PATTERN FORMATION DURING

CAENORHABDITIS ELEGANS VULVAL DEVELOPMENT

Thesis by

Minqin Wang

In Partial Fulfillment of the Requirements

for the Degree of

Doctor of Philosophy

California Institute of Technology

Pasadena, California

2000

(submitted May 18, 2000)

ii

ACKNOWLEDGMENTS

I am very fortunate to have Dr. Paul Sternberg as my research advisor. This project would not have been possible without his wisdom, encouragement, understanding and patience. He has been an ideal mentor and has influenced me in many different ways. His enthusiasm, optimism, and dedication to science have been an inspiration for me. I feel privileged to have worked with him.

I would like to thank members of my thesis committee and other faculty at the Division of Biology, Dr. David Anderson, Dr. Eric Davidson, Dr. Raymond Deshaies, Dr. Scott Fraser, Dr. Ed Lewis, and Dr. Elliot Meyerowitz, who have been truly helpful and generous with their time. Special thanks go to the *C. elegans* community for sharing reagents and advice.

Caltech is truly a unique place full of wonderful and talented people whom I enjoyed working with immensely. Lily Jiang, Jing Liu and myself came from similar backgrounds and have shared a lot of happy moments. Giovanni Lesa is the first lab member I have known and has been a great friend ever since. My first few years in the lab would have been a lot more difficult without his Italian and jokes. Tom Clandinin has always been there when I need a listener or a critic. I have enjoyed stimulating conversations with him and he has provided me with a lot of valuable advice. Maureen Barr has made my days in the lab much more pleasant and has been a reliable source of support and encouragement. Dave Sherwood has been a

wonderful friend, and it has been so much fun to have him around that I wish he had joined the lab earlier. He is always willing to express his opinions, and we never did quite figure out how to stop talking. I have enjoyed having intellectual discussions and being friends with Nadeem Moghal and Réné Garcia. John DeModena and Pheobe Tzou have helped me with experiments, and have been good friends from the very beginning. I learned a lot about science and life from Bino Palmer and will not forget him. José Luis Riechmann and Cathy Yuh taught me many tricks in molecular biology and made my first year at Caltech easier. I enjoyed those beautiful pictures José Luis took and playing pingpong with him. Other past and present members of the Sternberg Lab, Jeff, Byung, Keith, Chris, Aidyl, Neil, Charles, Mark, Martha, Wen, Hui, Yvonne, Jane, Mary, Bhagwati, Yen, Carol, Lisa, Takao, just to name a few, have made the lab a great place to work.

My parents Hebao and Deben Wang are truly the magicians who have made me who I am. They have devoted their lives to raising my sister, my brother and myself, and have encouraged me to think independently. My sister and my brother, Minhua and Minli, have always been there for me and given me emotional support whenever needed.

It was fate that brought me to Caltech where I met Huimin, who has made my life full of joy and happiness. He is the one who can finish my sentences and understand every one of my whimsical ideas. His positive attitude and his belief in me have been my driving force. I can not imagine my life without him.

v

ABSTRACT

Pattern formation during animal development involves at least three processes: establishment of the competence of precursor cells to respond to intercellular signals, formation of a pattern of different cell fates adopted by precursor cells, and execution of the cell fate by generating a pattern of distinct descendants from precursor cells. I have analyzed the fundamental mechanisms of pattern formation by studying the development of *Caenorhabditis elegans* vulva.

In *C. elegans*, six multipotential vulval precursor cells (VPCs) are competent to respond to an inductive signal LIN-3 (EGF) mediated by LET-23 (RTK) and a lateral signal via LIN-12 (Notch) to form a fixed pattern of 3°-3°-2°-1°-2°-3°. Results from expressing LIN-3 as a function of time in animals lacking endogenous LIN-3 indicate that both VPCs and VPC daughters are competent to respond to LIN-3. Although the daughters of VPCs specified to be 2° or 3° can be redirected to adopt the 1° fate, the decision to adopt the 1° fate is irreversible. Coupling of VPC competence to cell cycle progression reveals that VPC competence may be periodic during each cell cycle and involve LIN-39 (HOM-C). These mechanisms are essential to ensure a bias towards the 1° fate, while preventing an excessive response.

After adopting the 1° fate, the VPC executes its fate by dividing three rounds to form a fixed pattern of four inner vulF and four outer vulE

descendants. These two types of descendants can be distinguished by a molecular marker *zmp-1::GFP*. A short-range signal from the anchor cell (AC), along with signaling between the inner and outer 1° VPC descendants and intrinsic polarity of 1° VPC daughters, patterns the 1° lineage. The Ras and the Wnt signaling pathways may be involved in these mechanisms.

The temporal expression pattern of *egl-17::GFP*, another marker of the 1° fate, correlates with three different steps of 1° fate execution: the commitment to the 1° fate, as well as later steps before and after establishment of the uterine-vulval connection. Six transcription factors, including LIN-1(ETS), LIN-39 (HOM-C), LIN-11(LIM), LIN-29 (zinc finger), COG-1 (homeobox) and EGL-38 (PAX2/5/8), are involved in different steps during 1° fate execution.

TABLE OF CONTENTS

Chapter 1

Pattern formation during *C. elegans* vulval induction

Minqin Wang and Paul W. Sternberg

(prepared for publication as a review in

Current Topics in Developmental Biology)

Studies of *C. elegans* vulval development provide insights into the process of pattern formation during animal development. The invariant pattern of vulval precursor cell fates is specified by the integration of at least two signaling systems. Recent findings suggest that multiple, partially redundant mechanisms are involved in patterning the vulval precursor cells. The inductive signal activates the LET-60/RAS signaling pathway and induces the 1° fate, while the lateral signal mediated by LIN-12/Notch is required for specification of the 2° fate. Several regulatory pathways antagonize the RAS signaling pathway and specify the non-vulval 3° fate in the absence of induction. The temporal and spatial regulation of VPC competence and production of the inductive and the lateral signal are precisely coordinated to ensure the wild-type vulval pattern.

I. Introduction

The development of *C. elegans* vulva exemplifies the fundamental mechanisms of pattern formation during organogenesis. It has been chosen as a model system because of its well-defined and fixed cell lineage, amenability for analyses at a single-cell level, and availability of genetic, cellular and molecular tools (Horvitz and Sternberg, 1991). One basic feature of vulval pattern formation in *C. elegans* is its precision.

C. elegans proceeds through four larval stages (L1-L4) before adulthood. At the L1 stage, 12 ectoblasts, P1.p-P12.p, are aligned in an anterior to posterior row along the ventral midline of the hermaphrodite

body (Sulston and Horvitz, 1977). The six central ectoblasts, P3.p-P8.p, form the multipotential group of vulval precursor cells (VPCs). Although they are all competent to choose among three fates (1°, 2° and 3°) (Sulston and White, 1980; Kimble, 1981; Sternberg and Horvitz, 1986), a pattern of 3°-3°-2°-1°-2°-3° is always established in wild-type animals (Fig. 1). All six VPCs divide once about 4 hours after the L2 molt. The daughters of P3.p, P4.p and P8.p, that adopt the non-vulval 3° fate, fuse with the hyp7 epidermal syncytium shortly after they are born. The daughters of P6.p, which adopts the 1° vulval fate, divide two more times to generate a lineage of eight descendants, while the daughters of the flanking P5.p and P7.p, which assume the 2° vulval fate, give rise to a lineage of seven progeny (Fig. 2). In this review, we refer to Pn.p daughters as Pn.px, Pn.p granddaughters as Pn.pxx, and Pn.p great granddaughters as Pn.pxxx. At the L4 stage, the 22 descendants of P5.p, P6.p and P7.p can be classified as 7 distinct types (A, B1, B2, C, D, E and F), as they migrate dorsally and undergo cell fusion to form an epithelial tube consisting of 7 toroidal cells (A to F). This structure connects to the uterus and eventually everts at late-L4 to form a mature vulva (Sharma-Kishore *et al.,* 1999). Besides the canonical 1° and 2° lineages observed in wild-type animals, two kinds of aberrant VPC lineages, hybrid (sometimes called half-vulval) and intermediate, are observed when vulval patterning is disturbed. In hybrid lineages, one VPC daughter cell fuses with hyp7, while its sister behaves like a 1° or 2° VPC daughter. Intermediate lineages exhibit both 1° and 2° features (Katz *et al.,* 1995).

At least two different intercellular signaling pathways are involved in patterning VPC fates (Fig. 1; reviewed in Eisenmann and Kim, 1994; Sundaram and Han, 1996; Greenwald, 1997; Kimble and Simpson, 1997; Kornfeld, 1997; Sternberg and Han, 1998). The inductive signal LIN-3, an epidermal growth factor (EGF)-like molecule produced by the anchor cell (AC) in the somatic gonad, induces P6.p to adopt the 1° fate (Kimble, 1981; Hill and Sternberg, 1992; Katz *et al.*, 1995). This signal is transduced by the receptor tyrosine kinase LET-23 and a conserved signaling pathway that activates LET-60/RAS (Aroian *et al.*, 1990; Beitel *et al.*, 1990; Han and Sternberg, 1990; Katz *et al.*, 1996). Overexpression of *lin-3* or *let-60*, or constitutive activation of *let-23* or *let-60*, causes P3.p, P4.p or P8.p to adopt vulval fates in addition to P5.p-P7.p (a multivulva or Muv phenotype). Reduction-of-function mutations in genes of this pathway can cause P5.p-P7.p to assume the non-vulval 3° fate (a vulvaless or Vul phenotype) (Hill and Sternberg, 1992; Aroian *et al.,* 1990; Han *et al.*, 1990; Katz *et al.,* 1995). Lateral signaling between P6.p and its neighbors P5.p and P7.p utilizes a Notch/LIN-12 family receptor encoded by *lin-12* (Yochem *et al.,* 1988). All six VPCs can adopt a 2° fate when LIN-12 is activated by a gain-of-function mutation, while none of them adopt a 2° fate in a *lin-12* loss-of-function mutant background (Greenwald *et al.*, 1983; Sternberg, 1988; Sternberg and Horvitz, 1989). A third signal has been proposed to come from the surrounding hyp7 epidermal syncytium (Herman and Hedgecock, 1990; Hedgecock and Herman, 1995), although recent findings suggest that it may also function autonomously within the VPCs, as discussed later (Lu and Horvitz, 1998; Thomas and Horvitz, 1999; A. Gonzalez-Serricchio and

P. Sternberg, in preparation). It negatively regulates the basal activity of *let-23*, and ensures that no induction will occur in the absence of LIN-3 (Clark *et al.,* 1994; Huang *et al.,* 1994).

Two distinct, but not mutually exclusive, models have been proposed to explain VPC fate patterning. The morphogen model is based on evidence demonstrating that VPCs can be induced to adopt the 1° or 2° fate depending on the level of LIN-3 signal they receive (Sternberg and Horvitz, 1986; Katz *et al.,* 1995). Since P6.p is closer to the AC compared with flanking P5.p and P7.p, a graded signal from the AC would be able to directly induce both 1° and 2° fates in a dose-dependant manner. A null or sub-threshold dose of LIN-3 leads to the 3° fate, while a low and a higher dose of LIN-3 induces the 2° and 1° fates respectively. The sequential induction model is supported by results of genetic mosaic analysis of *let-23* (Koga and Ohshima, 1995; Simske and Kim, 1995). In particular, mosaic animals that have LET-23 in P6.p, but not in P5.p and P7.p, typically have wild-type vulvae. Thus, LET-23 signaling may not be required cell-autonomously in P5.p and P7.p to adopt the 2° fate, at least in most animals. According to this model, the AC only induces P6.p to become 1°, which subsequently produces a lateral signal to induce P5.p and P7.p to become 2° through LIN-12.

It is unclear whether either mechanism is sufficient to form the invariant pattern of VPC fates. The morphogen model requires either of two postulations to explain the role of LIN-12: either there is autocrine activation of a LIN-12-dependent pathway, or LIN-12 is not necessary for the 2° fate with a low LIN-3 level. In the sequential model, the infrequent

failure to induce LET-23 deficient neighbors to adopt the 2° fate by a wild-type P6.p suggests that P5.p and P7.p might normally be induced directly by the AC. It is possible that both mechanisms are used during normal development and are partially redundant. Additionally, detailed analysis of the patterning of VPC fates has indicated that almost all aspects of this process are strictly controlled to ensure that a functional vulva is always formed. In this review, we describe the latest advances in our understanding of the integration of multiple mechanisms to achieve precise pattern formation.

II. Spatial regulation of VPC competence

To establish the pattern of VPC fates, both the production of inductive signal and the response of VPCs must be spatially and temporally regulated. The production of LIN-3 is spatially controlled by restricting its expression to the AC (Hill and Sternberg, 1992). Consequently, the closest VPC to the AC, P6.p, always receives the highest level of LIN-3. One closely related issue is the relative positioning of the VPCs to the AC, which appears to involve the homeotic gene *mab-5* (Clandinin *et al.,* 1997). In some *mab-5(lf)* mutants, the relative positioning of the VPCs to the AC is shifted so that P7.p, instead of P6.p, is the closest VPC to the AC. Also, the amount of LIN-3 expressed by the AC needs to be controlled to limit its potentially graded distribution, since excessive secretion can induce ectopic vulval fates. For example, transgenic animals bearing multiple copies of the *lin-3* gene or heat shocked animals carrying a transgene expressing LIN-3 EGF domain under the control of a heat shock promoter (*hs-LIN-3*) display a multivulva

(Muv) phenotype (Hill and Sternberg, 1992; Katz *et al.,* 1995). Besides the limited production and potentially graded spatial distribution of LIN-3, spatially restricted VPC competence is another important mechanism to ensure the precision of vulval pattern formation.

A. *lin-39*

Of the epidermal Pn.p cells, P1.p-P11.p, the anterior P1.p-P2.p and the posterior P9.p-P.11p adopt the 4° (sometimes called F) fate, (i.e., they fuse with hyp7 at the L1 stage; Sulston and Horvitz, 1977). P3.p-P8.p remain unfused and form the group of vulval precursor cells (VPCs) competent to generate the vulva (Sulston and White, 1980; Kimble, 1981; Sternberg and Horvitz, 1986). Two genes in the homeotic cluster (HOM-C) of *C. elegans*, *lin-39* and *mab-5*, are expressed in all VPCs and the posterior two VPCs, respectively (Wang *et al.,* 1993; Clark *et al.,* 1993). *lin-39* is the ortholog of the *Drosophila* gene *Sex combs reduced/deformed/proboscipedia* and is required for VPC specification. In a *lin-39* loss-of-function background, P3.p-P8.p fail to become VPCs and fuse with hyp7 as do the more anterior and posterior Pn.p cells (Clark *et al.,* 1993). Thus, spatial limit of *lin-39* expression in P3.p-P8.p might restrict the number of VPCs capable of generating vulval lineages (Fig. 3).

LIN-39 activity is required not only in the L1 stage, but later as well, to keep VPCs unfused and maintain their identity. In wild-type animals, P3.p sometimes adopts the 4° fate, although it fuses with hyp7 at late-L2 rather than L1. The *bar-1* gene, which encodes a β-catenin/Armadillo homolog in the Wnt signaling pathway, has been proposed to control the

late 4° versus VPC fate decision in P3.p-P8.p by regulating *lin-39* expression (Eisenmann *et al.*, 1998). In *bar-1* loss-of-function mutants, VPCs including P3.p adopt the 4° fate at late-L2 more frequently, presumably due to insufficient LIN-39 expression in VPCs. This late function of LIN-39 extends through VPC induction, where LIN-39 plays a critical role in regulating VPC response to inductive signal (Clandinin *et al.*, 1997; Maloof and Kenyon, 1998; also see below).

B. *mab-5*

Recent genetic studies on the *Antennapedia* homolog *mab-5* suggest that MAB-5 reduces the competence of P7.p and P8.p, thus forming a non-uniform pattern of VPC competence (Clandinin *et al.*, 1997). Isolated P7.p and P8.p cells are less sensitive and have a reduced ability to respond to low levels of inductive signal compared with other anterior Pn.p cells, such as P6.p (Katz *et al.*, 1995). Loss of *mab-5* activity increases the sensitivity of P8.p to respond to both *hs-LIN-3* and the cell-autonomous activation of the inductive pathway by a *let-23* gain-of-function mutation (Clandinin *et al.*, 1997). MAB-5 is expressed in P7.p-P11.p, but not in P3.p-P6.p (Fig. 3; Salser *et al.*, 1993). Misexpression of MAB-5 in P3.p-P6.p (Salser and Kenyon, 1992) reduces their responsiveness to inductive signal in sensitized backgrounds (Clandinin *et al.*, 1997). The competence of P6.p to respond to the AC signal is likely initially distinct from that of P7.p and P8.p, and the positional information provided by the HOM-C genes accounts for at least some of this difference. It is not known whether more anteriorly expressed homeotic genes, such as *ceh-13* (Wang *et al.*, 1993; Wittmann *et al.*, 1997;

Brunschwig *et al.*, 1999), have similar functions to *lin-39* or *mab-5* to

regulate the responsiveness of P3.p-P5.p. Overall, P6.p may be predisposed

to be the one that perceives the highest level of inductive signal LIN-3.

III. Temporal regulation of VPC competence and commitment

Unlike the strict spatial limitation of LIN-3 expression, the temporal

expression of LIN-3 in the AC appears to span from early L2 to mid L4

according to a *lin-3::lacZ* reporter gene (Hill and Sternberg, 1992; Euling

and Ambros, 1996a). While such reporter genes do not necessarily reflect

the native gene expression in detail, we consider the issues that arise if

LIN-3 is expressed for a longer period than is apparently necessary.

Establishing windows of VPC competence to control timing of vulval

induction is likely of importance, unless the release of LIN-3 is temporally

regulated. In wild-type animals, the window of VPC competence is limited

to late L2 and early L3, which is the normal time of inductive and lateral

signaling. This makes sense in that induced VPCs need to be coordinated

in their cell divisions and morphogenesis of their descendants.

Furthermore, it is critical for a functional vulva to properly attach to the sex

musculature, which is aligned by the gonad during the L3 stage (Sulston

and Horvitz, 1977; Stern and DeVore, 1994). Proper attachment to the AC,

which organizes the uterine-vulval connection throughout the L3 and L4

stages, is also essential (Newman *et al.*, 1996).

Problems that arise during vulval development caused by

heterochronic mutations, which alter the timing of postembryonic

development of most tissues including the vulva, but not the gonad, are

consistent with these ideas. As in wild-type animals, vulval fates adopted by precociously dividing VPCs are dependent on the AC signal (Euling and Ambros, 1996a). This strongly supports that the AC signal is present earlier than needed and uncontrolled acquisition of VPC competence will result in untimely vulval development with deleterious consequences. As a result, these heterochronic mutants are defective in egg-laying because of abnormal vulval lineages and abnormal interaction between the vulva and neighboring tissues.

In general, two basic mechanisms can regulate the timing of inductive responses in development: cell cycle and absolute time. Inductive signaling is often related to cell division history of responding cells, and cells can measure time progression by counting cell cycles (e.g., Raff *et al.*, 1985). For example, cell cycle stage biases the decision of *Dictyostelium* cells to become either prespore or prestalk after starvation (Gomer and Firtel, 1987). In the mammalian cerebral cortex, S phase cortical progenitors are multipotent, whereas post-S cells are restricted in their competence (McConnell and Kaznowski, 1991). The other method of chronometry involves an internal clock of absolute time, proposed by muscle formation in *Xenopus* (reviewed in Cooke and Smith, 1990). Also, cell cycle progression is not required for cell differentiation in patterning of the epidermal cells in *Drosophila* and neuronal induction in *Xenopus* (Hartenstein and Posakony, 1990; Edgar and O'Farrel, 1990; Harris and Hartenstein, 1991).

A. The heterochronic pathway

Several recent studies have begun to elucidate the complex mechanisms

that regulate the timing of VPC competence and choices of cell fates (Euling

and Ambros, 1996a, 1996b; Ambros, 1999; Wang and Sternberg, 1999). In

wild-type animals, the 20-hour VPC cell cycle starts from mid-L1 to mid-L3

(Fig. 4). Based on measurement of DNA content and hydroxyurea

sensitivity, VPC S phase occurs approximately three hours before mitosis

(Fig. 4; Euling and Ambros, 1996a). Previous results indicate that VPCs

respond to inductive and lateral signals during the last four hours of the

VPC cell cycle, around the late L2 to early L3 stage (Kimble 1981;

Greenwald *et al.*, 1983; Sternberg and Horvitz, 1986; Ferguson *et al.*, 1987).

This last four hours of the VPC cell cycle corresponds to the end of the G1

phase, as well as S and G2 phases.

Analysis of the heterochronic pathway has demonstrated

coordination between VPC cell cycle progression and developmental signals

in wild-type animals. Heterochronic genes regulate the timing of

postembryonic development, and perhaps, in the case of VPC development,

by affecting cell cycle progression of specific cells. Mutations in

heterochronic genes have been shown to cause either precocious or delayed

vulval development (Ambros and Horvitz, 1984). Specifically, heterochronic

genes control the completion of the G1 phase of the VPC cell cycle without

altering the time that VPCs are born, the cell cycle of VPC progeny, or the

timing of inductive signal production. Loss-of-function mutations in *lin-14*

(a novel nuclear protein) or *lin-28* (a cytoplasmic RNA binding protein),

which cause precocious vulval development, specifically shorten the G1

phase of the VPC cell cycle (Ambros and Horvitz, 1984; Ambros and Horvitz, 1987; Wightman *et al.*, 1991; Euling and Ambros, 1996a; Moss *et al.*, 1997). In contrast, *lin-14(gf)* or *lin-4(lf)* mutations cause the opposite phenotype: delayed or blocked VPC divisions (Euling and Ambros, 1996a; Ambros and Horvitz, 1987). In summary, heterochronic genes control both the acquisition of VPC competence and the completion of G1, although it has not been directly demonstrated whether these two events are causally related.

Recent studies have identified a new gene, *cki-1*, as one of the regulatory targets of the heterochronic genes (Hong *et al.*, 1999). CKI-1 belongs to the CIP/KIP family of cyclin-dependent kinase inhibitors, and regulates G1 progression of blast cells including VPCs. In addition to its expression in cell-cycle arrested cells, *cki-1::GFP* is expressed during the G1 phase of the cell cycle in differentiating cells such as VPCs. Expression of CKI-1 specifically in P6.p under the control of the *egl-17* promoter (Burdine *et al.*, 1998) blocks the division of P6.p. In contrast, blocking *cki-1* activity by RNA-mediated interference (RNAi) causes the six central Pn.p cells to undergo precocious cell division in the L2 stage and produce 12 VPCs. These data coupled to the observation that *cki-1::GFP* expression is reduced in VPCs in a *lin-14(lf)* mutant background suggest that *lin-14* controls VPC cell cycle progression at least in part by regulating *cki-1* (Hong *et al.*, 1999).

B. Cell cycle regulation of VPC competence and commitment

Although the heterochronic gene pathway affects both VPC cell cycle and competence, it is not clear whether VPC cell cycle progression is directly coupled to VPC competence or specification of cell fates. Ambros (1999) has shown that different phases of VPC cell cycle are linked to decisions of cell fates, using activation of *egl-17::GFP* expression (Burdine *et al.*, 1998) and the downregulation of LIN-12::GFP (Levitan and Greenwald, 1998a) as two markers for differentiation of the 1° fate. A P6.p cell arrested in S phase by hydroxyurea treatment nonetheless exhibits features of a specified 1° VPC, including activation of *egl-17::GFP* expression, decreasing of *lin-12::GFP* expression, and inhibition of *egl-17::GFP* expression in its neighbors in a Muv mutant background. Thus, induction and differentiation of the 1° fate can occur prior to completion of the S phase of the VPC cell cycle. Temperature-shift experiments using a temperature sensitive gain-of-function allele of *lin-12* suggest that the 1° fate decision is difficult to reverse to the 2° fate after a VPC has traversed the S phase of the cell cycle. In contrast, the 3° fate is readily convertible to the 2° fate after the S phase has passed. Therefore, specification of VPC fates is temporally coordinated so that specification of the 1° fate occurs prior to the completion of the S phase and therefore specification of the 2° or 3° fate, which may require the S phase (Fig. 4; Ambros, 1999).

Complementary results have been obtained using a different approach, which addresses commitment rather than specification (Wang and Sternberg, 1999). In a sensitized background of reduced inductive signaling, the AC signal is required after the VPC division. By establishing

a heat shock inducible LIN-3 system, one is able to turn on LIN-3

expression at different times. When challenged by LIN-3, presumptive 3°

VPC (P3.p, P4.p and P8.p) daughters, 2° VPC (P5.p and P7.p) daughters

with wild-type LIN-12 activity, and 2° VPC (P3.p-P8.p) daughters with

activated LIN-12, are all competent to respond to LIN-3 and can be

converted to the 1° fate. Therefore, specified 2° or 3° VPCs are not yet

committed to their fates, and can later be switched to the 1° fate if LIN-3 is

received by their daughters (Fig. 4; Wang and Sternberg, 1999).

A pivotal step in vulval patterning is 1° fate specification and

commitment. The 1° vulval lineage is a critical component of a functional

vulva, while the 2° or 3° lineages are sometimes dispensable (Horvitz and

Sulston, 1980; Sulston and White, 1980; M. Barr and P. Sternberg,

unpublished). Moreover, the 1° VPC is required to laterally signal its

neighbors to become 2° after its specification, in order to produce the wild-

type vulval pattern. Combined mechanisms of establishing the sequence of

specification of VPC fates, maintaining the competence of VPC daughters,

and irreversibility of 1° fate decision are essential to achieve the

prioritization of 1° over 2° and 3° fates as well as the temporal coordination

of inductive and lateral signaling events (Fig. 4). A sequence of the 1° fate

specification prior to the 2° fate biases the 1° fate decision and is consistent

with the sequence of the inductive and lateral signaling process.

Expanding the window of VPC competence to adopt the 1° fate to VPC

daughters provides a greater window of time to maximize the possibility of

induction of a 1° fate, which is especially important when the inductive

signal is not sufficient. The irreversibility of the 1° fate decision, combined

with reversibility of the decisions to become 2° and 3°, ensures that specification to be 1° overcomes a prior decision to be 2° or 3° and a 1° fate is specified regardless of when it happens.

Since low levels of LIN-3 also appear to induce the 2° fate (Katz *et al.*, 1995), different VPC fates can be considered as representing different states of VPCs that interpret different amounts of LIN-3 received over time and 'ratchet' towards the final 1° fate. Similar models have been proposed in amphibia and *Drosophila* (Fig. 5A; Gurdon *et al.*, 1995; Freeman, 1997). When the extent of vulval differentiation is reduced by reduction of signaling in the inductive signaling pathway, 2° and other non-canonical VPC fates are observed at the expense of the 1° fate. The 'ratchet' model can explain hybrid or intermediate vulval lineages that arise under various conditions (Sulston and Horvitz, 1981; Sternberg and Horvitz, 1986; Ferguson *et al.*, 1987; Sternberg and Horvitz, 1989; Thomas *et al.*, 1990; Aroian and Sternberg, 1991; Han *et al.*, 1993; Miller *et al.*, 1993; Lackner *et al.*, 1994; Tuck and Greenwald, 1994; Beitel *et al.*, 1995; Katz *et al.*, 1995; Koga and Oshima, 1995; Simske and Kim, 1995; Katz *et al.*, 1996; Hajnal *et al.*, 1997; Miller *et al.*, 1996; Wang and Sternberg, 1999). In this model, different levels of inductive signaling and length of exposure to the inductive signal might generate a series of diverse responses and different states, which can be translated into a series of VPC fates (Fig. 5A). Thus, various fates of the VPCs can result from VPCs going through a common program and exiting at different times. In wild-type animals, the 3°, 2° and the 1° fates constitute the three basic states that VPCs go through when the level of the inductive signal is none, low, or high, respectively. Hybrid

lineages with both 3° and 2° or 3° and 1° features (3°/2° and 3°/1°), as well as intermediate lineages with both 2° and 1° features (1°/2°) could be the result of intermediate states between 3° and 1°. VPCs can go through these states when the level of, or the exposure time to, the inductive signal LIN-3 is not sufficient.

One interesting feature of hybrid lineages is that the VPC daughter closer to the signal source (the AC or the 1° VPC) is always the one generating the half vulval lineage, whereas the more distal daughter adopts the half 3° fate. While this can be explained by polarized VPCs in the 'ratchet' model, an alternative way of generating hybrid and intermediate lineages may be that daughters of uncommitted VPCs respond to later inductive or lateral signal independently (Fig. 5B). According to this scenario, daughters of a presumptive 3° VPC might be reprogrammed to generate hybrid lineages of 3°/2° or 3°/1°, or intermediate lineages of 2°/1°. Inducing daughters of a presumptive 2° VPC might lead to intermediate lineages of 2°/1°. It is probable that the combined action of both 'ratchet' and responding VPC daughter mechanisms is responsible for hybrid and intermediate lineages.

C. The identity of VPCs and VPC daughters

In wild-type animals, the six central Pn.p cells form multipotential VPCs, and Pn.px cells generated after one round of cell division become VPC daughters. One intriguing issue is what makes Pn.px cells different from their parents. Both cell cycle dependent and cell cycle independent mechanisms may be involved.

The cell cycle related mechanism counts the numbers of cell cycles Pn.p cells have undergone instead of real time. For example, hydroxyurea arrested Pn.p cells exposed to LIN-3 at a time when they are chronologically older than normal VPC daughters still respond as VPCs rather than VPC daughters (Wang and Sternberg, 1999). Furthermore, precocious VPCs in a *lin-14(lf)* or *lin-28(lf)* background acquire competence to express vulval fates and produce precociously differentiated VPC daughters, presumably by shortening G1 of the VPC cell cycle (Euling and Ambros, 1996a). In addition, Pn.px and Pn.pxx cells, but not Pn.pxxx cells, in *lin-28(lf)* or *lin-14(lf)* mutants can be reprogrammed to the multipotential VPC states upon post-dauer development (Euling and Ambros, 1996b), indicating the importance of the cell division history of Pn.p cells and their descendants.

Meanwhile, cell cycle independent mechanisms may exist to monitor the chronological age of central Pn.p cells and maintain their VPC identity until mid-L3, regardless of the cell division history of Pn.p cells or their progeny. Genes in the heterochronic pathway are probably involved. First, retarded cell divisions in a *lin-4(lf)* or *lin-14(gf)* background result in abnormal Pn.px cell identity (Euling and Ambros., 1996a), suggesting that they are not equivalent to retarded cell divisions resulting from hydroxyurea treatment, which are apparently normal. Second, although shortening the Pn.p cell cycle by *lin-14* or *lin-28* mutations share similar properties with blocking *cki-1* activity by RNAi, the results are distinct. In both cases, divisions of the central Pn.p cells occur precociously at the L2 stage, distinct from Pn.p divisions occurring at mid-L3 in wild-type

animals. However, unlike Pn.px cells from precocious Pn.p divisions in *lin-14(lf)* or *lin-28(lf)* mutants, which produce precocious VPC daughters, Pn.px cells in *cki-1* RNAi animals retain the developmental potential of VPCs after Pn.p cells enter the cell cycle and divide once (Hong *et al.*, 1999). These VPCs specified by Pn.px cells are similar to the extra VPCs caused by rare precocious divisions of Pn.p cells in *lin-31* and *lin-25* mutants (Ferguson *et al.*, 1987; Miller *et al.*, 1993). It is worth noting that the absolute timing of Pn.p divisions, rather than the potential of cells to undergo more than two rounds of cell divisions, is likely to play an important role in determining the identity of Pn.p and Pn.px cells. For example, when the cullin CUL-1 is mutated, although the Pn.p cells fail to exit cell cycle and divide excessively, the divisions occur at mid-L3 as in wild-type animals, and no extra VPCs are produced (Kipreos *et al.*, 1996).

IV. Downstream events of RAS signaling

The inductive signal LIN-3 produced by the AC activates the RAS signaling pathway in responding VPCs. Extensive genetic screens and molecular approaches have identified numerous components in this pathway. However, relatively little is known about the downstream targets of the inductive signaling pathway, and how activation of RAS is translated into vulval fates.

A. The RAS signaling pathway

In the RAS signaling pathway, *lin-3* encodes an EGF-like growth factor, the inductive signal produced by the AC (Hill and Sternberg, 1992). LET-23, a

receptor tyrosine kinase, is the receptor of the inductive signal (Aroian *et al.*, 1990). Consistent with this model, LET-23 is not only expressed in all VPCs, but also localized on the basolateral surface of VPCs, the side facing the AC (Simske *et al.*, 1996). As positive regulators of LET-23-mediated RAS activation, LIN-2, LIN-7 and LIN-10 have been identified as PDZ domain-containing proteins that are required to localize LET-23 basolaterally in VPCs (Simske *et al.*, 1996; Hoskins *et al.*, 1996; Kaech *et al.*, 1998; Whitfield *et al.*, 1999). Biochemical experiments have shown that LIN-2, LIN-7, and LIN-10 form a complex and bind to the C-terminus of LET-23 via their PDZ domains. Loss-of-function mutations in *lin-2*, *lin-7*, or *lin-10* result in mislocalization of LET-23 in the apical domain of the VPCs, which correlates with an incompletely penetrant Vul phenotype. In addition to allowing better access to LIN-3 from the AC, the basolateral clustering of LET-23 might also allow amplification or maximum activation of the RAS signaling pathway, which occurs after ligand binding. For example, multivulva mutants that might be independent of LIN-3 inductive signal have more VPCs adopting the vulval fates than do Muv animals with additional loss-of-function mutations in *lin-2, lin-7*, or *lin-10* (Ferguson *et al.*, 1987; Katz *et al.*, 1996; Lu and Horvitz, 1998; Thomas and Horvitz, 1999).

After the LIN-3 ligand activates its receptor LET-23, the signal is transduced by a series of factors. The essential genes in the pathway include *sem-5* (GRB2), *let-341* (SOS), *let-60* (RAS), *lin-45* (RAF), *mek-2* (MAP kinase kinase), and *mpk-1/sur-1* (MAP kinase) (Beitel *et al.*, 1990; Han and Sternberg, 1990; Clark *et al.*, 1992a, 1992b; Han *et al.*, 1993; Lackner *et al.*, 1994; Wu and Han, 1994; Kornfeld, 1995a; Wu *et al.*, 1995; C. Chang, N.

Hopper, and P. Sternberg, in preparation). *ptp-2* (a SH2-containing protein tyrosine phosphatase SHP2), *ksr-1* (a novel protein kinase), *sur-6* (a regulatory B subunit of protein phosphatase 2A PP2A-B) and *sur-8/soc-2* (a novel leucine-rich repeat containing protein) have been identified as positive regulators downstream or parallel of *let-60 ras* (Kornfeld *et al.*, 1995b; Sundaram and Han, 1995; Gutch *et al.*, 1998; Sieburth *et al.*, 1998; Sieburth *et al.*, 1999). *lin-25* and *sur-2* encode two novel proteins that are positive factors downstream of MPK-1 (Singh and Han, 1995; Tuck and Greenwald, 1995). LIN-31 (a winged helix transcription factor) and LIN-1 (a ETS domain transcription factor) are two downstream effectors that are regulated by MAP kinase phosphorylation (Miller *et al.*, 1993; Beitel *et al.*, 1995; Tan *et al.*, 1998).

It is known in other organisms that activation of RAS signaling directly and indirectly leads to changes of gene transcription. However, exactly what happens in the VPC nucleus and how the 1° fate is programmed after RAS activation remains a mystery and largely unexplored. The phenotypes of *lin-25, sur-2, lin-31* and *lin-1* mutants are complex and epistasis analysis fails to place the transcription factors involved in a linear pathway (Miller *et al.*, 1993; Beitel *et al.*, 1995; Singh and Han, 1995; Tuck and Greenwald, 1995). The molecular switch determining the 1° fate may be the accumulation of transcription factors upon activation of RAS, which, once a certain threshold is reached, may turn on a whole set of downstream genes needed to execute the 1° fate. These genes may include those required for immediate and later responses to RAS activation, such as initiation of lateral signaling, inhibition of cell

fusion, and promotion of cell division. This conceivably irreversible process could result in VPC commitment toward the final 1° fate.

B. Changes of gene expression upon activation of RAS

Several reports have addressed the issue of changes of gene expression in P6.p that manifest the differentiation of the 1° fate (Simske *et al.*, 1996; Clandinin *et al.*, 1997; Eisenmann *et al.*, 1998; Burdine *et al.*, 1998; Levitan and Greenwald, 1998a; Maloof and Kenyon, 1998). Currently, the known events following the activation of the RAS signaling pathway include upregulation of *lin-39* and *let-23* expression, downregulation of *lin-12* expression, and activation of *egl-17* expression.

Besides its early function to prevent fusion of P3.p-P8.p in L1 and specify the VPCs, the HOM-C gene *lin-39* is required later for VPCs to respond to the inductive signal from late L2 to early L3 (Clandinin *et al.*, 1997; Maloof and Kenyon, 1998). First, immunocytochemical experiments using LIN-39 antibodies reveal that *lin-39* expression is increased in P6.p during the time of vulval induction. Second, epistasis analysis indicates that LIN-39 functions downstream of the RAS signaling pathway. A reduction-of-function mutation of *lin-39* results in defective vulval lineages, and suppresses the Muv phenotype caused by *let-60(gf)*. Furthermore, when provided with early LIN-39 activity, but no LIN-39 activity at the time of vulval induction, unfused VPCs in a *lin-39(lf)* background adopt non-vulval fates. Along with the temperature-sensitive periods of LIN-39, these results offer convincing evidence that LIN-39 activity is required again later during the time of vulval induction. LIN-39 may be functionally important

for the responsiveness of VPCs to inductive signal, since *lin-39(rf)* reduces

the induction level in animals with a sensitized background of a Vul

mutation or low levels of *lin-3* expression (Clandinin *et al.*, 1997; Maloof and

Kenyon, 1998). When mutated, *bar-1*, acting in VPCs to maintain the

expression of *lin-39* during vulval induction, also causes defects in 1° and 2°

fate specification similar to those in a *lin-39(rf)* background (Eisenmann *et

al.*, 1998).

Adoption of the 4° fate at late-L2 by P3.p in some of the wild-type

animals and by some VPCs in *bar-1(lf)* mutants is reminiscent of the early

function of *lin-39* at L1. However, adoption of the 4° fate at late-L2 differs

from Pn.p cell fusion at L1 as to whether the 4° fate can be suppressed by

activation of the RAS pathway. Constitutive activation of the RAS pathway

by Muv mutations inhibits P3.p from adopting the 4° fate (Ferguson *et al.*,

1987; Clandinin *et al.*, 1997). In addition, in *bar-1(lf)* mutants, P5.p-P7.p

adopt the 4° fate significantly less frequently than P3.p, P4.p and P8.p

(Eisenmann *et al.*, 1998). The rescue of the late 4° fate appears to be a result

of positive regulation of *lin-39* expression by activation of the RAS pathway,

which does not take place in L1. It is therefore likely that both BAR-1 and

the RAS pathway regulate LIN-39 in P5.p-P7.p, while BAR-1 alone

regulates LIN-39 in P3.p, P4.p and P8.p.

Besides *lin-39*, the expression of *let-23* is also upregulated by RAS

signaling (Simske *et al.*, 1996). As the receptor for the inductive signal

LIN-3, LET-23 is required for the responsiveness of VPCs together with

LIN-39, whose mechanism of regulation of VPCs' response is less clear. It

is conceivable that increases in *lin-39* and *let-23* expression in P6.p

following the initial inductive signaling could provide the basis for an amplified response of the presumptive 1° VPC, thereby locking the commitment towards the 1° fate. Increase of *let-23* expression in P6.p could also serve to sequester more LIN-3 molecules on P6.p to prevent excess induction of distal VPCs (also see below).

According to a *lin-12::GFP* reporter construct, the level of LIN-12 is downregulated by RAS signaling (Levitan and Greenwald, 1998a). This is consistent with genetic epistasis results that LIN-12 acts downstream of LET-60 RAS (Han *et al.*, 1990), and is certainly expected if the specification of the 1° fate occurs prior to that of the 2° fate (Ambros, 1999). Activation of the RAS pathway may turn on or upregulate the expression of a ligand in P6.p that laterally signals P5.p and P7.p, and subsequently, ligand-induced downregulation of LIN-12 receptor expression in P6.p. Such a mechanism would not only predispose P6.p to the 1° fate and enhance the difference between P6.p and its neighbors, it would also facilitate the coordination of inductive and lateral signals. Similar mechanisms may be used in other development systems, such as planar polarity establishment in *Drosophila* eye development (Tomlinson and Struhl, 1999). In this case, a polarizing signal from the equator mediated by the seven-transmembrane receptor Frizzled, followed by interaction between the photoreceptors mediated by Notch, ensures that the cells closer to the equator become the R3 photoreceptors and the polar cells adopt the R4 fate.

C. Specificity of RAS signaling

It has been known for a long time that mutations of genes in the LET-60/RAS pathway affect multiple processes in addition to vulval patterning, including viability, male spicule development, and P12 neuroectoblast fate specification (Fixsen *et al.*, 1985; Aroian and Sternberg, 1991; Chamberlin and Sternberg, 1994; Jiang and Sternberg, 1998). How does activation of RAS in VPCs lead to adoption of vulval fates by the VPCs? The HOM-C gene *lin-39* may be one of the factors required for specificity of the RAS signaling pathway (Maloof and Kenyon, 1998). While *lin-39* is expressed in hermaphrodite VPCs, *mab-5* is expressed in male P9.p-P11.p, a posterior equivalence group similar to hermaphrodite VPCs, which divide three times to generate the hook structure in male. Ectopic expression of *mab-5* in VPCs lacking LIN-39 activity causes the central Pn.p cells in the hermaphrodite to adopt features of the male posterior equivalence group. In contrast, replacing MAB-5 with misexpressed LIN-39 under control of a heat shock promoter results in precursors in the male posterior equivalence group displaying vulval characteristics.

Another tissue-specific effector that specifies the outcome of the LET-60/RAS signaling is the winged helix transcription factor LIN-31 (Tan *et al.*, 1998). *lin-31* is expressed specifically in the VPCs during induction and apparently affects only vulval development when mutated. LIN-31 appears to prevent vulval induction by forming a complex with LIN-1, a general effector of activated RAS. RAS signaling induces vulval fates through the dissociation of LIN-31/LIN-1 complex upon phosphorylation of LIN-31 by MPK-1, a signal transducer downstream of RAS. Also, ectopic expression

of *lin-31* in another RAS responsive cell (P12) is sufficient to cause P12 to express a vulval specific marker, increased LET-23 expression.

V. Negative regulation of RAS signaling

As discussed above, the system of VPC fate patterning utilizes mechanisms to impose a bias on P6.p to adopt the 1° fate, and P5.p and P7.p to become 2°. Since the number of VPCs competent to adopt the vulval fates exceeds the three central VPCs that actually do so in wild-type animals, it is crucial that additional mechanisms serve to prevent the anterior P3.p and P4.p, and the posterior P8.p from being induced. Besides restricted spatial expression and level of LIN-3, the inductive signaling pathway is negatively regulated at two distinct levels.

A. Inhibition of the basal activity of LET-23 signaling pathway

Two functionally redundant pathways of synthetic multivulva (synMuv) antagonize the LET-23-mediated signal transduction (Horvitz and Sulston, 1980; Ferguson and Horvitz, 1985, 1989; Beitel, 1994; Clark *et al.*, 1994; Huang *et al.*, 1994; Lu and Horvitz, 1998; Hsieh *et al.*, 1999; Thomas and Horvitz, 1999; Solari and Ahringer, 2000). These synMuv genes fall into two classes, A and B. So far six genes (*lin-8, lin-15A, lin-38, lin-56, egr-1* and *egl-27*) have been found to belong to class A and ten genes (*lin-9, lin-15B, lin-35, lin-36, lin-37, lin-51, lin-52, lin-54, lin-55* and *tam-1*) have been placed into class B. Single or double mutants of genes belonging to the same class have a wild-type vulva, while double mutants of both class A and B genes display excessive induction of P3.p, P4.p and P8.p (a Muv phenotype).

Recently, it has been found that some synMuv genes (*lin-53, hda-1, rba-1, chd-3* and *chd-4*) function in both synMuvA and synMuvB pathways (Lu and Horvitz, 1998; Shi and Mello, 1998; Solari *et al.*, 1999; Solari and Ahringer, 2000).

Several of the synMuv genes, including *lin-15A, lin-15B, lin-36*, and *lin-9*, have been cloned and shown to encode novel proteins (Clark *et al.*, 1994; Huang *et al.*, 1994; Beitel, 1994; Thomas and Horvitz, 1999). *lin-35* and *lin-53* have recently been shown to encode proteins similar to the tumor suppressor Rb and its binding protein RbAp48 (Lu and Horvitz, 1998). Two class A synMuv gene products, EGR-1 and EGL-27, are similar to the human metastasis tumor associated protein MTA1, a member of the nucleosome remodeling and histone deacetylase (NURD) complex (Solari *et al.*, 1999; Solari and Ahringer, 2000).

Detailed analysis on the question of site of action of synMuv genes suggests that some of them function autonomously in VPCs and others non-autonomously in the hypodermal syncytium hyp7. Genetic mosaic analysis studies of *lin-15* (A and B) and *lin-37* (a class B gene) suggest that both genes function non-autonomously in hyp7 (Herman and Hedgecock, 1990; Hedgecock and Herman, 1995). However, data on *lin-35* (class B), *lin-53* (class A and B) and *lin-36* (class B) are consistent with the hypothesis that they function autonomously within the VPCs. Antibody staining demonstrates that LIN-35 protein is present in VPCs, but not in hyp7, while a *GFP::lin-53* reporter gene is expressed in both (Lu and Horvitz, 1998). Results of both genetic mosaics and reporter gene expression of *lin-36*

support that this particular class B gene acts autonomously in VPC nuclei (Thomas and Horvitz, 1999).

How do the synMuv pathways work to negatively regulate the RAS signaling pathway? The Muv phenotype caused by mutations in synMuv genes requires functional *let-23* and genes downstream of the *let-23* receptor, but does not require the gonad, the source of the LIN-3 ligand (Ferguson and Horvitz, 1989; Huang *et al.*, 1994). Therefore, the synMuv pathways may inhibit the basal, ligand-independent activity of LET-23-mediated signaling pathway, which can be elevated by binding of the LIN-3 ligand to the LET-23 receptor (Fig. 6A). Alternatively, they may function to limit LIN-3 expression in the AC. For example, LIN-3 could be ectopically expressed in synMuv mutants, thereby inducing ectopic vulval fates even in the absence of the gonad. Finally, it is also possible that the synMuv pathways inhibit the RAS pathway by blocking a second, nongonadal signal, since three EGF-like molecules in addition to LIN-3 have been identified in the worm genome as possible candidates of EGF receptor ligands (Plowman *et al.*, 1999).

To understand the molecular mechanism by which the synMuv pathways antagonize RAS signaling, one needs to define the point at which the synMuv pathways interface with the Ras pathway, which could be at the level of the LET-23 receptor, the nucleus, or both. *In vitro* binding experiments suggest interactions among LIN-35, LIN-53 and HDA-1 (a histone deacetylase involved in remodeling chromatin structure), as well as among LIN-53, LIN-36, LIN-37 and LIN-15A (Lu and Horvitz, 1998; Walhout *et al.*, 2000). These data support the notion that LIN-35 Rb-

mediated class B synMuv pathway may function by repressing transcription of target genes. The discovery of another synMuv B gene *tam-1*, which mediates context-dependent gene silencing, is consistent with a mechanism of transcriptional repression, possibly by chromatin remodeling (Hsieh *et al.*, 1999). Furthermore, recent findings of components (LIN-53, HDA-1, RBA-1, CHD-3 and CHD-4) in the nucleosome remodeling and histone deacetylase (NURD) complex functioning in both synMuvA and synMuvB pathways suggest that these two pathways might redundantly recruit a core NURD complex and repress gene transcription by chromatin remodeling (Solari and Ahringer, 2000). Besides the chromatin remodeling model, it is also tempting to speculate that the class B synMuv pathway regulates cell fate specification and commitment of VPCs by Rb-associated G1/S cell cycle progression, thereby negatively regulating vulval induction.

B. Inhibition of the ligand-induced activity of LET-23 signaling pathway

Genes that function at another level of negative regulation have been isolated as suppressors of the Vul phenotype of *let-23(rf)* or *lin-10(rf)* mutants. These include *unc-101, sli-1* and *gap-1* (Lee *et al.*, 1994; Jongeward *et al.*, 1995; Yoon *et al.*, 1995; Hajnal *et al.*, 1997). Other negative regulators, such as *ark-1* and *sur-5*, have been recovered in genetic screens to look for Muv mutants in a *sli-1* background and suppressors of dominant negative *let-60 ras* (Gu *et al.*, 1998; N. Hopper, J. Lee and P. Sternberg, unpublished). These negative regulators have been identified to encode a homolog of medium chain of the *trans*-Golgi clathrin-associated adaptin

complex, the oncoprotein c-CBL, a GTPase activating protein for RAS, a
tyrosine kinase, and a novel protein, respectively. Similar to single
mutations in synMuv pathway genes, single mutations in these genes do
not cause any vulval phenotype. However, unlike mutations in synMuv
pathways, mutations of these negative regulators do not synergize greatly
with synMuv mutations of either class. Also, double mutants of these
negative regulators are largely or wholly dependent on the LIN-3 inductive
signal in the gonad to display the Muv phenotype (Sternberg *et al.*, 1994).

Although each negative regulator may interface with the RAS
signaling pathway by different underlying mechanisms, studies on these
genes converge and reveal an antagonistic function mediated by LET-23
(Fig. 6B). This model was first proposed based on the hyperinduced (Hin)
phenotype, defined as higher than wild-type vulval induction, caused by *let-
23(n1045)* at 25°C (Aroian and Sternberg, 1991). The Hin phenotype is
fundamentally different from the Muv phenotype caused by mutations in
synMuv genes in that the excess induction is centered around the AC, is
dependent on the AC signal, and is caused by a decrease of LET-23 activity
(Aroian and Sternberg, 1991). Double mutants of certain reduction-of-
function mutation of *let-23, lin-2, lin-7* or *lin-10* and *sli-1, unc-101*, or *gap-1*
also exhibit a Hin phenotype (Lee *et al.*, 1994; Jongeward *et al.*, 1995; Yoon
et al., 1995; Hajnal *et al.*, 1997). Mosaic analysis of *let-23; gap-1* animals
has shed light on the underlying mechanisms of a cell-non-autonomous
inhibitory function of LET-23 (Hajnal *et al.*, 1997). In short, the LET-23
receptors presented by the central VPCs might bind and sequester the LIN-
3 molecules secreted by the AC, thereby reducing the amount of LIN-3 the

distal VPCs (P3.p, P4.p and P8.p) may receive (Fig. 6B). Increase of *let-23* expression in P6.p upon activation of RAS may also facilitate the antagonistic role of LET-23 in addition to its role to activate RAS. In Hin animals, the LET-23 receptor might have reduced ability to bind and sequester LIN-3 because of mutations in the receptor itself or mislocalization caused by *lin-2*, *lin-7*, or *lin-10*. This leads to expanded spatial distribution of LIN-3 to reach the distal VPCs, which might induce the distal VPCs when their sensitivity is enhanced by reduction-of-function mutations in *sli-1*, *unc-101*, *gap-1*, or the *n1045* allele of *let-23*.

VI. Lateral signaling

A. 2° fate specification

While the RAS pathway is required for the 1° fate, LIN-12 activity is required for the 2° fate. In the absence of LIN-12, the receptor for the lateral signal, VPCs never adopt the 2° fate (Greenwald *et al.*, 1983; Sternberg and Horvitz, 1989). Although an isolated VPC receiving low levels of inductive signal can become 2° (Sternberg and Horvitz, 1986; Thomas *et al.*, 1990; Katz *et al.*, 1995), this has been proposed to depend on the autocrine activity of LIN-12 (e.g., Sternberg and Horvitz, 1989).

Does lateral signaling prevent adjacent VPCs from both adopting the 1° fate or induce neighbors of a 1° VPC to adopt the 2° fate? In *lin-15* mutants, all VPCs adopt vulval fates, but they display an alternating 1°-2° pattern (Sternberg, 1988). In particular, an isolated VPC lacking neighboring VPCs always adopts the 1° fate, whereas two isolated VPCs display a 1°-2° (or 2°-1°) pattern. However, lateral signaling also functions

in an inductive mode rather than an inhibitory mode. In *let-23* mosaic

animals, when P6.p has LET-23 and is induced to become 1°, P5.p and P7.p

lacking LET-23 can still adopt the 2° fate (Koga and Oshima, 1995; Simske

and Kim, 1995). Strikingly, although never in wild-type animals, P4.p can

become 2° when its neighbor P5.p adopts the 1° fate. Therefore, lateral

signaling can induce the 2° fate in VPCs that do not receive the inductive

signal. In wild-type animals, the induced 1° VPC, P6.p, signals laterally

and might specify P5.p and P7.p to become 2°.

One can infer from these results that the amount of LIN-3 received by

P5.p and P7.p is controlled so that lateral signal always overrides inductive

signal. When *lin-3* is overexpressed, inductive signal can override lateral

signaling to induce adjacent 1° fates (Katz *et al.*, 1995). On the other hand,

a wild-type vulval pattern can nevertheless be established even though the

absolute level of LIN-3 produced by the AC appears to be flexible within a

certain range. In some *let-23* mosaic animals where P6.p lacks LET-23 and

therefore can not sequester the LIN-3 molecules, LIN-3 from the AC is able

to induce P5.p or P7.p to adopt the 1° fate (Koga and Oshima, 1995; Simske

and Kim, 1995). In *dig-1* mutants in which the gonad is dorsally displaced,

the AC often induces the 1° fate with 2° neighbors, although the AC is at a

great distance from all VPCs (Thomas *et al.*, 1990). Most surprisingly,

some animals are Hin despite the lack of AC proximity. Therefore, the

VPCs most likely interact with each other and compare the relative level

rather than perceive the absolute level of the AC signal. In wild-type

animals, the positioning of the AC and VPCs ensures that P6.p is biased

towards the 1° fate, even when the intensity of the AC signal is not precisely controlled.

It is not clear whether a morphogen mechanism or a sequential induction mechanism alone is sufficient to pattern the 2° fates invariantly. With respect to the morphogen model, although low levels of LIN-3 are capable of inducing VPCs to adopt the 2° fate (Katz *et al.*, 1995), it is not necessary for 2° fate specification. Activated LIN-12 can cause all VPCs to adopt the 2° fate even when LIN-3 is not available (Sternberg and Horvitz, 1989; Greenwald and Seydoux, 1990). It is also conceivably difficult to solely rely on the distance between the AC and the VPCs to make the 1° versus 2° decision correctly every time. As to the sequential induction model, lateral signaling from a 1° VPC is not always sufficient to induce the 2° fate. In a small percentage of LET-23 mosaic animals with no LET-23 activity in P5.p or P7.p, a 1° P6.p can have a hybrid neighbor (Koga and Ohshima, 1995). Further clarification of how a low level of LIN-3 induces the 2° fate will likely provide better understanding of both mechanisms.

One unique feature of the 2° lineage is its polarity, with D and C descendants closer to the 1° lineage and A and B descendants further away. This polarity may be unrelated to LIN-12 function and require a signal from the gonad, as well as two receptors, *lin-17* (a Wnt receptor) and *lin-18* (a receptor tyrosine kinase) (Ferguson *et al.*, 1987; Sternberg and Horvitz, 1988; Sawa *et al.*, 1996; W. Katz and P. Sternberg, unpublished).

B. Regulators of the lateral signaling pathway

Although the identity of the lateral signal acting among the VPCs has yet to
be revealed, screens for extragenic suppressors of the egg-laying defects in
lin-12 dominant gain-of-function mutants or *lin-12* reduction-of-function
mutants have identified additional components in the lateral signaling
pathway (Sundaram and Greenwald, 1993; Levitan and Greenwald, 1995;
Tax *et al.*, 1997). Some cloned suppressors include *sel-1* (an extracellular
protein), *sel-10* (an F-box/WD40 repeat-containing protein of the CDC4
family), *sel-12* (presenilin), and *sup-17* (a metalloprotease of the ADAM
family) (Levitan and Greenwald, 1995; Grant and Greenwald, 1996;
Hubbard *et al.*, 1997; Wen *et al.*, 1997).

The two negative regulators of *lin-12* activity, *sel-1* and *sel-10*, may be
involved in LIN-12 turnover. Specifically, SEL-10 may target LIN-12 for
ubiquitin-mediated degradation, which is consistent with its cell-
autonomous effect and its physical association with SKP-1 (a component of
E3 complex for ubiquitin-dependent degradation) and the intracellular
domain of LIN-12 (King *et al.*, 1996; Hubbard *et al.*, 1997; Walhout *et al.*,
2000).

The positive regulator *sup-17* is homologous to *Drosophila*
kuzbanian, and is probably involved in processing the extracellular domain
of LIN-12/Notch during its maturation before activation upon ligand
binding (Pan and Rubin, 1997; Wen *et al.*, 1997). SEL-12, a *C. elegans*
presenilin, specifically affects LIN-12 accumulation in the VPC plasma
membrane, and presenilin has been shown to physically interact with
Notch (Levitan and Greenwald, 1998b; Ray *et al.*, 1999). Since the reduction-

of-function mutation in *sel-12* only suppresses the activity of full-length LIN-12, but not constitutively activated, truncated LIN-12 possessing only the intracellular domain, *sel-12* is likely involved in trafficking and cleavage of LIN-12 during its maturation before ligand binds to it. A physical association between SEL-10 and SEL-12 demonstrated *in vitro* and in yeast cells further implies that SEL-12 may also regulate SEL-10 level in the VPCs (Wu *et al.*, 1998; Walhout *et al.*, 2000).

The level of LIN-12 activity may be regulated by closely related processes, such as proteolytic processing, intracellular trafficking, and protein degradation. Studies of the above regulators of the lateral signaling pathway raise the intriguing possibility that they are involved in regulating dynamic changes in LIN-12 activity, which is a critical element in patterning VPC fates (Levitan and Greenwald, 1998a). For example, RAS-dependent downregulation of LIN-12 in P6.p could be the result of LIN-3-induced degradation of LIN-12 that reinforces the difference between P6.p and its neighbors.

VII. Evolutionary implications

Comparative developmental studies in several nematode species within the same order as *C. elegans* have revealed that similar patterning of vulval fates can be accomplished by combination of a wide diversity of patterning mechanisms and cell signaling networks. These studies have brought us insight into the evolution of developmental processes, as well as deepened our understanding of *C. elegans* vulval development.

First, the role of a single gene product can vary significantly between different species. In *C. elegans*, *lin-39* functions both early and later in vulval cell fate specification (Clandinin *et al.*, 1997; Maloof and Kenyon, 1998). Although its later role is obviously instructive, it is unknown whether the early function of LIN-39 to specify the multipotential VPC group is achieved by preventing cell fusion of the central Pn.p cells or promoting vulval fates. In *Pristionchus pacificus*, VPCs lacking LIN-39 activity die by programmed cell death rather than fuse with the epidermal syncytium hyp7. Double mutants with loss-of-function mutations in *lin-39* and *ced-3* (a gene required for apoptosis) have a functional vulva (Eizinger and Sommer, 1997; Sommer *et al.*, 1998). Therefore, the *lin-39* homolog *Ppa-lin-39* functions permissively to specify VPCs by inhibiting programmed cell death and does not actively participate in later vulval induction.

Second, the mechanism by which the AC specifies a similar centered vulval pattern can differ. While a one-step AC induction before VPC division is sufficient in wild-type *C. elegans*, several other nematode species (e.g., *Panagrolaimus, Oscheius*) utilize a two-step gonadal induction to pattern the VPC fates (Félix and Sternberg, 1997). In *C. elegans* wild-type animals, the AC is no longer needed after VPC division to induce the 2°-1°-2° pattern. In *Oscheius*, ablation of the AC after VPC division results in all VPCs including P6.p adopting the same outer vulval fate normally only adopted by P5.p and P7.p. This observation suggests that two successive inductions are required for specification of the inner fates. The first induction of VPCs to adopt vulval fates in these species might correspond to

an initially shared common program of 1° and 2°, perhaps a transiently induced early state in *C. elegans* (Fig. 5A). The second induction of VPC daughters to specify inner versus outer vulval fates might correspond to the specification of 1° versus 2° fates in *C. elegans*.

Finally, the network of cell interactions may use an overlapping set of developmental mechanisms, but may change the relative contribution of redundant mechanisms to elicit similar outcomes. For instance in *C. elegans*, differences of developmental potential among VPCs play a minor role compared with precisely controlled inductive and lateral signaling to generate the invariant vulval pattern. However, in *Mesorhabditis*, the gonad is not required for vulval induction after hatching (Sommer and Sternberg, 1994). In *Pristionchus*, there are only three VPCs in the vulval multipotential group (Sommer and Sternberg, 1996, 1997). In these two species, positional differences among VPCs appear to be a major mechanism, probably more important, than the gonadal induction. Nonetheless, use of multiple and even redundant mechanisms is one central idea to achieve a high degree of precision in patterning of vulval fates in *C. elegans* and other nematode species.

VIII. Conclusions and future directions

There has been significant progress in understanding the mechanisms that are responsible for formation of the invariantly patterned *C. elegans* vulva. A comprehensive picture is emerging in which all aspects of cell interaction in this patterning process are under precise control. Meanwhile our deepened knowledge raises more questions.

While we continue to identify and functionally analyze new genes to describe the pathways involved, especially the lateral and inhibitory pathways, in greater detail, much effort is needed to understand the integration of these signaling pathways. We do not know whether any of the changes in the expression of *egl-17*, *let-23*, *lin-39*, and *lin-12* within the 1° VPC are immediate steps following activation of RAS, or whether they are well downstream of RAS activation. Complex phenotypes displayed by *lin-1* and *lin-31* mutants make genetic analysis at the transcription factor level difficult (Miller *et al.*, 1993; Beitel *et al.*, 1995). Careful analysis of transcriptional regulatory regions of these genes and definitive identification of the transcription factors that bind to them should provide important insight into the signaling network that guides the expression of these genes. Moreover, the molecular link between the inductive and lateral signaling pathways and the identity of the lateral signal remain obscure, although *lin-25* has been described to affect both pathways (Tuck and Greenwald, 1995). Neither do we know about the target genes of synMuv pathways and how they relate to the RAS pathway. Although the concepts of cell fate specification and commitment have been used for a long time, their precise molecular meaning is not clear. Further understanding in specification and commitment of the 1° and 2° fates will help elucidate the mechanisms underlying the bias of the 1° fate determination. Detailed studies of the molecular meaning of VPC competence to respond to both inductive and lateral signal, as well as its relationship to the cell-cycle machinery will address the directly related questions of VPC commitment. In summary, future investigations of *C.*

elegans VPC fate patterning using genetic and molecular tools will provide a further comprehension of complex signaling networks and the mechanisms underlying precise pattern formation in development.

References

Ambros, V. (1999). Cell cycle-dependent sequencing of cell fate decisions in *Caenorhabditis elegans* vulval precursor cells. *Development* **126**, 1947-1956.

Ambros, V. and Horvitz, H. R. (1984). Heterochronic mutants of the nematode *Caenorhabditis elegans*. *Science* **226**, 409-416.

Ambros, V. and Horvitz, H. R. (1987). The *lin-14* locus of *Caenorhabditis elegans* controls the time of expression of specific postembryonic developmental events. *Genes Dev.* **1**, 398-414.

Aroian, R. V., Koga, M., Mendel, J. E., Ohshima, Y. and Sternberg, P. W. (1990). The *let-23* gene necessary for *Caenorhabditis elegans* vulval induction encodes a tyrosine kinase of the EGF receptor subfamily. *Nature* **348**, 693-699.

Aroian, R. V. and Sternberg, P. W. (1991). Multiple functions of *let-23*, a *Caenorhabditis elegans* receptor tyrosine kinase gene required for vulval induction. *Genetics* **128**, 251-267.

Beitel, G. J., Clark, S. G. and Horvitz, H. R. (1990). *Caenorhabditis elegans ras* gene *let-60* acts as a switch in the pathway of vulval induction. *Nature* **348**, 503-509.

Beitel, G. J., Tuck, S., Greenwald, I. and Horvitz, H. R. (1995). The *Caenorhabditis elegans* gene *lin-1* encodes an ETS-domain protein and defines a branch in the vulval induction pathway. *Genes Dev.* **9**, 3149-3162.

Beitel, G. J. (1994). Genetic and molecular analysis of *let-60 ras*, *lin-1* and *lin-9*: genes that function in *C. elegans* vuval induction. Ph.D. thesis, Massachusetts Institute of Technology, Cambridge, Massachusetts.

Brunschwig, K., Wittmann, C., Schnabel, R., Bürglin, T. R., Tobler, H. and Müller, F. (1999). Anterior organization of the *Caenorhabditis elegans* embryo by the *labial*-like *Hox* gene *ceh-13*. *Development* **126**, 1537-1546.

Burdine, R. D., Branda, C. S. and Stern, M. J. (1998). EGF-17(FGF) expression coordinates the attraction of the migration sex myoblasts with vulval induction in *C. elegans*. *Development* **125**, 1083-1093.

Chamberlin, H. M. and Sternberg, P. W. (1994). The *lin-3/let-23* pathway mediates inductive signaling during male spicule development in *Caenorhabditis elegans*. *Development* **120**, 2713-2721.

Clandinin, T. R., Katz, W. S. and Sternberg, P. W. (1997). *Caenorhabditis elegans* HOM-C genes regulate the response of vulval precursor cells to inductive signal. *Dev. Biol.* **182**, 150-161.

Clark, S. G., Chisholm, A. D. and Horvitz, H. R. (1993). Control of cell fates in the central body region of *C. elegans* by the homeobox gene *lin-39*. *Cell* **74**, 43-55.

Clark, S. G., Lu, X. and Horvitz, H. R. (1994). The *Caenorhabditis elegans* locus *lin-15*, a negative regulator of a tyrosine kinase signaling pathway, encodes two different proteins. *Genetics* **137**, 987-997.

Clark, S. G., Stern, M. J. and Horvitz, H. R. (1992a). *C. elegans* cell-signaling gene *sem-5* encodes a protein with SH2 and SH3 domains. *Nature* **356**, 340-344.

Clark, S. G., Stern, M. J. and Horvitz, H. R. (1992b). Genes involved in two *Caenorhabditis elegans* cell-signaling pathways. *Cold Spring Harb. Symp. Quant. Biol.* **57**, 363-73.

Cooke, J. and Smith, J. C. (1990) Measurement of developmental time by cells of early embryos. *Cell* **60**, 891-894.

Edgar, B. A. and O'Farrel, P. H. (1990). The three postblastoderm cell cycles of *Drosophila* embryogenesis are regulated in G2 by *string*. *Cell* **62**, 469-480.

Eisenmann, D. M. and Kim, S. K. (1994). Signal transduction and cell fate specification during *Caenorhabditis elegans* vulval development. *Curr. Opin. Genet. Dev.* **4**, 508-516.

Eisenmann, D. M., Maloof, J. N., Simske, J, S., Kenyon, C. and Kim, S. K. (1998). The β-catenin homolog BAR-1 and LET-60 Ras coordinately regulate the Hox gene *lin-39* during *Caenorhabditis elegans* vulval development. *Development* **125**, 3667-3680.

Eizinger, A. and Sommer, R. J. (1997). The homeotic gene *lin-39* and the evolution of nematode epidermal cell fates. *Science* **278**, 452-455.

Euling, S. and Ambros, V. (1996a). Heterochronic genes control cell cycle progress and developmental competence of *C. elegans* vulval precursor cells. *Cell* **84**, 667-676.

Euling, S. and Ambros, V. (1996b). Reversal of cell fate determination in *Caenorhabditis elegans* vulval development. *Development* **122**, 2507-2515.

Félix, M.-A. and Sternberg, P. W. (1997). Two nested gonadal inductions of the vulva in nematodes. *Development* **124**, 253-259.

Ferguson, E. L. and Horvitz, H. R. (1985). Identification and genetic characterization of 22 genes that affect the vulval lineages of the nematode *Caenorhabditis elegans*. *Genetics* **110**, 17-72.

Ferguson, E. L. and Horvitz, H. R. (1989). The multivulva phenotype of certain *Caenorhabditis elegans* mutants results from defects in two functionally redundant pathways. *Genetics* **123**, 109-121.

Ferguson, E. L., Sternberg, P. W. and Horvitz, H. R. (1987). A genetic pathway for the specification of the vulval cell lineages of *Caenorhabditis elegans*. *Nature* **326**, 259-267.

Fixsen, W., Sternberg, P. W., Ellis, H. and Horvitz, H. R. (1985). Genes that affect cell fates during the development of *Caenorhabditis elegans*. *Cold Spring Harbor Symp. Quant. Biol.* **50**, 99-104.

Freeman, M. (1997). Cell determination strategies in the *Drosophila* eye. *Development* **124**, 261-270.

Gomer, R. H. and Firtel, R. A. (1987). Cell-autonomous determination of cell-type choice in Dictyostelium development by cell-cycle phase. *Science* **237**, 758-762.

Grant, B. and Greenwald, I. (1996). The *Caenorhabditis elegans sel-1* gene, a negative regulator of *lin-12* and *glp-1*, encodes a predicted extracellular protein. *Genetics* **143**, 237-247.

Greenwald I. (1997). Development of the vulva. *In "C. elegans II".* (D. Riddle, T. Blumenthal, B. Meyer and J. Priess, Ed.), pp.519-541. Cold Spring Harbor Laboratory Press, New York.

Greenwald, I. and Seydoux, G. (1990). Analysis of gain-of-function mutations of the *lin-12* gene of *Caenorhabditis elegans*. *Nature* **346**, 197-199.

Greenwald, I. S., Sternberg, P. W. and Horvitz, H.R. (1983). The *lin-12* locus specifies cell fates in *Caenorhabditis elegans*. *Cell* **34**, 435-444.

Gu, T., Orita, S. and Han, M. (1998). *Caenorhabditis elegans* SUR-5, a novel but conserved protein, negatively regulates LET-60 Ras activity during vulval induction. *Mol. Cell. Biol.* **18**, 4556-4564.

Gurdon, J. B., Mitchell, A. and Mahony, D. (1995). Direct and continuous assessment by cells of their position in a morphogen gradient. *Nature* **376**, 520-521.

Gutch, M. J., Flint, A. J., Keller, J., Tonks, N. K. and Hengartner, M. O. (1998). The *Caenorhabditis elegans* SH2 domain-containing protein tyrosine phosphatase PTP-2 participates in signal transduction during oogenesis and vulval development. *Genes Dev.* **12**, 571-585.

Hajnal, A., Whitfield, C. W. and Kim, S. K. (1997). Inhibition of *Caenorhabditis elegans* vulval induction by *gap-1* and by *let-23* receptor tyrosine kinase. *Genes Dev.* **11**, 2715-2728.

Han, M., Aroian, R. and Sternberg, P. W. (1990). The *let-60* locus controls the switch between vulval and non-vulval cell types in *C. elegans*. *Genetics* **126**, 899-913.

Han, M. and Sternberg, P. W. (1990). *let-60*, a gene that specifies cell fates during *C. elegans* vulval induction, encodes a ras protein. *Cell* **63**, 921-931.

Han, M., Golden, A., Han, Y. and Sternberg, P. W. (1993). *C. elegans lin-45 raf* gene participates in *let-60 ras*-mediated vulval differentiation. *Nature* **363**, 133-140.

Harris, W. A. and Hartenstein, V. (1991). Neuronal induction without cell division in *Xenopus* embryos. *Neuron* **6**, 499-515.

Hartentein, V. and Posakony, J. W. (1990). Sensillum development in the absence of cell division: the sensillum phenotype of the Drosophila mutant *string*. *Dev. Biol.* **138**, 147-158.

Hedgecock, E. M. and Herman, R. K. (1995). The *ncl-1* gene and genetic mosaics of *Caenorhabditis elegans*. *Genetics* **141**, 989-1006.

Herman, R. K. and Hedgecock, E. M. (1990). Limitations of the size of the vulval primordium of *Caenorhabditis elegans* by *lin-15* expression in surrounding hypodermis. *Nature* **348**, 169-171.

Hill, R. J. and Sternberg, P. W. (1992). The gene *lin-3* encodes an inductive signal for vulval development for *C. elegans*. *Nature* **358**, 470-476.

Hong, Y., Roy, R. and Ambros, V. (1999). Developmental regulation of a cyclin-dependent kinase inhibitor controls postembryonic cell cycle progression in *Caenorhabditis elegans*. *Development* **125**, 3585-3597.

Horvitz, H. R. and Sternberg, P. W. (1991). Multiple intercellular signaling systems control the development of the *Caenorhabditis elegans* vulva. *Nature* **351**, 535-541.

Horvitz, H. R. and Sulston, J. E. (1980). Isolation and genetic characterization of cell-lineage mutants of the nematode *Caenorhabditis elegans*. *Genetics* **96**, 435-454.

Hoskins, R., Hajnal, A. F., Harp, S. and Kim, S. K. (1996). The *C. elegans* vulval induction gene *lin-2* encodes a member of the MAGUK family of cell junction proteins. *Development* **122**, 97-111.

Hsieh, J., Liu, J., Kostas, S. A., Chang, C., Sternberg, P. W. and Fire, A. (1999). The RING finger/B-Box factor TAM-1 and a retinoblastoma-like protein LIN-35 modulate context-dependent gene silencing in *Caenorhabditis elegans*. *Genes Dev.* **13**, 2958-2970.

Huang, L. S., Tzou, P. and Sternberg, P. W. (1994). The *lin-15* locus encodes two negative regulators of *Caenorhabditis elegans* vulval development. *Mol. Biol. Cell* **5**, 395-412.

Hubbard, E. J. A., Wu, G., Kitajewski, J. and Greenwald, I. (1997). *sel-10*, a negative regulator of *lin-12* activity in *Caenorhabditis elegans*, encodes a member of the CDC4 family of proteins. *Genes Dev.* **11**, 3182-3193.

Jiang, L. I. and Sternberg, P. W. (1998). Interaction of EGF, Wnt and HOM-C genes specify the P12 neuroectoblast fate in *C. elegans*. *Development* **125**, 2337-2347.

Jongeward, G. D., Clandinin, T. R. and Sternberg, P. W. (1995). *sli-1*, a negative regulator of *let-23*-mediated signaling in *C. elegans*. *Genetics* **139**, 1553-1566.

Kaech, S. M., Whitfield, C. W. and Kim, S. K. (1998). The LIN-2/LIN-7/LIN-10 complex mediates basolateral membrane localization of the *C. elegans* EGF receptor LET-23 in vulval epithelial cells. *Cell* **94**, 761-771.

Katz, W. S., Hill, R. J., Clandinin, T. R. and Sternberg, P. W. (1995). Different levels of the *C. elegans* growth factor LIN-3 promote distinct vulval precursor fates. *Cell* **82**, 297-307.

Katz, W. S., Lesa, G. M., Yannoukakos, D., Clandinin, T. R., Schlessinger, J. and Sternberg, P. W. (1996). A point mutation in the extracellular

domain activates LET-23, the *Caenorhabditis elegans* Epidermal Growth Receptor homolog. *Mol. Cell. Biol.* **16**, 529-537.

Kimble, J. (1981). Alterations in cell lineage following laser ablation of cells in the somatic gonad of *Caenorhabditis elegans*. *Dev. Biol.* **87**, 286-300.

Kimble, J. and Simpson, P. (1997). The LIN-12/Notch signaling pathway and its regulation. *Ann. Rev. Cell Dev. Biol.* **13**, 333-361.

King, R. W., Deshaies, R. J., Peteres, J.-M. and Kirschner, M. W. (1996). How proteolysis drives the cell cycle. *Science* **274**, 1652-1658.

Kipreos, E. T., Lander, L. E., Wing, J. P., He, W. W. and Hedgecock, E. M. (1996). *cul-1* is required for cell cycle exit in *C. elegans* and identifies a novel gene family. *Cell* **85**, 829-839.

Koga, M. and Ohshima, Y. (1995). Mosaic analysis of the *let-23* gene function in vulval induction of *Caenorhabditis elegans*. *Development* **121**, 2655-2666.

Kornfeld, K. (1997). Vulval development in *Caenorhabditis elegans*. *Trends Genet.* **13**, 55-61.

Kornfeld, K., Guan, K.-L. and Horvitz, H. R. (1995a). The *Caenorhabditis elegans* gene *mek-2* is required for vulval induction and encodes a protein similar to the protein kinase MEK. *Genes Dev.* **9**, 756-768.

Kornfeld, K., Hom, D. B. and Horvitz, H. R. (1995b). The *ksr-1* gene encodes a novel protein kinase involved in *ras*-mediated signaling in *Caenorhabditis elegans*. *Cell* **83**, 903-913.

Lackner, M. R., Kornfeld, K., Miller, L. M., Horvitz, H. R. and Kim, S. K. (1994). A MAP kinase homologue, *mpk-1*, is involved in *ras* mediated induction of vulval cell fates in *Caenorhabditis elegans*. *Genes Dev.* **8**, 160-173.

Lee, J., Jongeward, G. D. and Sternberg, P. W. (1994). *unc-101*, a gene required for many aspects of *Caenorhabditis elegans* development and behavior, encoded a clathrin-associated protein. *Genes Dev.* **8**, 60-73.

Levitan, D. and Greenwald, I. (1995). Facilitation of *lin-12*-mediated signaling by *sel-12*, a *Caenorhabditis elegans* S182 Alzheimer's disease gene. *Nature* **377**, 351-354.

Levitan, D. and Greenwald, I. (1998a). LIN-12 protein expression and localization during vulval development in *C. elegans*. *Development* **125**, 3101-3109.

Levitan, D. and Greenwald, I. (1998b). Effects of SEL-12 presenilin on LIN-12 localization and function in *Caenorhabditis elegans*. *Development* **125**, 3599-3606.

Lu, X. and Horvitz, H. R. (1998). *lin-35* and *lin-53*, two genes that antaganize a *C. elegans* Ras pathway, encode proteins similar to Rb and its binding protein RbAp48. *Cell* **95**, 981-991.

Maloof, J. N. and Kenyon, C. (1998). The Hox gene *lin-39* is required during *C. elegans* vulval induction to select the outcome of Ras signaling. *Development* **125**, 181-190.

McConnell, S. K. and Kaznowski, C. E. (1991). Cell cycle dependence of laminar determination in developing neocortex. *Science* **254**, 282-285.

Miller, L. M., Gallegos, M. E., Morisseau, B. A. and Kim, S. K. (1993). *lin-31*, a *Caenorhabditis elegans* HNF-3/*fork head* transcription factor homolog, specifies three alternative cell fates in vulval development. *Genes Dev.* **7**, 933-947.

Miller, L. M., Waring, D. A. and Kim, S. K. (1996). Mosaic analysis using a *ncl-1(+)* extrachromosomal array reveals that *lin-31* acts in the Pn.p cells during *Caenorhabditis elegans* vulval development. *Genetics* **143**, 1181-1191.

Moss, E. G., Lee, R. C. and Ambros, V. (1997). Control of developmental timing in *C. elegans* by the cold chock domain protein LIN-28 and its regulation by the *lin-4* RNA. *Cell* **88**, 637-646.

Newman, A. P., White, J. G. and Sternberg, P. W. (1996). Morphogenesis of the *C. elegans* hermaphrodite uterus. *Development* **122**, 3617-3626.

Pan, D. and Rubin, G. M. (1997). Kuzbaninian controls proteolytic processing of Notch and mediates lateral inhibition during *Drosophila* and vertebrate neurogenesis. *Cell* **90**, 271-280.

Plowman, G. D., Sundarsanam, S., Bingham, J., Whyte, D. and Hunter, T. (1999). The protein kinases of *Caenorhabditis elegans*: a model for

signal transduction in multicellular organisms. *Proc. Natl. Acad. Sci. USA* **96**, 13603-13610.

Raff, M. C., Abney, E. R. and Fok-Seang, J. (1985). Reconstitution of a developmental clock in vitro: a critical role for astrocytes in the timing of oligodendrocyte differentiation. *Cell* **42**, 61-69.

Ray, W. J., Yao, M., Nowotny, P., Mumm, J., Zhang, W., Wu, J. Y., Kopan, R. and Goate, A. M. (1999). Evidence for physical interaction between presenilin and Notch. *Proc. Natl. Acad. Sci. USA* **96**, 3263-3268.

Salser, S. J. and Kenyon, C. (1992). Activation of a *C. elegans Antennapedia* homologue in migrating cells controls their direction of migration. *Nature* **355**, 255-258.

Salser, S. J., Loer, C. M. and Kenyon, C. (1993). Multiple HOM-C gene interactions specify cell fates in the nematode central nervous system. *Genes Dev.* **7**, 1714-1724.

Sawa, H., Lobel, L. and Horvitz, H. R. (1996). The *Caenorhabditis elegans* gene *lin-17*, which is required for certain asymmetric cell divisions, encodes a putative seven-transmembrane protein similar to the *Drosophila Frizzled* protein. *Genes Dev.* **10**, 2189-2197.

Sharma-Kishore, R., White, J. G., Southgate, E. and Podbilewicz, B. (1999). Formation of the vulva in *Caenorhabditis elegans*: a paradigm for organogenesis. *Development* **126**, 691-699.

Shi, Y. and Mello, C. (1998). A CBP/p300 homolog specifies multiple differentiation pathways in *Caenorhabditis elegans*. *Genes Dev.* **12**, 943-955.

Sieburth, D. S., Sun, Q. and Han, M. (1998). SUR-8, a conserved Ras-binding protein with leucine-rich repeats, positively regulates Ras-mediated signaling in *C. elegans*. *Cell* **94**, 119-130.

Sieburth, D. S., Sundaram, M., Howard, R. M. and Han, M. (1999). A PP2A regulatory subunit positively regulates Ras-mediated signaling during *Caenorhabditis elegans* vulval induction. *Genes Dev.* **13**, 2562-2569.

Simske, J. S., Kaech, S. M., Harp, S. A. and Kim, S. K. (1996). LET-23 receptor localization by the cell junction protein LIN-7 during *C. elegans* vulval induction. *Cell* **85**, 195-204.

Simske, J. S. and Kim, S. K. (1995). Sequential signaling during *Caenorhabditis elegans* vulval induction. *Nature* **375**, 142-146.

Singh, N. and Han, M. (1995). *sur-2*, a novel gene, functions late in the *let-60 ras*-mediated signaling pathway during *Caenorhabditis elegans* vulval induction. *Genes Dev.* **9**, 2251-2265.

Solari, F. and Ahringer, J. (2000). NURD-complex genes antagonise Ras-induced vulval development in *Caenorhabditis elegans*. *Curr. Biol.* **10**, 223-226.

Solari, F., Bateman, A. and Ahringer, J. (1998). The *Caenorhabditis elegans* genes *egl-27* and *egr-1* are similar to MTA1, a member of a chromatin regulatory complex, and are redundantly required for embryonic patterning. *Development* **126**, 2483-2494.

Sommer, R. J. (1997). Evolutionary changes of developmental mechanisms in the absence of cell lineage alterations during vulval formation in the Diplogastridae (Nematoda). *Development* **124**, 243-251.

Sommer, R. J., Eizinger, A., Lee, K.-Z., Jungblut, B., Bubeck, A. and Schlak, I. (1998). The *Pristionchus* HOX gene *Ppa-lin-39* inibits programmed cell death to specify the vulva equivalence group and is not required during vulval induction. *Development* **125**, 3865-3873.

Sommer, R. J. and Sternberg, P. W. (1994). Changes of induction and competence during the evolution of vulval development in nematodes. *Science* **265**, 114-118.

Sommer, R. J. and Sternberg, P. W. (1996). Apoptosis and change of competence limit the size of the vulva equivalence group in *Pristionchus pacificus*: a genetic analysis. *Current Biology* **6**, 52-59.

Stern, M. J. and DeVore, D. L. (1994). Extending and connecting signaling pathways in *C. elegans*. *Dev. Biol.* **166**, 443-459.

Sternberg, P. W. (1988). Lateral inhibition during vulval induction in *Caenohabditis elegans*. *Nature* **335**, 551-554.

Sternberg, P. W. and Han, M. (1998). Genetics of RAS signaling in *C. elegans*. *Trends Genet.* **14**, 466-452.

Sternberg, P. W. and Horvitz, H. R. (1986). Pattern formation during vulval induction in *C. elegans*. *Cell* **44**, 761-772.

Sternberg, P. W. and Horvitz, H. R. (1988). *lin-17* mutations *of Caenorhabditis elegans* disrupt certain asymmetric cell divisions. *Dev. Biol.* **130**, 67-73.

Sternberg, P. W. and Horvitz, H. R. (1989). The combined action of two intercellular signaling pathways specifies three cell fates during vulval induction in *C. elegans*. *Cell* **58**, 679-693.

Sternberg, P. W., Yoon, C. H., Lee, J., Jongeward, G. D., Kayne, P. S., Katz, W. S., Lesa, G., Liu, J., Golden, A., Huang, L. S. and Chamberlin, H. M. (1994). Molecular genetics of proto-oncogenes and candidate tumor suppressors in *Caenorhabditis elegans*. *Cold Spring Harb. Symp. Quant. Biol.* **59**, 155-163.

Sulston, J. E. and Horvitz, H.R. (1977). Postembryonic cell lineages of the nematode *Caenorhabditis elegans*. *Dev. Biol.* **56**, 110-156.

Sulston, J. E. and Horvitz, H. R. (1981). Abnormal cell lineages in mutants of the nematode *Caenorhabditis elegans*. *Dev. Biol.* **82**, 41-55.

Sulston, J. E. and White, J. G. (1980). Regulation and cell autonomy during postembryonic development of *Caenorhabditis elegans*. *Dev. Biol.* **78**, 577-597.

Sundaram, M. and Greenwald, I. (1993). Suppressor of a *lin-12* hypomorph define genes that interact with both *lin-12* and *glp-1* in *Caenorhabditis elegans*. *Genetics* **135**, 765-783.

Sundaram, M. and Han, M. (1995). The *Caenorhabditis elegans ksr-1* gene encodes a novel Raf-related kinase involved in Ras-mediated signal transduction. *Cell* **83**, 889-901.

Sundaram, M. and Han, M. (1996). Control and integration of cell signaling pathways during *C. elegans* vulval development. *Bioessays* **18**, 473-480.

Tan, P. B., Lackner, M. R. and Kim, S. K. (1998). MAP kinase signaling specificity mediated by the LIN-1 Ets/LIN-31 WH transcription factor complex during *C. elegans* vulval induction. *Cell* **93**, 569-580.

Tax, F. E., Thomas, J. H., Ferguson, E. L. and Horvitz, H. R. (1997). Identification and characterization of genes that interact with *lin-12* in *Caenorhabditis elegans*. *Genetics* **147**, 1675-1695.

Thomas, J. H. and Horvitz, H. R. (1999). The *C. elegans* gene *lin-36* acts cell autonomously in the *lin-35* Rb pathway. *Development* **126**, 3449-3459.

Thomas, J. H., Stern, M. J. and Horvitz, H. R. (1990). Cell interactions coordinate the development of the *C. elegans* egg-laying system. *Cell* **62**, 1041-1052.

Tomlinson, A. and Struhl, G. (1999). Decoding vectorial information from a gradient: sequential roles of the receptors Frizzled and Notch in establishing planar polarity in the *Drosophila* eye. *Development* **126**, 5725-5738.

Tuck, S. and Greenwald, I. (1995). *lin-25*, a gene required in vulval induction in *Caenorhabditis elegans*. *Genes Dev.* **9**, 341-357.

Walhout, A. J. M., Sordella, R., Lu, X., Hartley, J. L., Temple, G. F., Brasch, M. A., Thierry-Mieg, N. and Vidal, M. (2000). Protein interaction mapping in *C. elegans* using proteins involved in vulval development. *Science* **287**, 116-122.

Wang, B. B., Muller-Immergluck, M. M., Austin, J., Robinson, N. T., Chisholm, A. and Kenyon, C. (1993). A homeotic gene cluster patterns the anteroposterior body axis of *C. elegans*. *Cell* **74**, 29-42.

Wang, M. and Sternberg, P. W. (1999). Competence and commitment of *Caenorhabditis elegans* vulval precursor cells. *Dev. Biol.* **212**, 12-24.

Wen, C., Metzstein, M. M. and Greenwald, I. (1997). SUP-17, a *Caenorhabditis elegans* ADAM protein related to *Drosophila* KUZBANIAN, and its role in LIN-12/NOTCH signaling. *Development* **124**, 4759-4767.

Whitfield, C. W., Benard, C., Barnes, T., Hekimi, S. and Kim, S. K. (1999). Basolateral localization of the *Caenorhabditis elegans* epidermal

growth factor receptor in epithelial cells by the PDZ protein LIN-10. *Mol. Biol. Cell* **10**, 2087-2100.

Wightman, B., Burglin, T. R., Gatto, J., Arasu, P. and Ruvkun, G. (1991). Negative regulatory sequences in the *lin-14* 3'-untranslated region are necessary to generate a temporal switch during *Caenorhabditis elegans* development. *Genes Dev.* **5**, 1813-1824.

Wittmann, C., Bossinger, O., Goldstein, B., Fleischmann, M., Kohler, R., Brunschwig, K., Tobler, H. and Müller, F. (1997). The expression of the *C. elegans labial*-like *Hox* gene *ceh-13* during early embryogenesis relies on cell fate and on anteroposterior cell polarity. *Development* **124**, 4193-4200.

Wu, G., Hubbard, E. J. A., Kitajewski, J. K. and Greenwald., I. (1998). Evidence for functional and physical association between *Caenorhabditis elegans* SEL-10, a Cdc4p-related protein, and SEL-12 presenilin. *Proc. Natl. Acad. Sci. USA* **95**, 15787-15791.

Wu, Y. and Han, M. (1994). Suppression of activated Let-60 Ras defines a role of *Caenorhabditis elegans sur-1* MAP kinase in vulval differentiation. *Genes Dev.* **8**, 147-159.

Wu, Y., Han, M. and Guan, K.-L. (1995). MEK-2, a *Caenorhabditis elegans* MAP kinase kinase, functions in Ras-mediated vulval induction and other developmental events. *Genes Dev.* **9**, 742-755.

Yochem, J., Weston, K. and Greenwald, I. (1988). The *Caenorhabditis elegans lin-12* gene encodes a transmembrane protein with overall similarity to *Drosophila Notch*. *Nature* **335**, 547-550.

Yoon, C. H., Lee, J., Jongeward, G. D. and Sternberg, P. W. (1995). Similarity of *sli-1*, a regulator of vulval development in *C. elegans*, to the mammalian proto-oncogene *c-cbl*. *Science* **269**, 1102-1105.

Table 1. Genes involved in patterning of VPC fates.

VPC fates	Function	Genes	Predicted protein
Spatial competence	VPC specification and competence	*lin-39* *mab-5* *bar-1*	*Scr* homeodomain *Antp* homeodomain β-catenin
Temporal Competence	The heterochronic pathway	*lin-4* *lin-14* *lin-28*	Regulatory RNA Novel nuclear protein RNA binding protein
	Regulatory target of heterochronic genes	*cki-1*	Cyclin-dependent kinase inhibitor
1°	Ligand Receptor Signal transducers	*lin-3* *let-23* *sem-5* *let-341* *let-60* *lin-45* *mek-2* *mpk-1*	Epidermal growth factor Receptor tyrosine kinase SH3-SH2-SH3 adaptor Guanine nucleotide releasing protein RAS RAF MAP kinase kinase MAP kinase
	Localization of LET-23	*lin-2* *lin-7* *lin-10*	PDZ PDZ PDZ
	Positive regulators	*ptp-2* *ksr-1* *sur-6* *sur-8/soc-2* *lin-25* *sur-2*	Tyr phosphatase SHP2 Novel protein kinase Phosphatase 2A-B Leucine-rich repeat Novel, nuclear Novel, nuclear
	Transcription factors	*lin-1* *lin-31*	ETS Winged helix
3° protein	Negative regulators	*gap-1*	GTPase activating
	of the ligand-induced activity of LET-23	*unc-101* *sli-1* *ark-1*	AP47, Clathrin adaptin CBL Tyrosine kinase
	Negative regulator of RAS	*sur-5*	Novel

	Class A synMuv Negative regulators of the basal activity of LET-23	*lin-15A* *lin-8* *lin-38* *lin-56* *egr-1* *egl-27*	Novel Not cloned Not cloned Not cloned MTA1 MTA1
	Class B synMuv	*lin-15B* *lin-9* *lin-35* *lin-36* *lin-37* *lin-51* *lin-52* *lin-54* *lin-55* *tam-1*	Novel Novel Rb Novel Not cloned Not cloned Not cloned Not cloned Not cloned RING finger/B box nuclear protein
	Class A and B synMuv NURD complex	*lin-53* *hda-1* *rba-1* *chd-3* *chd-4*	Rb-associated protein Histon deacetylase Rb-associated protein Highly similar chromodomain helicase protein
2°	Receptor	*lin-12*	Notch
	Positive regulators	*sel-12* *sup-17*	Presenilin ADAM metalloprotease
	Negative regulators	*sel-1* *sel-10*	Extracellular protein CDC4

FIGURES

Figure 1. *C. elegans* vulval development.

Lateral view of an L3 hermaphrodite. Ventral is down; anterior is to the left. The anchor cell (AC) is part of the somatic gonad, and is dorsal to P6.p. Six vulval precursor cells (VPCs), P3.p-P8.p, lie along the ventral midline in the central body region, surrounded by the hypodermal syncytium (hyp7). At least two signals function during patterning of VPC fates. The AC produces the inductive signal (straight arrows) and induces the 1° fate at a high level and the 2° fate at a low level. The closest VPC to the AC, P6.p, adopts the 1° fate and signals P5.p and P7.p laterally (curved arrows) to cause them to adopt the 2° fate. It is not clear where the inhibitory signal comes from.
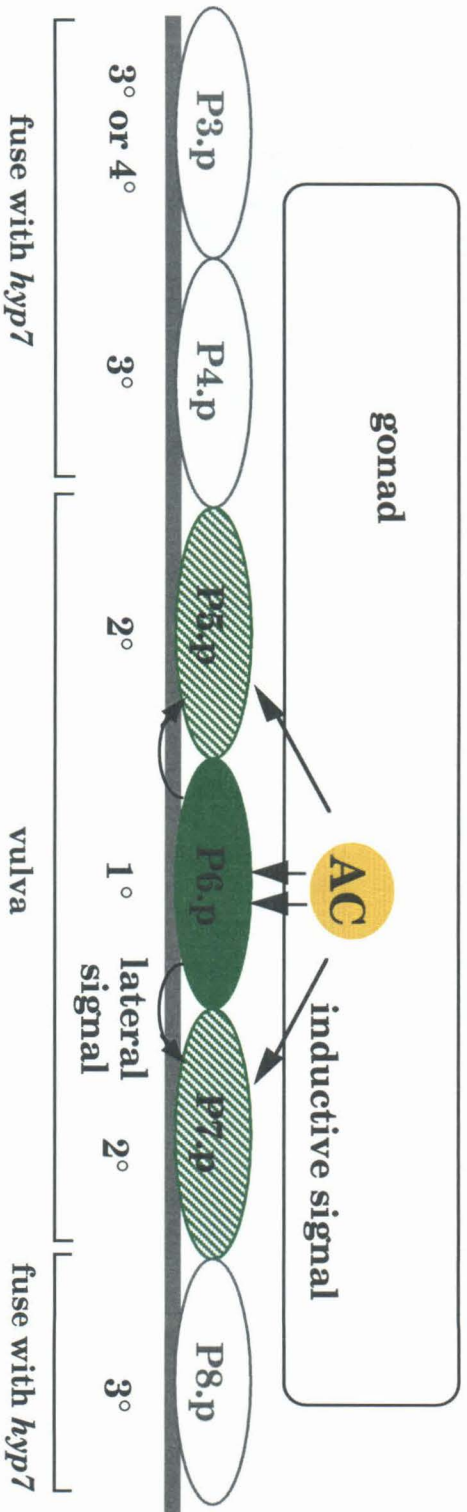
Figure 2. VPC lineages during wild-type development.

The axis at left is marked in hours after hatching. Each larval stage ends with a molt, including lethargus, when the animal is inactive and ceases pumping and locomotion (checked boxes), and ecdysis, when the old cuticle is shed and the animal resumes pumping and locomotion (short horizontal lines). VPC fates are characterized by the division pattern and the morphogenetic behavior of the VPC descendants. Horizontal lines indicate cell divisions and vertical lines represent individual cells. L, longitudinal division; underlining, strong adherence to the ventral cuticle. T, transverse division. N, division did not occur and nucleus compact. S, VPC daughters did not divide and fuse with the epidermis. In wild-type animals, P3.p could either fuse at late-L2, or divide once and fuse with the epidermis at mid-L3. A, B1, B2, C, D, E and F indicate seven types of vulval descendants.
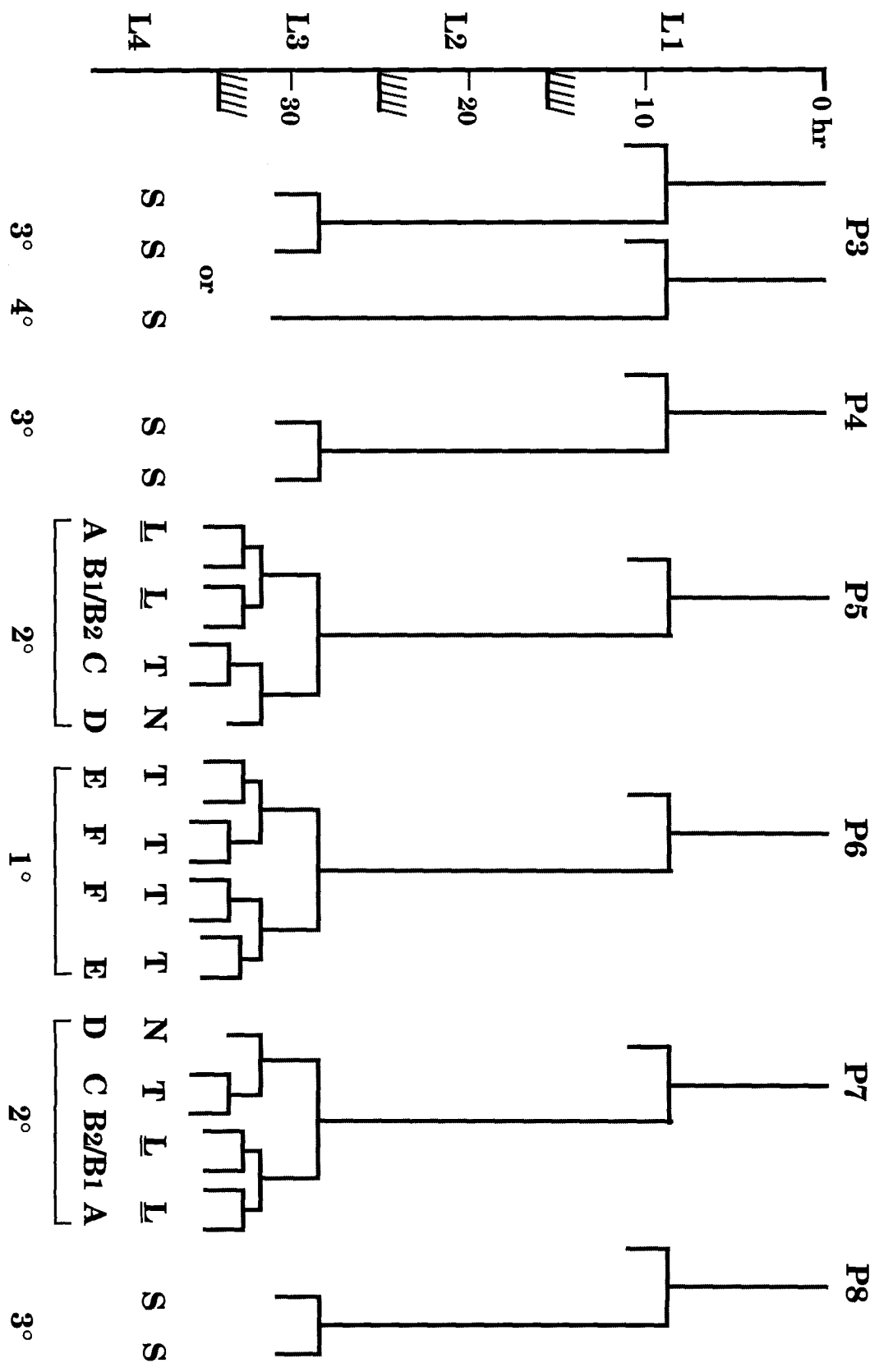
I-56

Figure 3. Spatial limitation of VPC competence.

The VPC multipotential group consists of the six central Pn.p cells. *lin-39* is expressed in P3.p-P8.p, while *mab-5* is expressed in posterior Pn.p cells including P7.p and P8.p. LIN-39 activity is required to specify P3.p-P8.p to be VPCs and promote their competence to respond to the inductive signal LIN-3. MAB-5 activity reduces the competence of P7.p and P8.p.
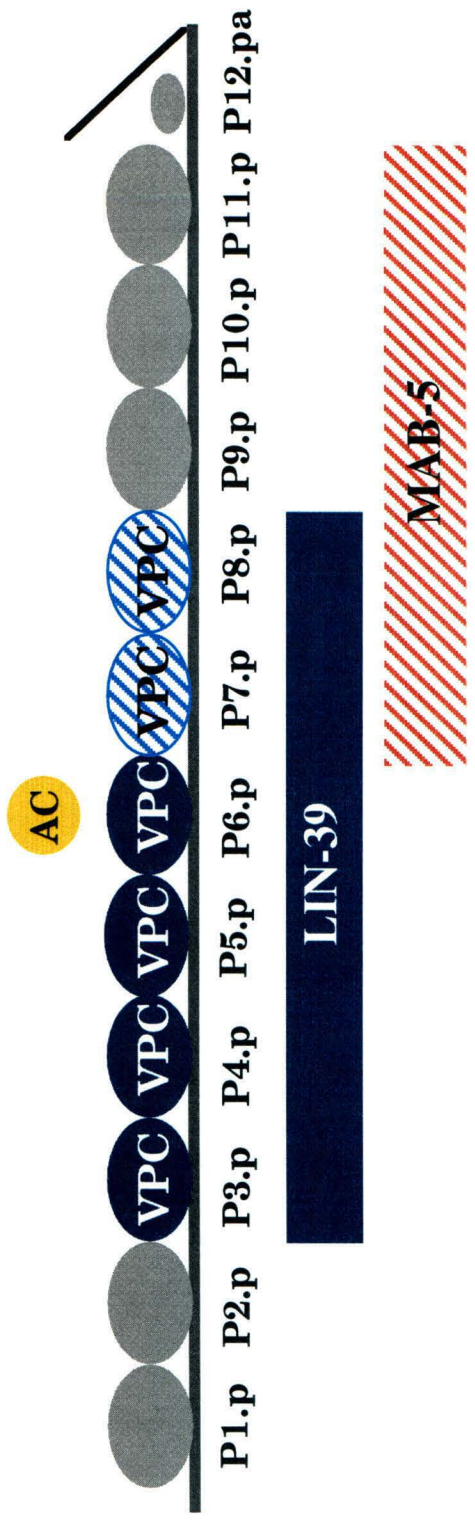
Figure 4. Temporal regulation of VPC competence and commitment.

The axis at left is marked in hours after hatching. Horizontal lines indicate cell divisions and vertical lines represent individual cells. The six VPCs are born during the L1 stage and divide approximately 20 hours later in the L3 stage. VPCs undergo S phase during the first hour of L3. VPCs mature during the late L2 stage and acquire a developmentally regulated competence to respond to inductive signal from late-L2 to L3 until they divide. Maintaining the competence of VPC daughters and prioritizing the VPC fates bias towards the 1° fate. In wild-type animals, P6.p receives the highest level of LIN-3 and is specified to be 1° before completion of S phase. The presumptive 1° VPC then laterally signals its neighbors to adopt the 2° fate after S phase.
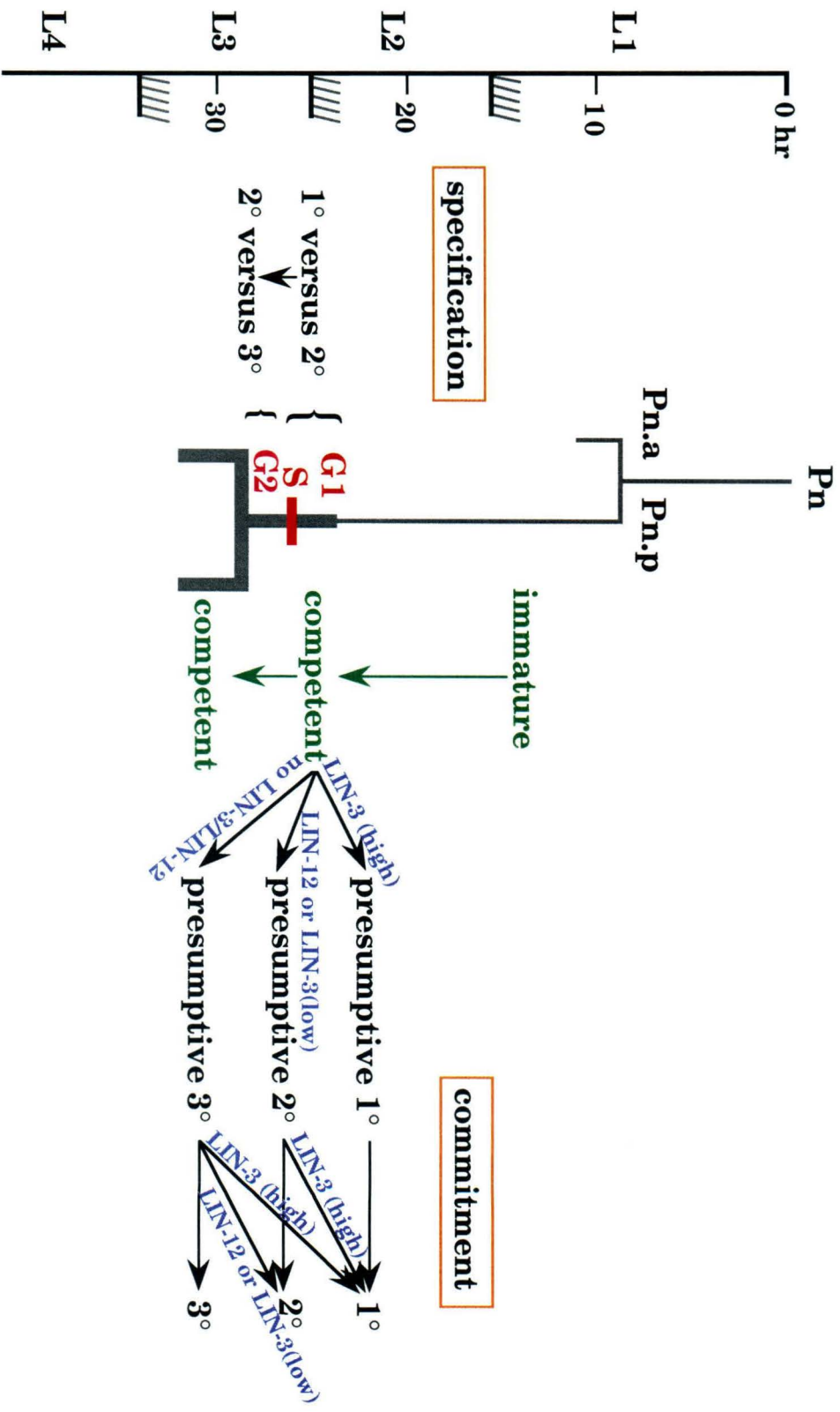
Figure 5. Models for hybrid and intermediate vulval lineages.

There are two possible explanations for the non-canonical lineages VPCs adopt when the inductive signaling pathway is perturbed. (A) According to the 'ratchet' model, VPCs move successively through a series of states depending on the length of time and the intensity of the inductive signal LIN-3. VPCs are able to switch from a lower state to a higher state, but not the reverse. VPCs can exit at any time to adopt different fates depending on their states and developmental history. (B) Competent VPC daughters might respond to inductive or lateral signals independently to generate half lineages of 3°, 2°, or 1°, leading to final lineages with mixed features.

A. The 'ratchet' model

LIN-3 ⟶ VPC state 0 ⟶ 3°

LIN-3 ⟶ VPC state 1 ⟶ hybrid (3°/2° or 3°/1°)

LIN-3 ⟶ VPC state 2 ⟶ 2°

LIN-3 ⟶ VPC state 3 ⟶ intermediate (2°/1°)

LIN-3 ⟶ VPC state 4 ⟶ 1°

B. Responding VPC daughters

hybrid (3°/2°)   hybrid (3°/1°)   intermediate (2°/1°)

LIN-3 or Lateral signal

e.g.   S L L   S T T   L L T T
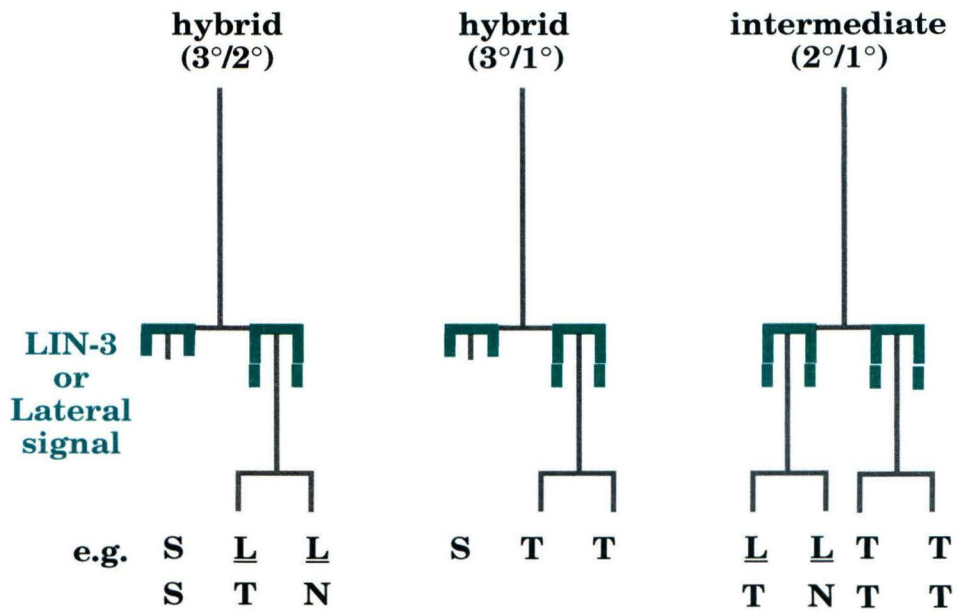   S T N   T N T T
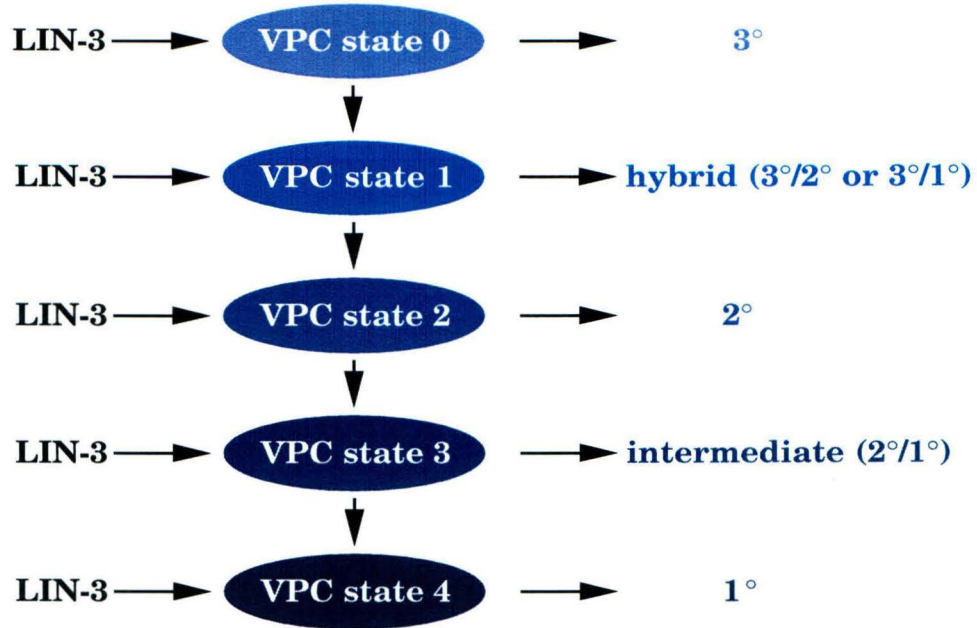
Figure 6. Negative regulation of RAS signaling.

(A) The RAS signaling output depends on both the ligand-independent and the ligand-dependent activities of LET-23. In all VPCs, genes in the synthetic multivulva pathway antagonize the basal activity of LET-23-mediated inductive pathway to prevent vulval induction when LIN-3 is absent. In P6.p, LIN-3 produced by the AC induces LET-23 to activate RAS signaling, while P3.p, P4.p and P8.p do not receive LIN-3 and adopt the non-vulval 3° fate. (B) LET-23 functions antagonistically in addition to activate the RAS pathway. LET-23 in P6.p sequesters LIN-3 and prevents the diffusion of LIN-3 molecules. Upon induction by LIN-3, LET-23 increases its expression level in P6.p, thereby limiting the amount of unbound LIN-3 molecules to reach distal VPCs.

A.

P6.p

P3.p, P4.p and P8.p

synMuv
genes

LET-23
basal activity

RAS

LIN-3

LET-23
induced activity

RAS

vulval fate

synMuv
genes

LET-23
basal activity

RAS

LET-23
induced activity

RAS

non-vulval fate

B.

3°

3°   LET-23

2°

1°   AC

2°

3°

LIN-3

Chapter 2

Competence and commitment of *Caenorhabditis elegans* vulval precursor cells

Minqin Wang and Paul W. Sternberg

(reprinted with permission)

Competence and Commitment of *Caenorhabditis elegans* Vulval Precursor Cells

Minqin Wang and Paul W. Sternberg[1]

Howard Hughes Medical Institute and Division of Biology, California Institute of Technology, Pasadena, California 91125

Multipotent *Caenorhabditis elegans* vulval precursor cells (VPCs) choose among three fates (1°, 2°, and 3°) in response to two intercellular signals: the EGF family growth factor LIN-3 induces 1° fates at high levels and 2° fates at low levels; and a signal via the receptor LIN-12 induces 2° fates. If the level of LIN-3 signal is reduced by a *lin-3* hypomorphic mutation, the daughters of the VPC closest to the anchor cell (AC), P6.p, are induced by the AC. By expressing LIN-3 as a function of time in LIN-3-deficient animals, we find that both VPCs and the daughters of VPCs are competent to respond to LIN-3, and VPC daughters lose competence after fusing with the hypodermis. We also demonstrate that the daughters of VPCs specified to be 2° can respond to LIN-3, indicating that 2° VPCs are not irreversibly committed. We propose that maintenance of VPC competence after the first cell cycle and the prioritization of the 1° fate help ensure that P6.p will become 1°. This mechanism of competence regulation might have been maintained from ancestral nematode species that used induction both before and after VPC division and serves to maximize the probability that a functional vulva is formed. © 1999 Academic Press

Key Words: induction; cell cycle; competence; EGF; pattern formation.

INTRODUCTION

While we have a reasonable understanding of how cells choose between two alternative developmental fates (Greenwald and Rubin, 1992; Horvitz and Herskowitz, 1992), the mechanisms by which a cell chooses appropriately among multiple fates remains unknown (reviewed by Gurdon, 1992; Morrison *et al.*, 1997; see also Dyson and Gurdon, 1998). For example, peripheral T lymphocytes choose among proliferation, death, or anergy (reviewed by Alberola-Ila *et al.*, 1997). CNS stem cells choose among differentiation as neurons, astrocytes, or oligodendrocytes (Johe *et al.*, 1996). Neural crest stem cells similarly choose among neuronal, glial, and smooth muscle fates in response to three peptide growth factors (Shah and Anderson, 1997). *Caenorhabditis elegans* vulval precursor cells (VPCs) also choose among three fates (Sternberg and Horvitz, 1986) and allow high-resolution study because their fates are invariant in an intact, wild-type animal (reviewed by Horvitz and Sternberg, 1991).

A separate, but as we shall see, related issue is how the competence of cells to respond to intercellular signals is

regulated. The restriction of the ability of precursor cells to respond only to correct cues by establishing windows of precursor cell competence complements strict control of when and where inductive signals are available. However, the mechanisms by which cells acquire, maintain, and lose such competence are not well understood (e.g., Slack, 1991; Gurdon, 1992).

C. elegans vulval development starts with six multipotent VPCs [P(3–8).p] (Sulston and Horvitz, 1977). Each VPC is competent to respond to the inductive signal from the somatic gonadal anchor cell (AC) and can adopt any of the three fates, 1°, 2°, or 3° (Sulston and White, 1980; Kimble, 1981; Sternberg and Horvitz, 1986; Thomas *et al.*, 1990). In wild-type hermaphrodites, the VPC nearest to the AC, P6.p, adopts the 1° fate, while the adjacent P5.p and P7.p adopt the 2° fate. The other three distal-most cells, P3.p, P4.p, and P8.p, adopt the nonvulval 3° fate. All VPCs divide once about 4 h after the molt from the L2 to L3 larval stage (L2 molt). The two daughters of VPCs that assume the 3° fate then fuse with the hyp7 epidermal syncytium. By contrast, daughters of VPCs that assume the 1° and 2° fates divide again about 2.5 h later and then a third time during the L3 molt to give rise to eight and seven progeny nuclei, respectively (Sulston and Horvitz, 1977; see Fig. 1).

[1] To whom correspondence should be addressed. Fax: (626) 568-8012. E-mail: pws@cco.caltech.edu.

The VPCs choose among three potential fates (1°, 2°, or 3°) in an invariant spatial pattern. Previous studies demonstrated that activation of distinct receptors correlates with each of the two induced fates. The inductive signal from the AC is the EGF-like growth factor LIN-3 (Hill and Sternberg, 1992; Katz et al., 1995) and acts via the receptor tyrosine kinase LET-23 (Aroian et al., 1990; Katz et al., 1996). A lateral signal between induced VPCs is mediated by LIN-12, a *Notch* homolog (Greenwald et al., 1983; Sternberg, 1988; Yochem et al., 1988; Sternberg and Horvitz, 1989; Koga and Ohshima, 1995; Simske and Kim, 1995). Strong LET-23 activation leads to 1° fates; LIN-12 activation leads to 2° fates (weak LET-23 activation also leads to 2° fates but whether this depends upon LIN-12 is still unclear). Current models of VPC fate patterning are based on these conclusions, along with the utilization of LIN-12-mediated lateral signaling to work in either an inductive or inhibitory mode. A sequential induction model posits that the inductive signal only induces P6.p to be 1°, which subsequently induces P5.p and P7.p to become 2° by lateral signaling mediated by LIN-12 (Koga and Ohshima, 1995; Simske and Kim, 1995; J. Liu and P. S., unpublished observations). A direct induction model posits that a graded inductive signal mediated by LET-23 induces and biases lateral signaling among VPCs, thus specifying both 1° and 2° fates in a dose-dependent manner (Sternberg and Horvitz, 1986; Katz et al., 1995). These models require that a presumptive 3° can become 1° or 2° by action of these receptors, but do not bear on when the VPCs commit to their fates and how the competence of VPCs to respond to signals is regulated. The hybrid lineages (1°/3°, see Fig. 1B) seen in various mutant backgrounds and experimentally manipulated animals (e.g., Sulston and Horvitz, 1981; Ferguson et al., 1987; Sternberg and Horvitz, 1986; Aroian and Sternberg, 1991; Katz et al., 1995) suggest that VPCs are not irreversibly committed to their fates. The heterochronic pathway affects both timing of acquisition of competence and cell cycle progression of VPCs (Euling and Ambros, 1996). HOM-C genes also influ-

ence the competence of VPCs (Clandinin et al., 1997; Maloof and Kenyon, 1998; Eisenmann et al., 1998).

Here we examine the commitment of VPCs to their fates and the window of VPC competence to respond to LIN-3.

MATERIALS AND METHODS

General Methods and Strains

C. elegans strains were handled at 20°C according to standard protocols (Brenner, 1974; Wood, 1988). The following alleles were used: for LGI, *ayIs4[egl-17::GFP; dpy-20(+)]*; LGII, *syIs12[hs-LIN-3EGF; dpy-20(+)]*; LGIII, *dpy-19(e1259)*, *unc-32(e189)*, *lin-12(n137)*, *lin-12(n676n909)*, *unc-69(e587)*; LGIV, *unc-24(e138)*, *let-59(s49)*, *unc-22(s7)*, *dpy-20(e1282)*, *lin-3(n378)*, *lin-3(n1059)*; LGX, *unc-3(e151)* (Brenner, 1974; Greenwald et al., 1983; Ferguson and Horvitz, 1985; Clark et al., 1988; Katz et al., 1995; Burdine et al., 1998).

The integrated transgenes *ayIs4* and *syIs12* carry *dpy-20(+)*. *ayIs4; syIs12; lin-3(n378) let-59 unc-22/unc-24 lin-3(n1059) dpy-20* animals were constructed by mating *ayIs4/+; syIs12/+; [lin-3(n378) let-59 unc-22 or unc-24 lin-3(n1059) dpy-20]/dpy-20* males to *ayIs4/+; syIs12/+; [lin-3(n378) let-59 unc-22 or unc-24 lin-3(n1059) dpy-20]/dpy-20* hermaphrodites. Vulvaless hermaphrodite cross-progeny were selected, placed on individual plates, and allowed to self-fertilize. Animals that did not segregate Dpy were kept, and their progeny were examined individually under Nomarski optics after heat shock for the presence of *ayIs4* and *syIs12*. These animals were therefore of genotype *ayIs4/(ayIs4* or +); *syIs12/(syIs12* or +); *lin-3(n378) let-59 unc-22/unc-24 lin-3(n1059) dpy-20*. Animals that contained *ayIs4* and *syIs12* in all their progeny were identified.

Heat Shock and Hydroxyurea Treatment of Transgenic Animals

Animals were mounted on agar pads, examined using Nomarski optics to confirm their stages (Sulston and Horvitz, 1977; Kimble and Hirsh, 1979), and then heat shocked. All heat-shock pulses were performed at 31.5°C for 20 min (except for the second half of


FIG. 1. Schematic outline of the response of VPCs when LIN-3 is expressed at different times. (A) Presumptive 3° VPCs can respond to LIN-3 and become 1°. (B) Newly born presumptive 3° VPC daughters can respond to LIN-3 and be induced to adopt the 1° or the hybrid fates. (C) Presumptive 2° VPCs can respond to LIN-3 and become 1°. (D) Presumptive 2° VPC daughters can respond to LIN-3 and be induced to adopt the 1° or the intermediate fates. L, longitudinal division; underlining, strong adherence to ventral cuticle. T, transverse division. N, division did not occur, and nucleus is compact. S, VPC daughters did not divide and fused with the epidermis. Green indicates expression of *egl-17::GFP* at L3 molt, a marker for 1° (Burdine et al., 1998).

FIG. 2. The AC is required after VPCs divide if VPCs did not receive sufficient signal. The horizontal axis shows the genetic background we used. Solid bar, intact animals; hatched bar, the AC was ablated immediately after P6.p had divided. (A) The strains used were *egl-17::GFP* and *egl-17::GFP; lin-3(e1417)*. The vertical axis indicates the percentage of P6.p cells that adopted the vulval fate. In wild type, 100% of the P6.p cells in intact animals adopted the vulval fates (n = many). This percentage remains unchanged when the AC was ablated immediately after P6.p had divided (n = 25). In a *lin-3(e1417)* background, 42% of the P6.p cells in intact animals were induced (n = 74). However, when the AC was ablated immediately after P6.p had divided, only 8% of the P6.p cells adopted the vulval fates (n = 32). (B) The strains used were *egl-17::GFP* and *egl-17::GFP; lin-3(sy91)*. The vertical axis indicates the percentage of P5.p and P7.p cells that adopted the vulval fate. In wild type, 100% of the P5.p and P7.p cells in intact animals adopted the vulval fates (n = many). This percentage remains unchanged when the AC was ablated immediately after P6.p had divided (n = 50). In an *lin-3(sy91)* background, 30% of the P5.p and P7.p cells in intact animals were induced (n = 130). However, when the AC was ablated immediately after P6.p had divided, only 7% of the P5.p and P7.p cells adopted the vulval fates (n = 66).

A.

B.

C.

D.

1

A.

B.

2   wild-type   *lin-3 (e1417)*
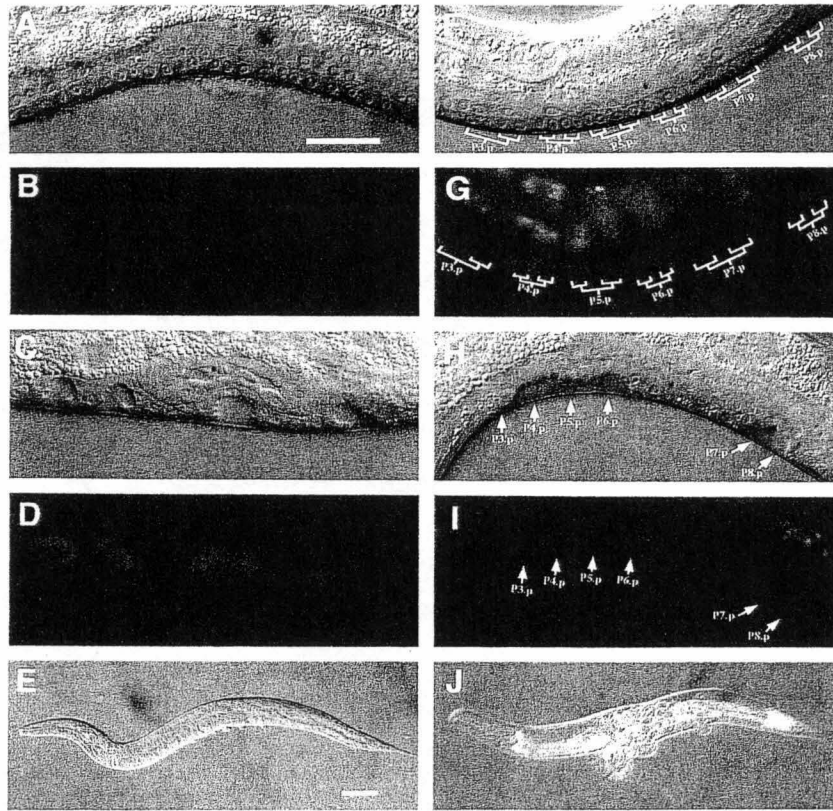
wild-type   *lin-3 (sy91)*
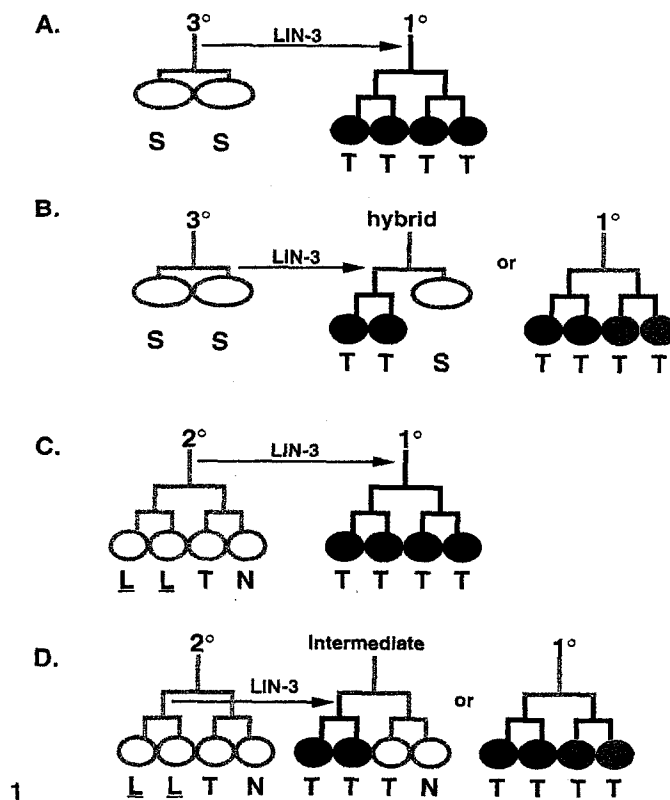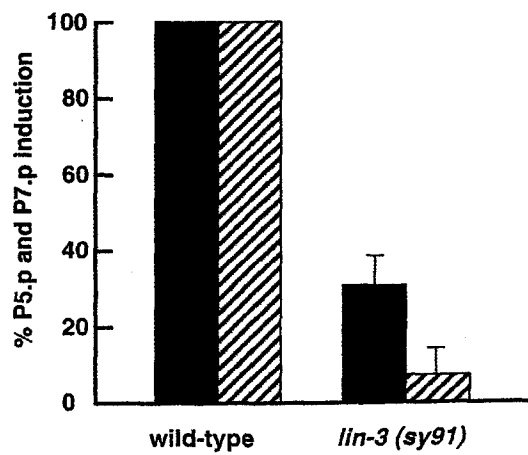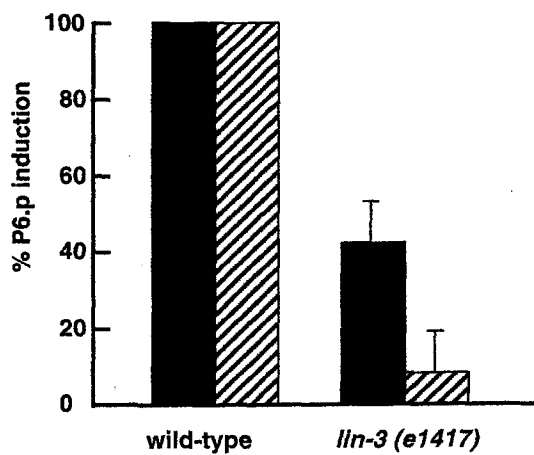
FIG. 3. The fate of VPCs in *egl-17::GFP; hs-LIN-3; lin-12(gf); lin-3(lf)* animals. Displays animals from Table 2. In all panels, ventral is down, anterior is to the left. In A–E, an animal without heat shock treatment; in F–J, an animal heat shocked at 31.5°C for 20 min after all its VPCs had divided. (A and B) Nomarski and fluorescence images of VPC granddaughters during L3 lethargus. None of the VPC granddaughters was expressing *egl-17::GFP*. (C and D) Nomarski and fluorescence images of vulval invagination of the same animal at mid-L4. For each VPC, some, but not all of its descendants were expressing *egl-17::GFP* strongly, showing that it adopted the 2° fate. (E) The same animal at adult stage. Small protrusions on the ventral side are the typical phenotype of 2° VPCs when they develop into adult stage (Greenwald *et al.*, 1983). (F, G) Nomarski and fluorescence images of VPC granddaughters during L3 lethargus. All descendants of P4.p, P5.p, P6.p (2/4 pattern), and P8.p (4/4 pattern) were expressing *egl-17::GFP*. (H, I) Nomarski and fluorescence images of vulval invagination of the same animal at mid-L4. No *egl-17::GFP* expression was detectable in any descendants of P4.p, P5.p, and P8.p, but the expression could be seen in descendants of P6.p and P7.p. Therefore, P4.p, P5.p, and P8.p of this animal matched all features of the 1° fate in terms of the *egl-17::GFP* expression pattern (see Materials and Methods). P3.p generated the lineage [S ss], and all three progeny were nonvulval epidermis. (J) Same animal at adult stage. Ruptured or large ventral protrusions imply the 1° fate adopted by some of the VPCs. The scale bars are 20 μm in A–D and F–I and 100 μm in E and J.

Table 1, 33°C for 30 min was used). Animals were placed on prewarmed plates of desired temperature, sealed with Parafilm, and then floated in a covered water bath of the same temperature. After heat shock, animals were transferred immediately to plates kept at 20°C until late L3 stage when they were scored for VPC fates. In many cases, the animals were replated and observed again during L4 stage.

Newly molted L3 *ayIs4; syIs12; lin-3(lf)* animals were examined using Nomarski optics and placed on plates containing 40 mM hydroxyurea and a small spot of *Escherichia coli* (Euling and Ambros, 1996) for 3 or 6 h. They then were mounted on agar pads and examined using Nomarski optics again to confirm that VPCs had not divided or started to divide during the period. These animals were put back on hydroxyurea plates and heat shocked at 31.5°C for 20 min prior to transfer to normal plates. Animals whose VPCs had divided or were starting to divide were discarded. Some of the 3-h hydroxyurea (HU)-treated animals were transferred to normal plates after treatment and cultured for 3 h. They then were

Wang and Sternberg

mounted and examined using Nomarski optics for a third time. Such animals were placed back on normal plates and heat shocked at 31.5°C for 20 min.

Cell Ablation and VPC Fate Assignment

AC ablation was performed with a laser microbeam (Sulston and White, 1980) when P6.p just finished its first division. Success of AC ablation was confirmed at the VPC four-cell stage.

Both VPC lineages and expression patterns of *egl-17::GFP* were followed after the four-cell stage using Nomarski optics and a Zeiss Axioplan microscope with a 200-W HBO UV source, using a Chroma High Q GFP LP filter set (450 nm excitation/505 nm emission). Photographs were taken with Fuji Provia ASA 400 film. VPC fates were assigned as the vulval fate or the nonvulval fate in Table 1, Fig. 2, and Fig. 5; the 1° or the non-1° fate was assigned in Table 2 and Fig. 3.

In Table 1, Fig. 2, and Fig. 5, we scored VPCs as adopting the vulval fate if they underwent at least two rounds of cell division and remained unfused based on observation under Nomarski optics. In Table 2 and Fig. 3, VPCs with 1° characteristic lineages at L3 lethargus, forming a symmetric invagination at mid-L4 stage without adhering to the ventral cuticle (Katz *et al.*, 1995), were scored as adopting the 1° fate for one set of experiments. For the other set of experiments, the expression *egl-17::GFP* was scored at both late L3 and mid-L4 stage. We scored VPCs as adopting the 1° fate only if GFP was expressed in all four descendants at L3 and faded completely at mid-L4.

RESULTS

AC Is Required after the First VPC Division if LIN-3 Signaling Is Reduced

Vulval induction occurs around the late L2 to early L3 stage (Kimble, 1981; Sternberg and Horvitz, 1986). Previous work showed that VPCs are able to adopt their correct fates if the AC is ablated just before their division (Kimble, 1981). However, it is unknown how long the LIN-3 protein made by the AC before the ablation will persist (e.g., in the extracellular matrix) after AC ablation, and thus the question remains whether VPC daughters need LIN-3 signaling provided by the AC to ensure a wild-type vulval pattern. To help answer this question, we examined whether the AC was required for vulval induction after VPCs had divided if there was a lower level of LIN-3 signal made by the AC. We used two *lin-3* hypomorphic alleles *e1417* and *sy91* to reduce the level of LIN-3 signaling (Liu, *et al.*, 1999). *e1417* does not have any mutation in either the coding region or the 5'-untranslated region of *lin-3*. The mutation is probably located in a noncoding region, such as the promoter. *sy91* contains a transposon insertion at an intron of *lin-3* that presumably decreases the level of *lin-3* mRNA (Hill and Sternberg, 1992). In intact *lin-3(e1417)* mutant animals, 42% of the P6.p cells were induced ($n = 74$), and none of the P5.p and P7.p cells was induced ($n = 148$). In intact *lin-3(sy91)* mutant animals, 45% of the P6.p cells were induced ($n = 65$), and 30% of the P5.p and P7.p cells were induced ($n = 130$).

We repeated the AC ablation experiment of Kimble (1981) and found that in wild-type animals 100% of the P6.p, P5.p, and P7.p cells adopted vulval fates if the AC was ablated after P6.p had divided ($n = 25$ animals). By contrast, when the AC was ablated immediately after P6.p had divided in a *lin-3(e1417)* background, the percentage of P6.p cells that were induced dropped dramatically from 42 to only 8% ($n = 32$, $P < 0.001$, Fig. 2A). In addition, when the AC was ablated immediately after P6.p had divided in a *lin-3(sy91)* background, the induction of the P5.p and P7.p cells dropped from 30 to 7% ($n = 66$, $P < 0.001$, Fig. 2B), and the induction of P6.p cells dropped from 45 to 27% ($n = 33$, $P = 0.12$). The percentage of P6.p cells that adopt the vulval fates clearly reflects the result of inductive signaling. Since specification of 2°, at least partially, involves induction by a 1° neighbor (Koga and Ohshima, 1995; Simske and Kim, 1995), the ability of P5.p and P7.p to become 2° is a rough measure of the extent to which P6.p laterally signals, which roughly parallels specification as 1° and other measures of induction of P6.p. Therefore, the results of these experiments demonstrate that AC can be required beyond the first VPC cell cycle.

Presumptive 3° VPC Daughters Are Competent to Respond to LIN-3 until They Differentiate as hyp7

The above experiments revealed that the daughters of VPCs are competent to respond to LIN-3. To test precisely how late the window of VPC competence extends, we induced LIN-3 expression at different times in a *lin-3* loss-of-function background, in which the inductive signal is missing and VPCs adopt the 3° fate (Figs. 1A and 1B). If the time of LIN-3 expression was before the end of VPC competence, VPCs would adopt vulval fates. We used a construct expressing the EGF domain of LIN-3 under the transcriptional control of an *hsp16* promoter (*syIs12*; henceforth *hs-LIN-3*; Hill and Sternberg, 1992; Katz *et al.*, 1995). To lower *lin-3* activity without loss of viability due to complete loss of *lin-3* activity, we used a heterozygous strain, *lin-3(n378/n1059)* [henceforth *lin-3(lf)*]. Without heat shock, all VPCs of *egl-17::GFP* (see below); *hs-LIN-3; lin-3(lf)* animals adopted the 3° fate (Table 1): they divided only once and their progeny fused with the hyp7 epidermis.

When the animals were mildly heat shocked (31.5°C for 20 min) before the first VPC division (Fig. 1A), from L2 lethargus (a period during which pharyngeal pumping ceases between L2 and L3) to mid-L3, the percentage of VPCs adopting vulval fates dropped gradually from 99 to 53% (Table 1). If the animals were mildly heat shocked after VPCs had divided once, all VPCs adopted the 3° fate ($n = 74$, Table 1). However, if the animals were strongly heat shocked (33°C for 20 min) after VPCs divided once, 2% ($n = 152$) of the presumptive 3° VPC daughters responded to LIN-3 by adopting the vulval fates (Table 1). To further examine whether VPC daughters can respond to LIN-3, we observed animals that were mildly heat shocked when some VPCs had divided while others had not. We found that

TABLE 1

Response of VPCs to *hs-LIN-3* at Different Times

Time of heat shock[a]	31.5°C for 20 min		33°C for 30 min	
	%[b]	n[c]	%[b]	n[c]
No heat shock	0	114	0	114
L2 lethargus (<0 h)	99	47	100	22
Early one-cell[d] (0–2 h)	87	77	92	26
Late one-cell[e] (2–4 h)	53	110	59	67
Early two-cell[f] (>4 h)	0	74	2	152

Note. egl-17::GFP; hs-LIN-3; lin-3(lf) animals were staged using Nomarski optics and heat shocked at 31.5°C for 20 min or at 33°C for 30 min.

[a] Stages of animals when heat shock began. Times referring to hours after L2 lethargus are in parentheses.

[b] A VPC was considered as adopting a vulval fate if it divided more than one round and remained unfused.

[c] Number of VPCs scored.

[d] Dorsal uterine cells had not divided.

[e] Dorsal uterine cells were dividing or had divided once. In some cases, the distal VPCs (P3.p, P4.p, or P8.p) started dividing, while the VPCs scored had not.

[f] The VPCs scored were dividing or had just divided.

very late stage VPCs could be induced to adopt vulval fates by heat shock starting at the onset of their mitosis (Fig. 1B and Table 1), while other divided VPCs in the same animal were not induced. In particular, in animals in which all VPCs but P6.p had divided, 23 of 42 (55%) P6.p daughters had vulval fates when the animals were heat shocked at the onset of P6.p mitosis. Among these 21 P6.p lineages we scored, both daughters of 7 were induced, only one daughter of 9 was induced (hybrid; also see Discussion), and neither daughter of 5 was induced.

Therefore, both VPCs and VPC daughters are competent to respond to LIN-3. Since presumptive 3° VPC daughters fuse with hyp7 epidermis shortly after they are born, the time when they lose competence is about the same time when they exit from the cell cycle and fuse with hyp7. VPC daughters are probably competent to respond to LIN-3 for a short period of time at the beginning of their cell cycle before fusion.

Wild-Type Presumptive 2° VPC Daughters Can Respond to LIN-3

We then tested whether extending the cell cycle of VPC daughters would make VPC daughters remain competent for a longer time. In wild-type hermaphrodites, P5.p and P7.p always adopt the 2° fates; therefore, their daughters always go through a full cell cycle without fusing with hyp7. By overexpressing LIN-3 in a wild-type background, we should be able to examine the competence of P5.p and P7.p daughters. In this same experiment, we should also be able to test whether the daughters of VPCs specified to be 2°

can respond to LIN-3 and be redirected to be 1°. If 2° VPCs are committed to their fates during their first cell cycle, 2° VPC daughters should not be affected by induction of LIN-3 expression after VPC division. We used *egl-17::GFP* as a marker for VPC fates, since wild-type 1° and 2° cells have distinct *egl-17::GFP* expression patterns (Burdine *et al.*, 1998). These patterns have been shown to correspond to different vulval fates by lineage analysis in various mutant backgrounds and ablation experiments (Burdine *et al.*, 1998; M. Wang and P. W. Sternberg, unpublished data). *egl-17::GFP* is expressed in 1° granddaughters at L3 and then fades completely in 1° descendants at mid-L4. In contrast, 2° granddaughters do not express *egl-17::GFP* at L3, but half of the 2° descendants (N and T) express GFP strongly at mid-L4.

TABLE 2

Response of VPCs to *hs-LIN-3* at Different Times in a *lin-12(gf)* Background

	VPCs induced to adopt 1° fates			
	Scored by lineage and morphogenesis		Scored by expression of egl-17::GFP at L3 and L4	
Time of heat shock[a]	%[b]	n[c]	%[b]	n[c]
No heat shock	0	66	0	86
Early/mid one-cell[d] (0–2 h)	36	28	41	22
Late one-cell[e] (3 h)	52	23	37	30
One-cell dividing[f] (4 h)	28	68	31	26
Early/mid two-cell[g] (5 h)	18	88	15	137
Late two-cell[h] (5.5 h)	7	15	0	22
Two-cell dividing and later[i] (>6 h)	0	46	0	31

Note. egl-17::GFP; hs-LIN-3; lin-12(gf); lin-3(lf) animals were staged using Nomarski optics and heat shocked at 31.5°C for 20 min.

[a] Stages of animals when heat shock began. Times referring to hours after L2 lethargus are in parentheses.

[b] We scored a VPC as 1°, either according to its lineages during L3 lethargus and morphogenesis at mid-L4 or according to the expression pattern of *egl-17::GFP* at both L3 lethargus and mid-L4 (see text). We scored the patterns of *egl-17::GFP* expression at L3 lethargus as 1°, if all four descendants of a VPC expressed GFP; however, a 2/4 pattern was observed instead of a 4/4 pattern (see text).

[c] Number of VPCs scored.

[d] Dorsal uterine cells had not divided or were still dividing.

[e] Other VPCs in the same animal were dividing or had divided to make two daughter cells at that time, while the VPCs scored had not.

[f] The VPCs scored were dividing to make two daughter cells.

[g] Dorsal uterine cells had not divided for a second time.

[h] Other VPC daughters in the same animal were dividing or had divided, while the VPC daughters scored had not.

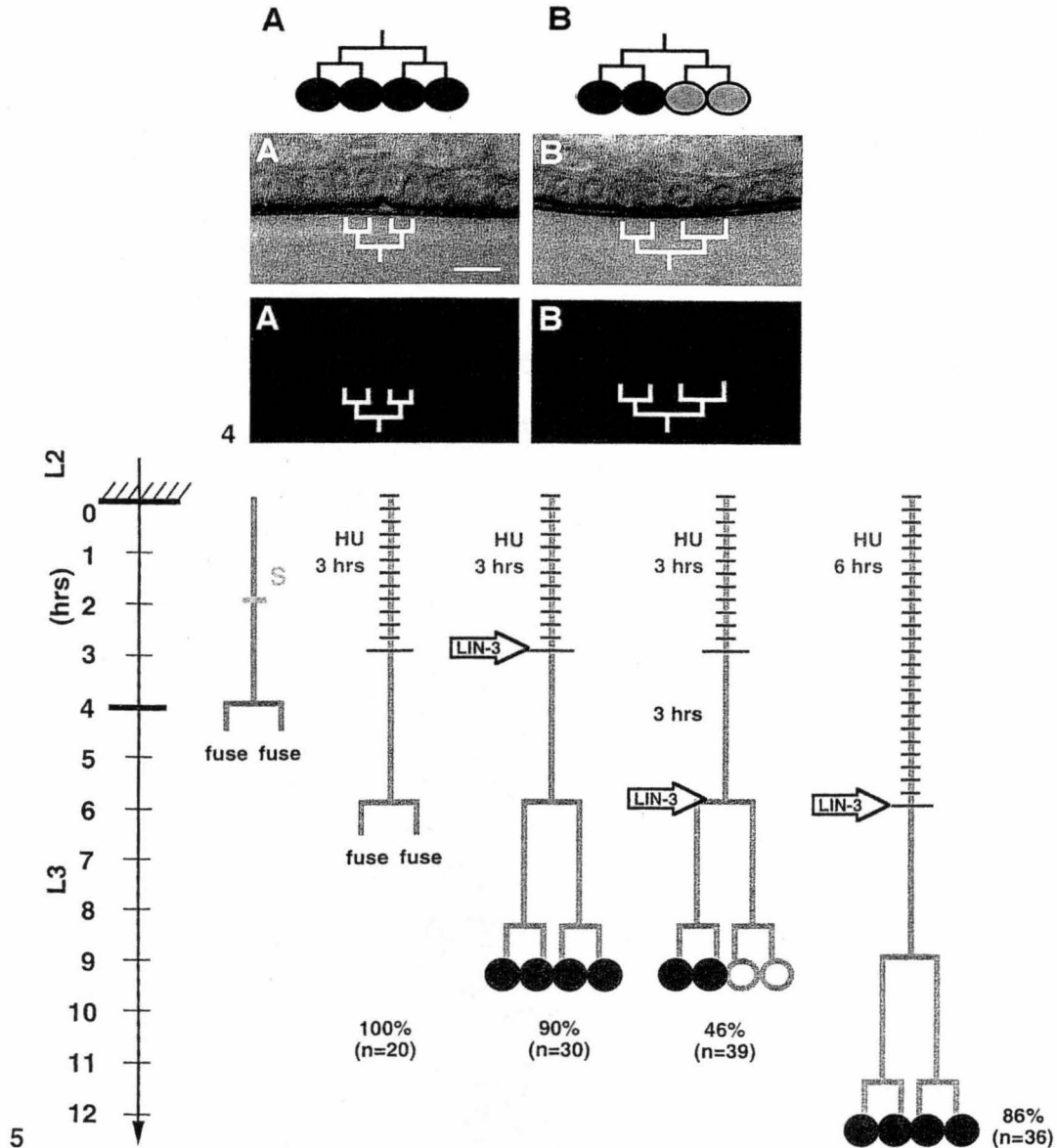[i] The VPC daughters scored were dividing or had divided.

FIG. 4. The 4/4 and 2/4 patterns of *egl-17::GFP* expression. Animals were photographed during L3 lethargus. In all panels, ventral is down, anterior is to the left. (A) The 4/4 pattern. All four granddaughters from one VPC were expressing the same level of *egl-17::GFP*, which is indistinguishable from the wild-type pattern. (B) The 2/4 pattern. The expression level of *egl-17::GFP* in two granddaughters derived from the same mother appeared the same within the two sisters, but different from that in their cousins. The scale bar is 5 μm.

FIG. 5. The timing mechanism of VPC competence measures cell cycles instead of real time. The axis at left is marked in hours after molt from L2 to L3. Arrows indicate the time when heat shock was performed to induce LIN-3 expression. The yellow bar indicates the estimated end of S phase in wild type based on Euling and Ambros (1996) and our results. Red bars indicate HU treatments. Green indicates expression of *egl-17::GFP* at L3 molt. The numbers are the percentages of VPCs that were induced to adopt the vulval fate. *n* is the number of VPCs scored. The strain used was *egl-17::GFP; hs-LIN-3; lin-3(lf)*. Without heat shock, HU alone does not induce VPCs to adopt vulval fates. The response of 6-h-old VPCs in S (take newly molted L3 as 0 h) resembled that of 3-h-old VPCs in S, but not that of 6-h-old VPCs in M. Both 3-h- and 6-h-old VPCs in S provided with heat shock LIN-3 displayed 4/4 patterns of *egl-17::GFP* expression suggesting that they responded as VPCs. Six-hour-old VPCs in M displayed 2/4 patterns indicating that they responded as VPC daughters.
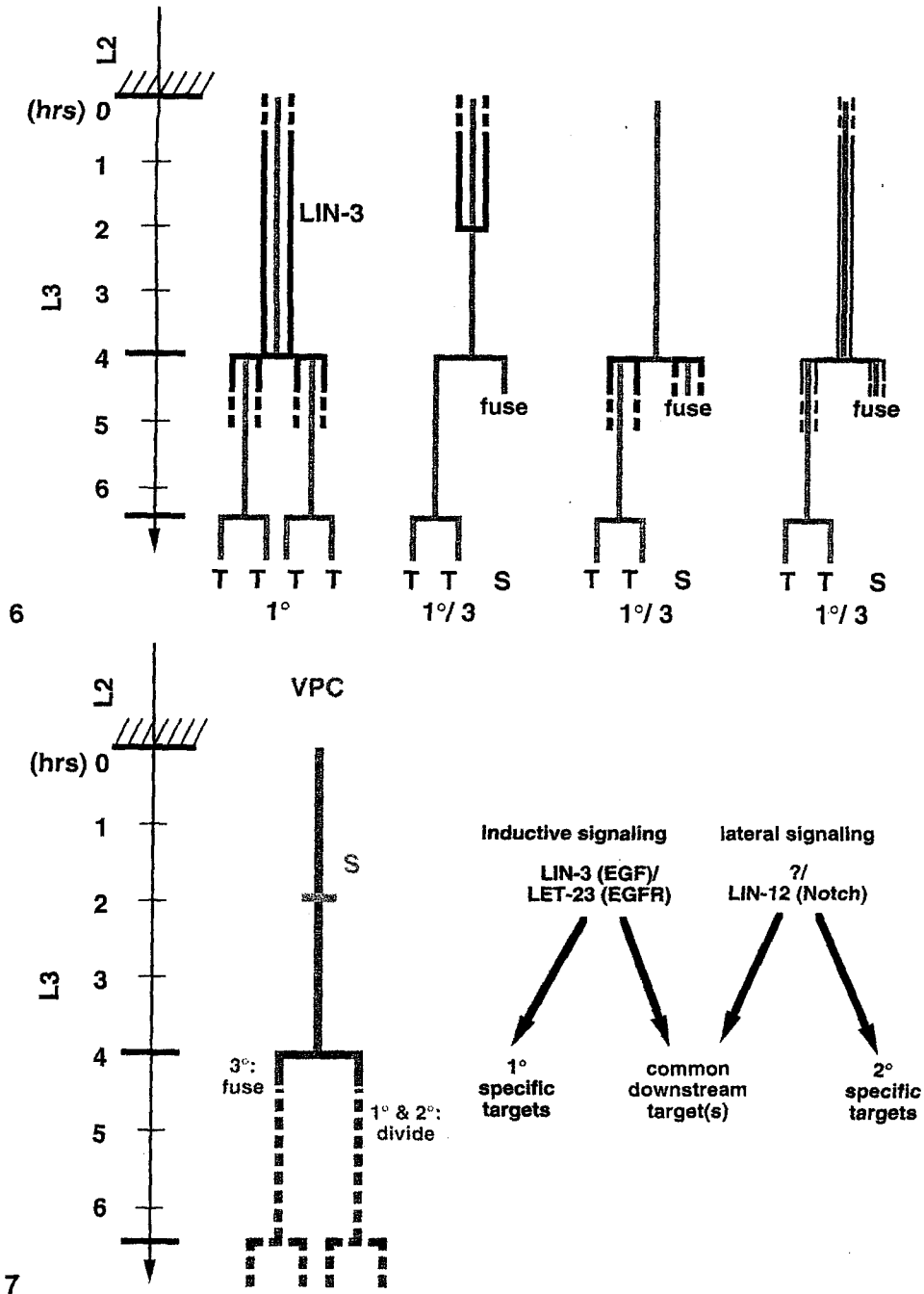
FIG. 6. Two ways to generate hybrid lineages. The axis at left is marked in hours after molt from L2 to L3. Green boxes indicate times when VPCs are exposed to LIN-3. The width of the green boxes indicates the level of LIN-3 signaling. 1°/3° hybrid lineages can be caused by truncation of LIN-3 signaling, too late LIN-3 expression, and/or too low a level of LIN-3 signaling.

FIG. 7. Hypothesis for cell cycle regulation of VPC fate specification. Both VPCs and VPC daughters are competent to respond to the inductive signal LIN-3. Maintaining competence to respond to LIN-3 to VPC daughters maximizes the probability that at least one VPC will be induced to be 1°. Specification to be 1° overcomes a prior specification to be 2°, while specification to be 1° cannot be reversed. 1° and 2° cells at first share a common pathway, thereby maintaining the ability to respond to further LIN-3 signaling. These two signaling pathways might act on the common downstream target(s) that determine the sensitivity of VPCs to LIN-3.

19

Without heat shock, *lin-3(+)* animals bearing *egl-17::GFP* and *hs-LIN-3* displayed wild-type vulval induction: P5.p and P7.p always adopted the 2° fate and never expressed *egl-17::GFP* at L3. When these animals were heat shocked after the VPCs had divided (Fig. 1D), in all 15 cases examined, the distal daughters of P5.p and P7.p were induced to express *egl-17::GFP* at the L3 stage. (Since in every case but one only distal daughters expressed *egl-17::GFP*, many of these P5.p and P7.p cells did not adopt bona fide 1° fates; also see below.) Proximal 2° VPC daughters directly adjacent to the daughters of P6.p (already 1°) expressed LIN-12 (Levitan and Greenwald, 1998) and were probably inhibited to respond to LIN-3 by lateral signaling. In contrast to the effects of LIN-3 induction on presumptive 2° VPC daughters, heat shock after the division of presumptive 3° VPCs had little if any effect (see above). Since the cell cycle of 3° VPC daughters is very short, one possibility is that 2° VPC daughters maintain their competence for a longer time by extending their cell cycle.

Presumptive 2° VPC Daughters with Activated LIN-12 Can Respond to LIN-3

To further test the competence of presumptive 2° VPC daughters and avoid the complication of having 1° neighbors present, we tested whether activated LIN-12 can prolong VPC daughters' competence. During vulval induction, *lin-12* is required for 2° fate specification (Greenwald *et al.*, 1983). In a *lin-12(gf)* background, all VPCs adopt the 2° fate even if LIN-3 is not available, but can be induced to adopt a 1° fate by LIN-3 provided by the anchor cell (Sternberg and Horvitz, 1989; Greenwald and Seydoux, 1990). Indeed, without heat shock, all VPCs of *egl-17::GFP; hs-LIN-3; lin-12(gf); lin-3(lf)* animals became 2° (Table 2 and Fig. 3A–3E). In this activated LIN-12 background, we induced LIN-3 expression at different times to determine the latest time when expression of LIN-3 induces VPCs to a 1° fate.

Heat shock before VPCs divide induced almost half of them to become 1° (Fig. 1C and Table 2). In contrast to nonresponsive daughters of presumptive 3° VPCs, if the animals were heat shocked after VPC division (Table 1), substantial proportions (15 and 18%, in different experiments) of *lin-12(gf)* VPC daughters responded to LIN-3 (Table 2, Fig. 1D, and Fig. 2). The adoption of the 1° fate by these presumptive 2° cells was supported by three lines of evidence. First, we observed lineages with 1° characteristics and nonadherence to the ventral cuticle at L3 lethargus, as well as the symmetric morphology of the vulval invagination at mid-L4 (Katz *et al.*, 1995, Fig. 3H and Table 2). Second, these cells expressed *egl-17::GFP* in a pattern similar to that seen in wild-type 1° cells (Burdine *et al.*, 1998; Fig. 1C, Figs. 3F–3I, and Table 2). Third, a significant percentage of the vulvae made by these VPCs ruptured during adulthood, a phenotype associated with adjacent 1° cells (Fig. 3J). If the animals were heat shocked when VPC daughters had started their division, no VPCs adopted the 1° fate (n = 77, Table 2). Since heat shock after the division of

presumptive 3° VPCs had little effect (see above), we thus conclude that the duration of VPC competence is extended well beyond the VPC division if LIN-12 is activated.

VPC Daughters Can Respond to LIN-3 Independently

In our experiments, we examined the percentage of competent VPCs that responded to LIN-3, as well as the patterns of *egl-17::GFP* expression, which we found to depend on the experimental perturbation. When we heat shocked the animals before the first VPC division in either the *lin-12(+)* or *lin-12(gf)* background, all four VPC granddaughters expressed GFP at the same level during L3 lethargus, as do wild-type 1° cells (Fig. 4A). We designate the pattern as 4/4. We interpret this pattern to mean that the VPCs became committed to the 1° fate and all of their granddaughters inherited this decision. When we heat shocked the animals at the onset of the first VPC division in a *lin-12(+)* or *lin-12(gf)* background, or after the first VPC division in a *lin-12(gf)* background, the expression levels in two granddaughters derived from the same VPC daughter appeared to be the same, but distinct from those in their cousins (Fig. 4B and Fig. 3G). We designate it the 2/4 pattern. This pattern suggests that these VPCs were not committed to the 1° fate, and their daughters responded to LIN-3 and were specified separately. The existence of the 2/4 pattern suggests that the daughters of VPCs can respond to LIN-3 independently.

Timing of VPC Competence Is Coupled to the Cell Cycle

To test whether the timing mechanism of VPC competence regulation measures cell cycles or real time, we used HU to reversibly block VPCs at S phase (Euling and Ambros, 1996) for different lengths of time and examined their competence by inducing LIN-3 expression after the block. If VPC cell cycle determines competence, then, no matter how long they have been blocked, VPCs would not be expected to differ significantly in competence. If real time is measured, chronologically older VPCs should be less competent to respond to LIN-3, regardless of their cell cycle phase.

Since HU is known to induce the expression of many stress genes, as a control we tested the effect of HU on *hs-LIN-3* expression and consequently vulval induction. Newly molted L3 *egl-17::GFP; hs-LIN-3; lin-3(lf)* animals were placed in HU for 3 h and then scored for vulval induction. All VPCs adopted the 3° fate (n = 20), indicating that without heat shock HU alone does not induce VPCs to adopt vulval fates (Fig. 5).

We analyzed VPCs in the S phase in an *egl-17::GFP; hs-LIN-3; lin-3(lf)* background (Fig. 5). In this experiment, VPCs would enter S phase and then exit S phase in the absence of inductive signal and HU. However, they were blocked at S phase by HU and then challenged with LIN-3

during the block or some time after the block was released. We used newly molted L3 animals and considered their VPCs as 0 h. The chronological age of the VPCs was counted by summing the time that the animals grew in HU as well as the time they grew without HU. We arrested animals with 0-h VPCs in HU for 3 or 6 h to keep VPCs at S phase (Euling and Ambros, 1996), and we refer to these cells as 3- or 6-h-old VPCs in S. We released animals with 3-h-old VPCs in S from HU for 3 h and found that these 6-h-old VPCs were close to the onset of mitosis ($n = 7$ animals). We thus refer to these cells as 6-h-old VPCs in M for simplicity.

Eighty-six percent of 6-h-old HU-arrested VPCs in S ($n = 36$) were competent to respond to LIN-3 and displayed 4/4 patterns of *egl-17::GFP* expression when induced, resembling the response of 3-h-old VPCs in S (90%, $n = 30$, $P > 0.7$, using Fisher's exact test; Fig. 5). However, only 46% of 6-h-old VPCs in M ($n = 39$) responded, and they displayed 2/4 patterns when expressing *egl-17::GFP* (Fig. 5, $P < 0.001$). Therefore, although the same age in real time, 6-h-old VPCs in M were less competent to respond to LIN-3 than 6-h-old VPCs in S phase. Moreover, the 2/4 pattern displayed by 6-h-old VPCs in M by inductive signal was qualitatively different from 6-h VPCs in S and took place after their division. Therefore, these experiments demonstrate that VPC competence depends on the state of the VPC cell cycle and not on the chronological age of the responding cell.

DISCUSSION

We have analyzed temporal aspects of vulval induction in *C. elegans* to explore how VPCs respond appropriately to the inductive signaling process. We show that VPC daughters require the inductive signal LIN-3 to adopt the vulval fates if LIN-3 signaling to VPCs is compromised. We have also found that VPC daughters can respond to the vulval inducing signal LIN-3, even if their parents were previously specified to be 2°. Our results reveal a coupling of VPC competence to the cell cycle as opposed to absolute developmental time. These findings have implications for the logic of how cells choose among three alternative fates to match the priorities of organogenesis.

Coupling of VPC Competence to the Cell Cycle

We have established an assay to examine VPC competence to respond to LIN-3. In this assay, we genetically remove most endogenous LIN-3 and then add back LIN-3 as a function of time using an inducible promoter. (Although this low level of endogenous LIN-3 remaining is unable to induce vulval fates, it is unknown whether this background affects VPCs' capability to respond to signaling.) The stereotyped cell lineages of *C. elegans* allow developmental time to be determined with considerable accuracy (within

30 min). We have found that VPCs are competent to respond to LIN-3 as are VPC daughters shortly after they are born. VPC daughters lose competence upon exit from the cell cycle, possibly by their terminal differentiation (fusion with the hyp7 epidermis). Keeping VPC daughters in the cell cycle by activated LIN-12 maintains VPC competence. We also note that blocking the cell cycle does not necessarily abolish VPC competence, as HU-arrested VPCs expressed a cell fate specific marker *egl-17::GFP*, although cell fate specific lineages are not executed (data not shown; Ambros, 1999).

Proposed roles of receptors of the LIN-12/Notch/GLP-1 family include maintaining cell competence by delaying cell fate determination (Coffman *et al.*, 1993; reviewed by Artavanis-Tsakonas *et al.*, 1995) or by controlling binary choices in cell fate (reviewed by Greenwald, 1994). Our observation that activation of LIN-12 [in either the *lin-12(+)* or *lin-12(gf)* background] extends competence to respond to the epidermal growth factor LIN-3 provides one class of explanation for the oncogenic action of some mammalian LIN-12 homologs (reviewed by Artavanis-Tsakonas *et al.*, 1995). Specifically, we see an inappropriate response to an EGF-like growth factor, likely via the RAS pathway, in cells that have activated LIN-12. Our results suggest that the effects of activated LIN-12 on competence of the VPC daughters may be caused by activated LIN-12 regulating cell cycle, as well as regulating cell differentiation.

Commitment to VPC Fates

Analysis of the commitment of cells to developmental fates has been difficult in *C. elegans* because traditional assays of transplantation and cell culture (reviewed by Gurdon, 1992) have not yet been applied to this organism. Manipulating the levels and the timing of growth factors involved with cell fate specification as we have done with LIN-3 in this study is another way of assessing their state of commitment. Ours is arguably the first study to use this approach to address cell fate commitment in *C. elegans*.

Our results demonstrate that VPC daughters with activated LIN-12 (hence specified to be 2°) remain competent to respond to LIN-3 and therefore can be respecified to adopt the 1° fate. We speculate that induced VPCs go through what is at first a common pathway of 1° and 2° fate specification, thus remaining competent to respond to further LIN-3 inductive signaling by becoming 1° (Fig. 7). There are indeed common and unique characteristics of the 1° and 2° fates. One common characteristic is that both fates involve stimulation of the cell cycle and generate grossly similar cell types. However, cells adopting each fate express molecular markers such as *egl-17::GFP* in distinct temporal and spatial patterns. As is often the case in development, differential gene expression precedes not only frank differentiation, but also commitment to a fate (Davidson, 1986). We believe that VPC fate specification usu-

ally takes place in the first cell cycle but that in relatively rare individuals—those that receive a lower level of LIN-3 during the first cell cycle—the patterning process extends into the second cell cycle.

Our results suggest that there are two ways in which the hybrid lineages of 1° and 3° seen under various conditions arise (e.g., Sulston and Horvitz, 1981; Ferguson *et al.*, 1987; Sternberg and Horvitz, 1986; Aroian and Sternberg, 1991; Katz *et al.*, 1995; this paper). In particular, we have provided evidence that these hybrids occur either because the VPCs failed to receive or transduce enough LIN-3 signal to be committed to the 1° fate or because they received LIN-3 too late and only one of two daughters responded (Fig. 6). If inductive signaling is truncated by anchor cell ablation, cells can generate 1°/3° hybrid lineages (Kimble, 1981; M. Wang and P. W. Sternberg, unpublished observations). We interpret these cases as resulting from insufficient signaling to become committed to vulval (1° or 2°). On the other hand, in our late LIN-3 expression experiments, VPCs did not receive LIN-3 until they divided, and 3°/1° (S TT) type hybrid lineages were likely caused by VPC daughters responding to LIN-3 independently (Fig. 1B). Similarly, 3°/2°–1°–2°/3° (i.e., S TN–TTTT–NT S) patterns could also be explained by lateral signaling from presumptive 1° daughters (e.g., Sulston and Horvitz, 1981; Koga and Ohshima, 1995; Simske and Kim, 1995). Finally, in *lin-3(e1417)* mutants, 17 of 74 P6.p lineages we scored were hybrids; in *lin-3(sy91)* mutants, 8 of 65 P6.p cells generated hybrid lineages, and 19 of 130 P5.p and P7.p cells were hybrids. These cases could result from both insufficient LIN-3 received by VPCs and continuous LIN-3 signaling to VPC daughters.

Evolutionary Implications and Prioritization of a Three-Way Decision

We believe that the maintenance of competence was necessary for vulval induction in ancestral nematodes and has been maintained in *C. elegans* because it helps ensure an appropriate pattern of cell types. In a number of other nematode species, vulval fate patterning is achieved through two successive inductions by the gonad (Félix and Sternberg, 1997). The first induction is of three VPCs to assume vulval fates; the second induction is of two VPC daughters to assume the inner vulval fates corresponding in cell type to the progeny of the 1° VPC. The vulval fates in these species might correspond to the first common part of the 1° and 2° program in *C. elegans* (stimulation of the cell cycle and blocking epidermal differentiation), presumably promoted by activated homologs of either LIN-12 or LET-23. The inner vulval fates might correspond to the final 1° fate in *C. elegans*, promoted by further LIN-3/LET-23 signaling in the second induction.

Of the three vulval fates in *C. elegans*, 1° is the most important fate to ensure a functional vulva. Hermaphrodites with only 1° but not 2° cells sometimes can still lay eggs, while animals with only 2° but not 1° cells never lay eggs (Sulston and White, 1980; Greenwald and Seydoux, 1990). Too little signal fails to induce a 1°, or induce a 1° that cannot laterally induce its neighbors to be 2°, resulting in animals with inefficient egg laying and copulation with males (Sulston and White, 1980; M. Barr and P. W. Sternberg, unpublished observations).

Prioritization of 1° over 2° fates could be achieved by maintaining VPC competence to respond to LIN-3 after they divide. The production of the LIN-3 signal may be difficult to be controlled precisely; it would thus be essential to have additional mechanisms to ensure the outcome of the signaling process. The maintenance of competence of VPC daughters in *C. elegans* provides a greater window of time for uncommitted 1° VPCs to respond to LIN-3 and commit to the 1° fate, thereby maximizing the probability that at least one VPC will be induced to be 1°.

Prioritization of 1° over 2° could also be achieved by making the decision to become 1° irreversible and making the decision to become 2° at the first VPC cell cycle reversible. Since low levels of LIN-3 signal induce a VPC to become 2° (Katz *et al.*, 1995, 1996), either VPCs must not commit to a fate until they have given enough time to receive LIN-3 or specification to be 1° supercedes specification to be 2° or 3°. Gurdon *et al.* (1995; Dyson and Gurdon, 1998) have argued for a ratchet mechanism of response to a morphogen, in which cells interpret signal received over time. Indeed, specification as 1° overcomes a prior specification to be 2° or 3°. We find that 2°-fated cells can be readily switched to 1° fates, and delivery of LIN-3 to VPC daughters induces them to display 1° characteristics. By contrast, it is more difficult for a presumptive 1° VPC to become 2°. In particular, very few presumptive 1° VPCs can be reversed to adopt the 2° fate even in S phase of the first cell cycle (Ambros, 1999). Also, challenge of 1° VPCs with a strong 2°-inducing signal (overexpression of the cytoplasmic domain of the LIN-12-like receptor GLP-1; Roehl and Kimble, 1993) failed to alter the fate of 1° VPCs (data not shown). Similarly, the 3° fate can lead to 1°, but not the reverse. Ambros (1999) has provided evidence that there is a temporal order to the specification of VPC fates in the first cycle: 1° fates are specified first, then 2° and 3° fates. Both his and our results suggest that the logic of VPC fate specification is biased toward ensuring that a 1° fate is specified.

In summary, inductive and lateral signaling would start from the first VPC cell cycle. Controlling the level of LIN-3 expression and lateral signaling between the VPCs ensures that there will not be excessive induction. P6.p (closest to the AC) receives the highest amount of LIN-3 and is normally induced to be 1°. In the case that P6.p did not receive sufficient signal, maintenance of competence to VPC daughters would then ratchet P6.p and its descendants to a 1° fate, locking in the 1° fate commitment. In *C. elegans* vulva induction, the patterning mechanism has evolved to ensure a 1° cell; coupling competence to the cell cycle helps ensure this pattern.

23

ACKNOWLEDGMENTS

Note added in proof. The manuscript referred to as "J. Liu, P. Tzou, R. Hill, and P. Sternberg, in preparation" is now in press at *Genetics* (Liu *et al.*, 1999).

REFERENCES

Alberola-Ila, J., Takaki, S., Kerner, J. D., and Perlmutter, R. M. (1997). Differential signaling by lymphocyte antigen receptors. *Annu. Rev. Immunol.* **15**, 125–154.

Ambros, V. (1999). Cell cycle-dependent sequencing of cell fate decisions in *Caenorhabditis elegans* vulva precursor cells. *Development, Development* **126**(9), 1947–1956.

Aroian, R. V., Koga, M., Mendel, J. E., Ohshima, Y., and Sternberg, P. W. (1990). The *let-23* gene necessary for *Caenorhabditis elegans* vulval induction encodes a tyrosine kinase of the EGF receptor subfamily. *Nature* **348**, 693–699.

Artavanis-Tsakonas, S., Matsuno, K., and Fortini, M. E. (1995). Notch signaling. *Science* **268**, 225–232.

Brenner, S. (1994). The genetics of *Caenorhabditis elegans*. *Genetics* **77**, 71–94.

Burdine, R. D., Branda, C. S., and Stern, M. J. (1998). EGL-17 (FGF) expression coordinates the attraction of the migrating sex myoblasts with vulval induction in *C. elegans*. *Development* **125**, 1083–1093.

Clandinin, T. R., Katz, W. S., and Sternberg, P. W. (1997). *Caenorhabditis elegans* HOM-C genes regulate the response of vulval precursor cells to inductive signal. *Dev. Biol.* **182**, 150–161.

Coffman, C. R., Skoglund, P., Harris, W. A., and Kintner, C. R. (1993). Expression of an extracellular deletion of *Xotch* diverts cell fate in *Xenopus* embryos. *Cell* **73**, 659–671.

Davidson, E. H. (1986). *In* "Gene Activity in Early Development," 3d ed. Academic Press, Orlando, FL.

Dyson, S., and Gurdon, J. B. (1998). The interpretation of position in a morphogen gradient as revealed by occupancy of activin receptors. *Cell* **93**, 557–568.

Eisenmann, D. M., Maloof, J. N., Simske, J. S., Kenyon, C., and Kim, S. K. (1998). The β-catenin homolog BAR-1 and LET-60 Ras coordinately regulate the Hox gene *lin-39* during *Caenorhabditis elegans* vulval development. *Development* **125**, 3667–3680.

Euling, S., and Ambros, V. (1996). Heterochronic genes control cell cycle progress and developmental competence of *C. elegans* vulval precursor cells. *Cell* **84**, 667–676.

Félix, M.-A., and Sternberg, P. W. (1997). Two nested gonadal inductions of the vulval in nematodes. *Development* **124**, 253–259.

Ferguson, E. L., and Horvitz, H. R. (1985). Identification and characterization of 22 genes that affect the vulval cell lineages of the nematode *Caenorhabditis elegans*. *Genetics* **110**, 17–72.

Ferguson, E. L., Sternberg, P. W., and Horvitz, H. R. (1987). A genetic pathway for the specification of vulval cell lineages of *Caenorhabditis elegans*. *Nature* **326**, 259–267.

Greenwald, I. (1994). Structure/function studies of *lin-12/Notch* proteins. *Curr. Opin. Gen. Dev.* **4**, 556–562.

Greenwald, I., and Rubin, G. M. (1992). Making a difference: The role of cell–cell interactions in establishing separate identities for equivalent cells. *Cell* **68**(2), 271–281.

Greenwald, I., and Seydoux, G. (1990). Analysis of gain-of-function mutations of the *lin-12* gene of *Caenorhabditis elegans*. *Nature* **346**, 197–199.

Greenwald, I. S., Sternberg, P. W., and Horvitz, H. R. (1983). The *lin-12* locus specifies cell fates in *Caenorhabditis elegans*. *Cell* **34**, 435–444.

Gurdon, J. B. (1992). The generation of diversity and pattern in animal development. *Cell* **68**, 185–199.

Gurdon, J. B., Mitchell, A., and Mahony, D. (1995). Direct and continuous assessment by cells of their position in a morphogen gradient. *Nature* **376**, 520–521.

Hill, R. J., and Sternberg, P. W. (1992). The gene *lin-3* encodes an inductive signal for vulval development in *C. elegans*. *Nature* **358**, 470–476.

Horvitz, H. R., and Herskowitz, I. (1992). Mechanisms of assymetric cell-division: To be or not to be, that is the question. *Cell* **68**(2), 237–255.

Horvitz, H. R., and Sternberg, P. W. (1991). Multiple intercellular signaling systems control the development of the *C. elegans* vulval. *Nature* **351**, 535–541.

Johe, K. K., Hazel, T. G., Muller, T., Dugich-Djordjevic, M. M., and McKay, R. D. G. (1996). Single factors direct the differentiation of stem cells from the fetal and adult central nervous system. *Genes Dev.* **10**(24), 3129–3140.

Katz, W. S., Hill, R. J., Clandinin, T. R., and Sternberg, P. W. (1995). Different levels of the *C. elegans* growth factor LIN-3 promote distinct vulval precursor fates. *Cell* **82**, 297–307.

Katz, W. S., Lesa, G. M., Yannoukakos, D., Clandinin, T. R., Schlessinger, J., and Sternberg, P. W. (1996). A point mutation in the extracellular domain activates LET-23, the *Caenorhabditis elegans* epidermal growth factor receptor homolog. *Mol. Cell. Biol.* **16**, 529–537.

Kimble, J. (1981). Alterations in cell lineage following laser ablation of cells in the somatic gonad of *Caenorhabditis elegans*. *Dev. Biol.* **87**, 286–300.

Kimble, J., and Hirsh, D. (1979). The postembryonic cell lineages of the hermaphrodite and male gonads in *Caenorhabditis elegans*. *Dev. Biol.* **70**, 396–417.

Koga, M., and Ohshima, Y. (1995). Mosaic analysis of the *let-23* gene function in vulval induction of *Caenorhabditis elegans*. *Development* **121**, 2655–2666.

Levitan, D., and Greenwald, I. (1998). LIN-12 protein expression and localization during vulval development in *C. elegans*. *Development* **125**, 3101–3109.

Liu, J., Tzou, P., Hill, R. J., and Sternberg, P. W. (1999). Structural requirements for the tissue-specific and tissue-general functions of the *C. elegans* epidermal growth factor LIN-3. *Genetics*, in press.

Maloof, J. N., and Kenyon, C. (1998). The Hox gene *lin-39* is required *during C. elegans* vulval induction to select the outcome of Ras signaling. *Development* **125**, 181–190.

Morrison, S. J., Shah, N. M., and Anderson, D. J. (1997). Regulatory mechanisms in stem cell biology. *Cell* **88**(3), 287–298.

Roehl, H., and Kimble, J. (1993). Control of cell fate in *C. elegans* by a GLP-1 peptide consisting primarily of ankyrin repeats. *Nature* 364, 632–635.

Shah, N. M., and Anderson, D. J. (1997). Integration of multiple instructive cues by neural crest stem cells reveals cell-intrinsic biases in relative growth factor responsiveness. *Proc. Natl. Acad. Sci. USA* 94(21), 11369–11374.

Simske, J. S., and Kim, S. K. (1995). Sequential signaling during *Caenorhabditis elegans* vulval induction. *Nature* 375, 142–146.

Slack, J. M. W. (1991). "From Egg to Embryo." Oxford Univ. Press, Oxford, England.

Sternberg, P. W. (1988). Lateral inhibition during vulval induction in *Caenorhabditis elegans*. *Nature* 335, 551–554.

Sternberg, P. W., and Horvitz, H. R. (1986). Pattern formation during vulval induction in *C. elegans*. *Cell* 44, 761–772.

Sternberg, P. W., and Horvitz, H. R. (1989). The combined action of two intercellular signaling pathways specifies three cell fates during vulval induction in *C. elegans*. *Cell* 58, 679–693.

Sulston, J. E., and White, J. G. (1980). Regulation and cell autonomy during postembryonic development of *Caenorhabditis elegans*. *Dev. Biol.* 78, 577–597.

Sulston, J. E., and Horvitz, H. R. (1977). Postembryonic cell lineages of the nematode *Caenorhabditis elegans*. *Dev. Biol.* 56, 110–156.

Sulston, J. E., and Horvitz, H. R. (1981). Abnormal cell lineages in mutants of the nematode *Caenorhabditis elegans*. *Dev. Biol.* 82, 41–55.

Thomas, J. H., Stern, M. J., and Horvitz, H. R. (1990). Cell interactions coordinate the development of the *C. elegans* egg-laying system. *Cell* 62, 1041–1052.

Wilkinson, H. A., and Greenwald, I. (1995). Spatial and temporal patterns of *lin-12* expression during *C. elegans* hermaphrodite development. *Genetics* 141, 513–526.

Wood, W. B. (Ed.) (1988). "The Nematode *Caenorhabditis elegans*." Cold Spring Harbor Laboratory Press, Cold Spring Harbor, NY.

Yochem, J., Weston, K., and Greenwald, I. (1988). The *Caenorhabditis elegans lin-12* gene encodes a transmembrane protein with overall similarity to *Drosophila Notch*. *Nature* 335, 547–550.

Chapter 3

The HOM-C gene LIN-39 and periodic competence of

C. elegans vulval precursor cells

Minqin Wang, John A. DeModena and Paul W. Sternberg

(prepared for submission)

SUMMARY

We have analyzed how the competence of vulval precursor cells (VPCs) to respond to the inductive signal is regulated during *C. elegans* vulval development. By testing the response of the tripotent VPCs to the EGF family growth factor LIN-3 as a function of time, we demonstrate that promoting cell cycle progression by a *cul-1* mutation or preventing cell fusion by overexpressing the HOM-C gene LIN-39 extends VPC competence. However, overexpressing the receptor LET-23 does not show such an effect. Our results suggest that LIN-39 activity, which is required for VPC responsiveness to LIN-3, may fluctuate during cell cycle progression, and thus provide a way of coupling competence to the cell cycle. Consistently, we find that VPCs may change competence periodically within each cell cycle: competent in S, but not in G2. Such a cell cycle coupled mechanism may be commonly used in regulating the competence of precursor cells.

INTRODUCTION

Spatially and temporally regulated cell signaling is required for cell proliferation and cell fate determination throughout animal development. In addition to strict control of when and where inductive signals are available, the competence of precursor cells to respond to such signals is also developmentally regulated (e.g., Slack, 1991; Gurdon, 1992). Developmental systems must therefore restrict the ability of precursor cells to only respond

to correct cues by establishing windows of precursor cell competence. However, the mechanism by which cells acquire, maintain and lose their competence is not well understood.

The intrinsic capacity of cells to respond to extracellular cues may be regulated cell-autonomously. First, cells may count their own age and lose their developmental potential progressively as they become older. For example, in mammalian cerebral cortex, late cortical progenitor cells lose competence to produce deep-layer neurons (Frantz and McConnell, 1996). Second, inductive signaling is often related to cell cycle progression of responding cells (e.g., Raff et al., 1985; Lumsden et al., 1994; Ferri et al., 1996). Cell cycle stage also biases the decision of Dictyostelium cells to become either prespore or prestalk after starvation (Gomer and Firtel, 1987). Third, other internal features of responding cells may also be important in tuning the response of multipotential progenitor cells. In vertebrate retina development, different expression levels of EGF receptor result in distinct fate determination of progenitor cells in response to the same extracellular signal (Lillien, 1995).

The *Caenorhabditis elegans* vulva provides an excellent model system to study regulation of cell competence, because induction can be analyzed at a single cell level (reviewed by Horvitz and Sternberg, 1991). Vulval development starts with six multipotential ectoblasts P(3-8).p, called the vulval precursor cells (VPCs) (Sulston and Horvitz, 1977). Each VPC is competent to respond to the inductive signal from the somatic gonadal anchor cell (AC), and can adopt any of the three fates, 1°, 2°, or 3° (Sulston and White, 1980; Kimble, 1981; Sternberg and Horvitz, 1986). In wild-type

animals, vulval induction occurs around late L2 to early L3 stage (Kimble, 1981; Sternberg and Horvitz, 1986). The VPC nearest to the AC, P6.p, adopts the 1° fate, while the adjacent P5.p and P7.p adopt the 2° fate. The other three distal-most cells P3.p, P4.p and P8.p adopt the non-vulval 3° fate. All VPCs divide once about 4 hours after the molt from the L2 to L3 larval stage (L2 molt). The two daughters of VPCs (Pn.px) that assume the 3° fate then fuse with the hyp7 epidermal syncytium. In contrast, daughters of VPCs (Pn.px) that assume the 1° and 2° fates divide a second and third time about 2 hours later and during L3 molt to give rise to 8 and 7 progeny nuclei, respectively, with different lineages (Sulston and Horvitz, 1977).

The highly reproducible pattern of VPC fates is probably the outcome of at least two signaling events (reviewed in Kenyon, 1995). The signals involved include an inductive signal LIN-3, an EGF homolog, from the AC (Hill and Sternberg, 1992; Katz et al., 1995), mediated by the receptor tyrosine kinase LET-23 (Aroian et al., 1990), and a lateral signal between VPCs, mediated by LIN-12, a *Notch* homolog (Greenwald et al., 1983; Sternberg, 1988; Yochem et al., 1988; Koga and Ohshima, 1995; Simske and Kim, 1995). Little is known about the mechanisms that regulate the competence of VPCs to respond to the inductive signal. The heterochronic pathway affects both timing of acquisition of competence and cell cycle progression of VPCs (Euling and Ambros, 1996). HOM-C genes also influence the competence of VPCs (Clandinin et al., 1997; Maloof and Kenyon, 1998).

Here we examine the end of the window of VPC competence, and find that perturbing the VPC cell cycle by a *cul-1* mutation, but not overexpressing the LET-23 receptor, affects the end of VPC competence. We

provide evidence that the level of the HOM-C gene LIN-39 activity affects VPC competence and that changes of the VPC competence might be coupled to progression of different phases of the VPC cell cycle. Our results suggest that LIN-39 expression level might also fluctuate during different phases of the cell cycle, implying that LIN-39 may tie in VPC competence regulation and cell cycle progression.

MATERIALS AND METHODS

General methods and strains

C. elegans strains were handled at 20°C according to standard protocols (Brenner, 1974; Riddle et al., 1997). The following alleles were used: for LGI, *ayIs4[egl-17::GFP; dpy-20(+)]*; LGII, *syIs12[hs-LIN-3EGF; dpy-20(+)]*; LGIII, *dpy-19(e1259), unc-32(e189), lin-12(n137), lin-12(n676n909), cul-1(e1756), unc-69(e587)*; LGIV, *unc-24(e138), let-59(s49), unc-22(s7), dpy-20(e1282), lin-3(n378), lin-3(n1059)*; LGV, *syIs31[let-23(+); dpy-20(+)]*; LGX, *unc-3(e151), muIs23[hs-LIN-39, dpy-20(+)]*. (Brenner, 1974; Greenwald et al., 1983; Ferguson and Horvitz, 1985; Katz et al., 1995; Kipreos et al., 1996; Burdine et al., 1998; G. M. Lesa, C. Lacenere and P. W. S., unpublished data; Maloof and Kenyon, 1998).

   ayIs4, syIs12 and *muIs23* integrated transgenes that carry *dpy-20(+)*. Strains bearing two or three of these constructs were built in a similar way. For example, *ayIs4; syIs12; lin-3(n378) let-59 unc-22 / unc-24 lin-3(n1059) dpy-20; muIs23* animals were constructed by mating *ayIs4 / +; syIs12 / +; [lin-*

3(n378) let-59 unc-22 or *unc-24 lin-3(n1059) dpy-20]/ dpy-20; muIs23/O*

males to *ayIs4/+; syIs12/+; [lin-3(n378) let-59 unc-22* or *unc-24 lin-3(n1059)*

dpy-20]/ dpy-20; unc-3 hermaphrodites. Vulvaless hermaphrodite cross

progeny were selected, placed on individual plates and allowed to self-

fertilize. Animals that segregated dead L1 larvae and Unc-3s were kept, and

their progeny were examined individually under Nomarski optics after heat

shock for the presence of *ayIs4* and *syIs12*. These animals were therefore of

genotype *ayIs4/ (ayIs4* or +); *syIs12/ (syIs12* or +); *lin-3(n378) let-59 unc-*

22/unc-24 lin-3(n1059) dpy-20; muIs23/ unc-3. Animals that did not

segregate Unc-3s and contained *ayIs4* and *syIs12* in all their progeny were

identified.

Heat shock and hydroxyurea treatment of transgenic animals

Animals were mounted on agar pads, examined using Nomarski optics to

confirm their stages (Sulston and Horvitz, 1977; Kimble and Hirsh, 1979) and

then heat shocked 15 minutes after they were staged. All heat shock pulses

were performed at 31.5°C for 20 minutes (except for Figure 1B, 33°C for 30

minutes was used). Animals were placed on prewarmed plates of desired

temperature, sealed with Parafilm, and then floated in a covered water bath

of the same temperature. After heat shock, animals were transferred

immediately to plates kept at 20°C until late L3 stage when they were scored

for VPC fates. In many cases, the animals were replated and observed again

during the L4 stage.

Newly molted L3 *ayIs4; syIs12; lin-12(+); lin-3(lf)* and *ayIs4; syIs12;*

lin-12(gf); lin-3(lf) animals as well as *ayIs4; syIs12; lin-12(gf); lin-3(lf)*

animals with very early Pn.px cells (dorsal uterine cells had not divided a second round, Kimble and Hirsh, 1979) were examined using Nomarski optics and placed on plates containing 40mM hydroxyurea and a small spot of *E. coli* (Euling and Ambros, 1996) for 3 or 6 hours. They then were mounted on agar pads and examined using Nomarski optics again to confirm that VPCs had not divided or started to divide during the period. For S phase VPC competence experiments, these animals were put back to hydroxyurea plates and heat shocked at 31.5°C for 20 minutes prior to transfer to normal plates. Animals whose VPCs had divided or were starting to divide were discarded. For G2 phase VPC competence experiments, staged animals were transferred to normal plates after HU treatment and cultured for 1.5 hours. They then were mounted and examined using Nomarski optics for a third time to confirm that VPCs had not yet entered mitosis. Such animals were placed back on normal plates and heat shocked for 31.5°C for 20 minutes.

VPC fate assignment

Both VPC lineages and expression patterns of *egl-17::GFP* were followed using Nomarski optics and a Zeiss Axioplan microscope with a 200-watt HBO UV source, using a standard GFP filter set. VPC fates were assigned as the vulval fate or the uninduced non-vulval fate in Table 1, Table 2, Figure 1 and Figure 3A; the 2° or the non-2° fate, in Figure 3B; and the s (divide twice and fuse) or the S fate (divide once and fuse) in Figure 1.

In Table 1, Figure 1 and Figure 3A, we scored VPCs as adopting the vulval fate if they underwent at least two rounds of cell division, remained unfused, and formed an invagination during the L4 stage. In Table 2, VPCs

were scored as adopting the vulval fate, if we observed *egl-17::GFP*

expression in all or part of their descendants during L3 lethargus, as well as

an invagination during the L4 stage. Expression patterns at mid-L4 stage

were not scored, since many *cul-1* mutants arrested at the L3 molt, and

therefore would not proceed into L4 (Kipreos et al., 1996). In Figure 3B,

VPCs were scored as assuming a different fate from their basal 2° fate, if any

of their descendants expressed *egl-17::GFP* during L3 lethargus. These fates

were considered as non-2° (not necessarily 1°). Expression patterns of *egl-*

17::GFP at L4 were not scored to simplify the protocol. In Figure 1, for single

hs-LIN-3 and double *hs-LIN-3 / hs-LIN-39* experiments, we scored vulval fates

of VPCs using the same criteria as we did in Table 1 and Figure 3A. For

single *hs-LIN-39* experiments, VPCs were scored as adopting the s fate if

they divided twice before they fuse with the epidermis and were scored as

adopting the S fate if they divided only once before they fuse as do wild-type

3° cells.

Immunostaining

lin-3(n378 / n1059); lin-12 (n137 / n676n909) L3 larvae were stained using

LIN-39 antibody, MH27 antibody, and DAPI. Worms were prepared for

whole mount immunofluorescence by a protocol developed by Finney and

Ruvkin (1990), and Miller and Shakes (1995), with slight differences in times

of fixation and incubation. For LIN-39 antibody staining, animals were

incubated with pre-adsorbed LIN-39 antibody as described in Maloof and

Kenyon, 1998.

RESULTS

To examine the end of VPC competence, we induced LIN-3 expression at different times in a *lin-3* loss-of-function background, in which the inductive signaling is missing and VPCs adopt the 3° fate. A heat shock inducible LIN-3 construct (*hs-LIN-3*) and a viable *lin-3* severe reduction-of-function mutant background *n378/n1059* [*lin-3(lf)*] were used (Hill and Sternberg, 1992; Katz et al., 1995; Wang and Sternberg, 1999).

Overexpression of LET-23 does not extend the end of VPC competence

Previous studies indicate that VPCs lose competence to respond to the AC signal LIN-3 shortly after they divide (Wang and Sternberg, 1999). One simple reason for loss of competence may be that the receptor levels are limiting. We therefore examined whether increasing the level of LET-23 would extend VPC competence. We used *syIs31*, which bears multiple copies of genomic *let-23* DNA and therefore presumably expresses a higher level of LET-23 than wild-type [henceforth *let-23(+++)*; Simske et al., 1996; C. Lacenere, G. Lesa, and P.W.S., unpublished; also see below].

When we induced LIN-3 expression by heat shock at different times in a *hs-LIN-3; lin-3(lf); let-23(+++)* background, we found that the sensitivity of VPCs to respond to LIN-3 was slightly increased in a *let-23(+++)* background (Table 1). In a *lin-3(n378/n1059)* background, 0% of VPCs (n=174) adopted the vulval fate if *let-23* was wild-type, whereas 6% of VPCs (n=105) adopted

the vulval fate with multiple copies of genomic *let-23* DNA (*P*<0.001, Fisher's exact test, Table 1). Overexpression of LET-23 probably does not cause ligand-independent activation of the signaling pathway, since *let-23(+++)* animals with the wild-type copy of the *lin-3* gene display wild-type vulval induction (C. Lacenere, G. Lesa, and P.W.S., unpublished). The *lin-3* genotype *(n378/n1059)* we used thus has residual *lin-3* activity, consistent with *n378* being a missense E to K mutation in the extracellular domain and *n378* homozygote mutants having significant vulval induction (Liu et al., 1999). Although wild-type VPCs are insensitive to this low level of signal, it may be detectable by more sensitive VPCs with higher levels of *let-23* expression. The percentage of VPCs induced to adopt vulval fates dropped when the start point of LIN-3 expression was delayed, and reduced to the control level when animals were heat shocked after VPCs had divided (7%, compared with 6%, *P*>0.99, Table 1). Therefore, although overexpression of LET-23 makes VPCs hypersensitive to LIN-3, it has no detectable effect on the end of the VPC competence window.

Driving the VPC cell cycle by *cul-1* extends VPC competence

Since the loss of VPC competence right after VPC division temporally corresponds with fusion with the hyp7 epidermal syncytium and exit from the cell cycle of the VPC daughters, we attempted to examine the effect of driving the VPC cell cycle or preventing VPC fusion separately.

As a test of the cell cycle dependence of VPC competence, we asked whether promoting the VPC cell cycle was sufficient to extend VPC

competence using a *cul-1* mutation. The cullin *cul-1* is required for cell cycle exit, but not for cell differentiation and cell fate determination (Kipreos et al., 1996). In *cul-1* mutant animals, all types of cells divide excessively including VPCs. Therefore, a *cul-1* mutation can promote cell division in a manner that is independent of the inductive signaling pathway.

We used a vulval cell fate marker *egl-17::GFP* (Burdine et al., 1998) to examine whether the vulval fates adopted by VPCs in a *cul-1* background are normal. In wild-type animals, *egl-17::GFP* is expressed in 1° granddaughters at L3 and then fades completely in 1° descendants at mid-L4. 2° granddaughters do not express *egl-17::GFP* at L3, but part of the 2° descendants express GFP strongly at mid-L4. We found that P5.p, P6.p and P7.p of *egl-17::GFP; cul-1* animals adopted vulval fates: their descendants displayed vulval-like lineages, expressed *egl-17::GFP* in an appropriate manner in P6.p, and displayed at least partial nonadherence to the ventral cuticle before forming an invagination at mid-L4 (data not shown). Thus, *cul-1* mutations do not affect vulval pattern formation in otherwise wild-type animals.

To examine the end of the VPC competence window in a *cul-1* mutant background, we constructed a strain of genotype *egl-17::GFP; hs-LIN-3; cul-1; lin-3(lf)*. Without heat shock, 22% (n=222) of the VPCs divided more than once while the remaining VPCs divided only once and fused with the epidermis as wild-type 3° cells do (Table 2). We infer that those VPCs that divided excessively did *not* adopt vulval fates, because most of their divisions were longitudinal, and their descendants neither detached from the ventral cuticle nor formed any invagination at mid L4 (data not shown). Moreover,

the descendants from the excessive divisions never expressed *egl-17::GFP* at any stage, whereas some or all descendants of 1° and 2° VPCs, as well as VPCs adopting non-canonical 1° and 2° fates, expressed the marker at either L3 or L4 (M.W. and P.W.S, unpublished results). Therefore, although causing excessive division of the VPCs, a mutation in *cul-1* does not promote vulval fates in the absence of inductive signal. Also, VPC fate assignment is not affected by the extra cell divisions caused by *cul-1* (see Experimental Procedures).

We then induced LIN-3 expression by heat shock at different times. Strikingly, VPC daughters, granddaughters and even great-granddaughters responded to LIN-3 (Table 2). After the VPC divisions, response dropped from 56% (n=135) to 45% (n=311) (*P*=0.05). This prolonged response was observed after the divisions of VPC daughters (20%, n=103), and was not completely abolished even after the divisions of VPC granddaughters (Table 2).

These results suggest that driving the VPC cell cycle through the loss of *cul-1* activity extends the end of VPC competence, and are consistent with a close relationship between cell cycle progression and VPC competence. It is possible that the VPCs in *cul-1* mutants divide earlier than their wild-type counterparts. However, that the VPCs respond to cell cycle rather than developmental time make this hypothesis unlikely (Wang and Sternberg, 1999). Another possibility is that *cul-1* might regulate the degradation of a key VPC regulatory protein (such as LIN-12, which can prolong VPC competence; Hubbard et al., 1997; Wang and Sternberg, 1999), or the unfused

state concomitant with VPC cell cycle progression is what extends VPC

competence.

Overexpressing LIN-39 extends the end of VPC competence

To mimic the effect of inhibiting VPC fusion, we used *muIs23*, which bears a

construct expressing LIN-39 under the transcriptional control of an *hsp16*

promoter (henceforth *hs-LIN-39*; Maloof and Kenyon, 1998). *lin-39*, one of

the genes in the HOM-C cluster of *C. elegans* specifying anterior/posterior

pattern, is a homolog of the Drosophila *Dfd/Scr/pb* gene and is expressed in

the VPCs (Wang et al., 1993). LIN-39 is both required for establishing the

identity of competent VPCs early in development and for determining the

response of VPCs to inductive signaling later (Clandinin et al., 1997; Maloof

and Kenyon, 1998). VPCs of *lin-39* loss-of-function mutants fuse with the

epidermis before vulval induction (Clark et al., 1993; Salser et al., 1993).

Conversely, overexpressing LIN-39 prevents VPC fusion (Maloof and Kenyon,

1998).

We built a strain carrying both *hs-LIN-3* and *hs-LIN-39*, as well as the

egl-17::GFP reporter gene, but lacking endogeneous LIN-3. We induced LIN-

3 and LIN-39 expression simultaneously by heat shock. Both mild and strong

heat shock induction of LIN-39 and LIN-3 simultaneously during late phase

of the VPC cell cycle partially restored competence of early stage VPC

daughters (14%, n=46, and 23%, n=116, respectively) (Figure 1A and 1B).

Therefore, overexpressing LIN-39 extends the end of VPC competence until

after the first VPC division. However, LIN-39 overexpression did not rescue

the loss of competence of already fused late stage VPC daughters (Figure 1A and 1B).

We found a synergistic effect of simultaneous overexpression of LIN-39 and LIN-3. Mild heat shock at the late Pn.p stage revealed that 76% (n=43) of VPCs were competent if both LIN-39 and LIN-3 were induced, but only 53% (n=110) if LIN-3 was induced alone ($P<0.01$, Figure 1A). Strong heat shock at the same stage yielded similar results: 86% (n=55) of the VPCs were competent if both LIN-39 and LIN-3 were induced, but only 59% (n=67) if LIN-3 was induced alone ($P<0.002$, Figure 1B). At the early Pn.px stage, mild heat shock revealed that 14% (n=46) of VPC daughters were competent if both LIN-39 and LIN-3 were induced, but 0% (n=74) if LIN-3 was induced alone ($P<0.001$, Figure 1A). At the same stage, strong heat shock revealed that 23% (n=116) of VPC daughters were competent if both LIN-39 and LIN-3 were induced, but only 2% (n=152) if LIN-3 was induced alone ($P<0.001$, Figure 1B). This synergy might not be obvious during early Pn.p stage, since the competent level of VPCs is already very high (92%, n=26, Figure 1B). We conclude that the level of LIN-39 activity continually affects the competence of VPCs, consistent with previous observations (Clandinin et al., 1997; Maloof and Kenyon, 1998).

When we overexpressed LIN-39 alone in the absence of LIN-3 during the late Pn.p stage, some VPCs divided twice before their progeny fused with the epidermis (Figure 1B). These VPCs never expressed *egl-17::GFP* (data not shown); they underwent one more round of cell division than normal 3° cells but nevertheless assumed the non-vulval fate (s instead of S, see

Experimental Procedures). Therefore, the level of LIN-39 activity might also regulate VPC cell cycle progression.

The occurrence of an extra division depended on when LIN-39 was induced. A heat shock pulse at the late Pn.p stage caused 11% of VPCs (n=121) to divide once more, while a heat shock pulse at the early Pn.p stage caused none (n=101) to do so ($P<0.001$, Figure 1B). Therefore, the activity of overexpressed LIN-39 may be transient, diminishing coordinately with VPC cell cycle progression.

LIN-39 expression shows fluctuation in VPCs

To examine whether the expression level of endogenous LIN-39 changes during VPC cell cycle progression, we used anti-LIN-39 antibodies (Maloof and Kenyon, 1998). In wild-type animals, LIN-39 is initially expressed at the same level in all VPCs before the AC induction, and then its expression level increases significantly in P6.p at the time of vulval induction (Maloof and Kenyon, 1998). To avoid the complication of increased LIN-39 expression upon Ras activation and examine LIN-39 expression in all six VPCs and their daughters with complete cell cycle progression, we observed LIN-39 expression in a *lin-3(lf); lin-12(gf)* background. In this background, the lack of LIN-3 disrupts Ras signaling, but VPCs undergo three rounds of cell division since LIN-12 is activated (Greenwald et al., 1983; Sternberg and Horvitz, 1989; Greenwald and Seydoux, 1990).

We found that in all animals we examined, LIN-39 is present in the neurons of the ventral cord (Figure 2). However, before VPCs' divisions, while LIN-39 is highly expressed uniformly in VPCs in 22/43 animals (Figure

2A and 2B), it is either completely absent or expressed at very low levels in 14 of 43 animals examined (Figure 2C and 2D). In particular, in 2 out of the 43 animals, P3.p or P8.p had divided according to MH27 staining of the cell junction, indicating that the central undivided VPCs were at the late stage (probably G2) of the cell cycle, and LIN-39 can not be detected in the central undivided VPCs. In the remaining 5 of 43 cases examined, while the central P6.p, or P6.p, along with P5.p and P7.p, had higher expression levels, the distal P3.p, P4.p and P8.p showed no or low levels of LIN-39 expression. This is consistent with the observation that the distal VPCs undergo mitosis slightly earlier than the central VPCs and P6.p is typically the last one to divide (data not shown). Alternatively, the residual LIN-3 signaling in the background may cause increased LIN-39 expression in P6.p (Maloof and Kenyon, 1998). We observed similar LIN-39 expression after VPC division. 8 of 14 animals observed had strong LIN-39 expression in all VPC daughters (Figure 2E and 2F), while in another 4 cases, the LIN-39 expression was very low or absent. In the remaining 2 animals, the central VPC daughters had stronger LIN-39 expression than did the distal ones. Therefore, LIN-39 protein levels might fluctuate, probably with the progression of the VPC cell cycle.

Our attempt to use a cell cycle phase marker, antibodies to phosphorylated histon H3 (Juan et al., 1998; Lieb et al., 1998), to mark the late G2 phase of cell cycle was successful in the *C. elegans* embryo, but not the larva. We were thus unable to correlate LIN-39 expression directly to different phases of VPC cell cycle. It remains possible that the different LIN-

39 expression we observed was variance among different individuals and unrelated to VPC cell cycle progression.

VPC competence is periodic and cell cycle regulated

LIN-39 appears to be a good candidate for VPC competence regulating factor. First, LIN-39 is required both early for Pn.p cells to remain unfused and become VPCs (Clark et al., 1993; Salser et al., 1993), and later downstream of Ras for VPC to respond to LIN-3 to adopt a vulval fate (Clandinin et al., 1997; Maloof and Kenyon, 1998). Second, the level of VPC competence appears to correlate with the level of LIN-39 activity when LIN-39 is overexpressed (Figure 1A and 1B). Previous studies indicate that the timing mechanism of VPC competence regulation is coupled to cell cycle instead of real time (Wang and Sternberg, 1999). The possible fluctuation of LIN-39 expression level in VPCs could thus mean changes of VPC competence during VPC cell cycle progression.

To test whether VPC competence remains constant within each cell cycle, we examined VPC competence during S and G2. We used hydroxyurea (HU) to reversibly block VPCs at S phase (Euling and Ambros, 1996; Ambros, 1999; Wang and Sternberg, 1999), and then induced LIN-3 expression during the block (S phase of the cell cycle), as well as 3 hours after the block but before the mitosis (G2 phase).

In an *egl-17::GFP; hs-LIN-3; lin-12(+); lin-3(lf)* background, 90% of VPCs in S phase (n= 30) and 60% of VPCs in G2 phase (n=63) of the first cell cycle responded to LIN-3 ($P<0.004$, Figure 3A), indicating that VPCs in G2 may be less competent than VPCs in S.

We then used activated LIN-12 to ask whether there is a periodic change in cell competence through each cell cycle. In an *egl-17::GFP; hs-LIN-3; lin-12(gf); lin-3(lf)* background, the percentage of competent VPCs in S and in G2 phase were 88% (n=17) and 61% (n=27) respectively ($P<0.05$, Figure 3B), confirming the earlier results. When we examined VPC daughters in S and in G2, we found that 48% of VPC daughters in S were competent (n=46, Figure 3B), not significantly different from their parent cells' response in G2 phase (61%, $P>0.46$). This number dropped to 8% (n=62, $P<0.0001$) for VPC daughters in G2 (Figure 3B). Therefore, VPC daughters in S phase may be as competent as VPCs in G2 phase of the first cell cycle, but more competent than VPC daughters in G2.

The difference in the percentage of VPCs that responded to LIN-3 between S and in G2 is not the only difference in VPC competence. In both *lin-12(+)* and *lin-12(gf)* backgrounds, LIN-3 induction in S phase of the first cell cycle resulted in VPCs expressing *egl-17::GFP* in 4/4 patterns (Figure 3; Wang and Sternberg, 1999). However, both VPCs in G2 and VPC daughters in S responded by producing 2/4 patterns. Therefore, the competence of VPCs in S may be qualitatively different from that of VPCs in G2, but VPCs in G2 and VPC daughters in S may respond to LIN-3 similarly. By contrast, 1/4 patterns were observed if the heat shock was performed in G2 of the second cell cycle (data not shown).

We conclude that VPCs in S can respond to LIN-3 as VPCs. Since LIN-3 expression while VPCs are in G2 has the same effect as LIN-3 expression while VPC daughters are in G1 or S, VPCs most likely do not respond to LIN-3 during G2 phase. Similarly, VPC daughters in S can

respond to LIN-3 as individual VPC daughters; VPC daughters most likely do not respond during G2 phase. We infer that VPC competence is cell cycle-regulated. After S phase of each cell cycle, VPCs may only respond as independent progeny cells in the next cell cycle. VPCs thus may not respond to LIN-3 after S phase in each cell cycle, but regain their competence by entering S of the next cell cycle.

It is unlikely that the 2/4 and 1/4 patterns of *egl-17::GFP* expression were artifacts caused by HU. Similar patterns were observed in our heat shock experiments in both wild-type and activated LIN-12 backgrounds without HU treatment (Table 1; data not shown), when animals were heat shocked during late stages of the VPC cell cycle (see Materials and Methods). Nor do these patterns seem to be a result of intrinsic polarity of VPCs, since both orientations of the expression pattern were observed although one was usually more frequent (for example, 30% anterior granddaughters of P7.p had stronger GFP expression than posterior granddaughters of P7.p, n=10; data not shown).

DISCUSSION

The challenge of understanding *C. elegans* development is to unravel the layers of regulation that ensure a precise outcome and thus reveal the underlying mechanisms. Our results have uncovered a coupling of vulval precursor cell (VPC) competence to cell cycle progression and maintaining of unfused state. We have also found that VPC competence shows periodic

change in difference phases of the VPC cell cycle, and that the HOM-C gene
lin-39 helps couple VPC competence to VPC cell cycle progression.

Driving VPC cell cycle or preventing cell fusion extends VPC competence

Failure of overexpression of the receptor LET-23 to extend the end of VPC
competence window suggests that the availability of the receptor may not be
a limiting factor when VPCs lose their competence. Promoting cell division
by a *cul-1* mutation or preventing cell fusion can extend VPC competence.
However, it is difficult to strictly separate cell cycle progression from cell
fusion inhibition. First, *cul-1* mutations cause maintaining of the unfused
state along with excessive VPC divisions. Second, LIN-39 overexpression
leads inhibition of VPC fusion, as well as additional cell divisions. Therefore,
it is not conclusive whether either cell cycle progression or cell fusion alone,
or both, is coupled to VPC competence regulation. It is possible that all three
processes share common regulatory factors, such as LIN-39.

Periodic competence and precision of VPC fate patterning

In addition to the observation that VPCs lose competence upon exit from the
cell cycle, possibly by fusion with the hyp7 epidermis, we find that VPCs may
be competent in S but not in G2 phase of the cell cycle. Based upon the
observation that when VPCs are presented with LIN-3 in their G2 phase it
may be their daughters that respond, we propose that cell fate may be
specified immediately after S or in the beginning of G2. At this time, VPCs

may choose fates and lose sensitivity to LIN-3 until their daughters regain

competence by entering the next cell cycle. Transplantation experiments in

the mammalian cerebral cortex have shown that S phase cortical progenitors

are multipotent, whereas cells after S phase are restricted in their

competence (McConnell and Kaznowski, 1991). A general feature of

developmental systems could thus be that responsiveness of precursor cells

undergoes a cyclic fluctuation coupled to cell cycle progression.

Restriction of cell responsiveness to part of the cell cycle has several

potential implications for the logic of developmental programming. It allows

sequential decision-making in response to intercellular signals, even using

the same signaling components. At a mechanistic level, developmental

changes in cell state, which involve changes in protein expression profiles,

can utilize the existing machinery that degrades proteins in a cell-cycle

dependent fashion. Moreover, if both signal production and cell

responsiveness are temporally regulated, then there can be more precise

boundaries to the time window of signaling.

One and only one 1° fate is absolutely required, among the three VPC

fates, to ensure a functional vulva (Horvitz and Sulston, 1980; Sulston and

White, 1980; M. Barr and P. W. S., unpublished). It has been proposed that

several mechanisms may be used to achieve the prioritization of 1° over 2°

and 3° fates (Ambros, 1999; Wang and Sternberg, 1999). Periodic VPC

competence appears to be another mechanism to ensure specification of a 1°

cell by providing multiple chances for a response to inductive signal, while

biasing against an excessive response (Figure 4). Regaining competence

during G1/S of the second cell cycle maximize the probability that at least one

VPC will be induced to be 1°. The reacquisition of competence by VPC daughters allows uncommitted 1° VPCs to respond to additional inductive signal and commit to 1°. Meanwhile, that VPCs progressively lose competence after S phase provides two ways to prevent excessive induction of 1° fates. First, limiting signaling to S phase cells caps the amount of response. Second, it might allow a period of lateral signaling to prevent extra 1° cells. Ambros (1999) has suggested that VPCs can laterally signal while in S phase, and specification of the 2° fate occurs in G2.

Multi-choice decisions in other systems might also utilize the cell cycle to prioritize the decisions and ensure that the appropriate ratio of cell types is produced by multipotent precursor cells. A general feature of many developmental systems appears to be that responsiveness of precursor cells undergoes a cyclic fluctuation coupled to cell cycle progression. In the mammalian cerebral cortex, S phase cortical progenitors are multipotent, whereas G2 progenitors are restricted in their competence; late cortical progenitor cells lose competence to produce deep-layer neurons (McConnell and Kaznowski, 1991; Frantz and McConnell, 1996). Inductive signaling is often related to cell cycle progression of responding cells (e.g., Raff et al., 1985; Lumsden et al., 1994). Cell cycle stage also biases the decision of *Dictyostelium* cells to become either prespore or prestalk after starvation (Gomer et al., 1987). Our results provide a mechanism to utilize the general cell cycle restriction mechanism to guide precursor cells to make appropriate choices among multiple fates and increase the precision of pattern formation. However, it should be noted that sometimes cell cycle progression does not affect cell differentiation at particular stages in some developmental systems

III-23

(Edgar and O'Farrell, 1990; Duronio and O'Farrell, 1994). One possibility is that in these cases cells might have already received appropriate signal(s) at previous cell cycles, and therefore could still execute their fates by differential gene expression when the cell cycle was disrupted. Or, a cell-cycle unrelated responding mechanism of precursor cells has been evolved in these systems.

LIN-39 activity may link VPC competence and the cell cycle

Two non-mutually exclusive classes of models can account for the cell cycle regulation of VPC competence. According to the first model, intrinsic changes, such as of chromatin structure, may occur during the completion of S phase, thus limiting major changes in gene expression profile to cell cycle transition. Or, there might be a cell-cycle regulated component(s) determining VPC competence whose activity undergo cyclic changes. This component(s) might be present and active through G1 and S phase of each cell cycle, becoming non-functional at the end of each S phase as well as when VPCs exit the cell cycle, thereby abolishing the competence of VPCs. This process may involve both transcriptional regulation and degradation of the protein product(s) (e.g., in yeast; Oehlen et al., 1996). *cul-1* may either indirectly regulate the activity of this component(s) by regulating the cell cycle, or it may affect the level of this component(s) by directly regulating its turnover.

While our data do not bear on the first model, we believe the second model is plausible. First, our LIN-39 overexpression experiments show that the level of VPC competence parallels the level of LIN-39 activity (Figure 1A

and 1B). Second, the LIN-39 expression level varies dramatically in VPCs, which is likely to correlate to different phases of the cell cycle (Figure 2). Another HOM-C gene in *C. elegans*, *mab-5*, has been observed to switch on and off repeatedly in the V5 lineage (Salser and Kenyon, 1996). In addition, both previous and our results suggest that LIN-39 protein decays rapidly after produced by heat shock induction (Maloof and Kenyon, 1998; Figure 1B), suggesting that the level of LIN-39 activity can change dramatically within a short period of time. Third, LIN-39 activity is required at the time of vulval induction for normal VPC response to the inductive signal LIN-3, probably as a downstream effector of the LIN-3/Ras signaling pathway (Clandinin et al., 1997; Maloof and Kenyon, 1998). Fourth, in *lin-39(n709)* mutants, VPCs often divide twice before they fuse with the hyp7 epidermal syncytium (s instead of S fate) (Clandinin et al., 1997). This phenotype, which is rarely, if ever, seen in other vulval induction mutants, implies that the behavior of VPC granddaughters can be uncoupled when *lin-39* is defective. Finally, it is unlikely that LIN-39 affects VPC competence solely by permitting an extra round of cell cycle when it is overexpressed. The percentage of VPCs that assumed the vulval fates when both LIN-3 and LIN-39 were induced by heat shock (14% and 23%) was much greater than the percentage of VPCs that adopted the s fate induced by LIN-39 overexpression alone (1% and 4%) (*P*<0.007, Figure 1A, and *P*<0.0001, Figure 1B). We postulate that LIN-39 might directly or indirectly regulate the cell-cycle regulated component(s) determining VPC competence or, more likely, is itself such a component (Figure 4).

lin-39 has been demonstrated to promote a pattern of VPC competence in both *C. elegans* and other nematode species (Clandinin et al., 1997; see also Sommer and Sternberg, 1994; Andreas and Sommer, 1997). *lin-39* also helps determine the specificity of the Ras pathway (Maloof and Kenyon, 1998). We propose that one mechanism that regulates VPC competence involves changes in HOM-C gene activity coupled to cell cycle progression (Figure 4). Providing both spatial and temporal information, LIN-39 may be an important common downstream target and mediate the common function of LET-23 and LIN-12 signaling, i.e., preventing cell fusion and promoting cell cycle progression. High LIN-39 activity is likely an important feature in the common part of $1°$ and $2°$ developmental programs. In vertebrates, the competence change and decision-making coupled to S and G2 phases of the cell cycle in cerebral cortical progenitors, suggested by transplantation experiments, are similar to that in *C. elegans* VPCs (McConnell and Kaznowski, 1991). A timing mechanism coupled to the cell cycle machinery and to HOM-C gene activity may be one mechanism used generally in regulating precursor cell competence.

Experimental caveats: heat shock induced LIN-3

We used an *hs-LIN-3* construct in a *lin-3* loss-of-function background to control the expression of LIN-3. Anti-LIN-3 antibodies will be necessary to examine the expression level of LIN-3 when heat shocked at different phases of the cell cycle and the time it takes for LIN-3 to be expressed after heat shock.

We think it unlikely that the drop of the percentage of competent VPCs in G2 is due to less efficient *hs-LIN-3* expression at different phases of the VPC cell cycle, since the AC is post-mitotic throughout the S and G2 phase of the VPC cell cycle. Furthermore, the *egl-17::GFP* expression patterns resulted from heat shock at these two phases were different (2/4 and 4/4, respectively). After a weak heat shock (at 31.5°C for 10 minutes) during the early Pn.p stage (0-2 hours after L2 lethargus), 5/22 VPCs expressed *egl-17::GFP*, all in a 4/4 pattern. This 23% response was much weaker than that to a 20 minutes 31.5°C heat shock at the same stage (41%, Table 2). Although the 23% response was close to that to a 20 minute 31.5°C heat shock at a later stage, the different expression pattern of *egl-17::GFP* (4/4 vs. 2/4) indicates that these two responses were qualitatively different.

Our results suggest that heat shock induction of LIN-3 expression in presumably G2 phase VPCs may not affect VPCs until the next cell cycle. However, another explanation of our observations is that the time it takes LIN-3 to act after heat shock is simply longer than the time VPCs need to complete G2. This is unlikely since several lines of evidence suggest that LIN-3 is being made and acts within an hour or less after the start of the heat shock.

First, we tested how long it took cells to show a positive response to LIN-3 after heat shock. We observed that animals started to express *egl-17::GFP* as early as 80 minutes after the beginning of the heat shock (20 minutes heat shock plus one hour waiting time, n=4). If the time required for *egl-17::GFP* transcription, translation, folding and fluorophore formation

(Heim et al., 1995) is considered, the LIN-3 protein should be present long before (at least 20 minutes) the GFP expression was observed.

Second, we found that VPCs at the end of their cell cycle could be induced to adopt vulval fates by heat shock starting at the onset of their mitosis, while other divided VPCs in the same animal were not induced (Table 1). Especially, in animals with all VPCs but P6.p having divided, 23 of 42 (55%) P6.p daughters were induced when the animals were heat shocked at the onset of P6.p mitosis. Among these 21 P6.p VPC lineages we scored, both daughters of 7 were induced, only one daughter of 9 were induced, and neither daughters of 5 were induced. Since P6.p cells were effectively induced by heat shock starting at the onset of their mitosis, the time it took for LIN-3 protein to be expressed by heat shock (including the 20 minutes used for heat shock) should be less than the time it took for these late stage VPCs to divide and fuse. We found that the time required for VPCs to divide and fuse with hyp7 was about one hour, by observing animals expressing MH27-GFP (Mohler et al., 1998) under Nomarski and fluorescence optics (data not shown). Therefore, LIN-3 protein should be present less than one hour after the start of heat shock, probably even earlier if we assume that induction has to take place before the fusion process starts or progresses.

Third, the *hs-LIN-3* construct probably started to produce *lin-3* transcripts before the heat shock process was finished. A 6-minute heat shock at 30°C (lower than 31.5°C used in our experiments) using the same construct can induce vulval development (Katz et al., 1995).

REFERENCES

Ambros, V. (1999). Cell cycle-dependent sequencing of cell fate decisions in *Caenorhabditis elegans* vulval precursor cells. *Development* **126**, 1947-1956.

Andreas, E. and Sommer, R. J. (1997). The homeotic gene *lin-39* and the evolution of nematode epidermal cell fates. *Science* **278**, 452-455.

Aroian, R. V., Koga, M., Mendel, J. E., Ohshima, Y. and Sternberg, P. W. (1990). The *let-23* gene necessary for *Caenorhabditis elegans* vulval induction encodes a tyrosine kinase of the EGF receptor subfamily. *Nature* **348**, 693-699.

Brenner, S. (1974). The genetics of *Caenorhabditis elegans*. *Genetics* **77**, 71-94.

Burdine, R. D., Branda, C. S. and Stern, M. J. (1998). EGL-17 (FGF) expression coordinates the attraction of the migrating sex myoblasts with vulval induction in *C. elegans*. *Development* **125**, 1083-1093.

Clandinin, T. R., Katz, W. S. and Sternberg, P. W. (1997). *Caenorhabditis elegans* HOM-C genes regulate the response of vulval precursor cells to inductive signal. *Dev. Biol.* **182**, 150-161.

Clark, S. G., Chisholm, A. D. and Horvitz, H. R. (1993). Control of cell fates in the central body region of *C. elegans* by the homeobox gene *lin-39*. *Cell* **74**, 43-55.

Duronio, R. J. and O'Farrell, P. H. (1994). Developmental control of a G1-S transcriptional program in *Drosophila*. *Development* **120**, 1503-1515.

Edgar, B. A. and O'Farrell, P. H. (1990). The three postblastoderm cell cycles of *Drosophila* embryogenesis are regulated in G2 by *string*. *Cell* **62**, 469-480.

Euling, S. and Ambros, V. (1996). Heterochronic genes control cell cycle progress and developmental competence of *C. elegans* vulval precursor cells. *Cell* **84**, 667-676.

Ferguson, E. L. and Horvitz, H. R. (1985). Identification and genetic characterization of 22 genes that affect the vulval lineages of the nematode *Caenorhabditis elegans*. *Genetics* **110**, 17-72.

Ferri, R. T., Eagleson, K. L. and Levitt, P. (1996). Environmental signals influence expression of a cortical areal phenotype *in vitro* independent of effects on progenitor cell proliferation. *Dev. Biol.* **175**, 184-190.

Finney, M. and Ruvkin, G. (1990). The *unc-86* gene product couples cell lineage and cell identity in *C. elegans*. *Cell* **63**, 895-905.

Frantz, G. D. and McConnell, S. K. (1996). Restriction of late cerebral cortical progenitors to an upper-layer fate. *Neuron* **17**, 55-61.

Gomer, R. H. and Firtel, R. A. (1987). Cell-autonomous determination of cell-type choice in Dictyostelium development by cell-cycle phase. *Science* **237**, 758-762.

Greenwald, I. and Seydoux, G. (1990). Analysis of gain-of-function mutations of the *lin-12* gene of *Caenorhabditis elegans*. *Nature* **346**, 197-199.

Greenwald, I. S., Sternberg, P. W. and Horvitz, H. R. (1983). The *lin-12* locus specifies cell fates in *Caenorhabditis elegans*. *Cell* **34**, 435-444.

Gurdon, J. B. (1992). The generation of diversity and pattern in animal development. *Cell* **68**, 185-199.

Heim, R., Cubitt, A. B. and Tsien, R. Y. (1995). Improved green fluorescence. *Nature* **373**, 663-664.

Hill, R. J. and Sternberg, P. W. (1992). The gene *lin-3* encodes an inductive signal for vulval development in *C. elegans*. *Nature* **358**, 470-476.

Horvitz, H. R. and Sternberg, P. W. (1991). Multiple intercellular signaling systems control the development of the *C. elegans* vulval. *Nature* **351**, 535-541.

Horvitz, H. R. and Sulston, J. E. (1980). Isolation and genetic characterization of cell-lineage mutants of the nematode *Caenorhabditis elegans*. *Genetics* **96**, 435-454.

Hubbard, E. J. A., Wu, G., Kitajewski, J. and Greenwald, I. (1997). *Sel-10*, a negative regulator of *lin-12* activity in *Caenorhabditis elegans*,

encodes a member of the CDC4 family of proteins. *Genes Dev.* **11**, 3182-3193.

Juan, G., Traganos, F., James, W. M., Ray, J. M., Roberge, M., Sauve, D. M., Anderson, H. and Darzynkiewicz, Z. (1998). Histon H3 phosphorylation and expression of cyclins A and B1 measured in individual cells during their progression through G2 and mitosis. *Cytometry* **32**, 71-77.

Katz, W. S., Hill, R. J., Clandinin, T. R. and Sternberg, P. W. (1995). Different levels of the *C. elegans* growth factor LIN-3 promote distinct vulval precursor fates. *Cell* **82**, 297-307.

Kenyon, C. (1995). A perfect vulva every time: gradients and signaling cascades in *C. elegans*. *Cell* **82**, 171-174.

Kimble, J. (1981). Alterations in cell lineage following laser ablation of cells in the somatic gonad of *Caenorhabditis elegans*. *Dev. Biol.* **87**, 286-300.

Kimble, J. and Hirsh, D. (1979). The postembryonic cell lineages of the hermaphrodite and male gonads in *Caenorhabditis elegans*. *Dev. Biol.* **70**, 396-417.

Kipreos, E. T., Lander, L. E., Wing, J. P., He, W. W. and Hedgecock E. M. (1996). *cul-1* is required for cell cycle exit in *C. elegans* and identifies a novel gene family. *Cell* **85**, 829-839.

Koga, M. and Ohshima, Y. (1995). Mosaic analysis of the *let-23* gene function in vulval induction of *Caenorhabditis elegans*. *Development* **121**, 2655-2666.

Lieb, J. D., Albrecht, M. R., Chuang, P.-T. and Meyer, B. J. (1998). MIX-1: an essential component of the *C. elegans* mitotic machinery executes X chromosome dosage compensation. *Cell* **92**, 265-277.

Lillien, L. (1995). Changes in retinal cell fate induced by overexpression of EGF receptor. *Nature* **377**, 158-162.

Liu, J., Tzou, P., Hill, R. J. and Sternberg, P. W. (1999). Structural requirements for the tissue-specific and tissue-general functions of the *Caenorhabditis elegans* Epidermal Growth Factor LIN-3. *Genetics* **153**, 1257-1269.

Lumsden, A., Clarke, J. D. W., Keynes, R. and Fraser, S. (1994). Early phenotypic choices by neuronal precursors, revealed by clonal analysis of the chick embryo hindbrain. *Development* **120**, 1581-1589.

Maloof, J. N. and Kenyon C. (1998). The Hox gene *lin-39* is required during *C. elegans* vulval induction to select the outcome of Ras signaling. *Development* **125**, 181-190.

McConnell, S. K. and Kaznowski, C. E. (1991). Cell cycle dependence of laminar determination in developing neocortex. *Science* **254**, 282-285.

Miller, D. M. and Shakes, D. C. (1995). Immunofluorescence microscopy. *Meth. Cell Biol.* **48**, 365-394.

Mohler, W. A., Simske, J. S., Williams-Masson, E. M., Hardin, J. D. and Whites, J. G. (1998). Dynamics and ultrastructure of developmental cell fusions in the *Caenorhabditis elegans* hypodermis. *Current Biology* **8**:1087-1090.

Oehlen, L. J. W. M., McKinney, J. D. and Cross, F. R. (1996). Ste12 and Mcm1 regulate cell cycle-dependent transcription of *FAR1*. *Mol. Cell. Biol.* **16**, 2830-2837.

Raff, M. C., Abney, E. R. and Fok-Seang, J. (1985). Reconstitution of a developmental clock in vitro: a critical role for astrocytes in the timing of oligodendrocyte differentiation. *Cell* **42**, 61-69.

Riddle, D., Blumenthal, T., Meyer, B. and Priess, J., Ed. (1997). *C. elegans* II. Cold Spring Harbor Laboratory Press, New York.

Salser, S. J. and Kenyon, C. (1996). A *C. elegans* Hox gene switches on, off, on and off again to regulate proliferation, differentiation and morphogenesis. *Development* **122**, 1651-1661.

Salser, S. J., Loer, C. M. and Kenyon, C. (1993). Multiple HOM-C gene interactions specify cell fates in the nematode central nervous system. *Genes Dev.* **7**, 1714-1724.

Simske, J. S. and Kim, S. K. (1995). Sequential signaling during *Caenorhabditis elegans* vulval induction. *Nature* **375**, 142-146.

Simske, J. S., Kaech, S. M., Harp, S. A. and Kim, S. K. (1996). LET-23 receptor localization by the cell junction protein LIN-7 during *C. elegans* vulval induction. *Cell* **85**, 195-204.

Slack, J. M. W. (1991). From egg to embryo (Oxford, England: Oxford University Press).

Sommer, R. J. and Sternberg, P. W. (1994). Change of induction and competence during the evolution of vulval development in nematodes. *Science* **265**, 114-118.

Sternberg, P. W. (1988). Lateral inhibition during vulval induction in *Caenorhabditis elegans*. *Nature* **335**, 551-554.

Sternberg, P. W. and Horvitz, H. R. (1986). Pattern formation during vulval induction in *C. elegans*. *Cell* **44**, 761-772.

Sternberg, P. W. and Horvitz, H. R. (1989). The combined action of two intercellular signaling pathways specifies three cell fates during vulval induction in *C. elegans*. *Cell* **58**, 679-693.

Sulston, J. E. and Horvitz, H. R. (1977). Postembryonic cell lineages of the nematode *Caenorhabditis elegans*. *Dev. Biol.* **56**, 110-156.

Sulston J. E. and White, J. G. (1980). Regulation and cell autonomy during postembryonic development of *Caenorhabditis elegans*. *Dev. Biol.* **78**, 577-597.

Wang, B. B., Muller, I. M., Austin, J., Robinson, N. T., Chisholm, A. and Kenyon, C. (1993). A homeotic gene cluster patterns the anteroposterior body axis of *C. elegans*. *Cell* **74**, 29-42.

Wang, M. and Sternberg, P. W. (1999). Competence and commitment of *Caenorhabditis elegans* vulval precursor cells. *Dev. Biol.* **212**, 12-24.

Yochem, J., Weston, K. and Greenwald, I. (1988). The *Caenorhabditis elegans lin-12* gene encodes a transmembrane protein with overall similarity to Drosophila *Notch*. *Nature* **335**, 547-550.

TABLES

Table 1. Response of VPCs to *hs-LIN-3* at different times in wild-type and *let-23* overexpression backgrounds.

Time of heat shock[a]	*let-23(+)*[g] VPCs induced		*let-23(+++)* VPCs induced	
	%[b]	n[c]	%[b]	n[c]
no heat shock	0%	114	6%	105
L2 lethargus	99%	47	98%	32
early Pn.p[d]	87%	77	90%	10
late Pn.p[e]	53%	110	77%	65
early Pn.px[f]	0%	74	7%	121

Table 1. *hs-LIN-3; lin-3(lf)* and *hs-LIN-3; lin-3(lf); let-23(+++)* animals were staged using Nomarski optics and heat shocked at 31.5°C for 20 minutes.

[a] Stages of animals when heat shock began.

[b] A VPC was considered as adopting a vulval fate if it divided more than one round and remained unfused.

[c] Number of VPCs scored.

[d] Dorsal uterine cells had not divided. The VPCs scored were likely in G_1/S phase of the first cell cycle.

[e] Dorsal uterine cells were dividing or had divided once. In some cases, the distal VPCs (P3.p, P4.p or P8.p) started dividing, while the VPCs scored had not. They were likely in G_2 phase of the first cell cycle.

[f] The VPCs scored were dividing or had just divided.

[g] Wang and Sternberg, 1999.

Table 2. Response of VPCs to *hs-LIN-3* at different times in a *cul-1* mutant background.

| Time of heat shock[a] | VPCs induced to express *egl-17::GFP* at L3 | |
	%[b]	n[c]
no heat shock	0%	222
Pn.p stage[d]	56%	135
Pn.px stage[e]	45%[f]	311
Pn.pxx stage[g]	20%	102
Pn.pxxx stage[h]	5%	19
later[i]	0%	23

Table 2. *cul-1* homozygotes segregated from *egl-17::GFP; hs-LIN-3; cul-1 / unc-69; lin-3(lf)* were staged using Nomarski optics and heat shocked at 31.5°C for 20 minutes.

[a] Stages of animals when heat shock began. We were unable to determine whether VPCs were at the early or late stage of the cell cycle because of uncoupled relative timing of VPC divisions in the same animal (see text).

[b] We scored a VPC as adopting vulval fates, if *egl-17::GFP* expression was seen in all or part of its descendants during L3 lethargus.

[c] Number of VPCs scored.

[d] The VPCs scored had not divided yet.

[e] The VPCs scored were dividing or had divided to make 2 daughter cells.

[f] The percentage was adjusted: The original number 10% was divided by 22%, the percentage of VPCs that underwent excessive cell division without heat shock (n=222). The data from later heat shock experiments were not adjusted this way, since all VPCs divided more than once were considered as dividing excessively, compared with wild-type 3° cells, and usually kept dividing several times more.

[g] The VPC daughters scored were dividing or had divided to make 4 granddaughters.

[h] The VPC granddaughters scored were dividing or had divided to make 8 progeny.

[i] More than 8 descendants from a single VPC were present when scored.

FIGURES

Figure 1. The effects of LIN-39 overexpression on VPC competence.
Open bars, *egl-17::GFP; hs-LIN-3; lin-3(lf)*; striped bars, *egl-17::GFP; hs-LIN-3; lin-3(lf); hs-LIN-39*; solid bars, *egl-17::GFP; lin-3(lf); hs-LIN-39*. The horizontal axis shows the time of heat shock. The vertical axis indicates the percentage of VPCs that adopted the vulval fate after heat shock, except for single *hs-LIN-39* experiments (solid bars), in which the vertical axis indicates the percentage of VPCs that adopted the s fate instead of the wild-type 3° S fate (see Experimental Procedures). (A) Heat shocked at 31.5°C for 20 minutes. Inducing LIN-3 and LIN-39 simultaneously at the early Pn.px stage restored VPC competence from 0% (*hs-LIN-3* alone) to 14%. Similar synergy was also obvious during the late Pn.p stage. However, VPC response to single *hs-LIN-39* was at too low a frequency to be analyzed under this condition. (B) Heat shocked at 33°C for 30 minutes. Double heat shock *hs-LIN-3* and *hs-LIN-39* at the early Pn.px stage increased VPC competence from 2% (*hs-LIN-3* only) to 23%. Similar synergy was also obvious during the late Pn.p stage. VPCs adopted the s fate if LIN-39 was overexpressed at the late Pn.p stage (11%) or early Pn.px stage (4%), but not early Pn.p stage (0%). N.D., not determined.

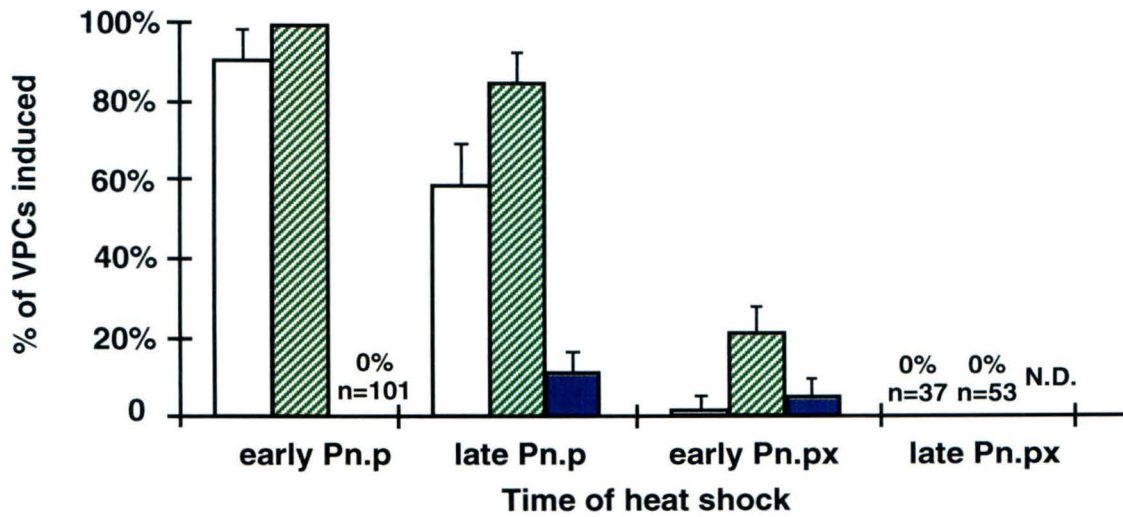**A. Mild heat shock**
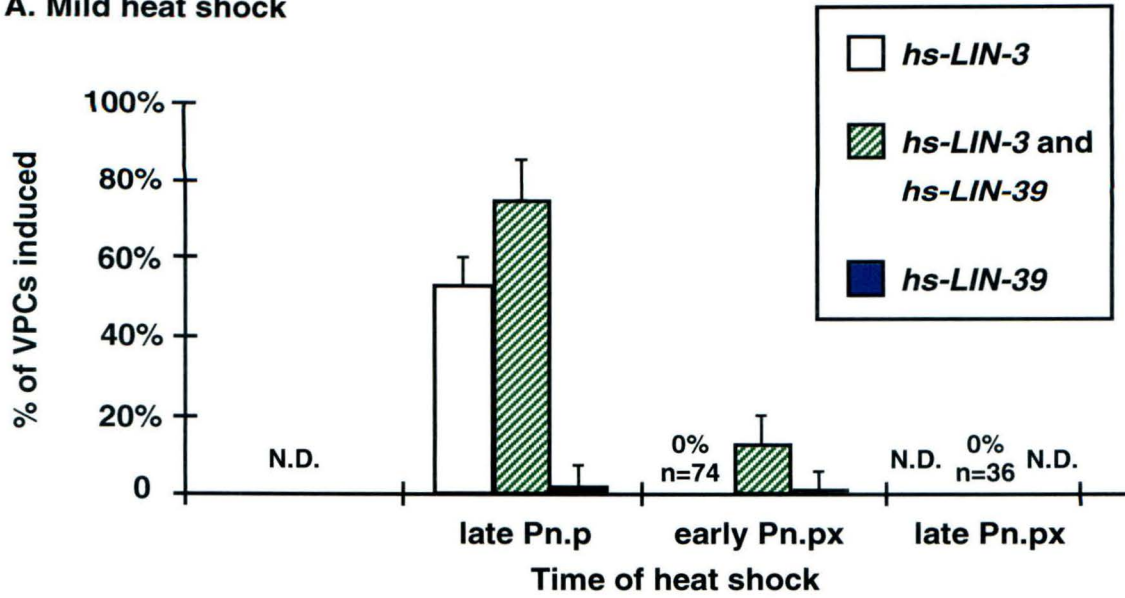
B. Strong heat shock

Figure 2. LIN-39 expression fluctuates in VPCs.

lin-3(lf); lin-12(gf) animals were stained using anti-LIN-39 antibodies and DAPI. In all panels, ventral is down, anterior is to the left. The scale bar is 10 μm. Arrowheads indicate VPC nuclei in (A)-(D) and VPC daughter nuclei in (E) and (F). (A), (C) and (E) are images of LIN-39 antibody staining, and (B), (D) and (F) are images of cell nucleus staining by DAPI. Staining in the neurons of the ventral cord can be seen as small nuclei between the VPCs in all panels. (A) and (B): An animal showing LIN-39 expression in all VPCs, except for P3.p, before VPC division. (C) and (D): An animal showing no or extremely faint LIN-39 expression in all VPCs before VPC division. (E) and (F): An animal showing LIN-39 expression in all VPC daughters after VPC division.
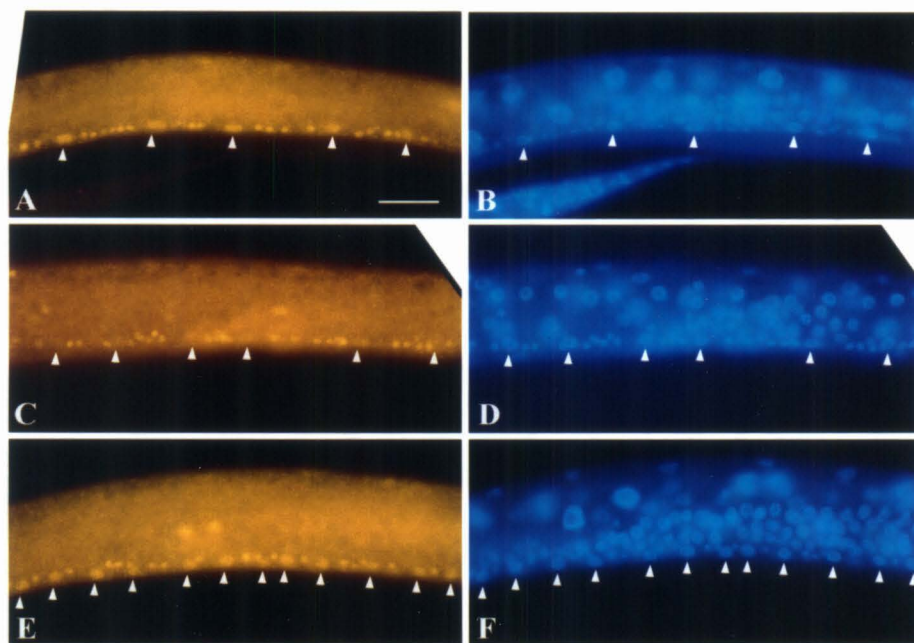
Figure 3. Competence of VPCs and VPC daughters in S and G2 phase of the cell cycle.

The axis at left is marked (A and B) in hours after molt from L2 to L3, and (B) in hours after VPCs' first division. Arrows indicate the time when heat shock was performed to induce LIN-3 expression. Yellow boxes indicate estimated S phase based on Euling and Ambros (1996) and our results. Red bars indicate HU treatment. The numbers are the percentage of VPCs that were induced to adopt (A) the vulval fate or (B) the non-2° vulval fate. n is the number of VPCs scored. (A) shows experiments done in an *egl-17::GFP; hs-LIN-3; lin-3(lf)* background. Without heatshock, HU alone does not induce VPCs to adopt vulval fates. VPCs in S of the first cell cycle provided with heat shock LIN-3 displayed 4/4 patterns of *egl-17::GFP* expression suggesting that they responded as VPCs. VPCs in G2 phase gave 2/4 patterns implying they responded as daughter cells. (B) shows experiments done in an *egl-17::GFP; hs-LIN-3; lin-12(gf); lin-3(lf)* background. The results of VPCs in S and in G2 phase of the first cell cycle were similar to those of (A). VPC daughters in S displayed 2/4 patterns indicating that they responded as VPC daughters, while VPC daughters in G2 responded as granddaughters, since they displayed 1/4 patterns.

A. *egl-17::GFP; hs-LIN-3; lin-3(lf)*

L2

(hrs)

0 1 2 3 4 5 6 L3 7 8 9 10 11 12

fuse fuse

S

HU 3 hrs

fuse fuse

100% (n=20)

LIN-3

HU 3 hrs

90% (n=30)

LIN-3

HU 3 hrs

1.5 hrs

60% (n=63)

LIN-3

HU 6 hrs

86% (n=36)

III-43

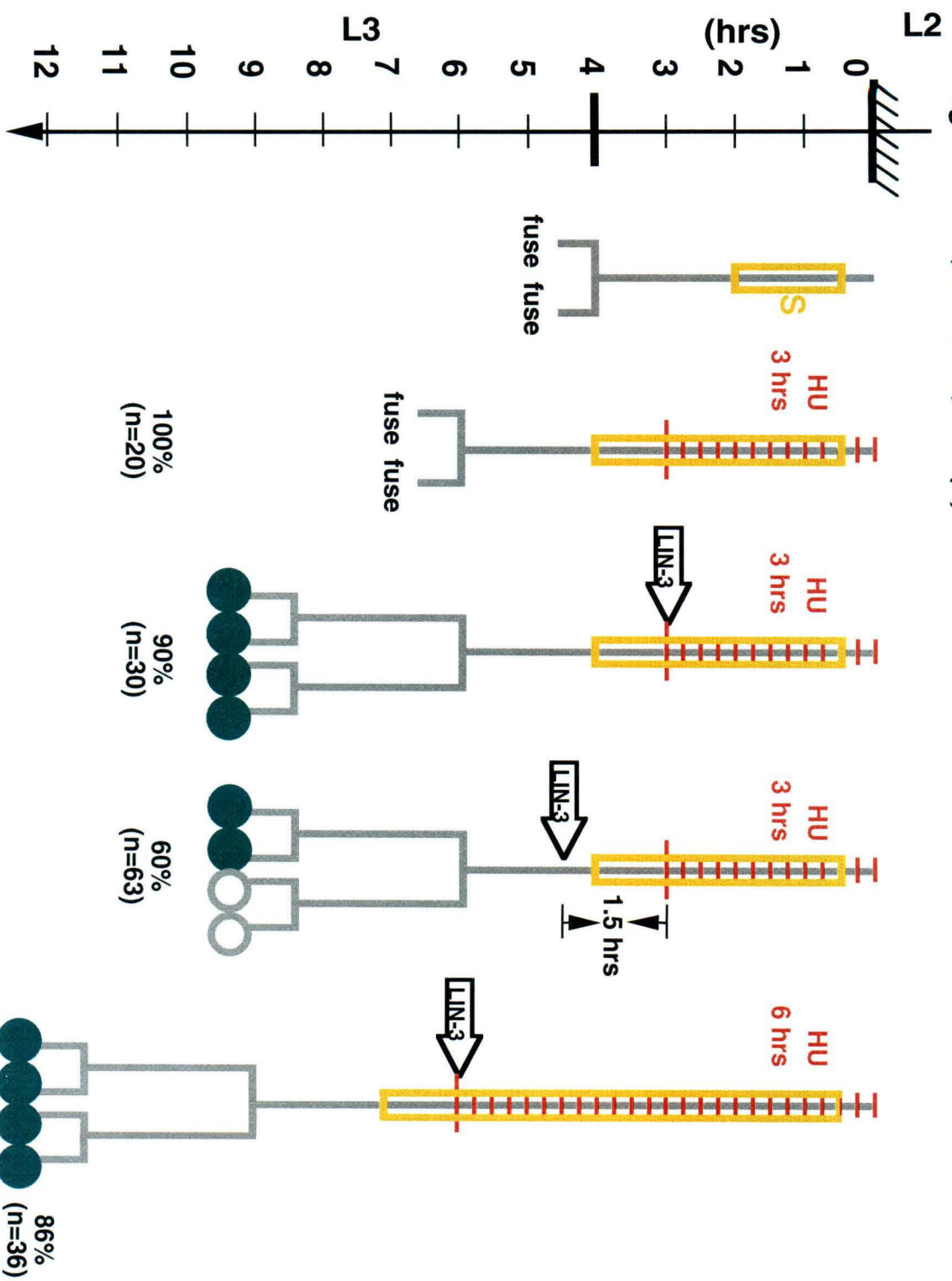B. *egl-17::GFP; hs-LIN-3; lin-12(gf); lin-3(lf)*

III-44

Figure 4. Hypothesis for cell cycle regulation of VPC competence.

VPCs are competent to respond to LIN-3, and presumably to the unknown

lateral signal, during G1 and S, but not the G2 phase of each cell cycle.

Change of LIN-39 activity coupled to cell cycle progression is proposed to

determine VPC competence. 1° and 2° cells at first share a common pathway,

then they are led to their specific fates by LET-23 or LIN-12 mediated

signaling. These two signaling pathways might act on the common

downstream target LIN-39, which mediates the common functions, including

preventing cell fusion and promoting cell cycle progression. VPCs that receive

neither the inductive and nor the lateral signal will eventually lose LIN-39

activity and fuse after a short G1 phase in the second cell cycle.
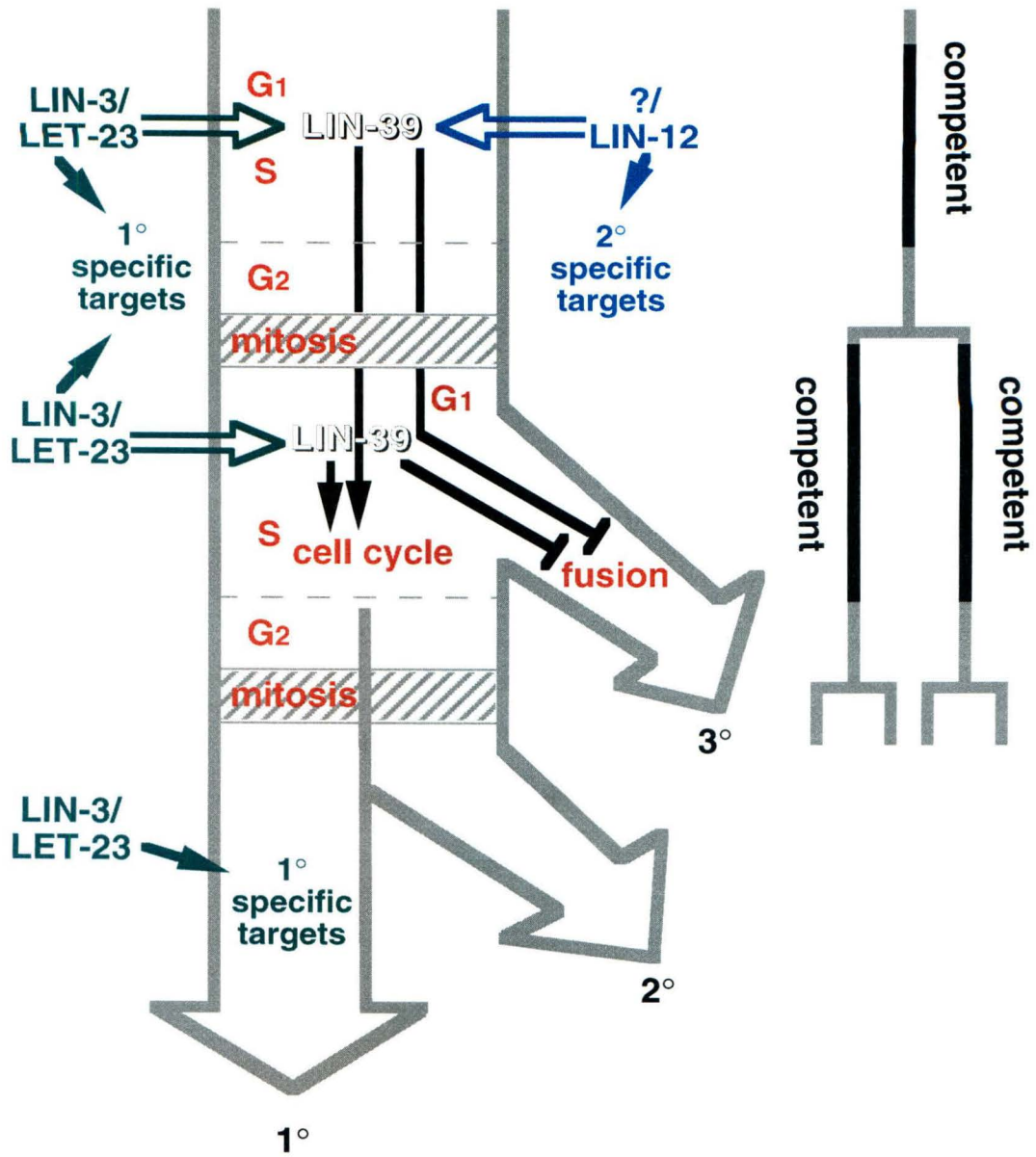
Chapter 4

Patterning of the 1° lineage in *C. elegans* vulval development

Minqin Wang and Paul W. Sternberg

(prepared for submission)

SUMMARY

In *C. elegans*, the descendants of the vulval precursor cell (VPC) that adopts the 1° fate establish a fixed spatial pattern of two different cell fates. The two inner granddaughters attach to the somatic gonadal anchor cell (AC) and generate four vulF cells, while the two outer granddaughters produce four vulE progeny. Using a molecular marker to distinguish these two fates, we find that *zmp-1::GFP* is expressed in vulE cells, but not vulF cells. Through perturbing one or more of the parameters in the 1° patterning process by laser ablation and use of different mutant backgrounds, we demonstrate that a short-range AC signal is required to ensure that vulE and vulF fates are properly specified. In addition, signaling between the inner and outer 1° VPC descendants, as well as intrinsic polarity of 1° VPC daughters, is involved in asymmetric divisions of 1° VPC daughters and proper orientation of the outcome. Finally, we show that Ras signaling may be used during AC signaling, while the LIN-17 Wnt receptor appears to mediate signaling between the inner and outer 1° VPC descendants.

INTRODUCTION

A basic question in developmental biology is how patterns of cell fates are formed. Studies into the development of ommatidia and the peripheral nervous system (PNS) in *Drosophila* have provided insight into underlying mechanisms that translate temporal and spatial information into patterns of cell fates (Banerjee and Zipursky, 1990; Jan and Jan, 1994; Freeman, 1997). Two kinds of patterning processes exist. First, unspecified precursor cells are induced to adopt different fates. Second, specified precursor cells execute their fates by dividing asymmetrically to form a defined pattern of different progeny cells. Although asymmetric cell division itself has been studied in a variety of developmental contexts (Horvitz and Herkowitz, 1992; Greenwald and Rubin, 1992; Schnabel and Priess, 1997; Jan and Jan, 1998), it remains unclear how precursors specified prior to their division execute their fates and generate correct patterns of descendants.

C. *elegans* vulval development is an excellent system for studying both types of pattern formation due to the ease of manipulation at the single cell level and the invariance of cell lineage in wild-type animals (Sulston and Horvitz, 1977; Sulston and White, 1980). Formation of a functional vulva can be divided into two major steps: the formation of the initial pattern of cell fates by the vulval precursor cells (VPCs), and the execution of different VPC fates through distinct cell divisions followed by morphogenesis of the descendants.

The first step, formation of the 3°-3°-2°-1°-2°-3° pattern of VPC fates, has been well studied. Six initially multipotential VPCs (P3.p-P8.p) are competent to adopt any of the three fates, 1°, 2° and 3° (Sulston and White, 1980; Kimble, 1981; Sternberg and Horvitz, 1986). Previous studies have revealed basic mechanisms that establish the fates of six VPCs (reviewed in Kenyon, 1995; Greenwald, 1997). The anchor cell (AC) in the somatic gonad produces a graded inductive signal LIN-3, an Epidermal Growth Factor, and induces the closest VPC, P6.p, to adopt the 1° fate (Sternberg and Horvitz, 1986; Hill and Sternberg, 1992; Katz et al., 1995). The LIN-3 signal activates signal transducers in the inductive signaling pathway, including LET-23, a receptor tyrosine kinase (RTK), and LET-60, a Ras homolog (Arioan et al., 1990; Beitel et al., 1990; Han and Sternberg, 1990). An induced 1° VPC laterally signals its immediate neighbors, P5.p and P7.p, to adopt the 2° fate through the LIN-12 receptor, a Notch homolog (Greenwald et al., 1983; Koga and Ohshima, 1995; Simske and Kim, 1995). *lin-15* negatively regulates the Ras signaling pathway and represses vulval fates in absence of LIN-3 (Clark et al., 1994; Huang et al., 1994).

This study focuses on how a specified VPC executes its fate decision to give rise to a distinct cell lineage. Using the 1° lineage as an example, we dissect the mechanisms that are involved in patterning the VPC lineage after VPC fate specification. Previous studies suggest that the VPCs are specified before their first division (Greenwald et al., 1983; Sternberg and Horvitz, 1986; Ferguson et al., 1987; Euling and Ambros, 1996). After P6.p *is induced* by the AC to adopt the 1° fate at the late L2 and early L3 stage (Kimble, 1981; Sternberg and Horvitz, 1986), it divides twice during the L3

stage. During L3 lethargus (the interval between L3 and L4), the four

granddaughters of P6.p (P6.pxx) form a line along the anteroposterior axis.

The AC attaches to the two inner P6.pxx cells (P6.pap and P6.ppa) and

away from the two outer P6.pxx cells (P6.paa and P6.ppp) (Figure 1A; also

see Results). All four P6.pxx cells then divide transversely, and the eight

great granddaughters (P6.pxxx) detach from the ventral cuticle, migrate

dorsally and form a symmetric invagination at the L4 stage (Figure 1B and

Figure 2A). In wild-type animals, 1° descendants produce a fixed spatial

pattern of cell fates: the four inner P6.pxxx cells become vulF, and the four

outer P6.pxxx cells become vulE. The four vulE cells fuse to form a toroidal

multinucleate cell, stacked beneath a ring formed by the analogous fusion

of the four vulF cells (Sharma-Kishore et al., 1999). At mid-L4,

establishment of the connection between the uterus and the vulva requires

separation of the vulval cells most proximal to the AC, the vulF cells, and

the formation of the uterine-seam (utse) syncytium through AC fusion with

the uterine π cells in the gonad (Newman et al., 1996). The vulval

invagination starts to evert at the late L4 stage, and the vulva lips are

formed during L4 lethargus (Figure 1C).

In this work, we analyze how a specified 1° VPC executes its fate by

generating a pattern of 8 descendants. We test possible roles for the AC, the

VU cells, the descendants of the 1° VPC, and the neighboring 2° VPCs. We

also manipulate the numbers of the AC as well as the relative positions of

the AC to the 1° VPC descendants. We have found that the 1° lineage

patterning may involve at least three different mechanisms. Besides a

short-range AC signal that patterns the inner and outer 1° VPC

descendants, signaling between the inner and outer 1° VPC descendants and intrinsic polarity of 1° VPC daughters contribute to the asymmetric divisions of 1° VPC daughters and the proper orientation of the results.

MATERIALS AND METHODS

General methods and strains

C. elegans strains were handled at 20°C according to standard protocols (Brenner 1974; Wood 1988). The following alleles were used: for LGI, *lin-17(n671)*; for LGII, *vab-1(dx31)*; for LGIII, *dig-1(n1321), dpy-19(e1259), lin-12(n137), lin-12(n676n909), pha-1(n2123ts), unc-32(e189)*; for LGIV, *dpy-20(e1282), syIs49[zmp-1::GFP; dpy-20(+)]*; for LGX, *unc-6(ev400)* (Brenner, 1974; Greenwald et al., 1983; Katz et al., 1995).

Transgenic lines were generated using the standard microinjection protocol that produces high copy number extrachromosomal arrays (Mello et al., 1991). The *zmp-1::GFP* transgene *syEx282* was obtained by microinjection of pJB100 (J. Butler and J. Kramer, personal communication) at 100ng/µl and pMH86 (*dpy-20(+)*) at 15ng/µl, into *dpy-20(e1282)* mutant animals. Heritable lines bearing the marker DNA [scored by rescue of *dpy-20(e1282)*] and GFP expression were isolated and treated with X-rays (3800rad) to promote chromosomal integration and generate *syIs49* (Way et al., 1991). The *hs-ras(dn)* transgene *syEx284* was obtained by microinjection of pPD49.83:ras149 (C. Sigrist and R. Sommer, personal

communication) at 100ng/μl and pBX *(pha-1(+))* at 100ng/μl, into *pha-1(e2123ts); him-5(e1490)* mutant animals. Heritable lines were scored by rescue of the lethality of *pha-1(e2123ts)* at 20°C.

Cell ablations

Cell ablations were performed with a laser microbeam according to standard methods (Sulston and White, 1980). For the AC ablation experiments in Table 1D, 5, 6, Figure 2, 4C and 4D, the AC was ablated when P5.px and P7.px were dividing or had just divided, and P6.px had not divided yet, were dividing, or had just divided. P5.p, P6.p, P7.p, and their descendants divide at approximately the same time, but the P6.px cells usually divide about 5 to 10 minutes later than the P5.px and P7.px cells (M. W. and P. W. S., unpublished). Therefore, the AC was ablated at the late P6.px stage or the early P6.pxx stage. For the AC ablation experiments in a *lin-12(lf)* background in Table 3A, 3C and Figure 3G, 3H, ACs were ablated at the early L3 stage when the DU cells had not divided. The success of the ablation was confirmed by observing under Nomarski optics 3-8 hrs after ablation during L3 lethargus when the position of the AC was scored. Intact animals and ablated animals were mounted on agar pads containing sodium azide for about 15 minutes before being put back on individual plates.

Heat shock of transgenic animals

Animals were mounted on agar pads, examined using Nomarski optics to confirm their stages (Sulston and Horvitz, 1977; Kimble and Hirsh, 1979)

and then recovered on seeded plates for 10 minutes before heat shock

treatment. All heat shock pulses were performed at 33°C for 30 minutes.

Animals were placed on prewarmed plates of desired temperature, sealed

with Parafilm, and then floated in a covered water bath of the same

temperature. After heat shock, animals were transferred immediately to

plates kept at 20°C until the mid-L4 stage and L4 lethargus when they were

scored for uterine-vulval connection and *zmp-1::GFP* expression in P6.pxxx

cells.

Scoring the 1° pattern

Expression patterns of *zmp-1::GFP* were observed using Nomarski optics

and a Zeiss Axioplan microscope with a 200-watt HBO UV source, using a

Chroma High Q GFP LP filter set (450nm excitation/ 505nm emission).

Photographs were taken with a Hamamatsu digital camera and the

Improvision Openlab 2.0.6 software.

The pattern of *zmp-1::GFP* expression in great granddaughters of the

1° VPC was scored during L4 lethargus. For experiments in Table 3C and

Figure 3, 8 of the 16 P5.pxxx and P6.pxxx cells at either the left or right side

(the upper focal plane) of the animals were scored. In many cases, the

other side was difficult to score, and therefore not included in the data. For

all other experiments, all P6.pxxx cells at both left and right sides of the

animals were scored.

RESULTS

1° vulval patterning in wild-type animals

In wild-type animals, all four granddaughters (P6.pxx) of the 1° VPC, P6.p,

divide transversely, and the outer and inner great granddaughters of P6.p

(P6.pxxx) produce two different cell types, vulE and vulF, respectively

(Sulston and Horvitz, 1977; Sternberg and Horvitz, 1986; Sharma-Kishore et

al., 1999; Figure 1). The inner and outer P6.p descendants differ in their

morphogenesis and fusion behavior. For example, during L3 lethargus,

the AC invariably attaches to the two inner P6.pxx cells (Figure 1A; D. R.

Sherwood and P. W. S., unpublished). Also, the inner P6.pxx cells divide

slightly later and are more dorsally positioned compared with their outer

counterparts (Sharma-Kishore et al., 1999). After P6.pxxx cells are

generated, the inner P6.pxxx cells (vulF) invaginate to a greater extent than

the outer P6.pxxx cells (vulE).

To look for markers that have differential expression patterns in vulE

and vulF cells, we examined the distribution of a *zmp-1::GFP* fusion protein

(J. Butler and J. Kramer, personal communication). *zmp-1* is a *C. elegans*

zinc metalloproteinase (Massova et al., 1998). We generated transgenic

lines containing integrated copies of the *zmp-1::GFP* reporter gene and

determined its expression pattern in wild-type animals. We found that

zmp-1::GFP was expressed in the AC throughout the L3 and the early L4

stage. It was not expressed in P6.p, P6.px, or P6.pxx cells. The expression

in the P6.pxxx cells began in late-L4. During L4 lethargus, *zmp-1::GFP*

was expressed in all four vulE cells, but not in any vulF cells, in all animals

observed (n=138, Figure 1C, 2B and 2C). The expression in vulE cells

persists in the adult stage. In wild-type animals, the transverse divisions

of P6.pxx result in two identical patterns of vulE and vulF cells at the left

and right sides of the animal (Figure 1C). In this paper, we consider the

pattern at each side as a half 1° lineage patterning unit to organize our

data.

Based on several lines of evidence, *zmp-1::GFP* can be used reliably to

distinguish the vulE and vulF fates. First, as described above, this marker

has a spatially and temporally invariable expression pattern in wild-type 1°

VPC great granddaughters. Second, the proper expression of *zmp-1::GFP*

correlates with the morphological criteria of a properly patterned 1°

lineage, i.e., a correct vulval-uterine connection required for egg-laying.

Mutant or experimentally manipulated animals with abnormal *zmp-*

1::GFP expression in the 1° lineage never formed a proper connection (0%,

n=174 animals, e.g., Figure 2G, 2H and 2I). Occasionally the 1°

descendants with a wild-type *zmp-1::GFP* expression pattern also failed to

form a connection between the uterus and the vulva (11%, n=207 animals;

also see below). Therefore, correct expression pattern of *zmp-1::GFP* may

reflect one aspect of the differentiation of the inner and outer great

granddaughters of the 1° VPC and it appears to be a prerequisite to indicate

proper patterning of the 1° lineage.

The neighboring 2° lineages are not required for 1° patterning

The generation of patterns of 1° descendants with different fates could rely

on intrinsic or cell signaling mechanisms. To examine whether any

signaling from other cells in the 1° VPC's vicinity or between neighboring cells of 1° descendants are required for 1° patterning, we ablated both 2° VPCs, part of the 1° descendants, or some gonadal cells, and examined the 1° pattern formation by using *zmp-1::GFP* as a marker.

To determine whether the neighboring 2° lineages are necessary for correct expression of *zmp-1::GFP* in 1° descendants, we ablated P5.p and P7.p, the two 2° VPCs flanking the presumptive 1° VPC P6.p, prior to the birth of any P6.p descendants. In these animals, the 1° lineage was correctly patterned as assessed by *zmp-1::GFP* expression (n=20 half 1° lineage patterning units, Table 1A), as well as by the morphological criteria of a proper vulval-uterine connection (data not shown). In addition, in *lin-12(lf)* mutants where the 2° fate is not specified, isolated 1° lineages invariably had the wild-type expression pattern of *zmp-1::GFP* (Greewald et al., 1983; Table 3A; also see below). Therefore, the 2° VPC neighbors may not be required for 1° patterning.

Each anterior and posterior half of the 1° lineage patterns autonomously

The developing vulva is mirror-symmetric and previous studies have shown that the anterior and posterior halves of the vulva develop autonomously during vulval morphogenesis and cell fusion (Sharma-Kishore et al., 1999; Shemer et al., 2000). When we ablated P6.pa or P6.pp, the other P6.px underwent its normal division to produce two outer P6.pxxx cells that expressed *zmp-1::GFP* and two inner P6.pxxx cells that did not express the marker (n=18 half 1° lineage patterning units, Table 1B). The morphology of the half 1° vulva left was also normal in these animals (data

not shown). Each anterior and the posterior half of the 1° lineage can therefore pattern autonomously.

The AC (but not VU) is required for 1° patterning

Besides the 2° VPCs and their descendants, the other set of cells in the vicinity of the 1° VPC and its descendants includes the AC and its surrounding VU precursors in the gonad (Kimble and Hirsh, 1979). Before the first division of the VPCs, the AC is surrounded by three VU precursors (Kimble and Hirsh, 1979). The VU precursors then divide twice, and their granddaughters become specified as π and ρ precursors which generate uterine cells, such as utse and uv1 (Kimble and Hirsh, 1979; Newman et al, 1996).

When we ablated all three VU precursor cells before their division at the early L3 stage (VPCs were also undivided at that time), the P6.pxxx cells had the wild-type *zmp-1::GFP* expression pattern (n=34 half 1° lineage patterning units, Table 1C, Figure 2E and 2F). At mid-L4, the vulval-uterine connection was otherwise normal except that it was blocked by the unfused AC, which failed to form utse in the absence of π cells (Figure 2D). Also, in *lin-12(lf)* mutants, where the π fate is not specified, isolated 1° lineages can invariably form a correct pattern (Newman, et al., 1995; Table 3A; also see below). Therefore, the VU precursor lineages are not requied in patterning the 1° lineage.

We then examined whether the AC is required for 1° lineage patterning. Previous AC ablation studies by Kimble (1981) suggest a

possible role for the AC after the induction of VPCs in making a functional vulval-uterine connection. To separate a possible late role for the AC in 1° patterning from its earlier function in VPC fate specification, we ablated the AC at the late P6.px stage or the early P6.pxx stage, after VPC fates are specified (Greenwald et al., 1983; Wang and Sternberg, 1999). Although all P5.p, P6.p, and P7.p were induced to divide three times after AC ablation as in intact animals, the inner P6.pxxx cells did not properly separate to form the uterine-vulval connection, and the vulva invariably had an abnormal morphology (Figure 2G). When we scored *zmp-1:::GFP* expression in P6.pxxx cells, the expression of *zmp-1::GFP* in P6.pxxx cells was disturbed in 51 of 70 resulting patterns (Table 1D, Figure 2H and 2I). The patterns of P6.pxxx cells lacking the AC appear variable: we observed all 10 possible patterns, but some patterns are obviously preferred (Table 1D and 7; also see Discussion). We conclude that the AC is required after the initial induction of the 1° VPC fate to ensure the wild-type patterning of the 1° lineage.

When we ablated the AC at the late P6.pxx stage, all resulting patterns had the wild-type *zmp-1::GFP* expression in P6.pxxx cells (n=20 half 1° lineage patterning units, Table 1E), as well as normal morphology of the 1° vulva (data not shown). Therefore, the AC may signal the P6.pxx cells, rather than P6.pxxx cells, to pattern the 1° lineage.

Wild-type 1° patterning requires the AC at short range

Although the AC is involved in 1° patterning, it is not clear whether a short distance between the AC and the 1° descendants is required. We therefore

examined the patterning of 1° VPCs, with or without AC attachment, in

dig-1 or *unc-6* mutants.

87% of *dig-1* mutant animals have an anteriorly-shifted gonad

(Thomas et al., 1990). In these animals, the AC is closest to P4.p or P5.p,

rather than P6.p, and the VPC closest to the AC invariably adopts the 1° fate

(Thomas et al., 1990). We found that the AC attached to the two inner

P4.pxx or P5.pxx cells at L3 (n=16 animals). We scored either P4.p or P5.p,

whichever was closest to the AC, and found that, in 44 of 45 these 1° VPCs,

a wild-type *zmp-1::GFP* expression pattern was formed (Table 2).

Therefore, P4.p and P5.p descendants are capable of forming a wild-type 1°

pattern if the AC is positioned nearby.

In 13% of *dig-1* mutant animals, the gonad primordium is displaced

to the dorsal side of the animal (Thomas et al., 1990). In these animals, the

AC is mispositioned dorsally along with the gonad, and the AC is at least

20μm (measured as a direct distance) away from the VPCs (Thomas et al.,

1990). Any of P4.p, P5.p, or P6.p, can be the closest VPC to the AC and can

then adopt the 1° fate. We found that only 4 of 38 1° VPCs (scored according

to detachment of descendants from ventral cuticle and symmetry of

invagination; Katz et al., 1995) with a dorsal gonad displayed a wild-type

zmp-1::GFP expression pattern in its descendants ($P<0.0001$, Fisher's exact

test, Table 2), suggesting that the AC is able to pattern the descendants of a

1° VPC locally, but not at long range.

In *unc-6* mutants, the gonad is positioned ventrally as in wild type.

However, in about 22% of the animals, the AC improperly migrates dorsally

or laterally within the ventral gonad (the distance between the AC and

P6.pxx cells is less than 20μm), rather than attaching to the inner P6.pxx

cells during L3 lethargus (Hedgecock et al., 1990; D. R. Sherwood and P. W.

S., unpublished). In 26 animals with a displaced AC, only 4 of 26 P6.p cells

had wild-type patterns of *zmp-1::GFP* expression in its progeny (Table 2).

In contrast, when the AC was correctly positioned and attached to inner

P6.pxx cells, all 37 P6.p cells formed the wild-type 1° pattern, indicating

that P6.p descendants are capable of forming a wild-type 1° pattern in an

unc-6 background, when the AC is correctly positioned (*P*<0.0001, Table 2).

These results indicate that proper patterning of the 1° lineage utilizes

a local signaling mechanism, possibly requiring direct cell-cell contact

between the AC and the 1° VPC granddaughters.

**Patterning of the 1° lineage with multiple ACs indicate that the AC signals
the 1° VPC granddaughters it contacts to ensure the production of vulF
progeny**

To clarify how the AC patterns the 1° lineage, we examined the *zmp-1::GFP*

expression pattern in VPC descendants in isolated 1° lineages with

multiple ACs. In *C. elegans*, LIN-12 is used repeatedly as the receptor for

lateral signaling. During early gonadal development, signaling between

two initially equivalent cells, Z1.ppp and Z4.aaa, is mediated by *lin-12* and

determines which cell becomes the AC and which becomes the ventral

uterine (VU) precursor cell (Kimble, 1981; Greenwald et al., 1983; Seydoux

and Greenwald, 1989). Afterwards, during vulval induction, LIN-12

functions again in lateral signaling between the VPCs to induce the 2° fate

(Sternberg, 1988; Sternberg and Horvitz, 1989; Koga and Ohshima, 1995; Simske and Kim, 1995).

In a *lin-12* loss-of-function mutant background, both Z1.ppp and Z4.aaa become ACs (Greenwald et al., 1983). In some cases, one or more of their sisters also undergoes transformation, resulting in more than two ACs (Sternberg and Horvitz, 1989; M.-A. Félix, personal communication). Out of 49 *lin-12(lf)* mutant animals examined, 32 had 4 ACs, 12 had 3 ACs, 4 had 2 ACs, and 1 had 5 ACs. Moreover, in the absence of LIN-12 activity, two or three central VPCs (P5.p and P6.p, or P5.p, P6.p and P7.p) adopt the 1° fate, while the distal VPCs (P3.p, P4.p and P8.p) adopt the 3° fate (Greenwald et al., 1983; Sternberg and Horvitz, 1989). We controlled the number of ACs and the 1° VPCs by laser ablation in a *lin-12(lf)* background.

We first ablated P5.p and P7.p, as well as all but one AC. In all 6 animals scored, the AC attached to the two inner P6.pxx cells during L3 lethargus. *zmp-1::GFP* was expressed in the outer P6.pxxx cells (as vulE), but not the inner cells (as vulF), during L4 lethargus (Table 3A). This indicates that a single 1° lineage with a single AC in a *lin-12(lf)* background patterns correctly, and that *lin-12* is not required for proper patterning of the 1° lineage.

We then examined patterning of isolated 1° lineages with multiple ACs. This time we ablated P5.p and P7.p, but left the multiple ACs intact. The ACs attached to the two inner P6.pxx cells in 12 of 14 animals, and the wild-type *zmp-1::GFP* expression pattern in P6.pxxx cells was observed (Table 3B, Figure 3A and 3B). The ACs in the remaining two animals attached to one of the two outer P6.pxx cells, in addition to the two inner

P6.pxx cells. Subsequently, the inner P6.pxxx cells, as well as the P6.pxxx progeny of the outer P6.pxx attached to the ACs, failed to express *zmp-1::GFP*, while the P6.pxxx progeny of the other outer P6.pxx expressed GFP (Table 3B, Figure 3C and 3D). Therefore, the AC can signal the P6.pxx cells that it contacts to generate vulF progeny.

To examine the patterning of two adjacent 1° lineages, we ablated P7.p in a *lin-12(lf)* background. When we left multiple ACs intact, the ACs attached to various numbers of posterior P5.pxxx cells and anterior P6.pxxx cells (data not shown). Subsequently, 137 of 144 central Pn.pxxx cells (P5.ppax, P5.pppx, P6.paax and P6.papx) behaved as vulF and did not express the marker (e.g., Figure 3E and 3F). When we ablated all ACs at early L3 before VPCs' first division, only 22 of 48 central Pn.pxxx cells did not express the marker ($P<0.0001$, Fisher's exact test). These results indicate that the AC may signal the P6.pxx cells that it contacts to ensure that vulF progeny will be generated.

Ras signaling may be used by the AC to pattern the 1° lineage

We tried to elucidate the signals and pathways that are utilized in 1° patterning. As shown above, *lin-12* is not required to pattern the 1° lineage. Since Ras LET-60 is the signal transducer during the initial AC induction of VPC fates, we tested whether Ras also functions later in patterning the 1° lineage.

To test the effect of interrupted Ras signaling on 1° patterning, we used a heat shock construct which encodes a putative dominant negative form of Ras from the closely related nematode *Pristionchus pacificus* (*hs-*

ras(dn); C. Sigrist and R. Sommer, personal communication). This Ras
variant is about 90% identical to LET-60 and contains a G10R mutation
(Sommer et al., 1996). In *C. elegans*, a G10R mutation of *let-60 ras* has a
dominant negative effect on the inductive signaling activity and causes a
vulvaless phenotype (Han and Sternberg, 1991).

We crossed *zmp-1::GFP* into the transgenic line carrying *hs-ras(dn)*,
heat shocked the animals at different times, and then scored the *zmp-
1::GFP* expression pattern in the 1° lineage. When we heat shocked
animals before VPCs' first division, P5.p, P6.p or P7.p always adopted the 3°
fate (n=16 animals), indicating that wild-type Ras activity was effectively
blocked by heat shock at this stage. When we tried to disrupt Ras signaling
after the 1° VPC was specified by heat shocking animals during the late
Pn.px or the early Pn.pxx stage, three central VPCs (P5.p-P7.p) were
induced to divide three times as in wild type, but the pattern of *zmp-1::GFP*
expression in P6.pxxx cells was abnormal (Table 4, Figure 4A and 4B). The
distribution of these abnormal patterns was very similar to the patterns of
1° lineage resulting from AC ablation (*P*=0.83, Fisher's exact test, Table 1),
suggesting that Ras may be used to transduce the AC signal to program the
1° VPC granddaughters. However, it remains possible that Ras is involved
in other aspects of the 1° patterning process, or affects the process
indirectly, such as by facilitating the function of the AC.

If the AC utilizes Ras signaling to pattern the 1° lineage, constitutive
activation of the receptor LET-23 might be able to bypass the requirement of
the AC. We used a gain-of-function allele of *let-23* (RTK), *sa62*, to
constitutively activate Ras signaling (Katz et al., 1996) and ablated the AC in

this background (Table 5). When the AC was ablated at the late P6.pxx or the early P6.pxxx stage in *let-23(sa62)* mutants, 13 out of 16 animals had wild-type *zmp-1::GFP* expression, which is significantly different from the result obtained from AC ablation in a wild-type background (*P*<0.0001, Table 5). This result indicates that the 1° patterning defects in the absence of the AC can be rescued by the ligand-independent activated LET-23, consistent with Ras activation being involved in transducing the AC signal to pattern the 1° lineage.

To examine whether all components connected with the Ras pathway during initial 1° VPC fate specification are also required in patterning of the 1° lineage, we examined *zmp-1::GFP* expression in various mutant backgrounds. To avoid disruption of the initial 1° VPC fate specification, we scored only mutants with at least wild-type levels of VPC induction (3 or more VPCs induced).

During the initial VPC fate specification, *lin-15* negatively regulates the Ras signaling pathway (Ferguson et al., 1987; Sternberg, 1988; Clark et al., 1994; Huang et al., 1994). In a *lin-15* loss-of-function background, all VPCs often adopt vulval fates, and P6.p is always the closest VPC to the AC and adopts the 1° fate. We observed wild-type *zmp-1::GFP* expression in 39 of 41 P6.p lineages (Table 5; the remaining two animals had an abnormal gonad). Therefore, the *lin-15* gene is not required for normal 1° patterning. Furthermore, unlike *let-23(gf)*, the *lin-15(lf)* mutation does not suppress the 1° patterning defect caused by the absence of the AC. When the AC was ablated at the late P6.px stage or the early P6.pxx stage, the expression patterns of *zmp-1::GFP* in P6.pxxx cells were disturbed in 17 of 19 animals

examined (P<0.0001, Table 5). This result indicates that *lin-15* may not be

involved or negatively regulate Ras signaling during 1° lineage patterning.

lin-1 encodes an ETS domain transcription factor and is a

downstream inhibitor of vulval induction that is negatively regulated by *let-60 ras* (Beitel et al., 1995). Similar to *lin-15* mutants, *lin-1* loss-of-function

mutants have all VPCs adopting vulval fates, and the AC is closest to P6.p,

which always becomes 1°. We found that the *zmp-1::GFP* expression

pattern in P6.pxxx was abnormal in 18 of 23 animals examined (Table 5),

indicating that *lin-1* may be involved in 1° lineage patterning.

LIN-31, a winged helix transcription factor, is another factor

functioning downstream of Ras signaling (Miller et al., 1993). In a *lin-31*

mutant background, VPCs adopt vulval or non-vulval fates randomly,

although P6.p is always the closest VPC to the AC. We scored the

patterning of P6.p descendants only when P6.p adopted the 1° fate (scored

according to detachment of descendants from ventral cuticle and symmetry

of invagination; Katz et al., 1995), and found that it displayed the wild-type

zmp-1::GFP expression pattern in its progeny in all cases (n=31 animals,

Table 5). Therefore, *lin-31* is not required during 1° lineage patterning.

Patterning of adjacent 1° lineages with a single AC reveals signaling between the inner and outer 1° VPC descendants

Besides AC signaling, it is possible that there are other intercellular

signaling mechanisms involved in 1° lineage patterning. To address this

issue, we ablated P7.p and all but one AC in a *lin-12(lf)* background to

examine patterning of adjacent 1° lineages with a single AC. In all 14

animals examined, the Pn.pxx cells that attached to the AC gave rise to progeny that did not express GFP (as vulF), while their flanking Pn.pxx cells always produced progeny that expressed GFP (as vulE) (Table 3C, Figure 3G and 3H). The rest of the Pn.pxxx cells showed a random pattern of GFP expression. These results show that the AC signals the 1° VPC granddaughters it contacts to produce vulF progeny. Their immediate neighbors invariably generate vulE progeny. However, the progeny of the more distal neighbors do not form an invariant pattern. Notably, the Pn.pxxx cells surrounding the AC that form the E-F-F-E pattern do not always descend from the same 1° VPC daughter and therefore do not always possess internal differences through intrinsically polar mother cells. We infer that in addition to AC signaling, there is likely signaling between the inner and outer 1° VPC descendants (P6.pxx or P6.pxxx cells) in patterning the 1° lineage.

In the above experiment, all 28 vulF cells that attached to the AC had a vulE neighbor (100%, Table 3C). In contrast, only 64 of 105 inner vulF cells in wild-type animals without an AC had an outer vulE neighbor (61%, Table 1D). Therefore, signaling between the inner and outer 1° VPC descendants may be partly triggered by AC signaling the inner 1° VPC descendants. Alternatively, the AC could also signal the outer 1° VPC descendants from a distance to produce the vulE progeny (see Discussion).

Bias of 1° lineage patterning in the absence of AC signaling reveals intrinsic polarity of 1° VPC daughters

Is there an intrinsic mechanism to generate polar 1° VPC daughters during 1° lineage patterning? Two lines of evidence suggest that the inner 1° VPC granddaughters are different from the outer cells prior to AC-dependent patterning of the 1° lineage.

First, positioning of the AC with respect to the 1° VPC progeny is biased in wild-type animals. Before P6.p's first or second division, the AC is not always in the middle of P6.p daughters. However, the AC invariably migrates and ends up attaching to the inner P6.pxx, but not the outer P6.pxx during L3 lethargus (D. R. Sherwood and P. W. S., unpublished). When both 2° neighbors and one of the 1° VPC daughters were ablated, the AC invariably attached only to the one presumptive inner granddaughter left, but not to the presumptive outer granddaughter (n=9 animals). Strikingly, when multiple ACs were present in a *lin-12(lf)* background, they attached to only the inner P6.pxx cells in 12 of 14 cases examined (Table 3B). Considering the relatively random position of the AC before the 1° VPC granddaughters were born, if the inner and outer granddaughters of the 1° VPC were equally attractive to the AC, the AC should have been positioned more randomly.

Second, the 1° descendants are predisposed in adopting the vulF or vulE fate when the AC is absent or Ras signaling is disrupted. Simply turning on Ras signaling through *let-23(gf)* can partially rescue the 1° patterning defect caused by the absence of the AC (Table 5), suggesting that the inner and outer 1° VPC descendants can differentiate from one another independent of the AC. Furthermore, when the AC was ablated, Ras signaling disrupted by heat shock induced Ras(dn) after the induction of the

VPC fates, or *lin-1* mutated, the 1° descendants expressed *zmp-1::GFP* in a variable fashion (Table 1D, 4 and 5). However, a careful examination of the pattern of *zmp-1::GFP* expression shows that among the pairs of 1° inner and outer P6.pxxx cells that adopted different fates, 64/70, 33/38, and 48/52 had the proper orientation with vulF facing the normal position of the AC, respectively (Table 7). Since unbiased signaling between the inner and outer 1° VPC descendants can not produce invariably oriented asymmetric divisions of 1° VPC daughters, such a bias towards specifically oriented 1° lineage pattern might involve an intrinsic mechanism that forms polar 1° VPC daughters.

LIN-17 may mediate signaling between the inner and outer 1° VPC descendants

lin-17 encodes a seven-transmembrane protein similar to *Drosophila Frizzled*, a Wnt receptor (Vinson et al., 1989; Sawa et al., 1996). In *lin-17* mutants, asymmetric divisions of many different types of cells are disrupted (Ferguson et al., 1987; Sternberg and Horvitz, 1988; Way et al., 1992; Chamberlin and Sternberg, 1995; Jiang and Sternberg, 1998). In the vulva, the asymmetric division of P7.p is either abolished or reversed. We suspected that LIN-17 could be involved in the asymmetric divisions of the 1° VPC daughter P6.px, despite that the 1° lineage patterning is wild-type in *lin-17(lf)* mutants (Table 6). First, a *lin-17::lacZ* reporter gene was expressed in all P6.pxx cells (Sawa et al., 1996). Second, and more importantly, double mutants of *lin-17* and *lin-18*, another gene involved in asymmetric divisions in the 2° vulval lineage, show defects in *zmp-1::GFP*

expression in P6.pxxx cells, although neither single mutant does (Table 6;

Ferguson et al., 1987; M. W., W. Katz and P. W. S., unpublished). This

suggests that *lin-17* may function redundantly with other genes during 1°

patterning.

To create a sensitized background to examine the effect of *lin-17* on 1°

patterning, we ablated the AC in a *lin-17* loss-of-function background. We

found that AC ablation in *lin-17* mutants during the late Pn.px or the early

Pn.pxx stage resulted in abnormal expression patterns of *zmp-1::GFP* in

P6.pxxx cells (Table 6, Figure 4C and 4D), and that these disturbed patterns

were distinct from those caused by AC ablation or disruption of Ras activity

in a wild-type background (Table 7). Strikingly, in *lin-17* mutants lacking

an AC, only 12% of the inner and outer P6.pxxx cells adopted different fates.

In contrast, in wild-type animals lacking an AC, 50% of the inner and outer

P6.pxx cells adopted different fates (*P*<0.0001, Fisher's exact test, Table 7).

Similarly, in animals with heat shock induced Ras(dn) and *lin-1* mutants,

50% and 57% of the inner and outer P6.pxx cells adopted different fates,

respectively (Table 7). Therefore, *lin-17* appears to function in parallel to

the AC signaling to promote the distinction of the inner and outer 1° VPC

descendants.

Among the pairs of inner and outer P6.pxxx cells that adopted

different fates in AC ablated wild-type animals, Ras(dn) induced animals,

or *lin-1* mutants, 64 of 70, 33 of 38, and 48 of 52 respectively, had the proper

orientation with vulF facing the normal position of the AC (Table 7). In *lin-17* mutants, 6 of 7 had the proper orientation (*P*>0.5, Table 7). Therefore, the

intrinsic bias for the inner and outer cells to adopt a proper orientation in

the 1° pattern is relatively normal when *lin-17* is mutated. If *lin-17* were involved in establishing the intrinsic polarity of 1° VPC daughters, we would expect such a bias to be disrupted. We infer that *lin-17* could facilitate the differentiation of 1° VPC descendants by mediating signaling between the inner and outer 1° VPC descendants (P6.pxx or P6.pxxx).

DISCUSSION

We have examined the mechanisms of 1° lineage patterning during *C. elegans* vulval development to understand how a precursor cell produces a pattern of different progeny cells when it executes a defined fate. We show that the AC, which induces the VPC to adopt the 1° fate, functions again later to ensure an appropriate pattern of cell fates. During AC pattering of the 1° lineage, the AC appears to function within a short-range and may require direct contact to signal the inner 1° VPC granddaughters. Our results suggest additional mechanisms, including intrinsic polarity of 1° VPC daughters and signaling between the inner and outer 1° VPC descendants, may also be involved in pattern formation of the 1° lineage. Finally, we find that the AC may use the Ras signaling pathway to pattern the 1° lineage, and LIN-17 the Wnt receptor may function during signaling between the inner and outer 1° VPC descendants.

The model of 1° lineage patterning

In wild-type animals, a final pattern of eight descendants of the 1° VPC is established by specification of two distinct cell types, vulE and vulF. We used *zmp-1::GFP* as a molecular marker to distinguish the vulE and vulF fates adopted by the 1° VPC great granddaughters. Our results suggest a model of 1° lineage patterning that is dependent on at least three different mechanisms: AC signaling the inner 1° VPC granddaughters, signaling between the inner and outer 1° VPC descendants, and intrinsic polarity of 1° VPC daughters (Figure 5).

First, in wild-type animals, the AC may signal the inner granddaughters of the 1° VPC through direct cell-cell contact to ensure vulF progeny to be produced (Figure 5). Analysis of situations in which the AC was ablated, properly attached to or at a distance from the 1° granddaughters indicates that the AC signal is required for 1° lineage patterning and functions locally (Table 1D, 2, and Figure 1G-1I). Moreover, when in contact, the AC can signal an outer 1° VPC granddaughter to generate vulF descendants (Table 3B, 3C, Figure 3C-3H).

Second, signaling between the inner and outer 1° VPC descendants (granddaughters or great granddaughters) may ensure proper differentiation of the vulF and vulE fates (Figure 5). This is largely based on the observation that vulF cells patterned by the AC are always flanked by vulE cells, even when they do not come from the same 1° VPC daughter (Table 3C). In addition, independent of AC signaling, the distinction between the inner and outer descendants can be significantly disrupted

without affecting the proper orientation of the outcome in rare cases with differentiated inner and outer cells (Table 6 and 7).

Third, the inner 1° VPC granddaughters are internally different from their outer cousins, probably a consequence of intrinsic polarity of 1° VPC daughters (Figure 5). By examining the 1° lineage patterning in the absence of the AC, we have found that the orientation of the pattern of the inner and outer cell pair is strongly biased in the absence of AC signaling, possibly through intrinsic polarity of 1° VPC daughters (Table 7). Such intrinsic program may lead to asymmetric segregation of cytoplasmic determinants during divisions of 1° VPC daughters. This bias is striking even if the inner 1° descendants might signal between them to differentiate from one another and therefore work against the intrinsic polarity mechanism. Also, homoiogenetic signaling between the inner 1° descendants, if such a mechanism does exist, can not explain the bias of the patterning orientation, should there be no intrinsic polarity of the 1° VPC daughters.

The precision of 1° patterning requires multiple mechanisms

Our results indicate that no single mechanism is sufficient and multiple mechanisms may act together to increase the reproducibility of 1° lineage patterning. Combined mechanisms of signaling between the inner and outer 1° VPC descendants and intrinsic polarity of 1° VPC daughters are apparently not enough to pattern the 1° lineage, since the AC is an indispensable component in patterning the 1° lineage precisely. In addition, our results support the notion that AC signaling alone may not be

sufficient and absolute levels of the AC signal received may not the sole factor that determines the fate of VPC descendants invariably, as discussed above.

It is possible that the mechanism of signaling between the inner and outer 1° descendants could be partially redundant with other mechanisms. LIN-17 activity appears to be required for signaling between the inner and outer 1° descendants, but is likely not involved in intrinsic polarity of 1° VPC daughters (Table 6 and 7). However, the 1° lineage patterns correctly in a *lin-17* loss-of-function background (Table 6). Moreover, ablation of a subset of the 1° VPC granddaughters does not affect patterning of the granddaughters left. When both inner P6.pxx cells (P6.pap and P6.ppa) were ablated, the two remaining outer cells (P6.paa and P6.ppp) underwent their normal divisions, and the four resulting progeny all expressed the marker (n=14 animals). When both outer P6.pxx cells (P6.paa and P6.ppp) were ablated, the two remaining inner cells (P6.pap and P6.ppa) developed normally, and none of the four resulting progeny expressed the marker (n=12 animals). Since the ablation of P6.pxx cells could only be performed after the mitosis of P6.px cells had completed, the ablation may not disrupt signaling between the inner and outer P6.pxx cells if they signal each other right after they are born. Alternatively, their signaling is redundant with other mechanisms in 1° patterning.

It is also probable that different mechanisms may partially depend on one another to work properly. We have found that vulF cells formed in the absence of the AC have more variable neighbors than vulF cells with an AC (Table 1D and 3C). Since the neighboring vulE and vulF cells do not

always descend from the same VPC daughter, the possibility of a mechanism of intrinsic asymmetric division can be excluded. Either signaling between the inner and outer 1° descendants partly relies on AC signaling, or the AC also signals from a distance to produce vulE cells. While both mechanisms may function simultaneously, it is unlikely that AC signaling at a distance is the only mechanism involved in patterning the vulE fate. If there were no signaling between the neighboring 1° VPC descendants, each cell would have to solely depend on interpretation of absolute levels of the AC signal received, or, the AC would have to send out different signals to VPC descendants in contact and those at a distance. However, this does not seem to be the case. In *unc-6* mutants, when the dorsally or laterally mispositioned AC had a similar distance from the outer 1° VPC granddaughters as in wild-type, the outer descendants did not consistently become vulE (Table 2, data not shown).

Our results indicate that the 1° patterning process may employ a triple assurance strategy, which includes the AC that signals the inner 1° VPC granddaughters, intrinsically different 1° VPC granddaughters, and different inner and outer 1° VPC descendants reinforced by signaling between them (Figure 5). The existence of partially redundant mechanisms may provide a backup and ensures the accuracy of 1° patterning should one of the other mechanisms goes wrong. Utilizing multiple mechanisms to ensure the precision of cell fate pattern formation may be a general scenario during pattern formation in many developmental systems, e.g., differentiation of mating type between mother and daughter cells in *S. cerevisiae*, four different progeny cells produced by

the sensory organ precursors in *Drosophila* (reviewed by Herskowitz, 1989; Jan and Jan, 1994).

Proteins that are involved in each mechanism

Several important questions remain to be answered. For example, how does each molecule in each mechanism act and how are they regulated? How is the network of interacting genes coordinated? Answering these questions requires the identification of the molecules that are involved in each mechanism.

Our results suggest that some components in the Ras pathway that act during initial VPC fate specification may also be involved in the later role of the AC in patterning the 1° lineage. Terminating Ras signaling after VPC specification has an equivalent effect to ablating the AC at this time (Table 1D, 4 and 7). This is consistent with the finding that Ras may be involved in vulval cell migration and cell fusion (Shemer et al., 2000), since the distinct morphogenesis and cell fusion behavior of vulE and vulF are likely downstream of their fate specification events. Rescue of the 1° patterning defect after AC ablation by a ligand-independent activated form of the LET-23 RTK is also consistent with this scenario (Katz et al., 1996). The multiple-tissue downstream effector of Ras, LIN-1, is required. However, the tissue-specific LIN-31 (reviewed in Tan and Kim, 1999) is not. LIN-15, the negative regulator of the pathway, during VPC induction does not seem to be involved in 1° lineage patterning. We speculate that the ligand of the AC signaling pathway might be a membrane bound protein, due to requirement of the AC to function at short range. Consistently, heat

shock induced LIN-3EGF expression (presumably diffusible) does not have any effect on 1° lineage patterning (data not shown).

Among other signaling pathways that may function in the vulva, the LIN-12/Notch signaling pathway is unlikely to be involved in AC signaling to pattern the 1° lineage. In *lin-12(lf)* mutants, a 1° lineage with a single AC has a wild-type pattern of *zmp-1::GFP* expression (Table 3A). Also, an RTK of the Eph receptor family, VAB-1, may not be required in 1° patterning, since *vab-1* mutants do not display any defects in 1° VPC specification and 1° lineage patterning (George, et al., 1998; data not shown).

This study shows for the first time that the Wnt receptor LIN-17 functions in asymmetric cell divisions of P6.p, although a loss-of-function *lin-17* mutation does not cause any defect in P6.p. Blocking LIN-17 activity significantly reduces the chance for the inner and outer 1° descendants to differentiate from one another, but does not affect the orientation of the pattern if they do choose to be different (Table 7). This supports the hypothesis that LIN-17 is involved in signaling between the inner and outer 1° descendants (which affects the difference between them only), rather than intrinsic polarity of 1° VPC daughters (which presumably affect both difference and polarity). Further characterization of molecules in each pathway involved in 1° lineage patterning may further clarify how multiple redundant mechanisms regulate the execution of the 1° fate.

REFERENCES

Banerjee, U. and Zipursky, S. L. (1990). The role of cell-cell interaction in the development of the *Drosophila* visual system. *Neuron* **4**, 177-187.

Beitel, G. J., Clark, S. G. and Horvitz, H. R. (1990). *Caenorhabditis elegans ras* gene *let-60* acts as a switch in the pathway of vulval induction. *Nature* **348**, 503-509.

Beitel, G. J., Tuck, S., Greenwald, I. and Horvitz, H. R. (1995). The *Caenorhabditis elegans* gene *lin-1* encodes an ETS-domain protein and defines a branch of the vulval induction pathway. *Genes Dev.* **9**, 3149-3162.

Brenner, S. (1994). The genetics of *Caenorhabditis elegans*. *Genetics* **77**, 71-94.

Chamberlin, H. M. and Sternberg, P. W. (1995). Mutations in the *Caenorhabditis elegans* gene *vab-3* reveal distinct roles in fate specification and unequal cytokinesis in an asymmetric cell division. *Dev. Biol.* **170**, 679-689.

Clark, S. G., Lu, X. and Horvitz, H. R. (1994). The *Caenorhabditis elegans* locus *lin-15*, a negative regulator of a tyrosine kinase signaling pathway, encodes two different proteins. *Genetics* **137**, 987-997.

Euling, S. and Ambros, V. (1996). Heterochronic genes control cell cycle progress and developmental competence of *C. elegans* vulval precursor cells. *Cell* **84**, 667-676.

Félix, M.-A. and Sternberg, P. W. (1997). Two nested gonadal inductions of the vulva in nematodes. *Development* **124**, 253-259.

Ferguson, E. L., Sternberg, P. W. and Horvitz, H. R. (1987). A genetic pathway for the specification of the vulval cell lineages of *Caenorhabditis elegans*. *Nature* **326**, 259-267.

Freeman, M. (1997). Cell determination strategies in the *Drosophila* eye. *Development* **124**, 261-270.

George, S. E., Simokat, K., Hardin, J. and Chisholm, A. D. (1998). The VAB-1 Eph receptor tyrosine kinase functions in neural and epithelial morphogenesis in *C. elegans*. *Cell* **92**, 633-643.

Greenwald, I. (1997). Development of the vulva. In *C. elegans* II. (ed. D. Riddle, T. Blumenthal, B. Meyer and J. Priess), pp.519-541. Cold Spring Harbor laboratory press, New York.

Greenwald, I. and Rubin, G. M. (1992). Making a difference: the role of cell-cell interactions in establishing separate identities for equivalent cells. *Cell* **68**, 271-281.

Greenwald, I. S., Sternberg, P. W. and Horvitz, H. R. (1983). The *lin-12* locus specifies cell fates in *Caenorhabditis elegans*. *Cell* **34**, 435-444.

Han, M. and Sternberg, P. W. (1990). *let-60*, a gene that specifies cell fates during *C. elegans* vulval induction, encodes a Ras protein. *Cell* **63**, 921-931.

Han, M. and Sternberg, P. W. (1990). Analysis of dominant negative mutations of the *Caenorhabditis elegans let-60 ras* gene. *Genes Dev.* **5**, 2188-2198.

Hedgecock, E. M., Culotti, J. G. and Hall, D. H. (1990). The *unc-5*, *unc-6*, and *unc-40* genes guide circumferential migrations of pioneer axons and mesodermal cells on the epidermis in *C. elegans*. *Neuron* **2**, 61-85.

Herskowitz, I. (1989). A regulatory hierarchy for cell specification in yeast. *Nature* **342**, 749-757.

Hill, R. J. and Sternberg, P.W. (1992). The gene *lin-3* encodes an inductive signal for vulval development in *C. elegans*. *Nature* **358**, 470-476.

Horvitz, H. R. and Herskowitz, I. (1992). Mechanisms of asymmetric cell division: two Bs or not two Bs, that is the question. *Cell* **68**, 237-255.

Huang, L. S., Tzou, P. and Sternberg, P. W. (1994). The *lin-15* locus encodes two negative regulators of *Caenorhabditis elegans* vulval development. *Mol. Biol. Cell* **5**, 395-412.

Jan, Y. N. and Jan, L. Y. (1994). Genetic control of cell fate specification in *Drosophila* peripheral nervous system. *Ann. Rev. Genet.* **28**, 373-393.

Jan, Y. N. and Jan, L. Y. (1999). Asymmetric cell division. *Nature* **392**, 775-778.

Jiang, L. I. and Sternberg, P. W. (1998). Interaction of EGF, Wnt and HOM-C genes specify the P12 neuroectoblast fate in *C. elegans*. *Development* **125**, 2337-2347.

Katz, W. S., Hill, R. J., Clandinin, T. R. and Sternberg, P. W. (1995). Different levels of the *C. elegans* growth factor LIN-3 promote distinct vulval precursor fates. *Cell* **82**, 297-307.

Katz, W. S., Lesa, G. M., Yannoukakos, D., Clandinin, T. R., Schlessinger, J. and Sternberg, P. W. (1996). A point mutation in the extracellular domain activates LET-23, the *Caenorhabditis elegans* epidermal growth factor receptor homolog. *Mol. Cel. Biol.* **16**, 529-537.

Kenyon C. (1995). A perfect vulva every time: gradients and signaling cascades in *C. elegans*. *Cell* **82**, 171-174.

Kimble, J. (1981). Alterations in cell lineage following laser ablation of cells in the somatic gonad of *Caenorhabditis elegans*. *Dev. Biol.* **87**, 286-300.

Kimble, J. and Hirsh, D. (1979). The postembryonic cell lineages of the hermaphrodite and male gonads in *Caenorhabditis elegans*. *Dev. Biol.* **70**, 396-417.

Koga, M. and Ohshima, Y. (1995). Mosaic analysis of the *let-23* gene function in vulval induction of *Caenorhabditis elegans*. *Development* **121**, 2655-2666.

Massova, I., Kotra, L. P., Fridman, R. and Mobashery, S. (1998). Matrix

metalloproteinases: structures, evolution, and diversification. *FASEB

J.* **12**, 1075-1095.

Mello, C. C., Kramer, J. M., Stinchcomb, D. and Ambros, V. (1991).

Efficient gene transfer in *C. elegans* after microinjection of DNA into

germline cytoplasm: extrachromosomal maintenance and

integration of transforming sequences. *EMBO J.* **10**, 3959-3970.

Miller, L. M., Gallegos, M. E., Morisseau, B. A. and Kim, S. K. (1993). *lin-

31*, a *Caenorhabditis elegans* HNF-3/*fork head* transcription factor

homolog, specifies three alternative cell fates in vulval development.

Genes Dev. **7**, 933-947.

Newman, A. P., White, J. G. and Sternberg, P.W. (1995). The

Caenorhabditis elegans lin-12 gene mediates induction of ventral

uterine specialization by the anchor cell. *Development* **121**, 263-271.

Newman, A. P., White, J. G. and Sternberg, P. W. (1996). Morphogenesis of

the *C. elegans* hermaphrodite uterus. *Development* **122**, 3617-3626.

Sawa, H., Lobel, L. and Horvitz, H. R. (1996). The *Caenorhabditis elegans*

gene *lin-17*, which is required for certain asymmetric cell divisions,

encodes a putative seven-transmembrane protein similar to the

Drosophila Frizzled protein. *Genes Dev.* **10**, 2189-2197.

Schnabel, R. and Priess, J. R. Specification of cell fates in the early embryo.

In *C. elegans* II. (ed. D. Riddle, T. Blumenthal, B. Meyer and J.

Priess), pp.361-382. Cold Spring Harbor laboratory press, New York.

Seydoux, G. and Greenwald, I. (1989). Cell autonomy of *lin-12* function in a

cell fate decision in *C. elegans*. *Cell* **57**, 1237-1245.

Sharma-Kishore, R., White, J. G., Southgate, E. and Podbilewicz, B. (1999). Formation of the vulva in *Caenorhabditis elegans*: a paradigm for organogenesis. *Development* **126**, 691-699.

Shemer, G., Kishore, R. and Podbilewicz, B. (2000). Ring formation drives invagination of the vulva in *Caenorhabditis elegans*: Ras, cell fusion, and cell migration determine structural fates. *Dev. Biol.* **221**, 233-248.

Simske, J. S. and Kim, S. K. (1995). Sequential signaling during *Caenorhabditis elegans* vulval induction. *Nature* **375**, 142-146.

Sommer, R. J., Carta, L. K., Kim, S.-Y. and Sternberg, P. W. (1996). Morphological, genetic and molecular description of *Pristionchus pacificus* sp. n. (Nematoda, Diplogasteridae). *Fund. Appl. Nematol.* **19**, 511-521.

Sternberg, P. W. (1988). Lateral inhibition during vulval induction in Caenorhabditis elegans. *Nature* **335**, 551-554.

Sternberg, P. W. and Horvitz, H. R. (1986). Pattern formation during vulval induction in *C. elegans. Cell* **44**, 761-772.

Sternberg, P. W. and Horvitz, H. R. (1988). *lin-17* mutations *of Caenorhabditis elegans* disrupt certain asymmetric cell divisions. *Dev. Biol.* **130**, 67-73.

Sternberg, P. W. and Horvitz, H. R. (1989). The combined action of two intercellular signaling pathways specifies three cell fates during vulval induction in *C. elegans. Cell* **58**, 679-693.

Sulston, J. E. and Horvitz, H. R. (1977). Postembryonic cell lineages of the nematode *Caenorhabditis elegans. Dev. Biol.* **56**, 110-156.

Sulston, J. E. and White, J. G. (1980). Regulation and cell autonomy during postembryonic development of *Caenorhabditis elegans*. *Dev. Biol.* **78**, 577-597.

Tan, P. O. and Kim, S. K. (1999). Signaling specificity, the RTK/RAS/MAP kinase pathway in metazoans. *Trends Genet.* **15**, 145-149.

Thomas, J. H., Stern, M. J. and Horvitz, H. R. (1990). Cell interactions coordinate the development of the *C. elegans* egg-laying system. *Cell* **62**, 1041-1052.

Vinson, C. R., Conover, S. and Adler, P. N. (1989). A *Drosophila* tissue polarity locus encodes a protein containing seven potential transmembrane domains. *Nature* **338**, 263-264.

Wang, M. and Sternberg, P. W. (1999). Competence and commitment of *Caenorhabditis elegans* vulval precursor cells. *Dev. Biol.* **212**, 12-24.

Way, J. C., Run, J.-Q. and Wang, A. Y. (1992). Regulation of anterior cell-specific *mec-3* expression during asymmetric cell division in *C. elegans*. *Dev. Dynamics* **194**, 289-302.

Way, J. C., Wang, L., Run, J.-Q. and Wang, A. (1991). The *mec-3* gene contains *cis*-acting elements mediating positive and negative regulation in cells produced by asymmetric cell division in *Caenorhabditis elegans*. *Genes Dev.* **5**, 2199-2211.

TABLES

Table 1. The AC is required for proper patterning of the 1° lineage, while the 2° lineages and the VU cells are not required.

experimental conditions	*zmp-1::GFP* expression in P6.pxxx during L4 lethargus	n		n
intact	◯◯ ●●	276/276		
(A) ablate P5.p and P7.p	◯◯ ●●	20/20		
(B) ablate one P6.p daughter	◯● ⊗	18/18		
(C) ablate VU precursors before VPCs divide	◯◯ ●●	34/34		
(D) ablate AC at the late P6.px stage to early P6.pxx stage	◯◯ ●◯	19/70	●● ◯◯	5/70
	◯◯ ◯◯	11/70	●● ◯◯	1/70
	◯◯ ●◯	13/70	●◯ ●◯	12/70
	●● ◯◯	1/70	●● ●◯	2/70
	●● ◯◯	1/70	●● ●◯	5/70
(E) ablate AC at the late P6.pxx stage	◯◯ ●●	20/20		

Table 1. L3 animals with integrated *zmp-1::GFP* were staged using Nomarski optics. In all panels, ventral is down. The panels indicate the expression patterns of *zmp-1::GFP* in P6.pxxx cells at the left or right side of the animal, observed by Nomarski optics during L4 lethargus. Filled circles indicate the P6.pxxx cells that expressed GFP; unfilled circles indicate the P6.pxxx cells that did not. Intact, control animals that were not ablated. n, the numerators indicate the number of half 1° lineage patterning units with the *zmp-1::GFP* expression pattern displayed; the denominators indicate the number of half 1° lineage patterning units scored.

(A) The 2° VPCs, P5.p and P7.p, were ablated.

(B) P6.pa or P6.pp was ablated.

(C) All the ventral uterine precursors (VU) were ablated at the early L3 stage (the three VU cells had not divided when ablated).

(D) The AC was ablated at the late L3 stage, just before, during, or right after the divisions of P6.px cells.

(E) The AC was ablated during L3 lethargus.

Table 2. Failure of AC contact with 1° descendants disrupts patterning of the 1° lineage.
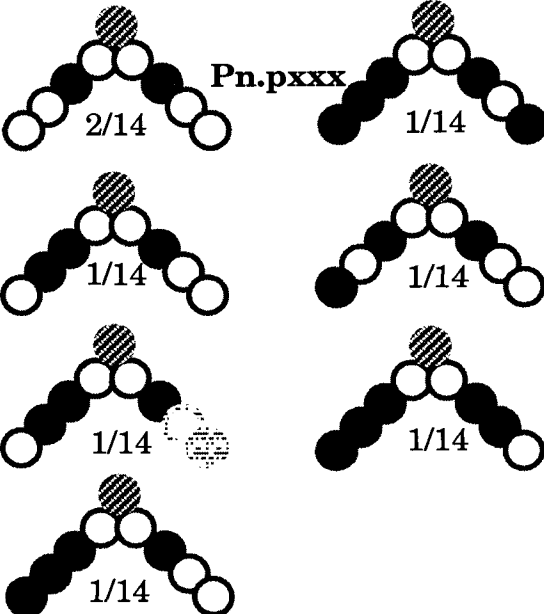
genotype	AC contact with 1° descendants[a]	1° VPC descendants scored[b]	wild-type *zmp-1::GFP* expression in Pn.pxxx
dig-1	contact (ventral gonad, anteriorly shifted)	P4.p or P5.p	44/45
	no contact (dorsal gonad)	P4.p, P5.p or P6.p	4/38
unc-6	contact	P6.p	37/37
	no contact	P6.p	4/26

Table 2. Animals were scored using Nomarski optics during L4 lethargus. The numerators indicate the number of VPCs whose descendants display the wild-type *zmp-1::GFP* expression pattern. The denominators indicate the number of VPCs scored. The full genotypes were: *dig-1(n1321); zmp-1::GFP* and *unc-6(ev400); zmp-1::GFP*.

[a] The position of AC at the Pn.pxx stage. In *dig-1* animals, when the gonad was positioned ventrally, but shifted anteriorly, it attached to the anterior P4.p or P5.p. When the gonad was mispositioned dorsally, it had no contact with any of the VPCs. In *unc-6* animals, the gonad was at the ventral side in all animals. However, the AC was sometimes misplaced at the dorsal part of the gonad, and therefore had no contact with VPCs and their descendants.

[b] In *dig-1* animals, we scored *zmp-1::GFP* expression in descendants of P4.p, P5.p, or P6.p, whichever was closest to the AC. In *unc-6* mutants, P6.p was always scored.

Table 3. The effect of adjacent 1° lineages and multiple ACs.

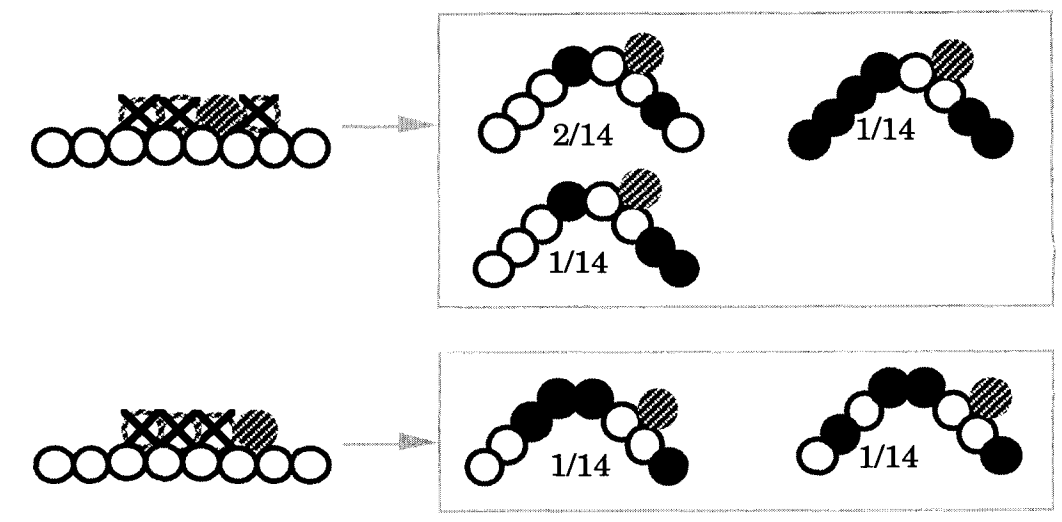| experimental conditions	*zmp-1::GFP* expression in Pn.pxxx during L4 lethargus	n
(A) a single 1° cell with a single AC *lin-12(lf)*	Pn.pxxx	6/6
(B) a single 1° cell with multiple ACs *lin-12(lf)*	Pn.pxxx	12/14
		2/14
(C) 2 adjacent 1° cells with a single AC *lin-12(lf)*	Pn.pxxx 2/14 1/14 1/14 1/14 1/14 1/14 1/14	

Table 3. *lin-12(lf); zmp-1::GFP* animals were scored using Nomarski optics. In all panels, ventral is down. All ablations were performed at the early L3 stage before VPCs' first division. The expression patterns of *zmp-1::GFP* in Pn.pxxx cells were scored by Nomarski optics during L4 lethargus. Filled circles indicate Pn.pxxx cells that expressed GFP; unfilled circles indicate those that did not. In panel C, only the expression patterns of *zmp-1::GFP* in P5.pxxx and P6.pxxx at the upper focal plane (either the left or right side of the animal) were scored. In all panels, the relative position of the AC(s) to P5.pxx and P6.pxx cells during L3 lethargus was scored and indicated. In *lin-12(lf)* mutants, the ACs fail to fuse with uterine π cells and therefore persist thoughout larval stages. Full genotypes: *unc-32(e189) lin-12(n676n909); zmp-1::GFP* and *unc-6(ev400); zmp-1::GFP*. n, the numerators indicate the number of animals whose 1° VPC descendants display the *zmp-1::GFP* expression pattern shown; the denominators indicate the number of animals scored.

(A) P5.p and P7.p, along with all ACs except for one, were ablated in *lin-12(lf)* mutants. The P6.p lineage was scored.

(B) P5.p and P7.p were ablated in *lin-12(lf)* mutants, and the P6.p lineage was scored.

(C) All ACs but one were ablated in *lin-12(lf)* mutants. P7.p was ablated, and the P5.p and P6.p lineages were scored.

Table 4. Expression of a dominant negative form of *ras* disrupts patterning of the 1° lineage.

experimental conditions	*zmp-1::GFP* expression in P6.pxxx during L4 lethargus			n[a]
no *hs-ras(dn)*[b]	⬤◯ / ⬤⬤	68/68		
induce *hs-ras(dn)* at the late P6.px or the early P6.pxx stage[c]	◯◯ / ⬤⬤	11/38	⬤◯ / ⬤◯	2/38
	◯◯ / ◯◯	7/38	⬤⬤ / ◯◯	1/38
	◯◯ / ⬤◯	6/38	⬤◯ / ⬤⬤	4/38
	◯⬤ / ⬤◯	1/38	⬤⬤ / ⬤◯	2/38
			⬤⬤ / ⬤⬤	4/38
induce *hs-ras(dn)* at the late Pn.pxx stage[d]	◯◯ / ⬤⬤	14/14		

Table 4. L3 animals were staged using Nomarski optics. In all panels, ventral is down. The panels indicate the expression patterns of *zmp-1::GFP* in P6.pxxx cells at the left or right side of the animal, observed by Nomarski optics during L4 lethargus. Filled circles indicate the P6.pxxx cells that expressed GFP, and unfilled circles indicate the P6.pxxx cells that did not. Full genotype: *hs-ras(dn); zmp-1::GFP*.

[a] The numerators indicate the number of half 1° lineage patterning units with the *zmp-1::GFP* expression pattern displayed. The denominators indicate the number of half 1° lineage patterning units scored.

[b] *hs-ras(dn); zmp-1::GFP* animals that were not heat shocked.

[c] *hs-ras(dn); zmp-1::GFP* animals were heat shocked at late-L3, just before, during or right after the divisions of P6.px cells.

[d] *hs-ras(dn); zmp-1::GFP* animals were heat shocked during L3 lethargus.

Table 5. Patterning of the 1° lineage in mutants of the Ras signaling pathway components.

background	AC ablation at the late P6.px or early P6.pxx stage	*zmp-1::GFP* expression in P6.p lineage
wild-type	intact	276/276
wild-type	AC ablated	6/35
let-23 (gf)	intact	49/49
let-23 (gf)	AC ablated	13/16
lin-15 (lf)	intact	39/41
lin-15 (lf)	AC ablated	2/19
hs-ras(dn)	untreated	34/34
hs-ras(dn)	heat shocked	3/19
lin-1 (lf)	intact	5/23
lin-31 (lf)	intact	31/31

Table 5. Animals were scored using Nomarski optics during L4 lethargus. AC ablation or heat shock were performed during the late P6.px or the early P6.pxx stage. The numerators indicate the number of P6.p cells whose descendants display the wild-type *zmp-1::GFP* expression pattern. The denominators indicate the number of P6.p cells scored. The full genotypes were: *let-23(sa62); zmp-1::GFP, lin-15(e1763); zmp-1::GFP, hs-ras(dn); zmp-1::GFP, lin-1(sy254); zmp-1::GFP,* and *lin-31(n301); zmp-1::GFP.*

Table 6. *lin-17* is involved in proper expression of *zmp-1::GFP* in the 1° lineage.

experimental conditions *lin-17(lf)*	*zmp-1::GFP* expression in P6.pxxx at L4 molt			n^a
intact[b]				144/144
ablate AC at the late P6.px to the early P6.pxx stage[c]		1/30		4/30
		10/30		3/30
		1/30		10/30
		1/30		
ablate AC at the late P6.pxx stage[d]				16/16

Table 6. L3 animals with integrated *zmp-1::GFP* were staged using Nomarski optics. In all panels, ventral is down. The panels indicate the expression patterns of *zmp-1::GFP* in P6.pxxx cells at the left or right side of the animal, observed by Nomarski optics during L4 lethargus. Filled circles indicate the P6.pxxx cells that expressed GFP; unfilled circles indicate the P6.pxxx cells that did not. Full genotype: *lin-17(n671); zmp-1::GFP*.

[a] The numerators indicate the number of half 1° lineage patterning units with the *zmp-1::GFP* expression pattern displayed. The denominators indicate the number of half 1° lineage patterning units scored.

[b] Control animals that were not ablated.

[c] The AC was ablated at late-L3, right before, during, or right after the second divisions of P6.p.

[d] The AC was ablated during L3 lethargus.

**Table 7. Distribution of patterns of *zmp-1::GFP* expression in P6.pxxx cells.**

background	peturbation	P6.pxxx pair with different inner and outer cells		proper orientation	
		%	n	%	n
wild-type	intact	100%	552	100%	552
wild-type	AC ablated	50%	140	91%	70
hs-ras (dn)	untreated	100%	136	100%	136
hs-ras (dn)	heat shocked	50%	76	87%	38
lin-1	intact	57%	92	92%	52
lin-17	intact	100%	288	100%	288
lin-17	AC ablated	12%	60	86%	7

Table 7. Results from Table 1, 4, 5 and 6 were summerized to compare the
results of AC ablation in wild type, a heat shock induced Ras(dn) background, a
lin-1(sy254) background, and AC ablation in a *lin-17(n671)* background. AC
ablation or heat shock were performed during the late P6.px or the early P6.pxx
stage. The expression patterns of *zmp-1::GFP* in P6.pxxx cells were scored
during L4 lethargus. Inner and outer P6.pxxx pairs that expressed *zmp-1::GFP*
differently were scored as P6.pxxx pairs with different inner and outer cells.
Among these P6.pxxx pairs with different inner and outer cells, those expressed
zmp-1::GFP in the outer cells were scored as those with the proper orientation.
n, the number of inner and outer P6.pxxx pairs scored.

FIGURES

Figure 1. Schematic outline of 1° lineage patterning

In all panels, ventral is down, anterior is to the left. In panel C, filled circles indicate the P6.pxxx cells that expressed *zmp-1::GFP*; unfilled circles indicate the P6.pxxx cells that did not express *zmp-1::GFP*. In panel B and C, the darker color indicates the P6.pxxx cells at the left side of the animal, and the lighter color indicates the P6.pxxx cells at the right side. Abbreviations: AC, anchor cell; E, vulE cells; F, vulF cells.

A. L3 lethargus
(P6.pxx cells)

P6.paa P6.pap P6.ppa P6.ppp
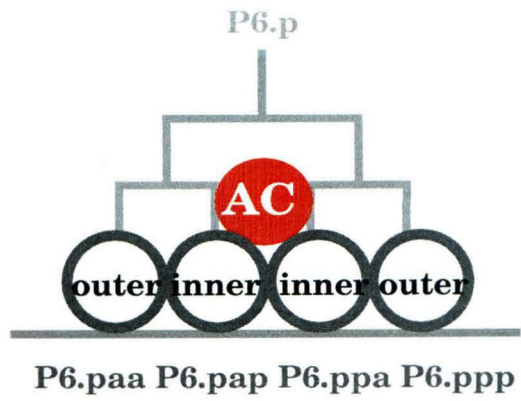
B. mid-L4
(P6.pxxx cells)
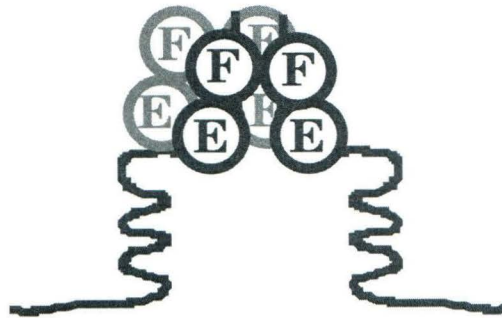
C. L4 lethargus
(P6.pxxx cells)

Figure 2. The AC is required for proper patterning of the 1° descendants.
Displays animals from Table 1. The strain used was *zmp-1::GFP*. In all
panels, ventral is down, anterior is to the left. Arrows point to the
connection between the uterus and the vulva at mid-L4; arrowheads
indicate the position of the great granddaughter nuclei of P6.p during L4
lethargus (some of the inner nuclei were out of focus). In (A)-(C), an intact
animal; in (D)-(F), an animal with all VU precursor cells ablated before
VPCs divide; in (G)-(I), an animal with the AC ablated at the early Pn.pxx
stage. (A): Nomarski image of the vulval invagination at the mid-L4 stage
of an intact animal. The vulva and the uterus were connected with a thin
line of utse. (B) and (C): Nomarski and fluorescence images of the four
P6.pxxx cells at the left side of the same animal during L4 lethargus.
Neither of the inner P6.pxxx cells expressed *zmp-1::GFP*, while both outer
cells expressed *zmp-1::GFP*. (D): Nomarski image of the vulval
invagination at the mid-L4 stage of an animal with all VU precursors
ablated. The unfused AC blocked the otherwise normal uterine-vulval
connection. (E) and (F): Nomarski and fluorescence images of the four
P6.pxxx cells at the left side of the same animal during L4 lethargus. The
expression pattern of *zmp-1::GFP* was the same as that in intact animals.
(G): Nomarski image of the vulval invagination at the mid-L4 stage of an
animal with the AC ablated at the late P6.px or the early P6.pxx stage. The
connection between the vulva and the uterus was abnormal. (H)-(I):
Nomarski and fluorescence images of the four P6.pxxx cells at the left side
of the same animal during L4 lethargus. Both outer P6.pxxx cells

expressed *zmp-1::GFP* as in intact animals, but one of the two inner cells

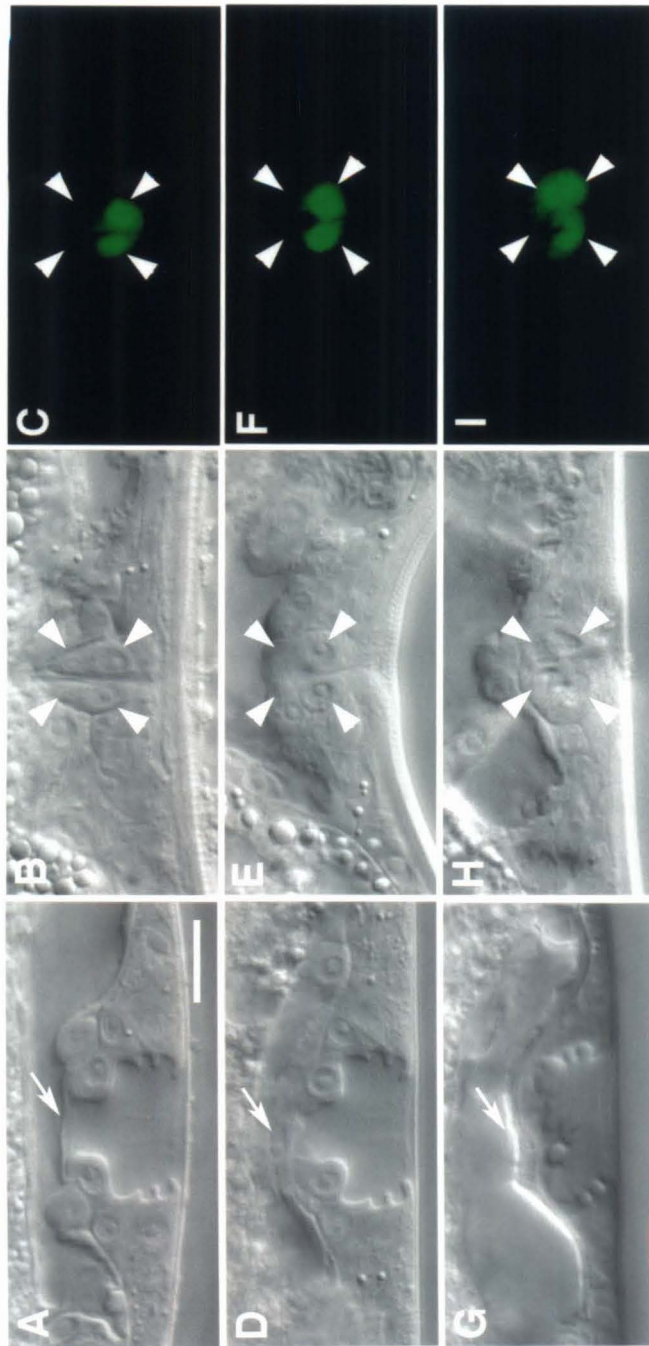also expressed *zmp-1::GFP*. The scale bar is 10 μm.

Figure 3. The expression pattern of *zmp-1::GFP* in the 1° VPC great granddaughters is determined by the proximity between the AC and the 1° VPC granddaughters.

Displays animals from Table 3. The strain used was *lin-12(lf); zmp-1::GFP*. In all panels, ventral is down, anterior is to the left. All animals were during L4 lethargus when photographed. Arrowheads indicate the positions of the great granddaughter nuclei of P5.p and P6.p. AC, the AC or multiple ACs remained unfused and expressed *zmp-1::GFP* during L4 lethargus in a *lin-12(lf)* background. In (A)-(D), two different animals with P5.p and P7.p ablated; in (E) and (F), an animal with P7.p ablated; in (G) and (H), an animal with P7.p and all ACs but one ablated. (A) and (B): Nomarski and fluorescence images of the four P6.pxxx cells at the left side of an animal. P5.p and P7.p were ablated at the early L3 stage. The four ACs attached to P6.pap and P6.ppa during L3 lethargus. During L4 lethargus, neither of the inner P6.pxxx cells expressed *zmp-1::GFP*, while both outer cells expressed *zmp-1::GFP*. (C) and (D): Nomarski and fluorescence images of the four P6.pxxx cells at the left side of an animal. P5.p and P7.p were ablated at the early L3 stage. The four ACs attached to P6.pap, P6.ppa and P6.ppp, but not P6.paa during L3 lethargus. During L4 lethargus, none of P6.papl, P6.ppal and P6.pppl expressed *zmp-1::GFP*, while P6.paal expressed *zmp-1::GFP*. (E) and (F): Nomarski and fluorescence images of the eight great granddaughters of P5.p and P6.p at the left side of an animal. P7.p was ablated at the early L3 stage. The four ACs attached to the five innermost granddaughters of P5.p and P6.p (P5.ppa, P5.ppp, P6.paa, P6.pap and P6.ppa) during L3 lethargus. During

L4 lethargus, P5.paal, P5.papl and P6.pppl expressed *zmp-1::GFP*, while

P5.ppal, P5.pppl, P5.paal, P6.papl and P6.ppal did not express *zmp-1::GFP*.

(G) and (H): Nomarski and fluorescence images of the eight P5.pxxx and

P6.pxxx cells at the left side of an animal. P7.p and all ACs except one were

ablated at the early L3 stage. The unablated AC attached to P5.ppp and

P6.paa during L3 lethargus. During L4 lethargus, P5.ppal and P6.papl

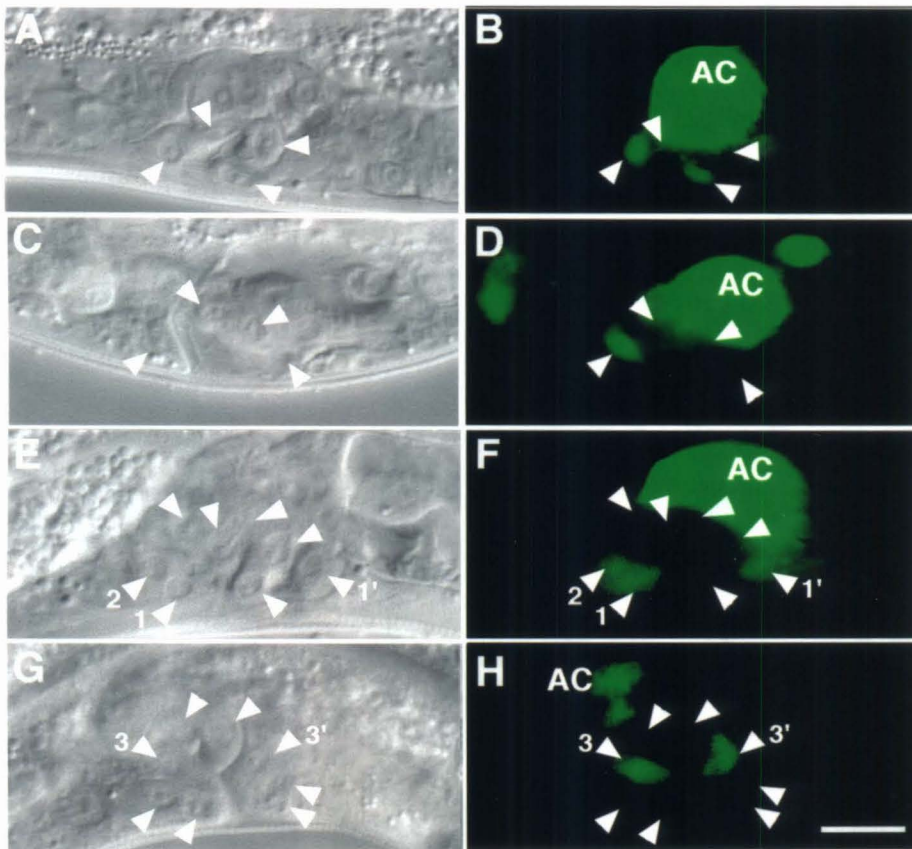expressed *zmp-1::GFP*, while the other six cells did not express *zmp-1::GFP*. The scale bar is 10 μm.

Figure 4. *ras* and *lin-17* might be involved in AC signaling and signaling between the 1° VPC descendants respectively in 1° vulval patterning. Displays animals from Table 4 and 6. The strains used were *hs-ras(dn); zmp-1::GFP,* and *lin-17(n671); zmp-1::GFP*. In all panels, ventral is down, anterior is to the left. Arrowheads indicate the position of P6.pxxx nuclei at the left side of the animal during L4 lethargus (some were out of focus). In (A) and (B), an animal with *hs-ras(dn)* was heat shocked at the early Pn.pxx stage. Nomarski and fluorescence images of the four P6.pxxx cells at the left side of the animal during L4 lethargus. All four P6.pxxx cells expressed *zmp-1::GFP*. In (C) and (D), an *lin-17(n671); zmp-1::GFP* animal with the AC ablated at the early P6.pxx stage. Nomarski and fluorescence images of the four P6.pxxx cells at the left side of the animal during L4 lethargus. The anterior inner and outer P6.pxxx cells expressed *zmp-1::GFP*, while the posterior inner and outer P6.pxxx cells did not express *zmp-1::GFP*. The scale bar is 10 μm.
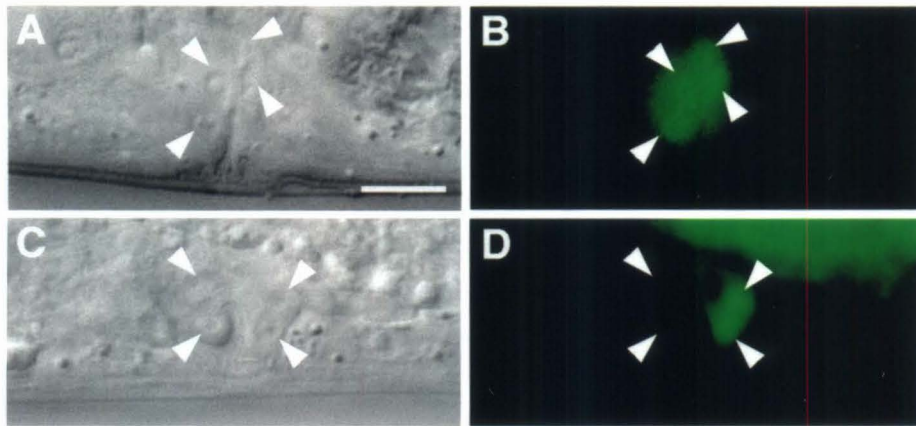
Figure 5. Model for patterning of the 1° vulval lineage.

After the early effect of the AC that induces the proliferation of the VPCs, the AC functions again later to pattern the 1° descendants. The inner 1° VPC granddaughters attract the AC better than the outer cells and lead to the AC attachment. Through cell-cell contact, the AC signals the inner 1° VPC granddaughters to ensure that vulF progeny will be produced. The inner 1° VPC granddaughters are internally different from the outer cells, caused by intrinsic polarity of 1° VPC daughters. In addition, signaling between the inner and outer 1° VPC descendants promotes the differentiation of the inner and outer cells. 1° VPC descendants can variably adopt the vulE or vulF fate without forming a fixed spatial pattern when one or more of the three mechanisms is disrupted.

I. Induction of the 1° fate
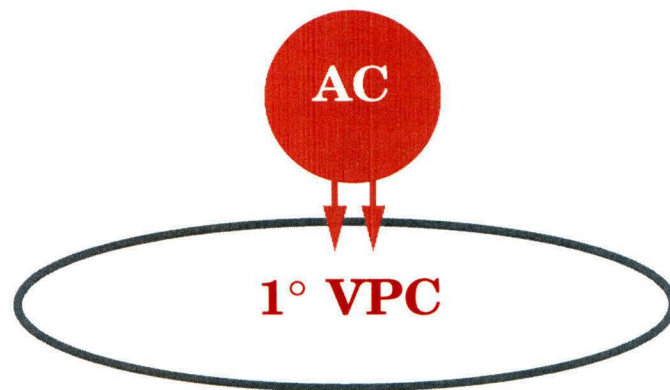
II. Patterning of the 1° lineage
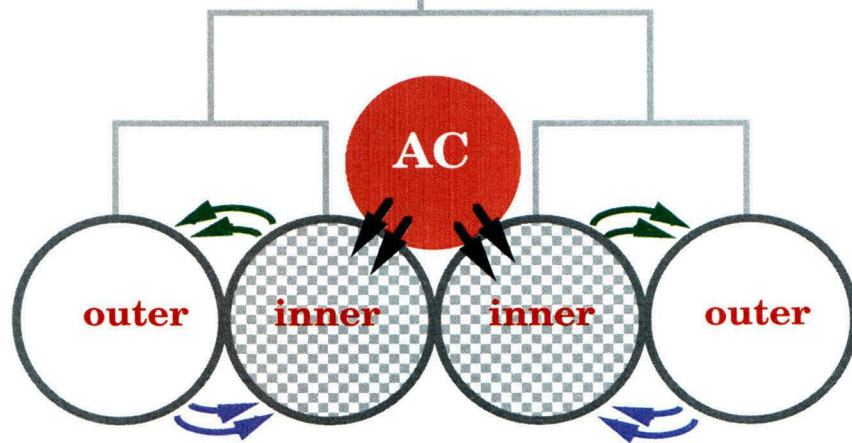
Chapter 5

A network of transcription factors facilitates temporal expression of *egl-17::GFP* during the execution of the 1° fate in *C. elegans* vulva

Minqin Wang and Paul W. Sternberg

(prepared for submission)

SUMMARY

During the development of *C. elegans* vulva, the Ras signaling pathway induces one of the vulval precursor cells (VPCs) to adopt the 1° fate. To understand how Ras signaling leads to changes in the activity of VPC specified as 1°, we used *egl-17::GFP* as a molecular marker to dissect the execution of the 1° fate, the events following 1° fate specification after Ras is activated. We find that the temporal expression pattern of *egl-17::GFP* correlates with progression of 1° fate specification and execution. In particular, the execution of the 1° fate can be divided into three steps, including commitment of the 1° fate, as well as later steps before and after establishment of the uterine-vulval connection. Each step involves functioning of different transcription factors. LIN-1 (ETS), LIN-39 (HOM-C) act during the first step; LIN-11 (LIM) and LIN-29 (zinc finger) are required during the second step; COG-1 (homeobox) and EGL-38 (PAX2/5/8) are involved during the third step. We show that the progression of each step is sequential and interrelated, and EGL-38 may function to specify the vulF fate of the 1° VPC descendants.

INTRODUCTION

Two major mechanisms that make multipotential precursor cells adopt different fates during animal development are autonomous mechanism and intercellular signaling. During cell-cell interactions, the signal can be

from cells other than the precursor cell group or among the precursors (reviewed in Greenwald and Rubin, 1992). Extensive studies have been devoted to identifying signaling molecules involved in different signaling pathways, such as the Ras and Notch signaling pathways (reviewed in Artavanis-Tsakonas et al., 1995; Wassarman et al., 1995; Sternberg and Han, 1998). However, how the activity of the cell changes and what happens in the cell nucleus after signaling molecules are activated are largely unexplored. Transcription factors have emerged as downstream targets of signaling which subsequently turn on other genes leading to cell differentiation and cell fate determination, and therefore provide unique insight into how developmental processes are regulated by intercellular signaling.

We used Ras signaling during *Caenorhabditis elegans* vulval development as a model system to study the downstream events following intercellular signaling. The *C. elegans* lineage is completely known and the vulval development has been well-studied (Sulston and Horvitz, 1977; Kimble and Hirsh, 1979; Greenwald, 1997; Kornfeld, 1997; Sternberg and Han, 1998). Cellular, molecular biological and genetic tools are all readily available. The development of *C. elegans* hermaphrodite proceeds through four larval stages (L1 to L4) before adulthood. Each stage ends with a molt, which includes lethargus, when the animal ceases feeding and is inactive, and ecdysis, when the old cuticle is shed and locomotion and pharynx pumping resume (Sulston and Horvitz, 1977). The vulval development process spans all four larval stages, from the L1 to the L4 stage. Formation of a wild-type vulva is functionally important for egg-laying and mating.

It has been proposed that vulval development can be divided into several steps, including VPC generation, VPC fate specification, execution of VPC fates and morphogenesis of VPC descendants (reviewed in Greenwald, 1997). During VPC generation, of the 12 ectoblasts (P1.p-P12.p) that are aligned anteroposteriorly along the ventral midline of the hermaphrodite body, six central ones (P3.p-P8.p) establish the multipotential group of vulval precursor cells (VPCs) (Sulston and Horvitz, 1977).

At least two intercellular signaling pathways are involved in the VPC fate specification. In wild-type animals, a pattern of 3°-3°-2°-1°-2°-3° is invariably established, despite the fact that all six VPCs are competent to choose among three fates, the non-vulval 3°fate and the vulval 1° and 2° fates (Sulston and White, 1980; Kimble, 1981; Sternberg and Horvitz, 1986). The anchor cell (AC) in the somatic gonad produces an epidermal growth factor (EGF)-like molecule, LIN-3, and induces the closest VPC, P6.p, to adopt the 1° fate (Kimble, 1981; Hill and Sternberg, 1992; Katz et al., 1995). The LIN-3 inductive signal is transduced by the receptor tyrosine kinase LET-23 and a conserved signaling pathway that activates LET-60 Ras (Aroian et al., 1990; Beitel et al., 1990; Han and Sternberg, 1990). Analysis of factors functioning downstream of Ras indicates a complex and branched pathway instead of a simple linear pathway (reviewed in Sternberg and Han, 1998). Lateral signaling between P6.p and its adjacent P5.p and P7.p, mediated by LIN-12, a Notch family receptor, causes P5.p and P7.p to adopt the 2° fate (Yochem et al., 1988; Greenwald et al., 1983; Koga and Oshima, 1995; Simske and Kim, 1995).

After VPC fates are specified, different fates are executed by generating different numbers and types of descendants that behave distinctively to form the adult vulva (reviewed in Greenwald, 1997). The execution of the vulval fate starts from the first divisions of the VPCs, and for the purpose of this paper, we consider it ends at the end of the L4 stage, including morphogenesis of VPC descendants. VPCs that adopt the 3° fate divide once during the early L3 stage and then fuse with the epidermal syncytium hyp7. All induced VPCs that adopt the 1° or the 2° fate behave similarly initially and divide twice to give rise to four granddaughter cells during the L3 stage. It is the divisions of VPC granddaughters that distinguish the lineages of VPCs adopting the 1° and 2° fates. While all 1° VPC granddaughters divide transversely to generate eight progeny (abbreviated TTTT), the 2° VPC granddaughters have a more complicated division pattern (abbreviated LLTN or NTLL). The two distal-most 2° VPC granddaughters divide longitudinally (LL, underline indicate attachment to the ventral cuticle during L3 lethargus), the one 2° VPC granddaughter right next to the 1° VPC descendants does not divide (N), and the one remaining 2° VPC granddaughter in the middle has transverse division (T). During the L4 stage, the 22 vulval cells undergo cell fusion to form 7 toroidal cells A, B1, B2, C, D, E and F (Sharma-Kishore *et al.*, 1999; Figure 1). This is consistent with that each different division in the 1° or 2° lineage translates into one different type of descendants (with the exception of the L division next to T in the 2° lineage, which results in two types of progeny, B1 and B2). In this study, we refer to VPCs as Pn.p cells, VPC daughters as

Pn.px cells, VPC granddaughters as Pn.pxx cell, and VPC great granddaughters as Pn.pxxx cells.

We have studied events after 1° fate specification, i.e., the execution of the 1° fate, to elucidate the developmental process in the VPCs following Ras activation. By examining the temporal expression pattern of *egl-17::GFP* in the 1° lineage, we show that the dynamic expression of this molecular marker correlates with specification, commitment, and later steps of execution of the 1° fate. Analysis of mutants recovered in our screen and other transcription factors that are involved in execution of the 1° fate suggest that 1° fate execution can be divided into three different steps. The sequential progression of these steps involve functioning of a network of transcription factors, including LIN-1 (ETS), LIN-39 (HOM-C), LIN-11 (LIM), LIN-29 (zinc finger), COG-1 (homeobox) and EGL-38 (Pax). Finally, we provide evidence that EGL-38 may function specifically in the vulF cells of the 1° lineage.

MATERIALS AND METHODS

General methods and strains

C. elegans strains were handled at 20°C according to standard protocols (Brenner 1974; Wood 1988), except for Table 4B, in which animals were grown at 25°C. The following alleles were used: for LGI, *ayIs4[egl-17::GFP; dpy-20(+)], lin-11(n389), unc-13(e51)*; for LGII, *cog-1(sy275), lin-29(n546), lin-29(sy292), rol-1(e91), unc-4(e120), unc-52(e444)*; for LGIV, *egl-38(n578), dpy-20(e1282), syIs49[zmp-1::GFP; dpy-20(+)]*; LGV, *him-5(e1490)* (Brenner, 1974; Ambros and Horvitz, 1984; Freyd et al., 1990; Rougvie and Ambros, 1995; Chamberlin et al., 1997; Burdine et al., 1998; R. Palmer and P. W. S., in preparation).

Complementation tests and strain construction

Candidate alleles of *lin-11, lin-29, lin-17* and *lin-18* from our screen were tested for complementation with *lin-11(n389), lin-29(sy292* and *n333), lin-17(n671)* and *lin-18(e620)*, respectively, in the same manner. For example, wild-type males were mated to *mut-x* hermaphrodites where *mut-x* is a candidate *lin-11* allele. Cross progeny males were selected and mated to *unc-13(e51) lin-11(n389)* hermaphrodites. Non-Unc hermaphrodite cross progeny were selected, placed on individual plates and scored for their ability to lay eggs.

    ayIs4 and *syIs49* were mapped to chromosome I and IV using *lin-17(n671)* and *dpy-20(e1282)*, respectively (R. Burdine and M. Stern, personal communication; data not shown). To examine the expression pattern of the

markers in mutants, we used the loss-of-function allele or the most severe reduction-of-function allele available in all experiments, except for *n1790*, the *lin-1* gain-of-function allele, used in Table 4 (Jacobs et al., 1998). *lin-1(sy254)*, *lin-11(n389)* are both loss-of-function alleles of each gene (Freyd et al., 1990; Beitel et al., 1995). *n333* and *sy292* are either loss-of-function or severe loss-of-function of *lin-29* (Rougvie and Ambro, 1995; T. Inoue, A. Newman and P. W. S., unpublished). We used *lin-39(n709)*, a temperature-sensitive reduction-of-function allele, since *lin-39* loss-of-function mutants do not form VPCs (Ellis, 1985; Clark et al., 1993). *n578*, a reduction of function allele of *egl-38*, was selected due to the lethality associated with the null allele (Chamberlin et al., 1997). The *cog-1(sy275)* mutation is recessive, has a single amino acid change (Y to N) in the conserved homeodomain, but not a null (R. Palmer, D. Sherwood and P. W. S., unpublished).

Double and triple mutant strains containing either marker were constructed similarly. *ayIs4 / +; unc-52(e444) / +; dpy-20(e1282); him-5(e1490) / +* males were mated to *ayIs4; egl-38(n578) dpy-20(e1282)* hermaphrodites, and cross progeny males were mated to *ayIs4; cog-1(sy275); dpy-20(e1282)* hermaphrodites. Non-Rol non-Dpy cross progeny were selected (*ayIs4 / ayIs4 or +; cog-1 / unc-52 or +; egl-38 dpy-20 or + / dpy-20*), placed on individual plates, and allowed for self-fertilize. Animals that segregated Unc progeny were kept and their egg-laying deficient progeny were put on individual plates again. Those that segregated Unc animals were kept and 12 animals were cloned to look for the loss of Unc animals in their progeny. *ayIs4; cog-1(sy275); egl-38(n578) dpy-20(e1282)* animals were identified and deconstructed to confirm the genotype.

ayIs4; unc-4(e120) lin-29(sy292) cog-1(sy275); dpy-20(e1282) animals were constructed as following: *ayIs4 / +; unc-4(e120) lin-29(sy292) rol-1(e91) / +; dpy-20(e1282); him-5(e1490)* males were mated to *ayIs4; cog-1(sy275); dpy-20(e1282)* hermaphrodites. Cross progeny egg-laying competent hermaphrodites (*ayIs4 / ayIs4 or +; unc-4 lin-29 rol-1 or + / cog-1; dpy-20*) were selected, placed on individual plates and allowed to self-fertilize. Animals that segregated Unc Rol progeny were kept, and the occasional Unc non-Rol recombinants were placed on individual plates again. The Unc progeny produced in the next generation were candidates of genotype *ayIs4; unc-4(e120) lin-29(sy292) cog-1(sy275); dpy-20(e1282)*, and were deconstructed to confirm the genotype.

Anatomy and heat shock

Animal anatomy and cell division patterns were examined under Nomarski optics as described by Sulston and Horvitz, 1997. For heat shock experiments, animals were mounted on agar pads, examined using Nomarski optics to confirm their stage (Sulston and Horvitz, 1977; Kimble and Hirsh, 1979) and then heat shocked at 33°C for 30 minutes. Animals were placed on prewarmed plates of desired temperature, sealed with Parafilm, and then floated in a covered water bath of the same temperature. After heat shock, animals were transferred immediately to plates kept at 20°C until the late L3 and mid L4 stages when they were scored for VPC fates.

GFP fluorecence microscopy

GFP expression was observed using Nomarski optics and a Zeiss Axioplan

microscope with a 200-watt HBO UV source, using a Chroma High Q GFP

LP filter set (450nm excitation/ 505nm emission). Photographs were taken

with Fuji Provia ASA 400 film.

RESULTS

Initial expression of *egl-17::GFP* in the VPC correlates with the

specification of the 1° fate

Previous studies have relied on three aspects of vulval development to score

vulval fates. They include axis of of Pn.pxx cell divisions, adherence of

Pn.pxxx cells to the ventral cuticle at the L3 molt, and morphogenesis of the

vulval tissue during the mid-L4 stage (Sternberg and Horvitz, 1986; Katz et

al., 1995). We chose to study the 1° fate since its lineage is less complex

than the 2° lineage and it has two types of descendants vulE and vulF rather

than five types (vulA, B1, B2, C and D) from the 2° lineage (Sharma-Kishore

et al., 1999). The three classical criteria of a 1° lineage are transverse

divisions of Pn.pxx cells, nonadherence to the ventral cuticle, and

symmetric invagination.

To facilitate studying specification and execution of the 1° vulval fate,

we sought molecular markers of the 1° vulval fate. *egl-17* encodes a

fibroblast growth factor (FGF), which acts as the signal for sex myoblast

migration (Burdine et al., 1997). The *egl-17::GFP* reporter construct is

expressed consistently in the 1° lineage (Burdine et al., 1998; Figure 1). The GFP expression starts in P6.p in most animals, and by mid-L3, in all animals, it is seen in both P6.px cells and all four P6.pxx cells. After P6.pxxx cells are born, the expression fades shortly after the early-L4 stage, right before the uterine-vulval connection is formed. It remains off in P6.pxxx cells at mid-L4 when *egl-17::GFP* is expressed strongly in the C and D descendants of the 2° VPCs, P5.p and P7.p (Burdine et al., 1998; Figure 1, 2A and 2B).

The temporal expression pattern of *egl-17::GFP* in the 1° lineage fits into different developmental steps of 1° fate specification and execution. In wild-type animals, the expression of *egl-17::GFP* in the 1° VPC, P6.p, starts from the late-L2 to early-L3 stage, and corresponds with P6.p induction by LIN-3 from the AC. This expression does not require completion of VPC S phase, indicating that it may reflect the specification of the 1° fate (Ambros, 1999).

To explore whether *egl-17::GFP* expression in the VPC requires any other later cellular behavior, we used a heat shock inducible LIN-3 construct (*hs-lin-3*; Katz et al., 1995) to induce VPCs to adopt various vulval fates and compared the marker expression in VPCs with their final fates scored with classical methods (Table 1). It has been shown that VPCs other than P5.p-P7.p can display the proper *egl-17::GFP* expression pattern if they adopt the 1° or 2° fate (Burdine et al., 1998). When we induced LIN-3 expression by heat shock, all VPCs may adopt vulval fates. We observed 16 VPCs initially expressed *egl-17::GFP*, and then the expression faded in their daughters or granddaughters (Table 1). These VPCs eventually

adopted the 3° or the 2° fate, indicating that the initial expression of *egl-17::GFP* in the VPCs does not require the later cellular behavior and therefore indicates specification rather than commitment of the 1° fate.

Temporal expressions of *egl-17::GFP* in Pn.pxx and Pn.pxxx indicate VPC fate commitment and later steps of execution

After VPC fate specification, the subsequent execution of the 1° fate occurs after the first round of VPC division and includes all three rounds of VPC divisions. Distinct types of descendants with different morphological behavior are generated during the L3 and L4 stages. The continued GFP expression in 1° VPC granddaughters may reflect commitment to the 1° fate which can occur after the VPC division, and therefore the first step to execute the 1° fate (Greenwald et al., 1983; Ambros, 1999; Wang and Sternberg, 1999). The decreased expression after the divisions of 1° VPC granddaughters could correlate with later steps of 1° fate execution.

We tested whether different expression patterns of *egl-17::GFP* in Pn.pxx and Pn.pxxx cells correspond to different VPC fates. To compare the *egl-17::GFP* expression pattern in VPC granddaughters at mid-L4 with the division pattern of the VPC granddaughters and the morphology of the invagination in more detail, we used the *hs-LIN-3* construct to generate various types of vulval fates. After heat shock, we scored the division pattern of granddaughters of induced VPCs during the L3 stage, adherence of Pn.pxxx cells to the ventral cuticle at the L3 molt, and morphogenesis of the vulval tissue at mid-L4, as well as *egl-17::GFP* expression in Pn.pxx cells at late-L3 and in Pn.pxxx cells at mid-L4. We found that among 88

VPC lineages defined as 1° according to three classical standards, 76 had the wild-type 1° expression pattern of *egl-17::GFP* (Table 1). The remaining 12 cases had abnormal *egl-17::GFP* expression at mid-L4, although they would have been considered as normal 1° fates based on the three classical standards. With regard to two types of aberrant (non-1° and non-2°) fate with abnormal cell division or morphogenesis pattern, the expression patterns of *egl-17::GFP* were abnormal (Table 1; Sternberg and Horvitz, 1986; Katz et al., 1995). The results of the 2° fate according to the marker also match the results of the classical scoring methods (Table 1). These results indicate that different temporal expression patterns of *egl-17::GFP* in Pn.pxx and Pn,pxxx cells correspond to different vulval fates. In the case of the 1° fate, the *egl-17::GFP* marker may be a more stringent and accurate tool than the classical methods of lineaging and scoring of attachment and vulval morphology. Therefore, the dynamic temporal *egl-17::GFP* expression profile in Pn.pxx and Pn.pxxx cells can be used as a marker for properly executed 1° fate.

A screen for genes involved in 1° fate execution recovered *lin-11* and *lin-29*

To identify genes involved in the execution of the 1° fate, we did a genetic screen using wild-type animals with *egl-17::GFP* integrated into the genome. Since many mutants with vulval defects have a protruding vulva (Pvul) after EMS-mutagenesis, we looked for mutants with a Pvul phenotype and then scored their vulval induction and the expression pattern of *egl-17::GFP* in VPCs and VPC descendants. We simplified our screen and later analysis by saving only fertile animals. We focused on

recovering 1° vulval mutants, but kept the 2° vulval mutants as well. We expected that mutations with the 1° or 2° specific function after VPC fate specification should not alter the number of VPCs that adopt vulval fates, but should affect the expression pattern of *egl-17::GFP*. Therefore, we discarded mutant lines with other than three-VPC induction, and retained candidates with three VPCs adopting vulval fates and abnormal *egl-17::GFP* expression.

Approximately 12,500 mutagenized haploid genomes were screened, and 6 independent mutant lines were obtained. Linkage analysis and non-complementation tests (see Materials and Methods) indicated that we had isolated two alleles of *lin-11* (*sy533* and *sy534*), two alleles of *lin-29* (*sy531* and *sy532*), one allele of *lin-17* (*sy565*), and one allele of *lin-18* (*sy540*) (Table 2). Consistent with altered P7.p lineages in these mutants, both *lin-17* and *lin-18* mutants displayed abnormal *egl-17::GFP* expression in P7.pxxx cells (Ferguson et al., 1987; Sternberg and Horvitz, 1988; W. Katz and P. W. S., unpublished). However, the recovery of *lin-11* and *lin-29* was unexpected.

The LIM domain transcription factor LIN-11 is known to be involved in the execution of the 2° lineage and uterine morphogenesis (Freyd et al., 1990; Newman et al., 1999). In *lin-11* mutants, the 2° VPCs generate two daughters with the same fate, rather than two different daughters. Consequently, P5.p and P7.p produce lineages of L̲L̲L̲L̲ instead of L̲L̲TN in wild-type animals. As expected, the expression of *egl-17::GFP* in the 2° lineages at mid-L4 is abolished due to the lack of C and D descendants (Burdine et al., 1998). Surprisingly, although the 1° descendants from P6.p had the normal lineage (Table 2) and P6.p, P6.px and P6.pxx cells

expressed GFP normally during the L3 stage, P6.pxxx cells continued to express GFP weakly at mid-L4, when the expression faded in wild-type animals (Table 3; Figure 2C and 2D). Such a subtle phenotype has not been observed previously and demonstrates for the first time that *lin-11* is involved in the execution of the 1° fate.

lin-29 is one of the heterochronic genes that control the timing and sequence of the development of most tissues in the larva except the gonad (Ambros and Horvitz, 1984; Ambros, 1989). It encodes a zinc finger transcription factor, and is required for vulval morphogenesis (Rougvie and Ambros, 1995; Bettinger et al., 1997). *lin-29* mutants have wild-type vulval lineages (Table 2) and it has been found that in these mutants, the vulva has normal invagination until it starts to evert during the final stage of morphogenesis at L4 molt (Bettinger et al., 1997). By examining the *egl-17::GFP* expression pattern in VPC descendants in *lin-29* mutants, we found that the vulval defects started much earlier than the final stage of vulval morphogenesis. In fact, the execution of both 1° and 2° fates was abnormal. In addition to failure of the 2° descendants to express the marker at mid-L4, faint *egl-17::GFP* expression persisted in all 1° VPC descendants during the mid-L4 stage (Table 3; Figure 2E and 2F). Overall, *lin-29* mutants have similar *egl-17::GFP* expression pattern to that of *lin-11* mutants, though distinct vulval morphology.

We proceeded to focus on studying the function of *lin-11* and *lin-29* in the execution of the 1° lineage.

cog-1 and egl-38 are also involved in the execution of the 1° fate

Apart from *lin-11* and *lin-29*, we examined additional genes implicated in the execution of the 1° fate, but did not come up in our screen. Two obvious candidates are *cog-1* and *egl-38*.

cog-1 is required in establishment of two kinds of connection during morphogenesis: uterine connection to the vulva in hermaphrodites and the vas deferens connection to the proctodeum in males (R. Palmer and P. W. S., unpublished). In the vulva, *cog-1(sy275)* mutants have a low penetrance (<50%) defect in the 1° lineage, in which one of P6.pap and P6.ppa has either delayed divisions or no division. *cog-1* encodes a homeodomain containing transcription factor (R. Palmer and P. W. S., unpublished). When we crossed *egl-17::GFP* into a *cog-1* mutant background, we observed normal expression of *egl-17::GFP* in P6.p, P6.px and P6.pxx cells during the L3 stage. However, 100% of the animals expressed GFP strongly in the four outer P6.pxx cells (P6.paax and P6.pppx) during the mid-L4 stage (Table 3; Figure 2G and 2H), indicating that the execution of the 1° fate in *cog-1* mutants is abnormal.

EGL-38 belongs to a subfamily of PAX2/5/8 transcription factors, which contains a paired domain and a homeodomain (Chamberlin et al., 1997). We analyzed *egl-38(n578)* because it is the only viable *egl-38* allele with an egg-laying defect. Besides developmental defects in the hermaphrodite uterus, the vulval morphology in *egl-38(n578)* mutants is abnormal. The four inner P6.pxxx cells (P6.papx and P6.ppax) fail to separate as in wild-type animals to form the proper uterine-vulval connection, indicating that the 1° vulval tissue might be defective (Chamberlin et al., 1997; Chang et al., 1999). However, both lineage and

egl-17::GFP expression in P6.p and its descendants are normal in *egl-38(n578)* mutants (Table 3; Figure 2I and 2J). We thus made a double mutant of *cog-1(sy275)* and *egl-38(n578)* and examined *egl-17::GFP* in this background. As in wild-type, all P6.p, P6.px and P6.pxx cells expressed *egl-17::GFP* during the L3 stage. However, all P6.pxxx cells expressed GFP strongly, similar to C and D descendants of the 2° lineage during the mid-L4 stage (Table 3; Figure 2K and 2L). Thus, *egl-38* is also involved in the execution of the 1° fate.

Four transcription factors regulate the second and third steps of 1° fate execution

To understand the process of 1° fate execution, we examined the temporal expression patterns of *egl-17::GFP* in *lin-11, lin-29, cog-1* and *egl-38* mutants in more detail. All *four* mutants have normal 1° vulval lineage (except for *cog-1*, in which one of P6.pap and P6.ppa occasionally has delayed or no division) and normal *egl-17::GFP* expression in P6.p, P6.px and P6.pxx during the L3 stage, indicating that specification and commitment of the 1° fate might be normal. Their defects in *egl-17::GFP* expression in P6.pxxx cells suggest that these genes are involved in later steps of 1° vulval execution, and may partly explain their failure to form a normal vulval morphology and functional uterine-vulval connection.

To further dissect the process of 1° fate execution, we first examined *egl-17::GFP* expression in wild-type animals more carefully. After GFP expression in P6.pxx cells at late-L3, the expression faded completely in P6.pxxx cells shortly after early-L4. Then after the inner P6.pxxx cells

separated and the uterine-vulval connection was formed, the expression

came on strongly in C and D descendants of the 2° lineage (Table 3). This

expression was considerably stronger than that in P6.pxx cells during the

L3 stage.

The misexpression of *egl-17::GFP* in outer P6.pxxx cells at mid-L4 in

cog-1 mutants was as strong as normal *egl-17::GFP* expression in 2°

lineages at mid-L4, and distinct from the moderate GFP expression in

P6.pxx cells at late-L3 (Table 3). We therefore asked whether it was an

elevated expression continuing from the expression in P6.pxx at L3, or it

was a different expression after the expression in P6.pxx and early P6.pxxx

cells was turned off after early-L4. We followed *cog-1* animals from late-L3

to mid-L4, and found that shortly after early-L4, the GFP expression in

P6.pxxx cells faded completely before the strong expression in outer P6.pxx

cells appeared (Table 3). Therefore, the execution of the 1° fate can be

divided into three steps according to the temporal *egl-17* expression pattern

(Figure 3). The first step is commitment to the 1° fate represented by

continuous *egl-17::GFP* expression in P6.px and P6.pxx cells during the L3

stage. The second step is fading of *egl-17::GFP* expression shortly after

early-L4 in P6.pxxx cells, before the separation of the inner P6.pxxx cells

and the formation of the uterine-vulval connection. The third step is

inhibition of *egl-17::GFP* expression in P6.pxxx at mid-L4, while the

expression is turned on in 2° lineages and the uterine-vulval connection is

formed. Accordingly, *cog-1* mutants are defective in the third step, rather

than the second step of 1° fate execution.

To test whether *cog-1; egl-38* double mutants have similar defects in the third step of 1° fate execution, we examined the double mutant animals from the late-L3 to mid-L4 stage. We observed that the *egl-17::GFP* expression in early P6.pxxx cells disappeared right after early-L4, and then the expression reappeared strongly in all P6.pxxx cells at mid-L4 (Table 3). As a result, just as in *cog-1* mutants, *cog-1; egl-38* double mutants are defective in the third step of 1° fate execution, but not the second step.

According to this model, *lin-11* and *lin-29* are involved in the second step of 1° fate execution, since the *egl-17::GFP* expression failed to be turned off in P6.pxxx cells after early-L4 when either gene is mutated (Table 3; Figure 2A-2D). The double mutants of *lin-11; lin-29* had similar defects in the second step of 1° fate execution as in the single mutants (Table 3), consistent with that the two genes function in the same step.

Although temporally the second step occurs prior to the third step, the question remains whether these two steps are sequentially or independently regulated. If turning off *egl-17::GFP* in the second step is required for turning on *egl-17::GFP* in the third step, the second step phenotype of *lin-11* or *lin-29* should be epistatic to the third step phenotype observed in *cog-1* when both genes are mutated. In other words, the double mutants should have persisting *egl-17::GFP* expression in P6.pxxx after early-L4, but no strong expression in outer P6.pxxx cells at mid-L4. If the two steps are unrelated, the double mutants should exhibit both defects in the second and third steps, i.e., fail to turn off *egl-17::GFP* in P6.pxxx cells at early-L4 and then have strong GFP expression in outer P6.pxxx cells at mid-L4. When we built the double mutants of *lin-11; cog-1* and *lin-29; cog-1*,

we found that both mutants were defective in the second step of 1° fate execution, but not the third step (Table 3). Moreover, *lin-11* and *lin-29* also suppressed the step three phenotype in *cog-1; egl-38* double mutants. The triple mutants *lin-11; cog-1; egl-38* and *lin-29; cog-1; egl-38* exhibited continuous weak expression of *egl-17::GFP* during the mid-L4 stage, similar to *lin-11* or *lin-29* mutants (Table 3; Figure 2M-2P). The fact that the second step defect is epistatic to the third step defect indicates that completion of the second step is a prerequisite for progression of the third step of 1° fate execution. It is possible that the second and the third steps share common regulatory factors such as *lin-11* and *lin-29*, which may be required during the third step in addition to the second step.

lin-1 and *lin-39* are required during the first step of 1° fate execution

We went on to test where *lin-11, lin-29, cog-1* and *egl-38* fit into the Ras signaling pathway, and looked for genes that may act during the first step of 1° fate execution.

LIN-1, an ETS transcription factor, is one of the downsteam targets of Ras signaling (Beitel et al., 1995). Based on available evidence, it has been proposed that the HOM-C gene *lin-39* also functions downstream of the Ras pathway (Clandinin et al., 1997; Maloof and Kenyon, 1998). In particular, epistasis analysis indicates that LIN-1 acts after LET-60 RAS, and phosphorylation of the C-terminal domain of LIN-1 by MAP kinase may regulate its function as an inhibitor of vulval fates (Han et al., 1990; Jacobs et al., 1998; Tan et al., 1998). Also, *lin-39(rf)* suppresses the multivulva phenotype of both *let-60(gf)* and *lin-1(lf)*, and *lin-39* expression is

upregulated by Ras activation (Clandinin et al., 1997; Maloof and Kenyon, 1998).

We tested whether *lin-1* or *lin-39* is involved in the execution of the 1° fate. When LIN-1, an inhibitor of vulval induction, is eliminated by a loss-of-function mutation, the animal display the multivulva phenotype and abnormal vulval morphology (Beitel et al., 1995). Most *lin-1(gf)* mutants have three VPCs adopting vulval fates, but also have grossly abnormal vulval invaginations (Jacobs et al., 1998). We crossed *egl-17::GFP* into *lin-1* gain-of-function and loss-of-function mutants, and found that none of the P6.pxx cells expressed GFP during the late L3 stage in either background, indicating that both mutants are defective in the first step of 1° fate execution (Table 4A; B. Gupta and P. W. S., unpublished). When we crossed *egl-17::GFP* into animals containing a heat shock inducible *lin-39* (*hs-lin-39*) construct integrated in the genome (Maloof and Kenyon, 1998) and heat shocked the animal during the early L3 stage, we found that P6.pxx cells expressed GFP strongly at late-L3 (Table 4A). In contrast, in *lin-39(rf)* mutants, P6.pxx cells had reduced *egl-17::GFP* expression than in the wild-type (Table 4B). Therefore, both *lin-1* and *lin-39* may be involved in the first step of 1° vulval execution.

We built strains bearing both a *lin-1* mutation and the *hs-lin-39* construct, and determined *egl-17::GFP* expression after heat shocking the animals at early-L3. We found that the phenotypes of both gain-of-function and loss-of-function mutations of *lin-1* were suppressed by heat shock induced *lin-39* overexpression (Table 4A), suggesting that LIN-39 might mediate LIN-1 function or regulate an effector of LIN-1.

We then tested whether the first and second steps of 1° fate execution are sequential or independent of each other. We were unable to use *lin-39(lf)* mutants, in which all Pn.p cells fuse with hyp7 during the L1 stage, and fail to form VPCs (Clark et al., 1993), and thus we constructed double mutants with *lin-39(rf)* and *lin-11* or *lin-29*. The second step phenotype in *lin-11* and *lin-29* mutants was suppressed by *lin-39(rf)* (Table 4B). Therefore, just like the sequential relationship between the second and the third steps, completion of the first step is required to regulate the second step of 1° fate execution. It is also possible that *lin-1* and *lin-39* themselves are necessary for later steps of 1° fate execution.

lin-11, lin-29 and *cog-1* function in all P6.pxxx cells, while *egl-38* is required in the inner P6.pxxx cells

Since *lin-11* and *lin-29* mutants have defective *egl-17::GFP* expression in all P6.pxxx cells, *lin-11* and *lin-29* are likely to function in all 1° VPC progeny. Likewise, *cog-1* may also function in all 1° VPC progeny, since the outer P6.pxxx cells have abnormal *egl-17::GFP* expression in *cog-1* mutants and the inner P6.pxxx cells show defects when both *cog-1* and *egl-38* are mutated. However, *egl-38* may act only in the inner P6.pxxx cells (Figure 3).

To further examine the function of the four genes, we utilized another vulval marker. The *zmp-1::GFP* reporter construct was made by inserting GFP coding sequence after the genomic sequence of *zmp-1* gene, which encodes a zinc metalloprotease (J. Butler and J. Kramer, personal communication). In wild-type animals, it is expressed in the outer P6.pxxx

cells (P6.papx and P6.ppax) at L4 lethargus, but not in the inner P6.pxxx

cells (P6.paax and P6.pppx) (Wang and Sternberg, in preparation).

Unlike wild-type, none of the P6.pxxx cells expressed *zmp-1::GFP* at

L4 lethargus in *lin-11*, *lin-29*, or *cog-1* mutants (Table 5). In contrast, all

P6.pxxx cells expressed *zmp-1::GFP* in *egl-38* mutants at that stage. This

confirms that 1° fate execution in *egl-38* mutants is deficient, although the

1° lineage has wild-type *egl-17::GFP* expression. We then built double

mutants using *egl-38* and the other three mutants. In all three double

mutants, the *zmp-1::GFP* expression in P6.pxxx cells in *egl-38* mutants

was suppressed by *lin-11, lin-29,* and *cog-1*, and none of the P6.pxxx cells

had *zmp-1::GFP* expression (Table 5), indicating that *lin-11, lin-29* and *cog-1* are required for *zmp-1::GFP* expression in all P6.pxxx cells (Figure 3). In

all *egl-38* single and double mutants, only the defects of inner 1° VPC

descendants, never the outer cells, in *zmp-1::GFP* or *egl-17::GFP*

expression were attributable to *egl-38* (Table 3 and 5). This supports the

hypothesis that *egl-38* may function only in the inner 1° VPC descendants,

and could be one of the distinguishing factor between the inner and outer 1°

descendants.

Transcription factors regulate the expression of one another during 1° fate

execution

For transcription factors to function autonomously during 1° fate execution,

they must be present in the 1° VPC descendants. In wild-type animals, the

anti-LIN-39 antibodies have revealed that LIN-39 protein is present in P6.p

and all its descendants throughout the L3 and L4 stage (M. W., J. A.

DeModena and P. W. S., unpublished). A *lin-11::GFP* transcriptional fusion construct is expressed in P6.pxx and P6.pxxx cells from the late L3 to the L4 stage (Hobert et al., 1998; S. Cameron and R. Horvitz, personal communication; B. Gupta and P. W. S., unpublished). Antibody staining of LIN-29 has also indicated accumulation of LIN-29 in P6.px, P6.pxx and P6.pxxx cells (Bettinger et al., 1997). Expression of a *cog-1::GFP* translational fusion construct capable of rescuing the *cog-1* mutant phenotype has been seen at least in the outer P6.pxxx cells throughout the L4 stage (R. Palmer and P. W. S., in preparation). We do not know about expression patterns of *lin-1* and *egl-38*.

We looked at *lin-11::GFP* and *cog-1::GFP* expression in various mutant backgrounds when other transcription factors were defective. We found that *lin-11::GFP* expression was significantly reduced in *lin-29* mutants, but not affected in *cog-1* or *egl-38* mutants (Table 6A). Furthermore, both *lin-11* and *egl-38* mutations cause inappropriate *cog-1::GFP* expression in the inner 1° VPC great granddaughters (Table 6B). Therefore, the expression and function of different transcription factors may be interrelated and form a complex network that defines the activity of the 1° VPC descendants during execution of the 1° fate.

DISCUSSION

We have analyzed the process of the execution of the 1° fate in *C. elegans* vulval development. At a cellular level, VPC fate specification leads to the

execution of the fate of choice. At the molecular level, activation of the Ras

signaling pathway results in changes of the protein expression profile

which can be translated into the activity of the VPCs. Our results reveal

three steps of 1° fate execution, indicated by the temporal expression pattern

of *egl-17::GFP* (Figure 3). The first step is the *egl-17::GFP* expression in the

1° VPC granddaughters. The second step is turn-off of the marker

expression in the 1° VPC great granddaughters after the early L4 stage,

right before the separation of the inner P6.pxxx cells and establishment of

the uterine-vulval connection. The third step is inhibition of *egl-17::GFP*

expression, while the expression is turned on in 2° lineages. We have

found that six transcription factors are involved in regulating the

progression of the three steps. While LIN-1 and LIN-39 are involved in the

first step, LIN-11 and LIN-29 act in the second step, and COG-1 and EGL-38

in the third step.

The temporal expression pattern of *egl-17::GFP* reveals three steps of 1° fate

execution

Activation of signaling pathways, such as the Ras signaling pathway, leads

to developmental decisions. In the 1° VPC, the immediate response of Ras

activation may be cell fate specification, which results in the presumptive 1°

VPC signaling its neighbors laterally and preventing its fusion with hyp7.

The transition between cell fate specification and commitment could be

accumulation of changes of gene expression in response to Ras activation,

which eventually leads to the irreversible commitment to the final 1° fate.

The further execution of the 1° fate then follow, as well as later events

caused by Ras activation, such as proceeding of cell cycle and cell division machinery and coordination of cell movements during vulval morphogenesis. Therefore, dynamic changes of gene expression upon Ras activation may reflect the progression of cell fate execution in detail.

The temporal *egl-17::GFP* expression pattern provides a useful tool to distinguish different stages of 1° lineage formation, although it may not necessarily accurately reflect the native gene expression in detail. Its expression starts in the 1° VPC during AC signaling from the early L3 stage (Burdine et al., 1998). This expression does not require completion of the S phase and the rest of the VPC cell cycle, as well as the subsequent cellular behavior, and therefore corresponds with the specification of the 1° fate (Ambros, 1999; Table 1). The execution of the 1° fate follows 1° fate specification, and spans the stage from the VPC division and the rest two rounds of cell divisions, till the end of morphogenesis of the VPC great granddaughters. Although the execution of the 1° fate clearly includes complex changes of the protein expression profile and cellular behavior, it can be divided into three relatively simple steps according to the temporal *egl-17::GFP* expression pattern. The expression of the marker in 1° VPC granddaughters during the first step may represent the final commitment to the 1° fate, since commitment of the 1° fate can occur after the VPC division (Ambros, 1999; Wang and Sternberg, 1999). The lack of *egl-17::GFP* expression in 1° VPC great granddaughters during the second and third steps can be divided by the separation of the inner 1° great granddaughters and the formation of the uterine-vulval connection.

A network of transcription factors functions in sequential execution of the 1° fate

How does activation of signaling pathways, such as the Ras signaling pathway, lead to developmental decisions? Most likely, immediate changes of gene expression resulting from Ras activation can be translated into choices of cell fates, and the subsequent changes of later gene expression can carry out or execute such a fate. Most of such changes can be attributed to transcription factors, which link intercellular signaling to transcriptional activity of the cell.

We have identified six transcription factors that regulate different steps of 1° fate execution, which occur sequentially after Ras signaling (Figure 3). It is known that LIN-1 and LIN-39 function downstream of Ras (Han et al., 1990; Clandinin et al., 1997; Jacobs et al., 1998; Maloof and Kenyon, 1998). By analyzing mutant phenotypes of several transcription factors (Table 2, 3, 4, and Figure 2), we have found that the first step during the execution of the 1° fate involves LIN-1 (ETS) and LIN-39 (HOM-C), while LIN-11 (LIM) and LIN-29 (zinc finger) function during the second step, and COG-1 (Homeobox) and EGL-38 (PAX) during the third step. The epistasis results of double and triple mutant of genes involved in different steps indicate the requirement of completion of an early step to display defects of a later step. Therefore, these three steps may be sequential, or genes involved in an early step may also be required during a later step.

Based on the available data, it is highly probable that some or even all of the discussed transcription factors are present in the 1° VPC descendants at the same time. It is therefore possible that they influence

each other's expression or activity. This is supported by the significant reduction of *lin-11::GFP* expression in the P6.pxxx cells in *lin-29* mutants, and the increase of *cog-1::GFP* expression in the inner P6.pxxx cells in *lin-11* and *egl-38* mutants (Table 6). As a result, the network of transcription factors is complex and activity of its members is related to each other.

Changes of expression of *egl-17::GFP* in 1° VPC descendants indicate that *lin-11, lin-29* and *cog-1* are all functionally required in all P6.pxxx cells, while *egl-38* may function only in inner P6.pxxx cells. Data obtained using the *zmp-1::GFP* marker confirm this result (Table 3, 4 and 5). Another construct that is expressed in the inner P6.pxxx cells during the L4 stage, *lin-3::GFP* or *lin-3::lacZ*, failed to express in the inner P6.pxxx cells in *lin-11, lin-29, cog-1* and *egl-38* mutants, which is consistent with this conclusion (Chang et al., 1999; B. J. Hwang and P. W. S., unpublished). The specific functioning of *egl-38* in the inner 1° VPC descendants implies that it may differentiate vulF from the vulE cells, while other transcription factors function in both types of cells.

It is worth noting that whenever *egl-17::GFP* failed to be turned off during the second step of 1° fate execution (in *lin-11, lin-29, lin-11; cog-1, lin-29; cog-1, lin-11; cog-1; egl-38,* and *lin-29; cog-1; egl-38* mutants), it also failed to be expressed in 2° lineages (Table 3 and Figure 2). In contrast, when *egl-17::GFP* was turned off successfully in the second step of 1° fate execution, even though the third step was abnormal (*cog-1* and *cog-1; egl-38*), it was expressed normally in the 2° lineage. Therefore, regulation of 2° fate execution and the second step of 1° fate execution may share common factors or mechanisms.

Regulation of gene transcription during the execution of the 1° fate

Our screen for genes specifically affecting the behavior of the 1° VPC

descendants, but not the early induction of the VPCs, has identified *lin-11*

and *lin-29*. However, some other genes involved may not come up due to

limitations of this screen. First, some genes involved in 1° fate execution,

for instance, *egl-38* does not change the expression pattern of *egl-17::GFP*

when mutated. Second, prescreen of the fertile protruding vulval

phenotype excludes all sterile mutants. If a gene affects both the vulva and

the somatic gonad to cause sterility, it will not be identified in our screen.

Many mutants with vulval morphgenesis or uterine-vulval

connection defects do not display defects in *egl-17::GFP* or *zmp-1::GFP*

expression in the 1° lineage. We crossed *egl-17::GPP* or *zmp-1::GFP* into

cog-2, *sqv-3*, *evl-4* and *evl-22* mutant backgrounds. *cog-2* encodes a Sox

domain transcription factor, and is required for establishing the uterine-

vulval connection (Hanna-Rose and Han, 1999). We found that *cog-2(ku194)*

mutants had wild-type expression pattern of *egl-17::GFP* and *zmp-1::GFP*

in P6.p descendants (data not shown). One class of genes called *sqv* affects

the morphology of the vulval invagination and identifies components of a

conserved glycosylation pathway (Herman et al., 1999; Herman and

Horvitz, 1999). We chose *sqv-3* as an example of the *sqv* mutants and found

that both *egl-17::GFP* and *zmp-1::GFP* are expressed normally in P6.p

descendants in *sqv-3(n2842)* mutants (data not shown). *evl* mutants were

identified by the abnormal morphology of the vulva, and were divided into

three different classes, in which class II and class III have a more severe

phenotype (Seydoux et al., 1993). We examined the phenotype of *evl-4(ar101)* of class II and *evl-22(ar104)* of class III. In both mutants, about 30% animals *either* had no 1°-like lineage formed or less than three VPCs induced (n=28, 27, respectively). The remaining animals had wild-type *egl-17::GFP* expression in P6.p descendants (data not shown). It remains possible that some of these genes do function in the execution of the 1° fate, although their mutants exhibit no defect using the available markers.

The complexity of the process of 1° fate execution leads us to speculate that there are many yet unidentified players in addition to the six genes identified. Notably, all six transcription factors belong to different families and possess distinct domains that are known to bind distinct DNA sequences. *egl-17, lin-12, lin-39* and *let-23* are the few genes that have been shown to change their expression in P6.p during vulval induction (Simske et al., 1996; Burdine et al., 1998; Levitan and Greenwald, 1998; Maloof and Kenyon, 1998). While these genes may be among the immediate targets of Ras signaling, *zmp-1* may be among the more downstream targets. Detailed promoter analysis of these genes and DNA binding assay with the known transciption factors may reveal the complex process of transciptional regulation in the VPC, which leads to specification, commitment and execution of the 1° fate.

Hanna-Rose and Min Han for *cog-2* mutants, Tory Herman and Bob Horvitz

for *sqv-3*, and Geraldine Seydoux and Iva Greenwald for Evl mutants.

Takao Inoue first observed that *egl-29* failed to complement *lin-29*. This

work was supported by USPHS grant HD23690 to P.W.S., an Investigator

with the Howard Hughes Medical Institute.

REFERENCES

Ambros, V. (1989). A hierarchy of regulatory genes controls a larval-to-
adult switch in *C. elegans*. *Cell* **57**, 49-57.

Ambros, V. (1999). Cell cycle-dependent sequencing of cell fate decisions in
Caenorhabditis elegans vulval precursor cells. *Development* **126**, 1947-
1956.

Ambros, V. and Horvitz, H. R. (1984). Heterochronic mutants of the
nematode *Caenorhabditis elegans*. *Science* **226**, 409-416.

Aroian, R. V., Koga, M., Mendel, J. E., Ohshima, Y. and Sternberg, P. W.
(1990). The *let-23* gene necessary for *Caenorhabditis elegans* vulval
induction encodes a tyrosine kinase of the EGF receptor subfamily.
Nature **348**, 693-699.

Artavanis-Tsakonas, S., Matsuno, K. and Fortini, M. E. (1995). Notch
signaling. *Science* **268**, 225-232.

Beitel, G. J., Clark, S. G. and Horvitz, H. R. (1990). *Caenorhabditis elegans*
ras gene *let-60* acts as a switch in the pathway of vulval induction.
Nature **348**, 503-509.

Beitel, G. J., Tuck, S., Greenwald, I. and Horvitz, H. R. (1995). The *Caenorhabditis elegans* gene *lin-1* encodes an ETS-domain protein and defines a branch in the vulval induction pathway. *Genes Dev.* **9**, 3149-3162.

Bettinger, J. C., Euling, S. and Rougie, A. E. (1997). The terminal differentiation factor LIN-29 is required for proper vulval morphogenesis and egg laying in *Caenorhabditis elegans*. *Development* **124**, 4333-4342.

Burdine, R. D., Branda, C. S. and Stern, M. J. (1998). EGF-17(FGF) expression coordinates the attraction of the migration sex myoblasts with vulval induction in *C. elegans*. *Development* **125**, 1083-1093.

Burdine, R. D., Chen, E. B., Kwok, S. F. and Stern, M. J. (1997). *egl-17* encodes an invertebrate fibroblast growth factor family member required specifically for sex myoblast migration in *Caenorhabditis elegans*. *Proc. Natl. Acad. Sci. USA* **94**, 2433-2437.

Chamberlin, H. M., Palmer, R. E., Newman, A. P., Sternberg, P. W., Baillie, D. L. and Thomas, J. H. (1997). The PAX gene *egl-38* mediates developmental patterning in *Caenorhabditis elegans*. *Development* **124**, 3919-3928.

Chang, C., Newman, A. P. and Sternberg, P. W. (1999). Reciprocal EGF signaling back to the uterus from the induced *C. elegans* vulval coordinates morphogenesis of epithelia. *Curr. Biol.* **9**, 237-246.

Clandinin, T. R., Katz, W. S. and Sternberg, P. W. (1997). *Caenorhabditis elegans* HOM-C genes regulate the response of vulval precursor cells to inductive signal. *Dev. Biol.* **182**, 150-161.

Clark, S. G., Chisholm, A. D. and Horvitz, H. R. (1993). Control of cell fates in the central body region of *C. elegans* by the homeobox gene *lin-39*. *Cell* **74**, 43-55.

Ellis, H. M. (1985). Genetic control of programmed cell death in the nematode *Caenorhabditis elegans*. Ph.D. thesis, Massachusetts Institute of Technology.

Ferguson, E. L. and Horvitz, H. R. (1985). Identification and characterization of 22 genes that affect the vulval cell lineages of the nematode *Caenorhabditis elegans*. *Genetics* **110**, 17-72.

Ferguson, E. L., Sternberg, P. W. and Horvitz, H. R. (1987). A genetic pathway for the specification of the vulval lineages of *Caenorhabditis elegans*. *Nature* **326**, 259-267.

Freyd, G., Kim, S. K. and Horvitz, R. H. (1990). Novel cysteine-rich motif and homeodomain in the product of the *Caenorhabditis elegans* cell lineage gene *lin-11*. *Nature* **344**, 876-879.

Greenwald I. (1997). Development of the vulva. *In* "*C. elegans* II". (D. Riddle, T. Blumenthal, B. Meyer and J. Priess, Ed.), pp.519-541. Cold Spring Harbor Laboratory Press, New York.

Greenwald, I. and Rubin, G. M. (1992). Making a difference: the role of cell-cell interactions in establishing separate identities for equivalent cells. *Cell* **68**, 271-281.

Greenwald, I. S., Sternberg, P. W. and Horvitz, H.R. (1983). The *lin-12* locus specifies cell fates in *Caenorhabditis elegans*. *Cell* **34**, 435-444.

Han, M., Aroian, R. and Sternberg, P. W. (1990). The *let-60* locus controls the switch between vulval and non-vulval cell types in *C. elegans*. *Genetics* **126**, 899-913.

Han, M. and Sternberg, P. W. (1990). *let-60*, a gene that specifies cell fates during *C. elegans* vulval induction, encodes a ras protein. *Cell* **63**, 921-931.

Hanna-Rose, W. and Han, M. (1999). COG-2, a Sox domain protein necessary for establishing a functional vulval-uterine connection in *Caenorhabditis elegans*. Development 126, 169-179.

Herman, T., Hartwieg, E. and Horvitz, H. R. (1999). *squ* mutants of *Caenorhabditis elegans* are defective in vulval epithelial invagination. *Proc. Natl. Acad. Sci. USA* **96**, 968-973.

Herman, T. and Horvitz, H. R. (1999). Three proteins involved in *Caenorhabditis elegans* vulval invagination are similar to components of a glycosylation pathway. *Proc. Natl. Acad. Sci. USA* **96**, 974-979.

Hill, R. J. and Sternberg, P. W. (1992). The gene *lin-3* encodes an inductive signal for vulval development for *C. elegans*. *Nature* **358**, 470-476.

Hobert, O., D'Alberti, T., Liu, Y. and Ruvkun, G. (1998). Control of neural development and function in a thermoregulatory network by the LIM homeobox gene *lin-11*. *J. Neuroscience* **18**, 2084-2096.

Jacobs, D., Beitel, G. J., Clark, S. G., Horvitz, H. R. and Kornfeld, K. (1998). Gain-of-function mutations in the *Caenorhabditis elegans lin-1* ETS gene identify a C-terminal regulatory domain phosphorylated by ERK MAP kinase. *Genetics* **149**, 1809-1822.

Katz, W. S., Hill, R. J., Clandinin, T. R. and Sternberg, P. W. (1995).
Different levels of the *C. elegans* growth factor LIN-3 promote distinct
vulval precursor fates. *Cell* **82**, 297-307.

Kimble, J. *(1981)*. Alterations in cell lineage following laser ablation of cells
in the somatic gonad of *Caenorhabditis elegans*. *Dev. Biol.* **87**, 286-300.

Kimble, J. E. and Hirsh, D. (1979). Post-embryonic cell lineages of the
hermaphrodite and male gonads in *Caenorhabditis elegans*. *Dev.
Biol.* **70**, 396-417.

Koga, M. and Ohshima, Y. (1995). Mosaic analysis of the *let-23* gene
function in vulval induction of *Caenorhabditis elegans*. *Development*
121, 2655-2666.

Kornfeld, K. (1997). Vulval development in *Caenorhabditis elegans*. *Trends
Genet.* **13**, 55-61.

Levitan, D. and Greenwald, I. (1998). LIN-12 protein expression and
localization during vulval development in *C. elegans*. *Development*
125, 3101-3109.

Maloof, J. N. and Kenyon, C. (1998). The Hox gene *lin-39* is required during
C. elegans vulval induction to select the outcome of Ras signaling.
Development **125**, 181-190.

**Newman, A. P., Acton, G. Z., Hartwieg, E., Horvitz, H. R. and Sternberg,
P. W.** (1999) The *lin-11* LIM domain transcription factor is necessary
for morphogenesis of *C. elegans* uterine cells. *Development* **126**, 5319-
5326.

Rougvie, A. E. and Ambros, V. (1995). The heterochronic gene *lin-29* encodes a zinc finger protein that controls a terminal differentiation event in *Caenorhabditis elegans*. *Development* **121**, 2491-2500.

Seydoux, G., Savage, C. and Greenwald, I. (1993). Isolation and characterization of mutations causing abnormal eversion of the vulva in *Caenorhabditis elegans*. *Dev. Biol.* **157**, 423-436.

Sharma-Kishore, R., White, J. G., Southgate, E. and Podbilewicz, B. (1999). Formation of the vulva in *Caenorhabditis elegans*: a paradigm for organogenesis. *Development* **126**, 691-699.

Simske, J. S., Kaech, S. M., Harp, S. A. and Kim, S. K. (1996). LET-23 receptor localization by the cell junction protein LIN-7 during *C. elegans* vulval induction. *Cell* **85**, 195-204.

Simske, J. S. and Kim, S. K. (1995). Sequential signaling during *Caenorhabditis elegans* vulval induction. *Nature* **375**, 142-146.

Sternberg, P. W. and Han, M. (1998). Genetics of RAS signaling in *C. elegans*. *Trends Genet.* **14**, 466-472.

Sternberg, P. W. and Horvitz, H. R. (1986). Pattern formation during vulval induction in *C. elegans*. *Cell* **44**, 761-772.

Sternberg, P. W. and Horvitz, H. R. (1988). *lin-17* mutations *of Caenorhabditis elegans* disrupt certain asymmetric cell divisions. *Dev. Biol.* **130**, 67-73.

Sulston, J. E. and Horvitz, H. R. (1977). Postembryonic cell lineages of the nematode *Caenorhabditis elegans*. *Dev. Biol.* **56**, 110-156.

Sulston, J. E. and White, J. G. (1980). Regulation and cell autonomy during postembryonic development of *Caenorhabditis elegans*. *Dev. Biol.* **78**, 577-597.

Tan, P. B., Lackner, M. R. and Kim, S. K. (1998). MAP kinase signaling specificity mediated by the LIN-1 Ets/LIN-31 WH transcription factor complex during *C. elegans* vulval induction. *Cell* **93**, 569-580.

Wang, M. and Sternberg, P. W. (1999). Competence and commitment of *Caenorhabditis elegans* vulval precursor cells. *Dev. Biol.* **212**, 12-24.

Wassarman, D. A., Therrien, M. and Rubin, G. M. (1995). The Ras signaling pathway in *Drosophila*. *Curr. Opin. Genet. Dev.* **5**, 44-50.

Yochem, J., Weston, K. and Greenwald, I. (1988). The *Caenorhabditis elegans lin-12* gene encodes a transmembrane protein with overall similarity to *Drosophila Notch*. *Nature* **335**, 547-550.

TABLES

Table 1. The temporal patterns of *egl-17::GFP* expression indicate different vulval fates.

egl-17::GFP expression pattern			Fate	Lineage	M	n
Early-L3 (~28 hrs)	Late-L3 (~31 hrs)	Mid-L4 (~40 hrs)				
+	+	-	1°	TTTT/TDDT/ODDT/TD TT/OTTT/TODD/TOTT/ OOOT/OOOO/TDTD/TO TO/OOTO/OODT/DOLO /ODOO/OOTT/OTTO/O OTD/TOOT/TDDL/TLD L/LODL/LOOL/LTTT/L LLO/LOOO/LLLL/LOTT /LLOT	Sn	76
+	+	+ or +++	Abe- rrant	ODDO/OOTT/TOTT/LT TT/OTOT/OOTO/OTTT/ TTDT/TLTT	Sn	12
				LLOD/LOTD/LDDD/LD DT/LTTT/ LOOO/ULLL	An	10
+	-	-	3°	SS	N/A	6
+	-	+++	2°	LLTN/LLON/LLDN/LL OO//LLTL/LLDD	Aa	10
-	-	-	Abe- rrant	LLLL/ULLL/LTOL	Sa	4
-	-	+++	2°	LLTN/LLLN/LLDN/?LT N/LLON/LLLN/OLLN/ TLLN/LLON/LLON/LL LD/LLTL/LLOD/LUOO	Aa	97

Table 1. *egl-17::GFP; hs-LIN-3; lin-3(lf)* animals were heat shocked at 31°C

for 15 minutes during the L2 molt, and GFP expression were observed in

Pn.p cells at early L3, Pn.pxx cells at late-L3, and Pn.pxxx cells mid-L4

stage. The time indicated in the parentheses is number of hours from

hatching at 20°C. The developmental stage and time were deduced

according to the development of the gonad and the Pn.p lineages (Sulston

and Horvitz, 1977). +, the expression of GFP was observed; +++, the

expression of GFP was very strong; -, the expression of GFP was not

observed. Lineage, vulval lineages observed since the late L3 stage.

Abbreviations for divisions of Pn.pxx nuclei are based on Sternberg and

Horvitz (1986). T, transverse division; O, oblique division; D, division

occurred but axis not observed; N, division did not occur and the Pn.pxx

nucleus showed distinct morphology; U, division did not occur; L,

longitudinal division; underlining indicates Pn.pxxx progeny adhered to

the ventral cuticle at the L3 molt. M, vulval morphogenesis at mid-L4 (Katz

et al., 1995): the first letter indicates the vulval morphology, either

symmetric (S) or asymmetric (A), while the second letter describes the

adherence of vulval tissue to the ventral cuticle which can be either

adherence (a) or nonadherence (n). N/A, not applicable. n, number of

VPCs scored.

Table 2. Mutations identified in a screen for defects in *egl-17::GFP* expression.

Mutants(allele)	Defects in *egl-17::GFP* expression pattern	Defects in vulval lineages
lin-11(sy533)	1° & 2°	2°
lin-11(sy534)	1° & 2°	2°
lin-29(sy531)	1° & 2°	wild-type
lin-29(sy532)	1° & 2°	wild-type
lin-17(sy565)	2°	2°
lin-18(sy540)	2°	2°

Table 2. Animals were scored for the expression of *egl-17::GFP* in P6.pxx cells during the late-L3 stage and in P6.pxxx cells during the mid-L4 stage. We also scored vulval lineages from the mid-L3 to early-L4 stage.

Table 3. The network of *lin-11*, *egl-29*, *cog-1* and *egl-38* functions during the second and third steps of 1° fate execution.

Genotype	Expression pattern of *egl-17::GFP* in P6.p descendants				n
	Late-L3 (31 hrs)	Post early-L4 (37 hrs)	Mid-L4 (40 hrs)		
	P6.pxx	P6.pxxx	outer	inner	
wild-type	+	-	-	-	59
lin-11	+	+/-	+/-	+/-	45
lin-29	+	+/-	+/-	+/-	43
lin-11; lin-29	+	+/-	+/-	+/-	38
cog-1	+	-	+++	-	46
egl-38	+	-	-	-	38
cog-1; egl-38	+	-	+++	+++	37
lin-11; cog-1	+	+/-	+/-	+/-	43
lin-29; cog-1	+	+/-	+/-	+/-	40
lin-11; cog-1; egl-38	+	+/-	+/-	+/-	35
lin-29; cog-1; egl-38	+	+/-	+/-	+/-	36

Table 3. Animals were scored for the expression of *egl-17::GFP* in P6.pxx cells at the late-L3 stage, and in P6.pxxx cells at the post early-L4 stage and the mid-L4 stage. +, GFP expression was observed; +/-, weak GFP expression was observed; +++, strong GFP expression was observed; -, GFP expression was not observed. n, number of animals observed. Alleles used are: *lin-11(n389)*, *lin-29(sy292)*, *cog-1(sy275)*, and *egl-38(n578)*.

Table 4. *lin-39* and *lin-1* are required during the first step of 1° fate execution.

A.

Genotype	Expression of *egl-17::GFP* in P6.p descendants		n
	Late-L3 (31 hrs) P6.pxx	Mid-L4 (40 hrs) P6.pxxx	
wild-type	+	-	59
lin-1(gf)	-	-	48
lin-1(lf)	-	-	66
hs-lin-39	++	-	52
lin-1(gf); hs-lin-39	++	-	43
lin-1(lf); hs-lin-39	++	-	49

B.

Genotype	Expression of *egl-17::GFP* in P6.p descendants		n
	Late-L3 (31 hrs) P6.pxx	Mid-L4 (40 hrs) P6.pxxx	
wild-type	+	-	31
lin-39	+/-	-	40
lin-11	+	+/-	38
lin-29	+	+/-	39
lin-11; lin-39	+/-	-	32
lin-29; lin-39	+/-	-	33

Table 4. Animals were scored for the expression of *egl-17::GFP* in P6.pxx

cells during the late-L3 stage and in P6.pxxx cells during the mid-L4 stage.

+, GFP expression was observed; -, GFP expression was not observed; ++,

strong GFP expression was observed; +/-, weak GFP expression was

observed. For heat shock experiments, animals were heat shocked at 33°C

for 30 minutes during the early L3 stage. For experiments in part A,

animals were grown at 20°C, in part B, animals were grown at 25°C. n,

number of animals observed. Alleles used are: *lin-1(n1790gf), lin-1(sy254),*

lin-11(n389), lin-29(sy292), lin-39(n709ts).

Table 5. *lin-11, egl-29, cog-1* **and** *egl-38* **regulate the expression of** *zmp-1:GFP* **in vulE and vulF at the L4 molt.**

Genotype	Expression pattern of *zmp-1::GFP* in P6.pxxx	n
wild-type	+ - - +	80
lin-11	- - - -	55
lin-29	- - - -	50
cog-1	- - - -	52
egl-38	+ + + +	48
lin-11; egl-38	- - - -	52
lin-29; egl-38	- - - -	56
cog-1; egl-38	- - - -	56

Table 5. Animals were scored for the expression of *zmp-1::GFP* in P6.pxxx during the L4 molt. +, GFP expression was observed; -, GFP expression was not observed. The symbols of + and − correspond to GFP expressions in outer, inner, inner, and outer great granddaughters of P6.p (P6.paax, P6.papx, P6.ppax, and P6.pppx) in one of the two identical patterns at the left or right side of the animal. n, number of animals observed. Alleles used are: *lin-11(n389)*, *lin-29(sy292)*, *cog-1(sy275)*, and *egl-38(n578)*.

Table 6. *lin-11*, *egl-29*, *cog-1* and *egl-38* regulate the expression of one another in the 1° VPC descendants.

A. Expression pattern of *lin-11::GFP*

Genotype	Expression pattern of *lin-11::GFP* in P6.pxxx	n
wild-type	+ + + +	67
lin-29	- - - - or +/- +/- +/- +/-	85
cog-1	+ + + +	48
egl-38	+ + + +	42

B. Expression pattern of *cog-1::GFP*

Genotype	Expression pattern of *cog-1::GFP* in P6.pxxx	n
wild-type	+ - - +	75
lin-11	+ + + +	58
lin-29	+ - - +	51
egl-38	+ + + +	62

Table 6. Animals were scored for the expression of (A) *lin-11::GFP* or (B) *cog-1::GFP* in P6.pxxx during the mid-L4 stage. +, GFP expression was observed; +/-, GFP expression was very faint; -, GFP expression was not observed. The symbols of + and − correspond to GFP expressions in outer, inner, inner, and outer great granddaughters of P6.p (P6.paax, P6.papx, P6.ppax, and P6.pppx) in one of the two identical patterns at the left or right side of the animal. n, number of animals observed. Alleles used are: *lin-11(n389)*, *egl-29(sy292)*, *cog-1(sy275)*, and *egl-38(n578)*. We used *syEx198* for translational fusion of *cog-1::GFP* (R. A. Palmer and P. W. S., unpublished), and *nIs96* for transcriptional fusion of *lin-11::GFP* (S. Cameron and H. R. Horvitz, personal communication).

FIGURES

Figure 1. Schematic outline of the expression of *egl-17::GFP* in vulval lineages.

Outline of a lateral view of a hermaphrodite during the L3 and L4 stages. In all panels, ventral is down, anterior is to the left. In panel A, three induced VPCs, P5.p-P7.p, produce four granddaughters each after two rounds of cell division. After a third round of cell division, VPC descendants undergo morphogenesis and form an invagination. The darker circles indicate the Pn.pxxx cells at the left side of the animal, and the lighter circles indicate the Pn.pxxx cells at the right side. In panel B, six VPCs adopt three different fates during vulval development. VPC fates are determined by the division pattern and the morphogenesis behavior of the VPC progeny. Horizontal lines indicate cell divisions and vertical lines represent individual cells. L, longitudinal division; underlining, strong adherence to the ventral cuticle. T, transverse division. N, division did not occur and nucleus compact. S, VPC daughters did not divide and fuse with the epidermis. A, B1, B2, C, D, E and F indicate seven types of vulval descendants. In both panels, filled circles indicate VPC descendants that expressed *egl-17::GFP*. Unfilled circles indicate VPC descendants that did not express *zmp-1::GFP*.
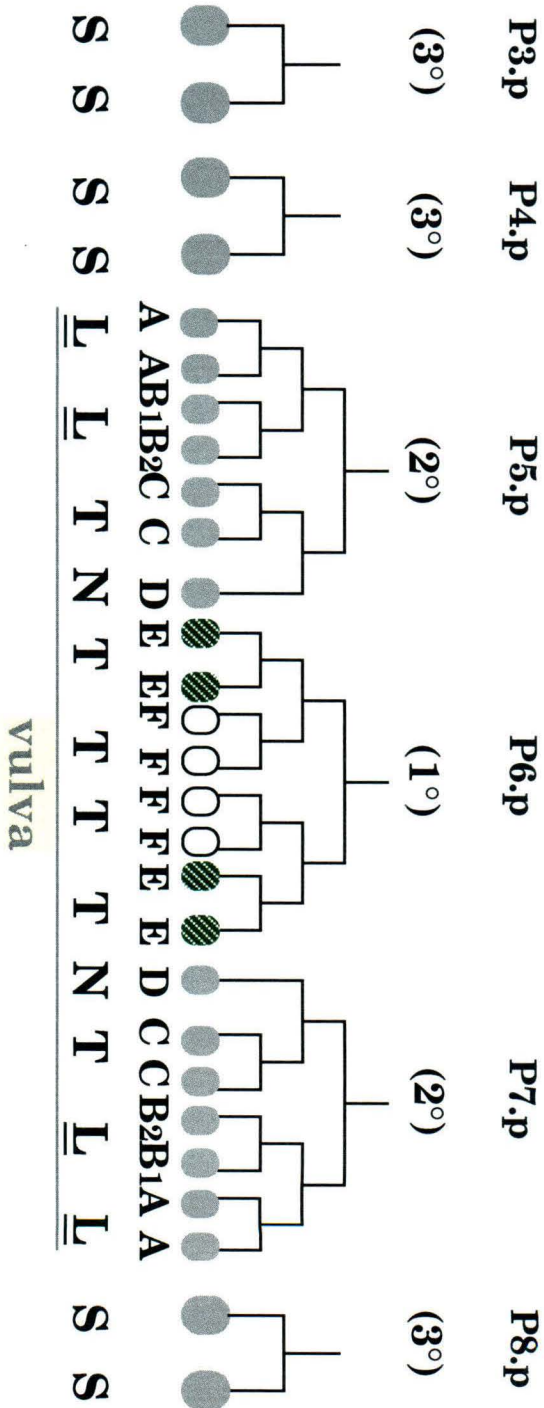
A.

step 1
(L3)

step 2
(post early-L4)

step 3
(mid-L4)

P5.p

P6.p

P7.p
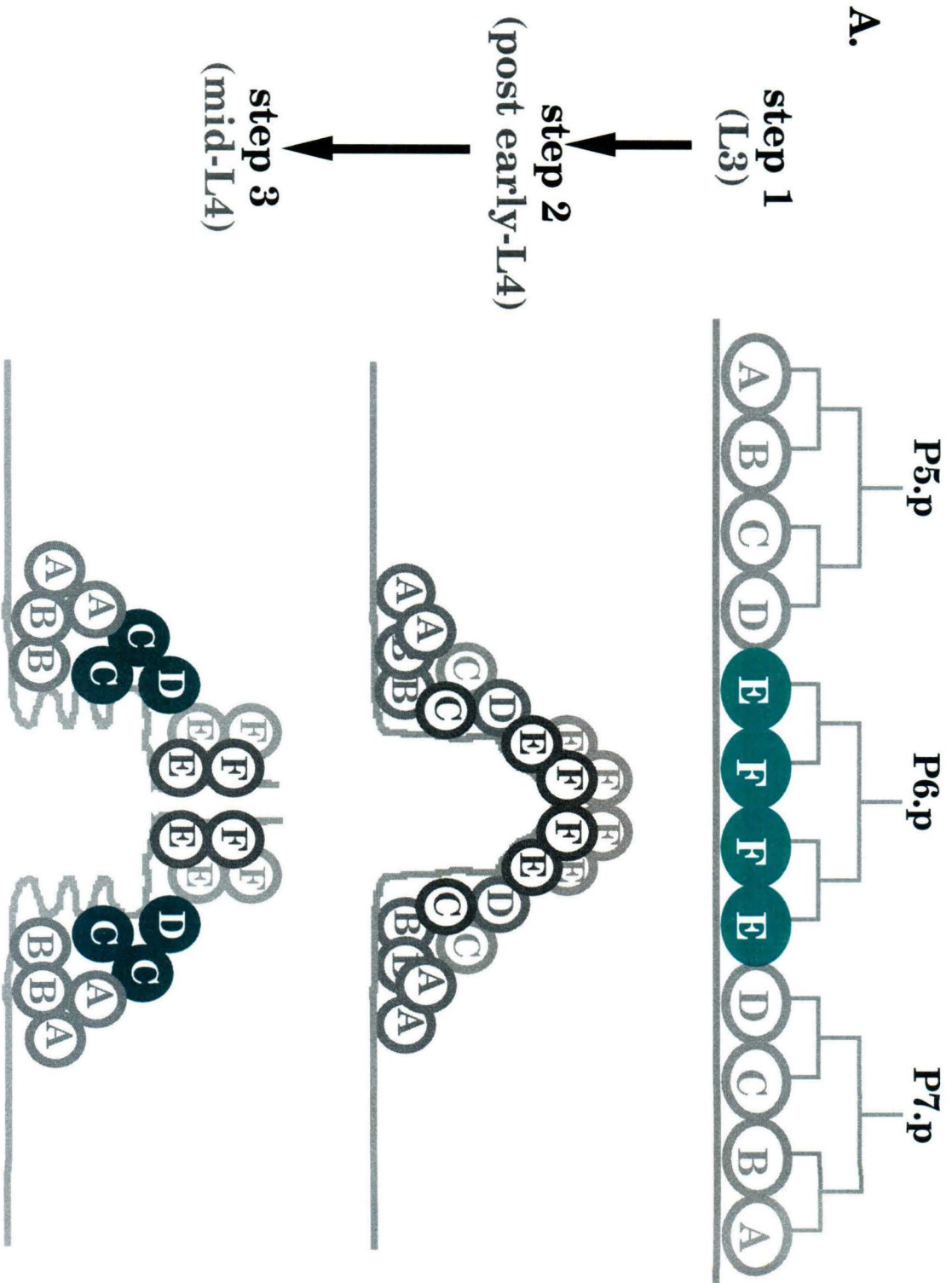
B.

Figure 2. *lin-11, lin-29, cog-1* **and** *egl-38* **are involved in the second and third steps of 1° fate execution.**

Displays animals from Table 3. In all panels, ventral is down, anterior is to the left. Arrowheads indicate the position of the visible P6.pxxx nuclei during the mid L4 stage. Abbreviations: i, inner P6.pxxx; o, outer P6.pxxx. All animals displayed had *egl-17::GFP* in their background, and the four P6.pxxx cells at the left side of the animal during the mid-L4 stage were photographed. The scale bar is 10 μm. (A) and (B): Nomarski and fluorescence images of a wild-type animal. P6.pxxx cells did not express *egl-17::GFP*, while the C and D descendants of the 2° lineages expressed GFP strongly. (C) and (D): Nomarski and fluorescence images of a *lin-11(n389)* animal. All P6.pxxx cells had faint *egl-17:::GFP* expression, while none of the 2° VPC descendants expressed GFP. (E) and (F): Nomarski and fluorescence images of a *lin-29(sy292)* animal. All P6.pxxx cells expressed *egl-17:::GFP* weakly, while none of the 2° VPC descendants expressed GFP. (G) and (H): Nomarski and fluorescence images of a *cog-1(sy275)* animal. The outer P6.pxxx cells expressed *egl-17::GFP* strongly, the inner P6.pxxx cells did not express the marker. The GFP expressions beside the inner P6.pxxx cells were from the T descendants of the 2° lineages. (I) and (J): Nomarski and fluorescence images of an *egl-38(n578)* animal. P6.pxxx cells did not express *egl-17::GFP* at this stage, while the C and D descendants of the 2° lineages expressed GFP strongly at this stage. (K) and (L): Nomarski and fluorescence images of a *cog-1(sy275); egl-38(n578)* animal. All P6.pxxx cells, as well as the T descendants of the 2° lineages expressed *egl-17::GFP* strongly. (M) and (N): Nomarski and fluorescence

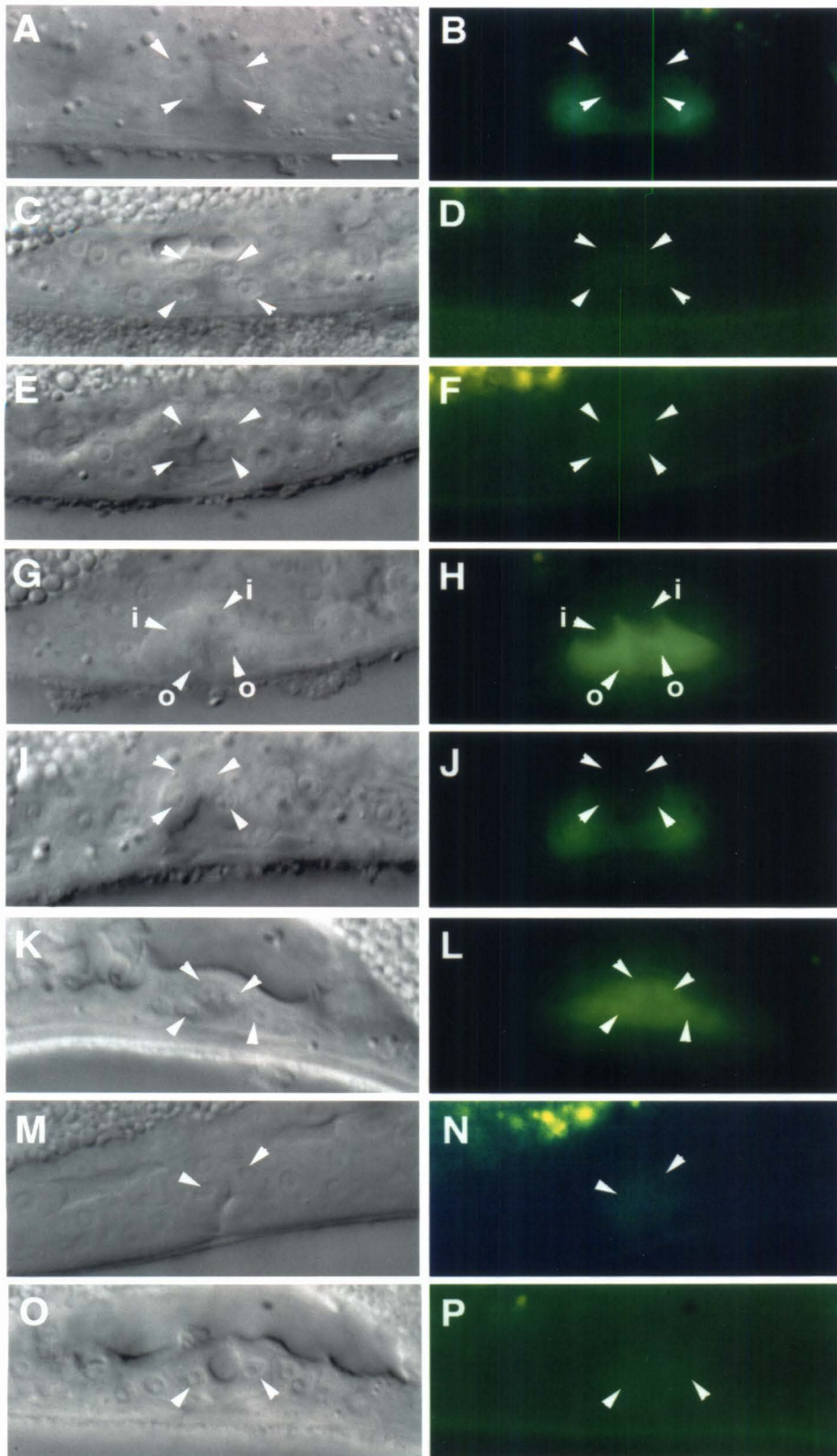images of a *lin-11(n389); cog-1(sy275); egl-38(n578)* animal. All P6.pxxx cells had faint *egl-17:::GFP* expression, while none of the 2° VPC descendants expressed GFP. (O) and (P): Nomarski and fluorescence images of a *lin-29(sy292); cog-1(sy275); egl-38(n578)* animal. All P6.pxxx cells had faint *egl-17:::GFP* expression, while none of the 2° VPC descendants expressed GFP.

Figure 3. A transcription factor network regulates three steps of 1° fate execution.

In wild-type animals, the AC induces P6.p to adopt the 1° fate through the Ras signaling pathway from the late L2 to the early L3 stage. AC induction leads to *egl-17:GFP* expression in P6.p, which indicates 1° fate specification. *lin-1* and *lin-39* regulate the first step of 1° fate execution when commitment to the 1° fate occur, where *egl-17::GFP* is expressed continuously in the P6.p daughter and granddaughters. During the second step, *lin-11* and *lin-29* suppress *egl-17::GFP* expression in all P6.pxxx cells, right before the separation of the inner P6.pxxx cells and establishment of the uterine-vulval connection. Afterwards, the expression of *egl-17::GFP* expression is suppressed by *egl-38* in the inner P6.pxxx cells and *cog-1* in all P6.pxxx cells during the third step. At the end of vulval morphogenesis, *lin-11, lin-29* and *cog-1* promote *zmp-1::GFP* expression in all P6.pxxx cells, while *egl-38* suppresses *zmp-1::GFP* expression in the inner P6.pxxx cells.
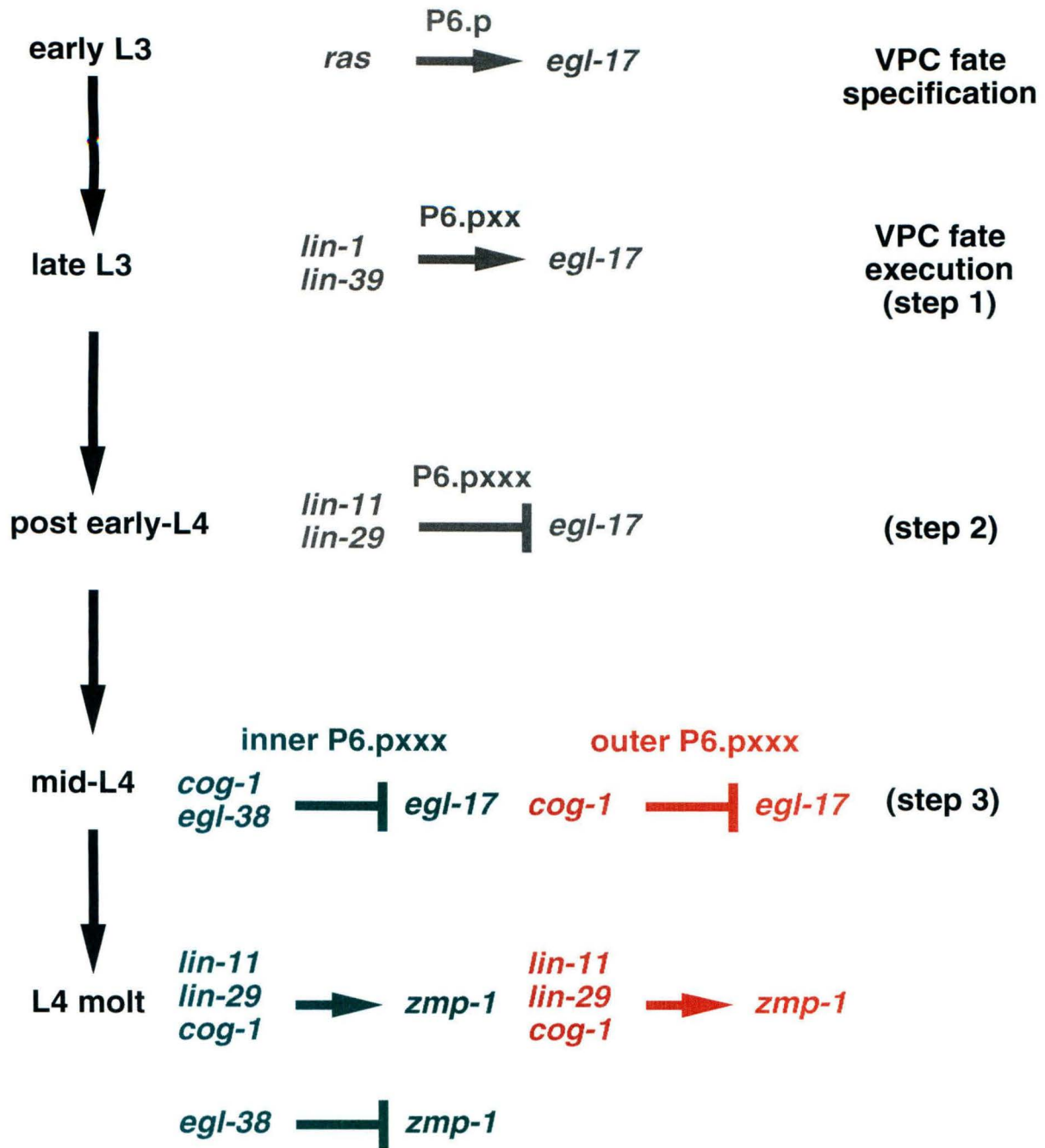
Appendix

DNA-binding properties of *Arabidopsis*

MADS domain homeotic proteins

APETALA1, APETALA3, PISTILLATA and AGAMOUS

José Luis Riechmann, Minqin Wang and Elliot M. Meyerowitz

(reprinted with permission)

DNA-binding properties of *Arabidopsis* MADS domain homeotic proteins APETALA1, APETALA3, PISTILLATA and AGAMOUS

José Luis Riechmann, Minqin Wang and Elliot M. Meyerowitz*

Division of Biology 156-29, California Institute of Technology, Pasadena, CA 91125, USA

ABSTRACT

The MADS domain proteins APETALA1 (AP1), APETALA3 (AP3), PISTILLATA (PI), and AGAMOUS (AG) specify the identity of *Arabidopsis* floral organs. AP1 and AG homocomplexes and AP3–PI heterocomplexes bind to CArG-box sequences. The DNA-binding properties of these complexes were investigated. We find that AP1, AG and AP3–PI are all capable of recognizing the same DNA-binding sites, although with somewhat different affinities. In addition, the three complexes induce similar conformational changes on a CArG-box sequence. Phasing analysis reveals that the induced distortion is DNA bending, oriented toward the minor groove. The molecular dissection of AP1, AP3, PI and AG indicates that the boundaries of the dimerization domains of these proteins vary. The regions required to form a DNA-binding complex include, in addition to the MADS box, the entire L region (which follows the MADS box) and the first putative amphipathic helix of the K box in the case of AP3–PI, while for AP1 and AG only a part of the L region is needed. The similarity of the DNA-binding properties of AP1, AP3–PI and AG is discussed with regard to the biological specificity that these proteins exhibit.

INTRODUCTION

According to a well-established genetic model (1–3), the identities of the organs of an *Arabidopsis* flower are specified by the action of at least five homeotic genes: *APETALA1 (AP1)*, *APETALA2 (AP2)*, *APETALA3 (AP3)*, *PISTILLATA (PI)* and *AGAMOUS (AG)* (4–8). While these genes have been extensively characterized at the genetic level, little is known about the molecular mechanisms by which the organ-identity proteins act. AP1, AP3, PI and AG are all MADS domain proteins (4,6–8). The MADS domain is a conserved DNA-binding/dimerization region present in a variety of transcription factors from different organisms (SRF, serum response factor; MCM1; the MEF2 family) (9,10). Within the family of MADS domain proteins, a particular characteristic of the plant proteins is that the vast majority of them contain another conserved region, the K box (11,12). This region has similarity to the coiled-coil segment of

keratin, suggesting that the K box may form amphipathic alpha helices, perhaps involved in protein–protein interactions (11,13). SRF and MCM1 recognize CArG-box sequences (consensus $CC(A/T)_6GG$) (14,15), and *in vitro* experiments have shown that AG (16–20), AP1 and AP3–PI (20) complexes bind to such sites. These four proteins exhibit partner specificity for the formation of DNA-binding complexes: neither AP3 nor PI have been found to bind DNA by themselves or in combination with either AP1 or AG (20).

Since these four related proteins act to specify the development of different organ types in the *Arabidopsis* flower, we were interested in comparing the DNA binding properties of the AP1, AP3–PI and AG complexes, which are dimers, in an effort to understand how the biological specificity of these (presumed) transcription factors is achieved. We show that the DNA-binding specificities of AP1, AP3–PI and AG dimers are very similar, since they recognize the same DNA-binding sites, although differences in affinities were detected. The three complexes are also similar in the distortion that they induce on the DNA, that is (at least in part) DNA bending toward the minor groove. In addition, the molecular dissection of AP1, AP3, PI and AG has revealed differences in the regions that are required for dimerization among these four proteins, which correlate with the partner specificity that they exhibit.

MATERIALS AND METHODS

Plasmids for *in vitro* transcription/translation

pSPUTK (Stratagene)-derived plasmids to produce AP1, AP3, PI and AG in *in vitro* transcription/translation reactions have been described previously (20). Several derivatives of *AP3*, *PI* and *AG* sequences were synthesized by PCR in order to make N- and C-terminal truncated proteins, as listed below, and cloned into pSPUTK. Throughout this article, the N- (N-terminal extension that precedes the AG MADS-box), M- (MADS domain), L- (linker between the MADS domain and the K box), K- (K box) and C- (C-terminal) regions of AP1, AP3, PI and AG, as well as the corresponding amino acid numbering, are as shown in Figure 1 of ref. 20. AP3ΔMLCK: AP3 protein lacking the first 26 aa of the MADS box (Asn residue at position 26 is changed into the initiation Met). AP3ML: truncated AP3 protein comprising only the MADS box and the L region (a stop codon was

introduced after the Gln residue at position 88). PIML: truncated PI protein comprising only the MADS box and the L region. AGΔMLCK: AG protein lacking the N region and the first half of the MADS box (Asn residue is changed into the initiation Met). AGLKC: the AGLKC protein lacks the N region and the entire MADS box except the two last aa (it therefore starts with the sequence Met-Glu-Tyr-Ser...). AGNM: truncated AG protein comprising only the N region and the MADS box. AGNML: truncated AG protein comprising the N, MADS and L regions. AGNMLK: truncated AG protein lacking the C-terminal region.

DNA-binding site probes

Seven different probes (A–G) were used. Probes A and B are derived from the promoters of the *Arabidopsis AP3* and *SUPERMAN (SUP)* genes, respectively, and have been described previously (20); probe D is derived from the *Arabidopsis AGL5* promoter (19); sites C and E were obtained in sequence-selection experiments performed with AG (17; site clones #85 and #41, respectively); sites F and G were obtained in sequence-selection experiments performed with AGL3 (21; site clones #3 and #103, respectively). All binding sites were cloned into pGEM vectors. Probe A, 5′-*ggatcc*TCACTTAGTTTTCATCAACTTCTGAAC-TTACCTTTCATGGATTAGGCAATACTTT<u>CCATTTTTAGT</u>-AACT*aagctt*-3′, (an additional CArG-box like sequence is also present in this probe, but it was determined by site-directed mutagenesis that it is not recognized by any of the proteins used in this study); probe B, 5′-*ggatcc*TAAGAAAAATGGGAGAA-AGGAACATCCACTTTT<u>CCATTTTTGG</u>TATAAAACTTTT-GATATAATATGTCCTTTTGCT*aagctt*-3′; probe C, 5′-*aagcttgc*-atgcctgcaggtcgactctagaggatccacagcAATACATT<u>CCATATTTG</u>-<u>GC</u>AGGTGGCtcc*ggaattc*-3′; probe D, 5′-*ggatcc*CAATAAAAA-GAAAAGGAGAATAAAAGGGATTA<u>CCAAAAAAGG</u>AA AGTTTCCAAAAGGTGATTCTGATGA*agctt*-3′; probe E, 5′-*tctaga*ctcaggaattcggtacccgggtATACTTTA<u>CCGAATGGGG</u>-TTAGACTAt*ggatcc*-3′; probe F, 5′-*tctaga*ctcgaggaattcggtaccc-gggtTCAACC<u>CCATTTATAG</u>CCACGTCAGTt*ggatcc*-3′; probe G, 5′-*tctaga*ctcgaggaattcggtacccgggtACGCATGCA<u>CCACAT</u>-<u>ATAG</u>TAACGTGt*ggatcc*-3′; (the CArG-boxes are underlined and the plasmid-derived linker sequences are in lower case). Binding probes were prepared as described (20).

In vitro transcription and translation

Proteins were synthesized using the TNT coupled transcription/translation reticulocyte lysate system (Promega). Labeled ([35S]methionine) *in vitro* translation reactions demonstrated that the proteins were produced in similar amounts. Some of the C-terminal deletion derivatives of AP1, AP3, PI and AG proteins were obtained by digesting the plasmids encoding the full-length proteins with internal restriction sites prior to the *in vitro* transcription reaction. AP1M–2, AP1M+3, AP1M+15, AP1M+29, AP1M+33, AP1ML+6, and AP1ML+34 proteins were obtained from RNAs synthesized from pSPUTK-AP1 linearized with *Bst*BI, *Hinf*I, *Rsa*I, *Ple*I, *Bsr*I, *Afl*II and *Alw*NI, respectively. To obtain AP3ML+12, AP3ML+31 and AP3ML+42, pSPUTK-AP3 was linearized with *Ple*I, *Alw*NI and *Fok*I, respectively. The PI open reading frame was linearized at *Ecl*136II and *Bpm*I sites to generate PIML+16 and PIML+20, respectively. AGNM+22 and AGNM+28 were obtained after digestion of pSPUTK-AG with *Ase*I and *Msp*I. The RNAs were purified by agarose gel electrophoresis prior to their

use in *in vitro* translation reactions performed with standard reticulocyte lysate (Promega).

DNA-binding assays and immunoprecipitation experiments

In vitro translated proteins were tested for DNA-binding activity by electrophoretic mobility shift assay (EMSA). Binding reactions were performed as described previously (20). Gels for resolving protein–DNA complexes were 5% (except when indicated otherwise) polyacrylamide:bisacrylamide (60:1) in 1× TBE. Immunoprecipitation experiments were carried out as described previously (20).

Apparent K_d values in DNA binding

Saturation-binding assays to determine the dissociation constants (K_d) were carried out by incubating a fixed amount of *in vitro* translated proteins (2 μl of the translation reaction) with increasing amounts of probes A or B under the standard conditions (the incubation time after addition of the probe was extended to 90 min to allow the binding reactions to reach equilibrium, as determined in pilot experiments). Probes were used at concentrations between 1 and 80 nM, the concentration range depending on the protein/probe combination. After gel electrophoresis, bound and free probe were quantitated with a phosphorimager (Molecular Dynamics). The production of both the full-length and a truncated AP1 protein in the *in vitro* translation reactions resulted in the formation of three different AP1 DNA-binding complexes. The amount of probe bound by all of them was quantitated, and the values obtained were used for the calculations as the total amount of bound probe. DNA-binding reactions with AG also showed band shifts originated by truncated AG proteins, but the amount of probe that was bound in the AG reactions is very low. This ensured that the concentration of free probe at equilibrium was approximately equal to the concentration of total probe, and therefore that the values obtained for the probe bound only by full-length AG could be used to calculate the apparent K_ds. K_ds were estimated by the method of Scatchard and calculation of the least-square fit line of the primary data, wherein $K_d = -1/\text{slope}$ (22).

Circular permutation and phasing analyses

For circular permutation analysis, two annealed complementary oligonucleotides containing the site A CArG-box, 5′-CTAGAG-CAATACTTT<u>CCATTTTTAG</u>TAACTCAAGTC-3′ and 5′-TCG-AGACTTGAGTTA<u>CTAAAAATGG</u>AAAGTATTGCT-3′, were cloned into the *Xbal/Sal*I sites of pBend2 (23), generating plasmid pBendA. Probes were prepared by digestion of pBendA with the appropriate restriction enzymes and labeling of the purified fragments with 32P using T4 polynucleotide kinase. The magnitude of apparent DNA bending was calculated using the formula $\mu_{min}/\mu_{max} = \cos(\alpha_D/2)$ (24), where α_D is the distortion angle, and μ_{min} and μ_{max} are the relative mobilities of the slowest and fastest migrating species. The values of μ_{min} and μ_{max} were calculated from the curve produced after fitting the data using a computer function (Cricket Graph III, Cricket Software).

For the phasing analysis, sequences containing the site A CArG-box separated by a linker of variable length from an A tract (intrinsically bent toward the minor groove by approximately 54°; 25) were cloned into the *Xbal/Sal*I sites of pBend2 (23). The distance between the center of the CArG-box and the center of the

A-4

3136 *Nucleic Acids Research, 1996, Vol. 24, No. 16*

A tract was 21, 23, 26, 28 or 30 bases. Sequences were as follows:
5'-ctcagaTTTCCATTTTTAGTATAAAAACGGGCAAAAAC-
GGGCAAAAACGgtcgac-3'; 5'-ctcagaTTTCCATTTTTAGTA-
AGCAAAAACGGGCAAAAACGGGCAAAAACGgtcgac-3';
5'-ctcagaTTTCCATTTTTAGTAACTGGCAAAAACGGGCA-
AAAACGGGCAAAAACGgtcgac-3'; 5'-ctcagaTTTCCATTT-
TTAGTAACTGTAGCAAAAACGGGCAAAAACGGGCAA
AAACGgtcgac-3'; and 5'-ctcagaTTTCCATTTTTAGTAACTG-
TACTGCAAAAACGGGCAAAAACGGGCAAAAACGgtc-
gac-3' (the CArG-box and the A tract are underlined). Probes of
164–173 bp in length were prepared by digestion of the resulting
plasmids with *Pvu*II, and labeling of the purified DNA fragments
with ^{32}P using T4 polynucleotide kinase.

RESULTS

Comparison of DNA-binding by AP1, AP3–PI and AG complexes

The DNA-binding capabilities of AP1, AP3–PI and AG com-
plexes were compared using several CArG-box containing
sequences as binding sites. *In vitro* translated AP1, AP3, PI and
AG were incubated with probes A, B, C and D, and the
protein–DNA complexes analyzed by electrophoretic mobility
shift assays (EMSA) (Fig. 1). Probes A, B and D contain CArG
sequences that are found in the promoters of three *Arabidopsis*
genes (see Materials and Methods), while probe C is based on a
synthetic AG-binding site identified in sequence-selection ex-
periments (17). The probes were labeled to the same specific
activity, allowing direct comparison between the reactions
containing the same protein. The shifted bands present in the
reactions with AP1 and AG correspond to protein–DNA com-
plexes formed by the full-length proteins as well as by truncated
proteins also produced in the translation reactions. AP1 showed
the strongest binding to probes A and D, recognizing the probes
in the order A~D>B>C (Fig. 1). A similar behavior was observed
for AP3–PI, while the affinities of AG for probes A, B and D were
comparable and higher than that for probe C (Fig. 1). The binding
of AG to probe C is revealed in a longer exposure of the
autoradiogram (Fig. 1, lane 13).

Apparent dissociation constants (K_ds) were estimated by
Scatchard analyses of saturating binding assays (22) in which a
constant amount of *in vitro* translated protein was titrated with
increasing amounts of the A and B probes (Fig. 2). AP1 showed
a higher affinity for probe A (K_d = 4.6 nM, Fig. 2) than for probe
B (K_d = 43.4 nM; r^2 value for the least square fit line was 0.893).
The AP3–PI complex showed a similar behavior, although with
somewhat lower affinities: K_d for probe A was 12.5 nM (r^2 =
0.942), while that for probe B could not be estimated because
saturation was not reached in the range of probe concentration
used. AG has comparable affinities for probes A and B: K_ds were
3.8 (r^2 = 0.744) and 2.7 (r^2 = 0.820), respectively. Similar results
were obtained in duplicated experiments. The fact that the
intensities of the bands due to AG were substantially weaker than
those of the bands produced by AP1 or AP3–PI complexes (Fig.
1) indicates that only a very minor fraction of the AG protein
synthesized was active in DNA-binding, since the amounts of
AP1, AP3, PI and AG that are produced by the *in vitro* translation
reactions are comparable (not shown) and AG binds with high
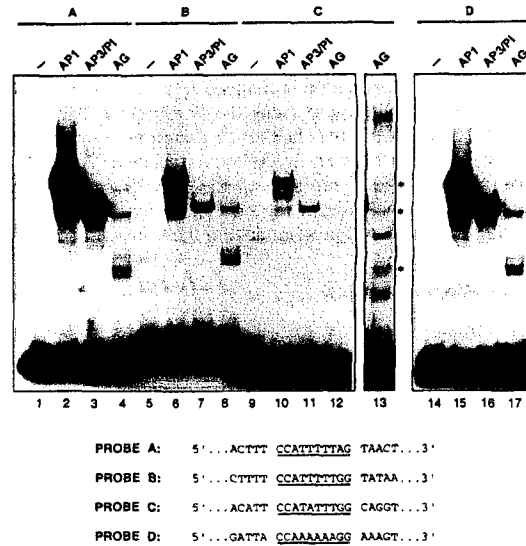affinity to probes A and B.

Figure 1. AP1, AP3–PI, and AG complexes bind to CArG-box containing
sequences. *In vitro* translated AP1, AP3 and PI (cotranslated), and AG were
assayed for DNA-binding activity with probes A, B, C and D. Controls with
unprogrammed lysate for each of the probes are included (lanes 1, 5, 9 and 14).
Lane 13 shows a longer exposure of lane 12. The shifted bands visible on lane
13 that are specific to the presence of AG in the reaction are indicated by
asterisks; additional shifted bands are non-specific and originated by the
reticulocyte lysate.

PROBE A: 5'...ACTTT CCATTTTTAG TAACT...3'
PROBE B: 5'...CTTTT CCATTTTTGG TATAA...3'
PROBE C: 5'...ACATT CCATATTTGG CAGGT...3'
PROBE D: 5'...GATTA CCAAAAAGG AAAGT...3'

AP1, AP3–PI and AG DNA-binding activity was assayed with
three additional CArG-box containing sequences, probes E, F and
G, derived from sequence-selection experiments performed with
either AG or AGL3 (17,21). AP1, AP3–PI and AG bind to all
three probes (a single exception being AP1 and probe E, a
combination for which no binding could be detected in the
experimental conditions used) (data not shown). AP1, AP3–PI
and AG bound probes E, F and G with much lower affinities than
probes A, B, C and D, consistent with the fact that the former vary
more from the canonical $CC(A/T)_6GG$ site and the consensus
sequence [5'-(T/a)(T/a)(A/T/g)CC(A/T)_4(A/T/g/c)_2(G/a)(G/t)(A/
T/C)(A/t)(A/t/g/c)-3'] deduced from AG-sequence-selection experi-
ments (17,18) (data not shown).

DNA bending by AP1, AP3–PI and AG complexes

Circular permutation analysis was used to determine whether
AP1, AP3–PI and AG complexes induce conformational changes
on the DNA upon binding to a CArG-box sequence. This assay
is based on the position-dependent effects of DNA distortion on
the electrophoretic mobility of DNA fragments of the same length
(26). A series of probes were prepared in which the position of the
site A CArG-box varies with respect to the ends of the fragments,
that are otherwise of identical sequence (Fig. 3A). These
circularly permutated probes were used in EMSAs with AP1,
AP3–PI and AGNML. In all cases, protein–DNA complexes in
which the CArG-box sequence is localized toward the center of
the DNA fragment (probes 3, 4 and 5) showed lower mobility
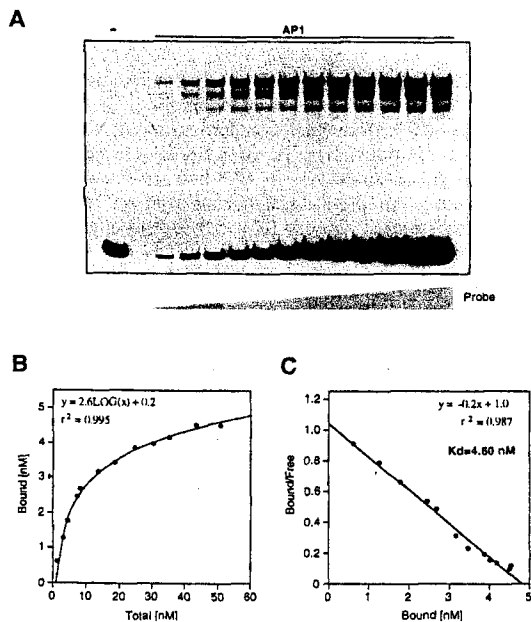than those in which the CArG-box is located near either end

A

B

$y = 2.6\text{LOG}(x) + 0.2$
$r^2 = 0.995$

C

$y = -0.2x + 1.0$
$r^2 = 0.987$

$Kd = 4.80\ nM$

Figure 2. Measurement of DNA-binding affinity of AP1 for probe A. (A) Saturation binding assay with increasing concentrations of probe A (from 1 to 50 nM) and a constant amount of *in vitro* translated AP1. The production of a truncated AP1 protein as a minor product of the *in vitro* translation reaction results in the formation of three different protein–DNA complexes. Free and bound (by all the AP1 complexes) probe were quantitated. A control with unprogrammed lysate and probe A at 12 nM is included (left lane). (B) The amount of bound probe is plotted as a function of total input. (C) Scatchard plot (ratio of bound and free versus bound) of the saturation curve shown in (B). A linear correlation was observed between the two variables, allowing calculation of the dissociation constant ($K_d = -1/$slope). This value is an average of the K_ds for the various AP1 protein complexes with DNA.

A

B

C

Figure 3. Circular permutation analysis of DNA distortions induced by AP1, AP3–PI and AGNML complexes. (A) The probes used for circular permutation analysis were generated by restriction endonuclease cleavage of pBendA, containing the site A CArG-box sequence (black box) flanked by two tandem polylinker sequences, with the seven enzymes shown (1–7). (B) Electrophoretic mobility shift analysis of AP1, AP3–PI and AGNML bound to circularly permutated probes. The faster migrating complexes visible in the reactions with AP1 are due to the presence of truncated proteins also produced in the translation reactions. Reactions with AGNML showed an additional band of lower mobility. (C) The relative mobilities of the AP1-, AP3–PI- and AGnml–DNA complexes were normalized for slight differences in probe mobilities and plotted as a function of the distance between the center of the CArG-box and the center of the probes.

(probes 1, 2, 6 and 7) (Fig. 3B), indicating that AP1, AP3–PI and AGNML induce DNA conformational changes. The unbound probes possessed similar mobilities, regardless of the position of the CArG-box, suggesting that they do not contain significant intrinsic DNA bends (data not shown). The distortion angles were calculated from the data obtained in the circular permutation analysis (Fig. 3C), and estimated to be 53° (AP1 and AP3–PI), and 73° (AGNML). The full-length AG protein was also used in EMSAs with the circularly permutated probes, and its induced apparent bend angle was estimated to be 70° (data not shown).

The DNA distortions induced by AP1, AP3–PI and AGNML were further investigated using phasing analysis (27–29), which determines the direction of the protein-induced bend with respect to an intrinsic DNA bend. A series of DNA probes were prepared such that the site A CArG-box sequence is separated by a linker of variable length from a 25 bp sequence that contains an A tract intrinsically bent toward the minor groove (25). In this set of probes, the distance between the center of the CArG-box and the center of the A tract is varied from 21 to 30 bp, almost a helical turn, to place the CArG-box on different faces of the DNA relative to the intrinsic bend (Fig. 4A). If AP1, AP3–PI or AGNML complexes bend the DNA at the CArG-box in the same
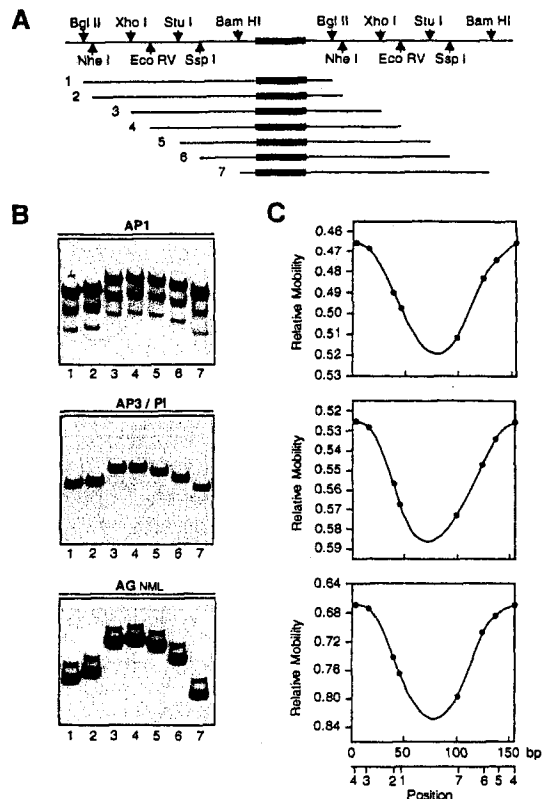
orientation as the A tract, the two bends cooperate to increase the overall extent of bending, resulting in a slow-moving complex in the mobility shift assays. If, on the contrary, the protein induced bend and the intrinsic bend counteract each other, a faster-moving complex will be formed. The DNA–protein complexes formed between the phasing probes and AP1, AP3–PI and AGNML showed variations in electrophoretic mobility that depended on the spacing between the CArG-box and the intrinsic DNA bend, confirming that these MADS-domain proteins induce directed DNA bends (Fig. 4B and C). In all three cases, binding to probe 21, in which the centers of the two bends are separated by ~2 helical turns, resulted in the complex with the slowest mobility (Fig. 4B and C). Therefore, since the two bends cooperate when their centers are in phase, the net orientation of DNA bending
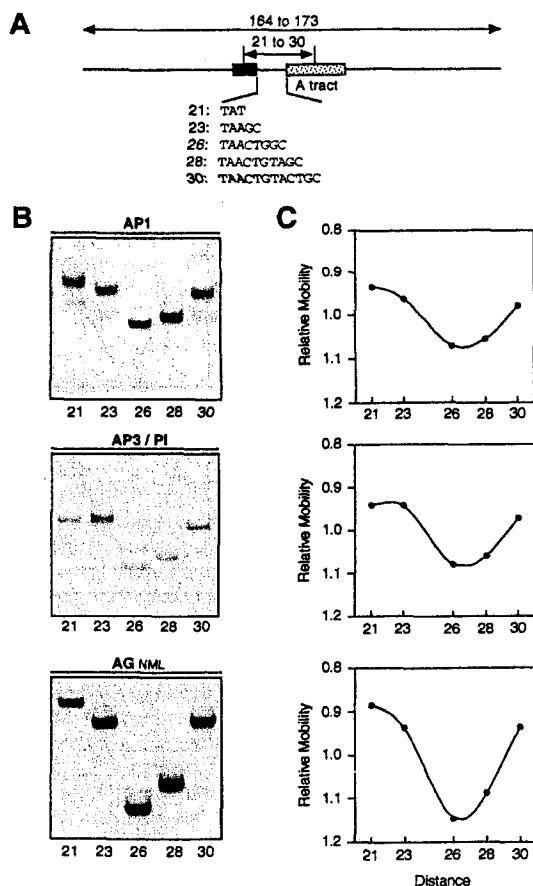
A

21: TAT
23: TAAGC
26: TAACTGGC
28: TAACTGTAGC
30: TAACTGTACTGC

B   AP1

C

AP3 / PI

AG NML

Distance

Figure 4. Phasing analysis of DNA bending by AP1, AP3–PI and AGNML complexes. (A) The probes used for phasing analysis contained the site A CArG-box sequence (black box) separated by a linker of variable length from an A tract sequence (dotted box) that is bent intrinsically toward the minor groove. The distance between the center of the CArG-box and the center of the A tract in the different probes was 21, 23, 26, 28 or 30 bp. (B) Electrophoretic mobility shift analysis of AP1, AP3–PI and AGNML bound to phasing analysis probes. (C) Relative mobilities of the AP1–, AP3–PI– and AGNML–DNA complexes plotted as a function of the distance between the center of the CArG-box and the A tract. In each case, mobility of each protein–probe complex was normalized to the average mobility of all the complexes.

induced by these proteins with respect to the center of the CArG-box is toward the minor groove. The amplitude of the phasing curve obtained with AGNML was larger than those from AP1 and AP3–PI (Fig. 4C), which is indicative of a more pronounced bend (29), as was suggested by the circular permutation analysis.

The observation that AP1, AP3–PI and AGNML induce DNA bending toward the minor groove is in agreement with recent results obtained using circular permutation and phasing analyses that indicated that SRF induces bending in the same orientation (30), and with the crystal structure of core SRF bound to DNA that showed the DNA bent around the protein by 72° (9).

DNA-binding domains of AP1, AP3, PI and AG proteins

To investigate the role of the K box and other regions that are C-terminal to the MADS box in DNA-binding complex formation, a series of C-terminal deletion derivatives of AP1, AP3, PI and AG were produced by *in vitro* transcription/translation. Regions C-terminal to the AP1 MADS box are required to form a DNA-binding complex, since neither AP1M-2 nor AP1M+3 derivatives have such activity (Fig. 5A; AP1M-2 and AP1M+3 truncated proteins lack the last two amino acids of the MADS box or contain the first three amino acids of the L region, respectively). The K box is not required for DNA binding, as AP1M+15, AP1M+29 and AP1M+33 truncated proteins were capable of DNA binding (Fig. 5A). Therefore, the 'core' AP1 protein (minimal DNA-binding domain) consists of the MADS box and part of the L region. AP1M+15 binds to DNA, but at much reduced levels compared with AP1M+29 (Fig. 5A; comparable amounts of the truncated proteins were produced in the *in vitro* translation reactions). AP1 truncated proteins were also used to show that the DNA-binding complex is a protein dimer. The presence of both AP1M+29 and AP1ML+34 in the DNA-binding reaction leads to the formation of a single additional complex of intermediate mobility, corresponding to a heterodimer of both protein forms (Fig. 5A, lanes 10–12).

Similar results were obtained for the AG protein: AGNM+22 bound DNA, whereas AGNM did not (Fig. 5B). Thus, the minimal DNA-binding domain of both AP1 and AG encompasses the MADS box and part of the L region. Curiously, in those reactions with AG truncated proteins that do not include the K box (AGNM+22, AGNM+28, and AGNML) the amount of shifted probe was greater than that when assaying AGNMLK or AG (Fig. 5B). This did not result from substantial differences in the amounts of protein that were produced in the translation reactions (data not shown) or from differences in the DNA-binding affinities (K_ds for AGNML and probes A and B were determined and found to be in the same range as those of AG; data not shown). It may be that the full-length protein has more difficulty in folding properly in the *in vitro* translation. Reactions with AGNM+22, AGNM+28, and AGNML showed an additional retarded band, of weaker intensity, that could be due to a different conformation or shape of the protein–DNA complexes. AG truncated proteins were also used to show that the DNA-binding complex is a protein dimer (Fig. 5B, lanes 8–12).

In contrast with the results obtained for AP1 and AG, AP3ML truncated protein did not show DNA-binding activity when assayed together with PI or PIML (Fig. 5C, lanes 2 and 3), and neither did the PIML protein with several AP3 derivatives (Fig. 5C, lanes 3, 6, 11, 16 and 21). The first 12 amino acids of the AP3 K box were not enough to restore DNA-binding complex formation (AP3ML+12 variant; Fig. 5C, lanes 4–8), while AP3ML+31 and AP3ML+42 were functional when combined with an appropriate PI derivative or with full-length PI (Fig. 5C, lanes 9–18). PIML+16 and PIML+20 truncated proteins could form DNA-binding complexes together with AP3ML+31 (Fig. 5C, lanes 12 and 13) and AP3ML+42 (Fig. 5C, lanes 17 and 18) but, curiously, not with the full-length AP3 protein (Fig. 5C, lanes 22 and 23). In summary, the minimal DNA-binding domains of AP3 and PI differ from those of AP1 and AG. AP3 and PI proteins require amino acids in the K box, in addition to the MADS domain and the L region, to form a DNA-binding complex.
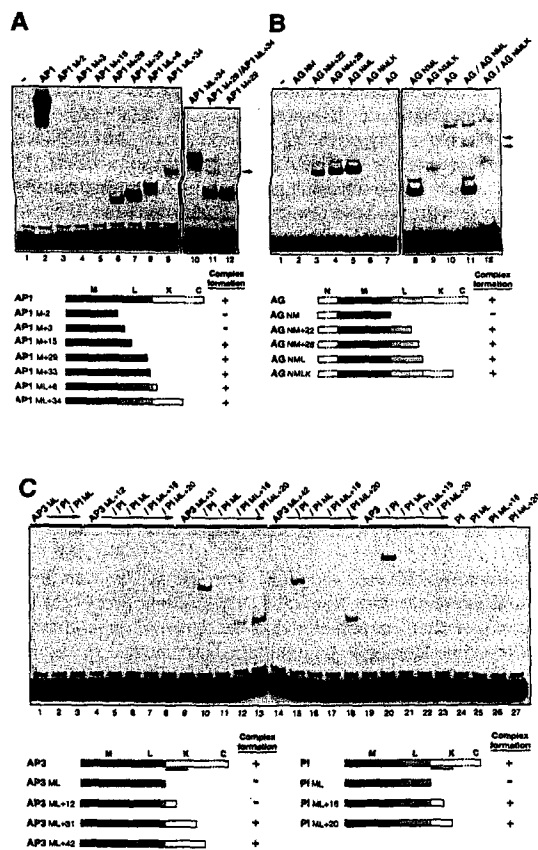
Figure 5. Analyses of C-terminal deletion mutants of AP1, AG, AP3 and PI. (A) Electrophoretic mobility shift analysis using C-terminal deletion derivatives of AP1, assayed with probe A. The structure of the different protein variants is represented in a schematic form below the panel, with the M, L, K and C regions indicated. The ability to form a complex with DNA is indicated with a + sign. That AP1 binds to DNA as a dimer is also shown (lanes 10–12; a 8% gel was used): when cotranslated AP1M+29 and AP1ML+34 (lane 11) were assayed, only one new band appeared, corresponding to a heterodimer of both protein forms (indicated by an arrow). (B) C-terminal deletion derivatives of AG tested with probe B. Protein–DNA complexes were separated from the free probe on a 7% gel. AG binds to DNA as a dimer (lanes 8–12; a 5% gel was used): AG was mixed with AGNML (lane 11) and with AGNMLK (lane 12), and in both cases only one new band appeared, corresponding to a heterodimer between the full-length and the truncated protein (indicated by an arrow). (C) Different combinations of AP3 and PI derivatives tested for DNA-binding with probe A. Protein–DNA complexes were separated from the free probe on 7% gels. The solid line in the diagram represents the first putative amphipathic helix of the K box. The ability to form a heterodimer complexed with DNA is indicated with a + sign.

The ability of N-terminally truncated proteins to dimerize was investigated by immunoprecipitation experiments. AGΔmlkc and AP3Δmlkc (which start at amino acid 26 of the MADS box) were still capable of interacting with AG and PI, respectively, although these interactions are reduced in comparison with those of the full-length AG and AP3 proteins (Fig. 6A). Complete removal of the AG MADS box (AGlkc protein) resulted in a
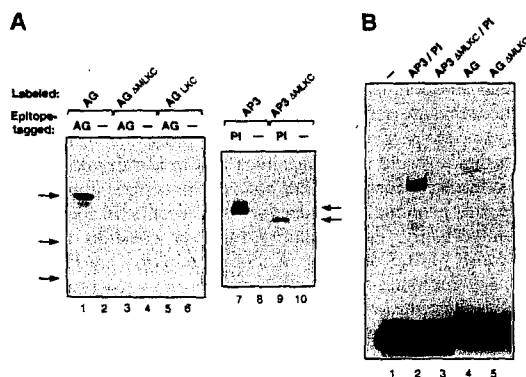

Figure 6. N-terminal deletion analysis of AG and AP3. (A) Similar amounts of [^{35}S]methionine-labeled *in vitro* translated AG, AGΔMLKC, and AGLKC were coimmunoprecipitated with epitope-tagged AG; labeled AP3 and AP3ΔMLKC were coimmunoprecipitated with epitope-tagged PI. Reactions with unprogrammed lysate (as control for non-specific precipitation) were included (even-numbered lanes). Arrows indicate the positions to which the different proteins migrate (B) Gel shift analysis of AGΔMLKC and AP3ΔMLKC assayed with probe A.

protein incapable of interacting with AG (Fig. 6A), in agreement with previous data showing that the MADS box was required for the interaction between AP3 and PI (7). DNA-binding experiments showed that neither AGΔMLKC nor AP3ΔMLKC–PI complexes could bind to probe A (Fig. 6B), indicating that a dimeric MADS protein complex requires the MADS-domains of both monomers to bind DNA. These results are in agreement with the recently determined crystal structure of SRF bound to DNA, which shows that residues in the N-terminal α-helix of the MADS box are involved in both DNA binding and forming part of the dimerization interface, while residues in the C-terminal half of the MADS box are critical for dimer formation (9).

DISCUSSION

Similarity of the DNA-binding properties of AP1, AP3–PI and AG complexes

AP1, AP3–PI and AG dimers were tested for DNA-binding with seven different CArG-box containing sequences, and of the resulting 21 different protein–DNA combinations only one failed to show DNA-binding, that between AP1 and probe E. Some of the probes used were synthetic binding sites identified in random sequence-selection experiments performed with either AG or AGL3 (17,21), but were nevertheless also bound by AP1 and AP3–PI. These results indicate that the sets of sequences recognized by AP1, AP3–PI and AG dimers are largely overlapping. Moreover, *AGL5* has been proposed to be regulated by AG (19); however, the CArG-box (probe D in this study) that might mediate such regulation is also very efficiently bound by AP1 and AP3–PI. Similarly, a CArG-box present in the *AP3* promoter (probe A), that might be involved in the autoregulation of *AP3* expression by AP3–PI (7,31,32), is also bound by AP1 and AG; and the three complexes recognized the probe derived from the *SUP* promoter (probe B). It is noteworthy that the three probes that are derived from the *Arabidopsis* genome were bound

with much higher affinities than those obtained from sequence-selection experiments, showing that the sequence-selection experiments did not unequivocally identify the highest affinity binding sites, and questioning the biological significance of the consensus sequences that are defined in those experiments. The similarity (or identity) of the sequences recognized by AP1, AP3–PI and AG implies that it would not be feasible to try to identify downstream genes of each particular MADS box protein complex by scanning *Arabidopsis* genomic sequences for CArG motifs. In addition, and most importantly, this similarity raises a question about the *Arabidopsis* MADS domain homeotic proteins that has been asked previously for other transcription factors: how do proteins that recognize the same or very similar sets of binding sites regulate the expression of different groups of downstream genes?

Although AP1, AP3–PI and AG recognize similar sets of target sites, their intrinsic DNA-binding specificities are not identical: differences in the *in vitro* DNA-binding affinities are detected. It is possible that these differences contribute to the biological specificity of these proteins. However, if subtle differences in DNA-binding affinities are, by themselves, the main determinants of the functional specificity of these four homeotic proteins, their concentrations in the cell should be critical and thus finely regulated. The available data, on the contrary, have not revealed a tight link between protein concentration and developmental outcome. First, none of the *ap1, ap3, pi* or *ag* alleles studied to date has been shown to be a haplo-insufficient mutation with respect to organ identity. In addition, *AG, AP3* and *PI* have been ectopically expressed under the control of the constitutive 35S promoter and shown to produce the expected organ identity changes (31–33). These data indicate that the levels of expression of AP1, AP3, PI and AG can be varied within a certain range without affecting their control of organ identity (it remains an open possibility that the level of protein of each gene is also regulated posttranscriptionally). Certain thresholds of homeotic protein concentration or function likely exist: the phenotype that is conferred by the ectopic expression of *AG* or *AP3* can vary in its severity between different transgenic lines, presumably owing to different levels of transgene expression (31,33). Nonetheless, the only functions identified in the ectopic expression experiments are those that are particular to the wild-type expression of each of those genes, and no new or different functions are shown by these proteins in the different transgenic lines. Therefore, the thresholds of protein concentration or function could in part be related to the DNA-binding activity of each of these proteins, but they do not indicate that the specific functions of each protein can be changed by under- or overexpression, as would be expected if subtle DNA affinity differences were responsible for specific functions.

AP1, AP3–PI and AG dimers were found to induce similar degrees of DNA bending toward the minor groove. It is noteworthy that a truncated core AG protein, AGNML, induced the same DNA distortion as the full-length AG protein, suggesting that the results obtained in the circular permutation and phasing analysis experiments were not affected by a possible extended shape of the proteins (as has been described in other cases; 34). In addition, the crystal structure of core SRF bound to DNA has recently been determined and showed the DNA bent around the protein (9). The similarity of the conformational changes induced by AP1, AP3–PI and AG dimers suggests that the different regulatory specificities of these three complexes do not arise through the generation of different DNA structures that could

direct the formation of transcripton complexes with distinct functional properties. It therefore seems at least possible that the biological specificity of AP1, AP3, PI and AG cannot be explained on the basis of their intrinsic DNA-binding properties alone. Consistent with this interpretation, *in vivo* analyses of the activity of chimeric genes formed by swapping regions between AP1, AP3, PI and AG have shown that, at least in some cases, the MADS domains can be interchanged without them determining the specific functions of the resulting chimeric proteins (35). In addition, we have recently found that the DNA-binding specificity of AP1, AP3, PI and AG can be altered without affecting their functions *in vivo* (J. L. Riechmann and E. M. Meyerowitz, unpublished results). Another possible mechanism by which the MADS domain homeotic proteins could direct the development of different organs is that they may act in conjunction with cofactors that modulate their ability to regulate the transcription of downstream genes. This could be a process in which DNA bending by the plant MADS-domain proteins might be involved, through determining DNA topology in nucleoprotein complexes, allowing interactions with other proteins that may bind to adjacent DNA sites, or facilitating the recognition by accessory proteins of their respective target sites, as has been suggested for SRF (9).

This situation of diverse and highly specific *in vivo* functions by related proteins with similar DNA-binding properties is reminiscent of that encountered for the *Drosophila* homeotic selector proteins. Homeodomain proteins also show very similar intrinsic DNA-binding specificities *in vitro* (with affinities on the order of $K_d = 10^{-8}–10^{-9}$ M) (36). Some differences in the DNA-binding specificities are also detected, which might contribute in part to the functional specificity of the proteins (37). However, the analyses of different mutant and chimeric proteins in ectopic expression experiments have shown that the specificity of action of the homeodomain proteins *in vivo* also depends on protein–protein interactions (38). Examples of direct interactions between the MADS box proteins of animals and fungi and additional cofactors are already abundant. Some of these interactions result in modulation of the MADS box protein activity and a concomitant cell-specific differential gene expression, eventually leading to cell specialization or to different developmental pathways. The yeast MADS domain protein MCM1 is required for transcription in the three yeast cell types, but through interactions with different cofactors (α1 protein, α2 homeodomain protein) it regulates the transcription of cell-type specific genes. Thus the regulatory activities of MCM1 are determined by the availability of accessory proteins in conjunction with the sequence context of the MCM1 binding sites (10,39). The MADS domain protein MEF2A physically interacts with muscle bHLH transcription factors to control the cascade of myogenic development through cooperative activation of muscle gene expression (40,41).

Organization of AP1, AP3, PI and AG proteins

As expected from the high degree of sequence similarity, the organization of the AG, AP3 and PI MADS boxes is similar to that of SRF: the basic N-terminal half is essential for DNA-binding and the C-terminal half is required for dimerization (9,42). Since the MADS box proteins bind to DNA as dimers, the minimal DNA-binding domain includes the conserved 56 aa MADS box, and an additional C-terminal extension, whose

sequence is not conserved throughout the family but is necessary for dimerization. This extension is of ~24 aa in SRF and MCM1 (9,16,42). In addition to the MADS box, the minimal DNA-binding domains of AP1 and AG include extensions of ~20 amino acids (part of the L region), and similar results have been obtained recently with the *Arabidopsis* AGL2 protein, whose core includes the MADS domain and the first 21 aa of the L region (43). On the other hand, core AP3 and PI proteins comprise the entire L region and part of the K box (a total C-terminal extension to the MADS domain of ~50 aa). The involvement of the first amino acids of the K-box in dimerization has also been recently shown for the *Antirrhinum* homologous proteins of AP3 and PI: DEF and GLO, respectively (44). The difference in the size of the core proteins, AG and AP1 on one hand, and AP3 and PI on the other, correlates with the partner specificity that these proteins possess: AG and AP1 form DNA-binding homodimers but not DNA-binding heterodimers with AP3 or PI, which form a DNA-binding AP3–PI heterodimer (20).

Based on the presumptive coiled-coil structure of the K box, and by analogy to leucine zipper proteins, it has been suggested that this region could be involved in promoting dimerization (12). The analysis of C-terminal deletion mutants described here shows that the entire K box (in the case of AP1 and AG), or a substantial part of it (in the case of AP3 and PI), is dispensable for the formation of DNA-binding dimers. It is possible that the K box plays a role in dimer stabilization, but might not be required in the mild conditions used in the DNA-binding experiments. Consistent with this notion, it has been shown that deletion of part of the K box of an epitope-tagged PI protein (a deletion that did not include the region shown here as forming part of the core protein) reduced, but did not abolish, the immunoprecipitation of labeled AP3 protein (7). Alternatively, the K-box could be involved in interactions with additional (unknown) cofactors of the plant MADS box proteins.

In summary, the finding of differences in the organization of the AP1, AG and AP3 and PI proteins, and its correlation with the partner specificity that these proteins exhibit for the formation of DNA-binding dimers (20), support the idea that selective dimerization is part of the mechanism by which these proteins achieve their functional specificity. On the other hand, the DNA-binding activities of these dimers (AP1, AP3–PI and AG) are very similar, suggesting that the biological specificity that these proteins possess may not be explained on the basis of their intrinsic DNA-binding specificity alone. It is likely that at least part of their biological specificity is achieved through selective interactions with additional transcription factors, a mechanism that appears to be a common theme for the MADS box proteins of animals and fungi.

ACKNOWLEDGEMENTS

REFERENCES

1   Coen,E.S. and Meyerowitz,E.M. (1991) *Nature*, **353**, 31–37.
2   Ma,H. (1994) *Genes Dev.*, **8**, 745–756.
3   Weigel,D. and Meyerowitz,E.M. (1994) *Cell*, **78**, 203–209.
4   Mandel,M.A., Gustafson-Brown,C., Savidge,B. and Yanofsky,M.F. (1992) *Nature*, **360**, 273–277.
5   Jofuku,K.D., den Boer,B.G.W., van Montagu,M. and Okamuro,J.K. (1994) *Plant Cell*, **6**, 1211–1225.
6   Jack,T., Brockman,L.L. and Meyerowitz,E.M. (1992) *Cell*, **68**, 683–697.
7   Goto,K. and Meyerowitz,E.M. (1994) *Genes Dev.*, **8**, 1548–1560.
8   Yanofsky,M.F., Ma,H., Bowman,J.L., Drews,G.N., Feldmann,K.A. and Meyerowitz,E.M. (1990) *Nature*, **346**, 35–39.
9   Pellegrini,L., Tan,S. and Richmond,T.J. (1995) *Nature*, **376**, 490–498.
10   Shore,P. and Sharrocks,A.D. (1995) *Eur. J. Biochem.*, **229**, 1–13.
11   Ma,H., Yanofsky,M.F. and Meyerowitz,E.M. (1991) *Genes Dev.*, **5**, 484–495.
12   Davies,B. and Schwarz-Sommer,Z. (1994) In Nover,L. (ed.), *Plant Promoters and Transcription Factors*. Springer-Verlag, Berlin, pp. 235–258.
13   Pnueli,L., Abu-Abeid,M., Zamir,D., Nacken,W., Schwarz-Sommer,Z. and Lifschitz,E. (1991) *Plant J.*, **1**, 255–266.
14   Pollock,R. and Treisman,R. (1990) *Nucleic Acids Res.*, **18**, 6197–6204.
15   Wynne,J. and Treisman,R. (1992) *Nucleic Acids Res.*, **20**, 3297–3303.
16   Mueller,C.G.F. and Nordheim,A. (1991) *EMBO J.*, **10**, 4219–4229.
17   Huang,H., Mizukami,Y., Hu,Y. and Ma,H. (1993) *Nucleic Acids Res.*, **21**, 4769–4776.
18   Shiraishi,H., Okada,K. and Shimura,Y. (1993) *Plant J.*, **4**, 385–398.
19   Savidge,B., Rounsley,S.D. and Yanofsky,M.F. (1995) *Plant Cell*, **7**, 721–733.
20   Riechmann,J.L., Krizek,B.A. and Meyerowitz,E.M. (1996) *Proc. Natl. Acad. Sci. USA*, **93**, 4793–4798.
21   Huang,H., Tudor,M., Weiss,C.A., Hu,Y. and Ma,H. (1995) *Plant Mol. Biol.*, **28**, 549–567.
22   Cao,Z., Umek,R.M. and McKnight,S.L. (1991) *Genes Dev.*, **5**, 1538–1552.
23   Kim,J., Zwieb,C., Wu,C., and Adhya,S. (1989) *Gene*, **85**, 15–23.
24   Thompson,J.F. and Landy,A. (1988) *Nucleic Acids Res.*, **16**, 9687–9707.
25   Koo,H.S., Drak,J., Rice,J.A. and Crothers,D.M. (1990) *Biochemistry*, **29**, 4227–4234.
26   Wu,H.-M. and Crothers,D.M. (1984) *Nature*, **308**, 509–513.
27   Zinkel,S.S. and Crothers,D.M. (1987) *Nature*, **328**, 178–181.
28   Kerppola,T.K. and Curran,T. (1991) *Cell*, **66**, 317–326.
29   Kerppola,T.K. and Curran,T. (1993) *Mol. Cell. Biol.*, **13**, 5479–5489.
30   Sharrocks,A.D. and Shore,P. (1995) *Nucleic Acids Res.*, **23**, 2442–2449.
31   Jack,T., Fox,G.L. and Meyerowitz,E.M. (1994) *Cell*, **76**, 703–716.
32   Krizek,B.A. and Meyerowitz,E.M. (1996) *Development*, **122**, 11–22.
33   Mizukami,Y. and Ma,H. (1992) *Cell*, **71**, 119–131.
34   Sitlani,A. and Crothers,D.M. (1996) *Proc. Natl. Acad. Sci. USA*, **93**, 3248–3252.
35   Krizek,B.A. and Meyerowitz,E.M. (1996) *Proc. Natl. Acad. Sci. USA*, **93**, 4063–4070.
36   Gehring,W.J., Affolter,M. and Bürglin,T. (1994) *Annu. Rev. Biochem.*, **63**, 487–526.
37   Dessain,S., Gross,C.T., Kuziora,M.A. and McGinnis,W.M. (1992) *EMBO J.*, **11**, 991–1002.
38   Mann,R.S. (1995) *Bioessays*, **17**, 855–863.
39   Johnson,A.D. (1995) *Curr. Opin. Genet. Dev.*, **5**, 552–558.
40   Kaushal,S., Schneider,J.W., Nadal-Ginard,B. and Mahdavi,V. (1994) *Science*, **266**, 1236–1240.
41   Molkentin,J.D., Black,B.L., Martin,J.F. and Olson,E.N. (1995) *Cell*, **83**, 1125–1136.
42   Norman,C., Runswick,M., Pollock,R. and Treisman, R. (1988) *Cell*, **55**, 989–1003.
43   Huang,H., Tudor,M., Su,T., Zhang,Y., Hu,Y. and Ma,H. (1996) *Plant Cell*, **8**, 81–94.
44   Zachgo,S., de Andrade Silva,E., Motte,P., Tröbner,W., Saedler,H. and Schwarz-Sommer,Z. (1995) *Development*, **121**, 2861–2875.